Editorial

PET in radiotherapy planning: Particularly exquisite test or pending and experimental tool?

Vincent Gregoire [a,*], Arturo Chiti [b]

[a] Radiation Oncology Department, Université catholique de Louvain, Brussels, Belgium; [b] Nuclear Medicine Department, Humanitas, Milan, Italy

In medicine, clinical practice cannot resist fashion: in the year 2000, 9 publications dealt with the "*use of PET in radiotherapy planning*"; by the end of 2005, 187 articles have been published on this subject, and by the end of June 2010, PubMed indicated 565 hits using the same keywords!

But are we sure that this is fashion? Isn't it a reflection of a medical progress that translated into practice change? And if so, what would have made the use of PET so exquisite in radiotherapy planning? Answering this question requires a profound understanding of the process of radiotherapy planning and the key elements that are likely to impact on it.

Radiotherapy planning is a multiple step process that starts with a decision of a multidisciplinary tumor board to irradiate a malignant tumor with a given T–N–M stage, and end with the signature of a board certified Radiation Oncologist on a treatment plan comprising a dose prescription, a set of dose distribution together with a set of technical parameters that will be transferred to the linear accelerator (or equivalent machine) for the plan execution [1].

In this process, the appropriate selection and delineation of target volumes (TVs) and Organs At Risk (OARs) – typically performed on contrasted CT and/or MRI – by a trained Radiation Oncologist is of paramount importance. It requires the proper use of both extremely sensitive (very few false negative examination, or with a high negative predictive value) and specific (very few false positive examination, or with a high positive predictive value) imaging modalities. In other words, we want the images to give us the truth, all the truth and only the truth…! In addition, for the delineation aspect, one needs imaging modalities that have a high spatial resolution, typically in the order of 1–2 mm. Both CT and MRI fulfill this criterion.

How is the picture with PET? PET has an intrinsic advantage, which is that it could image any physiopathological pathways within a tumor or a normal tissue, providing an ad hoc tracer can be injected to the patient. And tracers of metabolism, proliferation, hypoxia, apoptosis, gene expression (e.g. EGFR), etc. have been validated and are available if not all for routine clinical practice, at least for clinical studies. But PET has potential limitations, which are its relatively lower spatial resolution and the low signal-to-background ratio observed with some tracers; both limitations could compromise the overall sensitivity and specificity of PET compared to CT and/or MRI. The lower spatial resolution is a complex issue resulting from several factors, and among them the energy of the positron, the size of the detector and the low counting efficiency are the most important. These factors may require the use of appropriate acquisition protocols (e.g. correction for movement artifacts) and special reconstruction algorithms to sharpen the edges of the volume of interest. The low signal-to-background ratio typically results from the tracer metabolism, which ideally should distribute evenly into the body, get fixed to the site(s) of interest while the unfixed tracer should get cleared from the body. And all these processes should be done as quickly as possible, and for sure within a time frame compatible with the half-life of the tracer. But as one knows, the reality is far from this ideal picture…

Several articles have been recently published on the use of PET for radiotherapy planning in oesophageal, lung, head and neck, brain, prostate, and anal canal tumors [2–12]. No definitive conclusion could be drawn from these publications, PET influencing target volume selection and delineation in some studies, not in others. But what seems consistently observed in all these publication is the importance of the use of well-defined protocols for image acquisition, reconstruction and segmentation.

In this framework, in this special issue of *Radiotherapy & Oncology*, we ought to summarize the state-of-the-art knowledge on the use of PET for radiotherapy planning, from tracers and data acquisition to clinical use in various tumors. It starts with a summary of the various PET radiopharmaceuticals available in oncology [13], and the state-of-the-art equipment and protocols for data acquisition and transfer [14]. Then a series of contribution deals with patient immobilization on PET–CT camera [15], image reconstruction and segmentation [18], image quantitation [16], correction of movement artifacts [17], and the use of PET for dose optimization [19]. Thereafter, a article from Chiti and Gregoire [20] set the scene for the use of PET images in radiotherapy planning: what are we looking for? Last, this special issue ends with a systematic review on the use of PET for the main tumor sites, e.g. brain tumors [21], head and neck tumors [22], lung tumors [23], gastro-intestinal tumors [24], genito-urinary tumors [25] and gynecological tumors [26].

It is expected that this special issue of Radiotherapy & Oncology will contribute to increase the awareness of Radiation Oncologist,

* Corresponding author. Address: Radiation Oncology Department and Laboratory of Molecular Imaging and Experimental Radiotherapy, Université catholique de Louvain and St-Luc University Hospital, 10 Ave. Hippocrate, 1200 Brussels, Belgium.
E-mail address: vincent.gregoire@uclouvain.be (V. Gregoire).

Nuclear Medicine physicians and other related specialists on the proper use of PET in radiotherapy planning.

References

[1] ICRU. International Commission on Radiation Units and Measurements. Prescribing, recording and reporting Intensity-Modulated Photon-Beam Therapy (IMRT). In: ICRU Report 83, J. ICRU. Oxford: Oxford University Press.

[2] Thorwarth D, Alber M. Implementation of hypoxia imaging into treatment planning and delivery. Radiother Oncol 2010. doi:10.1016/j.radonc.2010.05.012.

[3] Moule RN, Kayani I, Mouddin SA, Meer K, Lemon C, Goodchild K, et al. The potential advantages of 18FDG PET/CT-based target volume delineation in radiotherapy planning of head and neck cancer. Radiother Oncol 2010. doi:10.1016/j.radonc.2010.04.025.

[4] Muijs CT, Beukema JC, Pruim J, Mul VE, Groen H, Plukker JT, et al. A systematic review on the role of FDG-PET/CT in tumour delineation and radiotherapy planning in patients with esophageal cancer. Radiother Oncol 2010. doi:10.1016/j.radonc.2010.04.024.

[5] Henriques de Figueiredo B, Barret O, Demeaux H, Lagarde P, De-Mones-Del-Pujol E, Kantor G, et al. Comparison between CT- and FDG-PET-defined target volumes for radiotherapy planning in head-and-neck cancers. Radiother Oncol 2009;93:479–82.

[6] Seppälä J, Seppänen M, Arponen E, Lindholm P, Minn H. Carbon-11 acetate PET/CT based dose escalated IMRT in prostate cancer. Radiother Oncol 2009;93:234–40.

[7] Muijs CT, Schreurs LM, Busz DM, Beukema JC, van der Borden AJ, Pruim J, et al. Consequences of additional use of PET information for target volume delineation and radiotherapy dose distribution for esophageal cancer. Radiother Oncol 2009;93:447–53.

[8] Schinagl DA, Hoffmann AL, Vogel WV, van Dalen JA, Verstappen SM, Oyen WJ, et al. Can FDG-PET assist in radiotherapy target volume definition of metastatic lymph nodes in head-and-neck cancer? Radiother Oncol 2009;91:95–100.

[9] MacManus M, Nestle U, Rosenzweig KE, Carrio I, Messa C, Belohlavek O, et al. Use of PET and PET/CT for radiation therapy planning: IAEA expert report 2006–2007. Radiother Oncol 2009;91:85–94 [Review].

[10] Nguyen BT, Joon DL, Khoo V, Quong G, Chao M, Wada M, et al. Assessing the impact of FDG-PET in the management of anal cancer. Radiother Oncol 2008;87:376–82.

[11] van Loon J, Offermann C, Bosmans G, Wanders R, Dekker A, Borger J, et al. 18FDG-PET based radiation planning of mediastinal lymph nodes in limited disease small cell lung cancer changes radiotherapy fields: a planning study. Radiother Oncol 2008;87:49–54.

[12] Ollers M, Bosmans G, van Baardwijk A, Dekker A, Lambin P, Teule J, et al. The integration of PET–CT scans from different hospitals into radiotherapy treatment planning. Radiother Oncol 2008;87:142–6.

[13] Haubner R. PET radiopharmaceuticals in radiation treatment planning: synthesis and biological characteristics. Radiother Oncol 2010;96:280–7.

[14] Sattler B, Lee JA, Lonsdale M, et al. PET/CT (and CT) instrumentation, image reconstruction and data transfer for radiotherapy planning. Radiother Oncol 2010;96:288–97.

[15] Coffey M, Vaandering A. Patient setup for PET-CT acquisition in radiotherapy planning. Radiother Oncol 2010;96:298–301.

[16] Weber WA. Quantitative analysis of PET studies. Radiother Oncol 2010;96:308–10.

[17] Bettinardi V, Picchio M, Di Muzio N, et al. Detection and compensation of organ/lesion motion using 4D-PET/CT respiratory gated acquisition techniques. Radiother Oncol 2010;96:311–6.

[18] Lee JA. Segmentation of positron emission tomography images: some recommendations for target delineation in radiation oncology. Radiother Oncol 2010;96:302–7.

[19] Thorwarth D, Geets X, Paiusco M. Physical radiotherapy treatment planning based on functional PET/CT data. Radiother Oncol 2010;96:317–24.

[20] Chiti A, Kirienko M, Gregoire V. Clinical use of PET–CT data for radiotherapy planning: What are we looking for? Radiother Oncol 2010;96:277–9.

[21] Grosu AL, Weber WA. PET for radiation treatment planning of brain tumours. Radiother Oncol 2010;96:325–7.

[22] Troost ECG, Schinagl DAX, Bussink J, et al. Clinical evidence on PET–CT for radiation therapy planning in head and neck tumours. Radiother Oncol 2010;96:328–34.

[23] De Ruysscher D, Kirsch C-M. PET scans in radiotherapy planning of lung cancer. Radiother Oncol 2010;96:335–8.

[24] Lambrecht M, Haustermans K. Clinical evidence on PET–CT for radiation therapy planning in gastro-intestinal tumors. Radiother Oncol 2010;96:339–46.

[25] Pichio M, Giovannini E, Crivellaro C, et al. Clinical evidence on PET–CT for radiation therapy planning in prostate cancer. Radiother Oncol 2010;96:347–50.

[26] Haie-Meder Ch, Mazeron R, Magné N. Clinical evidence on PET–CT for radiation therapy planning in cervix and endometrial cancers. Radiother Oncol 2010;96:351–5.

Editorial

Clinical use of PET-CT data for radiotherapy planning: What are we looking for?

Arturo Chiti [a,*], Margarita Kirienko [a], Vincent Grégoire [b]

[a] Department of Nuclear Medicine, Istituto Clinico Humanitas, Milan, Italy; [b] Department of Radiation Oncology, St-Luc University Hospital, Brussels, Belgium

Personalized medicine is the new driving force in the modern era of medicine. In oncology, personalized management of a patient's disease means the application of specific therapeutic strategies that are best suited for an individual patient and for the particular type of tumour, which the therapy is aiming to target. Molecular diagnostics influences cancer management in several ways that aid personalisation and this is why research has now focused on individualizing treatment strategies by incorporating a combination of physiological variables, genetic characteristics and environmental factors together with the traditional tumour characteristics that currently drive clinical decision making.

Imaging is playing a major role in individualizing treatment strategies and the approach differs depending on whether the target is a single disease control point or a general disease control point applicable to a number of treatment paradigms (e.g. proliferation, angiogenesis, inflammation, etc.). Among the many different imaging tools that are available nowadays, Positron emission tomography (PET) can be used to visualize molecular alterations in the living subject, thus facilitating early diagnosis and treatment of disease. The state of art of molecular imaging with PET requires the use of integrated PET and computed tomography (CT) scanners, which are able to offer combined information on molecular and morphological characteristics of tumours.

PET-CT using fluoro-deoxy-glucose as a molecular probe of glucose metabolism in cancer cells has been demonstrated to have high accuracy for detection of many tumour types [1]. Along with diagnosis, staging, detection of relapse, restaging and follow-up, one of the main applications of PET-CT is the assessment of therapy response and treatment planning. In routine practice, structural and tumour volume changes are used to guide therapeutic strategies and to measure the disease-free and overall survival. However, tissue metabolism changes more rapidly than morphology, and changes in tumour FDG uptake may therefore predict alterations in volume [2].

The use of FDG-PET as a surrogate tool for monitoring therapy response offers better patient care by individualizing treatment and avoiding ineffective chemotherapy. The use of PET, not only with FDG, to identify patients who can benefit from targeted therapies with monoclonal antibodies has also been demonstrated to be useful, as well as to evaluate the response to therapy in those patients selected for treatment [3,4].

Like other imaging tools PET can be used to inform decision-making, e.g. whether a surgical approach is advisable, which intervention will be most appropriate and whether advanced therapies are feasible. It can also further improve tailoring of therapy by guiding radiation therapy planning and improving definition of tumour target volumes, as is described in the other contributions of this journal's issue. Although CT remains the gold standard for depicting anatomy for the purpose of target volume definition and dose calculation, PET-CT could help with respect to the dose constraints for organs at risk, if the hypermetabolic component is smaller than the morphological appearance of the tumour, reducing the gross tumour volume. Further, PET could permit the inclusion of FDG-avid, but non-enlarged, lymph nodes within the field of treatment or could modify the TNM staging, resulting in a shift in treatment modality from curative to palliative.

Radiation oncologists rely only on the representation through imaging tools to select and delineate target volumes. The limitation is the fact that none of the imaging modalities has sensitivity and specificity of 100% because of their spatial resolution, the specific affinity of the tracer or the contrast medium used to visualize different characteristics of the neoplastic tissue.

Sensitivity and the specificity of a diagnostic tool depend also on the criteria used for the image interpretation. CT acquisition and reconstruction parameters are standardized, Hounsfield unit (HU) is easily correlated with tissue density and patterns of vascular enhancement through contrast medium are well-defined. This accounts for the high reliability of contrast enhanced CT in oncology. The high specificity is counterbalanced by suboptimal sensitivity in some neoplasm due to the fact that only morphological and density parameters are taken into account. Magnetic resonance imaging (MR) adds functional information to high resolution images particularly in some tissues, like brain. New sequences are very promising for tissue characterization but the clinical utilization is still to be assessed. Different carriers for gadolinium are available to study different tissues increasing signal specificity when compared to CT.

PET radiopharmaceuticals have the theoretical advantage of high specificity due to specific binding to particular targets. Tracers may be viewed as probes for specific metabolic pathways: i.e. hexokinase activity, apoptosis, hypoxia, etc. [5]. In the clinical setting this specificity is limited by the fact that the same metabolic pathways are activated in neoplastic and non-neoplastic tissues. Diagnostic accuracy might be flawed by inflammatory reaction and physiological pattern of distribution of the tracer. For instance

* Corresponding author.
E-mail address: arturo.chiti@humanitas.it (A. Chiti).

granulomatous lesions might have FDG uptake as high as very aggressive tumours, or the high background uptake of 11C-choline in the liver might hinder huge metastatic invasion. Limited spatial resolution is also an issue: for instance micro-embolic nodal metastases are missed in PET and this reduces the accuracy of the method to assess micrometastases [6]. Furthermore, different radiopharmaceuticals should be used to image different tumour types. For instance, bladder cancer is known not to be FDG avid (Fig. 1), while prostate cancer can be detected with high sensitivity with 11C-choline (Fig. 2).

Image standardization has been recently established for FDG PET to overcome several differences existing in reported images, which accounted for a lack of confidence in the technique from radiation oncologist and oncologist [7]. Nonetheless, since PET is going to be used even more frequently with radiopharmaceutical

different than FDG, the problem of standardization will still exist for other radiopharmaceuticals as soon as they enter the clinical use.

The use of imaging to better delineate the radiation treatment target is a particular example of personalized treatment [8]. In fact, instead of using a prior established field, the radiation dose is shaped on the tumour for each single patient. The advantage of functional imaging with PET is the possibility of further increasing the accuracy of target delineation including only metabolic active tissue.

The clinical setting and the objective of the treatment are essential in choosing the most appropriate imaging modality. If for a particular case the objective is to avoid the miss of the localization of tumour cells, the most sensitive imaging modality or, in case of PET, the most sensitive tracer and highly sensitive criteria for the
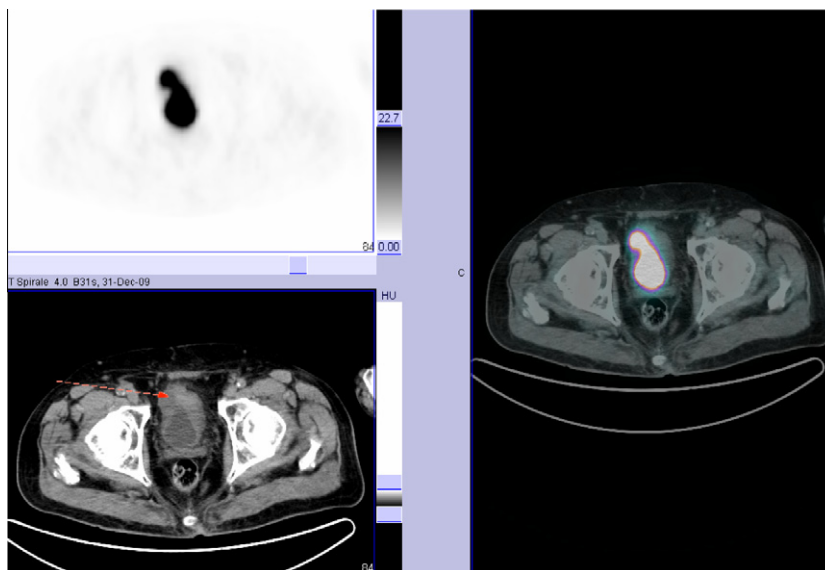

Fig. 1. Primary bladder cancer. Axial slices of 18F-FDG PET (upper left), CT (lower left) and fusion images (right). The primary tumour is clearly depicted on CT images (arrow) but, due to low glucose consumption, no abnormality can be seen on PET images. Physiological elimination of the radiopharmaceutical in the bladder is easily recognized.
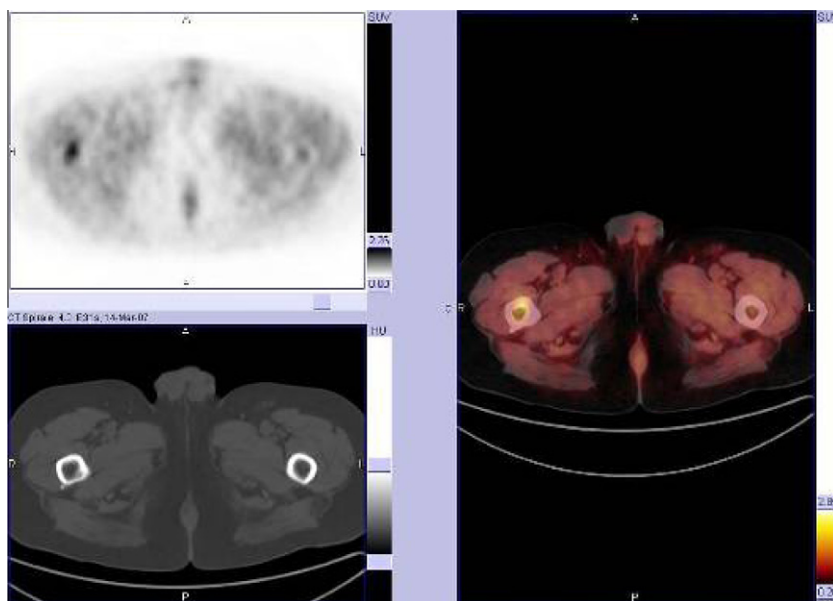

Fig. 2. Metastatic prostate cancer. Axial slices of 11C-choline PET (upper left), CT (lower left) and fusion images (right). Focal uptake of the radiopharmaceutical is clearly seen in the right proximal femur, without any abnormality on CT images.

Table 1

PET sensitivity and specificity for different tumour types. Results often show large variations in range due to the patients selection and lesions sizes, particularly for lymph node staging. Therefore, this table should be used just as a reference. Further details are described in the dedicated chapters of this journal's issue. FDG is considered unless otherwise stated.

Site		Sensitivity (%)	Specificity (%)
Brain	Primary[a]	78–94	93–100
H&N	Primary	93–100	90–100
	Nodes[b]	76–85	33–67
NSCLC	Primary[c]	90	79–96
	Nodes	83	89
Oesophagus	Primary	94	92
	Nodes	24–82	81–99
Cervical	Primary	75	96
	Nodes	38–91	83–100
Endometrial	Primary	89–97	50
	Nodes	53–100	99

[a] Amino acid PET.
[b] N0 neck.
[c] Lung nodules.

image interpretation have to be chosen. This can determine that non-neoplastic tissue (false positive finding) would be included in the target volume. On the other hand almost all neoplastic, if not absolutely all, cells would be irradiated, because of the high negative predictive value that this procedure gives.

If the objective is to preserve non-neoplastic tissue and include in the target volume only the tissue that is certainly neoplastic, the most specific modality and specific criteria for the interpretation have to be preferred. The price for that could be that some neoplastic cells (false negative findings) would not be included in the target volume. On the other hand we will avoid including non-neoplastic tissue in the target volume, because of the high positive predictive value. Table 1 briefly summarize data available for sensitivity and specificity of PET imaging for different tumours entities.

Thresholding for target delineation with PET is still a matter of debate [9]. In fact no methodology has been assessed to be useful in every clinical setting. As described in another session of this journal's issue, delineation of target volumes on PET images can be done by hand or using automated segmentation methods. The operator's hand approach has the main limitation of a large variability of resulting contours. This operator dependent method requires a lot of expertise and strict guidelines for the display devices, without any robust standard to follow still defined. PET-CT

images are considered easier to delineate but it makes poor sense to use an anatomic modality to better delineate functional images. Another approach to reduce the variability of the delineation consists in relying on automatic or semi-automatic segmentation methods.

Whichever approach is going to be used, the fine tuning of the method is going to affect diagnostic accuracy. The operator's mind might want to be set towards a more specific or sensitive reading of images, therefore setting the threshold for the target volume in different ways. In the same way, different parameters of the automatic segmentation program might affect the final target volume identification.

In conclusion, in order to get a really personalized approach of radiation target volume delineation in each patient, many parameters must be taken into account. The inclusion of clinical parameters pertaining to a single patient is going to heavily affect the therapeutic approach, which should be the result of the best use of technical and clinical information. This means the physicians in charge of choosing the best treatment strategy for the patient have still to choose whether they prefer to use a sensitive or specific approach to obtain the patient's best outcome.

References

[1] Gambhir SS, Czernin J, Schwimmer J, Silverman DH, Coleman RE, Phelps ME. A tabulated summary of the FDG PET literature. J Nucl Med 2001;42:1S–93S.
[2] Ben-Haim S, Ell P. 18F-FDG PET and PET/CT in the evaluation of cancer treatment response. J Nucl Med 2009;50:88–99.
[3] Groves AM, Win T, Haim SB, Ell PJ. Non-[18F]FDG PET in clinical oncology. Lancet Oncol 2007;8:822–30.
[4] Wahl RL, Jacene H, Kasamon Y, Lodge MA. From RECIST to PERCIST: Evolving Considerations for PET response criteria in solid tumors. J Nucl Med 2009;50:122S–50S.
[5] Busk M, Horsman MR, Jakobsen S, Hansen KV, Bussink J, van der Kogel A, et al. Can hypoxia-PET map hypoxic cell density heterogeneity accurately in an animal tumor model at a clinically obtainable image contrast? Radiother Oncol 2009;92:429–36.
[6] Christian N, Lee JA, Bol A, De Bast M, Jordan B, Grégoire V. The limitation of PET imaging for biological adaptive-IMRT assessed in animal models. Radiother Oncol 2009;91:101–6.
[7] Boellaard R, O'Doherty MJ, Weber WA, et al. FDG PET and PET/CT: EANM procedure guidelines for tumour PET imaging: version 1.0. Eur J Nucl Med Mol Imaging 2010;37:181–200.
[8] MacManus M, Nestle U, Rosenzweig KE, Carrio I, Messa C, Belohlavek O, et al. Use of PET and PET/CT for radiation therapy planning: IAEA expert report 2006–2007. Radiother Oncol 2009;9:85–94.
[9] Ollers M, Bosmans G, van Baardwijk A, Dekker A, Lambin P, Teule J, et al. The integration of PET-CT scans from different hospitals into radiotherapy treatment planning. Radiother Oncol 2008;87:142–6.

Review

PET radiopharmaceuticals in radiation treatment planning – Synthesis and biological characteristics

Roland Haubner *

Medizinische Universität Innsbruck, Innsbruck, Austria

A R T I C L E   I N F O

A B S T R A C T

During the last decade several different PET radiopharmaceuticals entered into the clinic and positron emission tomography (PET) became an important tool for staging of cancer patients and assessing response to therapy. Meanwhile FDG-PET has also found application in radiation treatment planning. Potential radiopharmaceuticals for radiation treatment planning may also include tracers allowing monitoring of proliferation, amino acid metabolism, hypoxia, lipid metabolism and receptor expression. Here the syntheses of a selection of clinically tested promising tracers are summarized and the different molecular mechanisms for accumulation are discussed which may help to choose the appropriate tracer for planning radiation treatment strategies.

© 2010 European Society for Therapeutic Radiology and Oncology and European Association of Nuclear Medicine. Published by Elsevier Ireland Ltd. All rights reserved. 96 (2010) 280–287

Positron emission tomography (PET) scanning is a significant advance in cancer imaging and has improved the management of patients with cancer. The most commonly used radiopharmaceutical is 2-[^{18}F]fluoro-2-D-deoxyglucose ([^{18}F]FDG). FDG-PET, especially when combined with structural imaging, such as computed tomography (CT), provides the most accurate information for staging of many common cancers. However, over the last decade more and more PET radiopharmaceuticals are entering the clinics. These include radiolabelled amino acids, nucleoside derivatives, choline derivatives, nitroimidazole derivatives, and peptides targeting a variety of different receptors. Thus, molecular imaging using PET enables the visualization of various molecular pathways in tumour biology including metabolism, proliferation, oxygen delivery, protein synthesis as well as receptor and gene expression.

PET with these radiopharmaceuticals can be used for tumour staging, for prediction of tumour response to therapy, for the detection of early recurrence, and for the evaluation of modifications in organ function after treatment [1]. PET and especially FDG-PET has also taken on increasing importance for radiation treatment planning [2]. Here it can provide additional information for target volume selection and delineation. But, not only [^{18}F]FDG may supply helpful information which may influence radiation treatment planning, for example ^{11}C-methionine is currently one of the best available PET tracer for delineating brain tumour con-

tours [3]. but also ^{18}F-fluorotethyltyrosine has potential for radiation treatment planning in patients with brain tumours [4]. For imaging prostate cancer ^{11}C- and ^{18}F-labelled choline derivatives are promising tracers [5]. Also tracers allowing non-invasive determination of the oxygen supply of the tumour are of interest for radiation treatment planning. Tracers allowing imaging of hypoxic tumour cells include [^{18}F]FMISO, [^{18}F]FAZA, and [^{64}Cu]ATSM [6]. ^{18}F-Fluorothymidine [7] is a nucleoside derivative which allows monitoring of thymidine kinase activity, a surrogate for proliferation, which may also add information to adequate radiation treatment planning (a summary of the tracers discussed is found in Table 1).

In this chapter the syntheses of a variety of different radiopharmaceuticals for PET imaging are summarized and the molecular processes which are responsible for tracer accumulation are discussed. There may be a variety of other compounds which are in preclinical testing or even in initial clinical trials or which never became a tracer with broad use in clinical routine. These compounds are not discussed in this chapter which should help in choosing the appropriate tracer for planning corresponding radiation treatment strategies.

Imaging of glucose metabolism

Accumulation mechanism and synthesis of [^{18}F]FDG

As already mentioned molecular imaging using PET has brought an additional dimension to the treatment management of cancer

---

* Address: Medizinische Universität Innsbruck, Anichstr. 35, Innsbruck, Austria.
  E-mail address: roland.haubner@i-med.ac.at

Table 1

Summary of the tracer discussed. This includes the most common tracers of each category or tracers which are already in first clinical studies. No tracers are listed which are only under preclinical development.

Molecular uptake mechanism	Tracer	Isotope	Organs of highest physiological uptake[a]	Availabiltiy
Amino acid transport and protein synthesis	Methionine	C-11	Liver, salivary glands, lachrymal glands, bone marrow, pancreas, bowels, renal cortical, urinary bladder	In-house production/cyclotron
	Fluoroethyltyrosine	F-18	Pancreas, kidneys, liver, heart, brain, colon, muscle	In-house production/cyclotron[b]
	FDOPA	F-18	Pancreas, liver, duodenum, kidneys, gallbladder, biliary duct	Commercially available
Glucose metabolism	FDG	F-18	Brain, myocardium, breast, liver, spleen stomach, intestine, kidney, urinary bladder, skeletal muscle, lymphatic tissue, bone marrow, salivary glands, thymus, uterus, ovaries, testicle, brown fat	Commercially available
Proliferation	FLT	F-18	Bone marrow, intestine, kidneys, urinary bladder, liver	In-house production/cyclotron[b]
Hypoxia	FMISO	F-18	Liver, urinary excretion	In-house production/cyclotron[b]
	FAZA	F-18	Kidneys, gallbladder, liver, colon	In-house production/cyclotron
	Cu-ATSM	Cu-64	Liver, kidneys, spleen, gallbladder[c]	In-house production/cyclotron[b]
Lipid metabolism	Choline	C-11	Liver, pancreas, spleen, salivary glands, lachrymal glands, renal excretion, bone marrow, intestine	In-house production/cyclotron
	Fluoroethylcholine	F-18	Liver, kidneys, salivary glands, urinary bladder, bone marrow, spleen	In-house production/cyclotron[b]
	Acetate	C-11	Gastrointestinal tract, prostate, bone marrow, kidneys, liver, spleen, pancreas	In-house production/cyclotron
Angiogenesis/integrin binding	Galacto-RGD	F-18	Bladder, kidneys, spleen, liver	In-house production/cyclotron
	AH111585	F-18	Bladder, liver, intestine, kidneys	In-house production/cyclotron
SSTR binding	DOTATOC	Ga-68	Pituitary and adrenal glands, pancreas, spleen, urinary bladder, liver, thyroid	In-house production/generator
	DOTATATE	Ga-68	Spleen, urinary bladder, liver	In-house production/generator

[a] Uptake ranking is from higher to lower organ activity concentration.
[b] In some countries commercially available but yet without marketing authorization.
[c] Estimated from calculations using ^{60}Cu-ATSM-PET.

patients. The most commonly used radiotracer is 2-[^{18}F]fluoro-2-D-deoxyglucose ([^{18}F]FDG), which allows to assess the metabolic state of malignant lesions. Thus, also most published radiation treatment planning studies involve [^{18}F]FDG (for review see e.g. [2]).

[^{18}F]FDG is a glucose derivative where the hydroxy function in position 2 is replaced by the radioactive fluorine isotope. The accumulation of [^{18}F]FDG (for review see e.g. [8]) is based on enhanced glycolysis, which has often been associated with the growth rate and malignancy potential of the tumour. Glucose is an important nutrient for all cells playing an essential role in the cellular energy metabolism. [^{18}F]FDG is similar as glucose transported via glucose transporters (mainly GLUT-1 and GLUT-3) into the cell and phosphorylated via hexokinase. Because of the missing hydroxy function in position 2 subsequent metabolism via G6-phosphate isomerase, as found for glucose-6-phospate, is not possible. Hence, the [^{18}F]FDG-6-phosphate is not further degraded and, additionally, due to the negative charge, can not penetrate the cell membrane leading to the trapping in the cell (for schematic presentation of the uptake mechanism see Fig. 1). Thus, [^{18}F]FDG can be used to study alterations in glucose uptake, which is a marker for the viability of cells [9].

In tumour cells glucose transport and metabolism is altered leading to an increased [^{18}F]FDG uptake compared to normal cells. One mechanism for the high glycolytic rate in tumour cells appears to be the over-expression of GLUT-1 and GLUT-3 [10] another is found in the highly active hexokinase bound to tumour mitochondria, a phenomenon which is not present in normal cells [11]. However, not only tumour cells show high [^{18}F]FDG uptake. E.g. High background glucose metabolism of normal grey matter structures results in low tumour-to-background ratios when imaging brain tu-

mours. Moreover, due to repair processes induced by reactions after therapeutic interventions, macrophages will also infiltrate the tumour showing comparable [^{18}F]FDG uptake as viable tumour cells. In one study it has been shown that a maximum of approx. 25% of the total [^{18}F]FDG uptake measured in the tumour tissue was due to uptake in macrophages and granulation tissue [12]. Moreover, it is suggested that hypoxia increases uptake of [^{18}F]FDG through activation of the glycolytic pathway (e.g. an increased expression of GLUT-1 was found in hypoxic breast cancer cells) [13]. Thus, analysis of [^{18}F]FDG PET data has to be carried out carefully also taking into account the limitations of this technique.

Based on the synthesis described by Ido et al. in 1977 [14] two different strategies have been developed. One is focused on the electrophilic fluorination of 3,4,6-triacetyl-D-glucal (TAG) using acetylhypofluorite [15]. The other introduced an aminopoly-ether-supported nucleophilic substitution of 1,3,4,6-tetracetyl-2-trifluoromethan sulfonyl-β-D-mannose [16]. Due to the higher radiochemical purity and especially higher specific activity available, in addition with the advantage of getting an epimeric pure product, the latter strategy is now the almost exclusive way of producing [^{18}F]FDG (for overview see [9]). For this process a variety of automated synthesis modules are available which allow production of high amounts of [^{18}F]FDG in high radiochemical yield (approx. 70% uncorrected) in short reaction times (approx. 30 min).

Imaging amino acids transport and protein synthesis

Available amino acid radiopharmaceuticals

Radiolabelled amino acids are well-established for tumour imaging. Although lesion detection remains an important aspect,
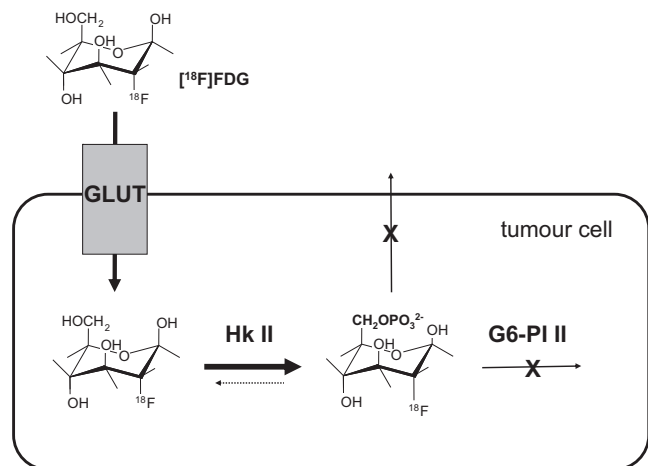
Fig. 1. Schematic presentation of the [18F]FDG uptake mechanism: [18F]FDG is transported into the cell via glucose transporters (GLUT). Mainly used transporters are GLUT-1 and GLUT-3. In the cell [18F]FDG is phosphorylated via hexokinase II (HK II). Introduction of the negative charge via the phosphate group is responsible for intracellular trapping. Due to the missing hydroxyl function at position 2′ [18F]FDG-phosphate is not tolerated by glucose-6-phosphate isomerase II (G6-PI II).

Fig. 2. Schematic presentation of amino-acid uptake mechanism: [11C]MET and [18F]FET are predominantly transported via amino acid transport (AAT) system L (leucine preferring) into the cell. Because of the isotopic labelling [11C]MET can also be incorporated into proteins. The unnatural amino acid [18F]FET is not incorporated. Despite this difference comparison of [11C]MET and [18F]FET uptake in brain tumour patients showed similar distribution patterns and tumour-to-blood ratios indicating that the rate determining step is the transport into the cell for both tracers. However, unnatural amino acids may have the advantage of improved metabolic stability avoiding problems with kinetic analysis.

there is a growing emphasis on therapy planning, evaluating response to treatment and providing prognostic information. For this purpose [11]C- as well as ^{18}F-labelled amino acid derivatives are available. A variety of amino acids have been labelled with ^{11}C-carbon. This includes the naturally occurring L-[11C]leucine [17], L-[methyl-11C]methionine ([11C]MET) [18], and L-[1-11C]tyrosine [19] as well as unnatural aliphatic (e.g. [11C]AIB) and alicyclic (e.g. [11C]ACPC) amino acids (for review see [20]). However, the most well-established ^{11}C-labelled amino acid is [11C]MET. [11C]MET can be prepared by various synthetic pathways (see e.g. [21]). All methods rely on the alkylation of the sulphide anion of L-homocysteine with either [11C]methyl iodide or [11C]methyl triflate. Variations in the synthesis routes lead only to negligible differences in e.g. specific activity as well as enantiomeric, radiochemical and chemical purity.

In contrast to ^{11}C-labelled amino acids labelling with ^{18}F-fluorine always results in unnatural amino acids. Most commonly aromatic amino acids were used for labelling with [18]F. The most well-established tracer for clinical studies are O-(2-[18F]fluoroethyl)-L-tyrosine ([18F]FET) and 3,4-dihydroxy-6-[18F]fluoro-L-phenylalanine ([18F]FDOPA). [18F]FET can be prepared either in a two-step synthesis directly from the disodiumsalt of L-tyrosine using [18F]fluoroethyltosylate as prosthetic group or via direct nucleophilic ^{18}F-fluorination of N-protected O-(2-tosyloxyethyl)-L-tyrosine in good radiochemical yields and high specific activities [22]. In contrast, [18F]FDOPA is mainly produced via electrophilic radiofluorodestannylation of N-formyl-3,4-di-tert-butoxycarbonyl-6-(trimethylstannyl)-L-phenylalanine using [18F]F$_2$ followed by acidic removal of the protecting groups [23].

Biological characteristics of amino acid-based tracer

Amino acid tracers were initially developed with the intention to measure protein synthesis rates. However, the rate of amino acid transport rather than the protein synthesis rate seems to be the major determinant of tracer uptake in tumour imaging studies (schematic uptake mechanism is presented in Fig. 2).

Tumour cells express a variety of amino acid transporters. So far the development of PET imaging agents has focused on substrates of systems L and/or A [20]. However, most tracers are transported by mo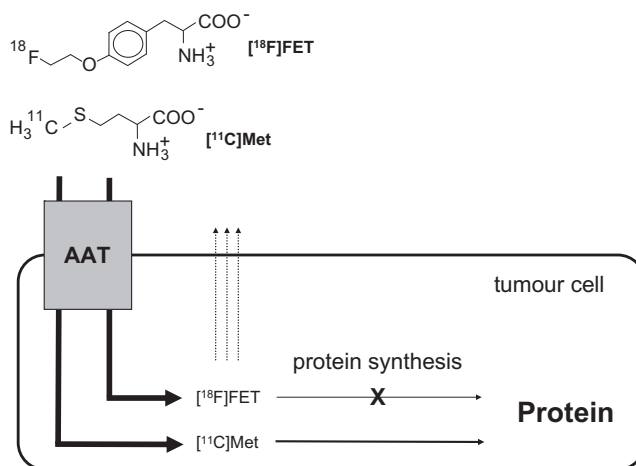re than one system as the different amino acid transport systems demonstrate an overlapping substrate specificity. For example [11C]MET is predominately transported via system L but to a lesser extent also via system A and ASC. The transport system L (leucine preferring) is sodium independent and carries amino acids with large neutral side chains. There are at least four subtypes named LAT1 to LAT4. Systems A (alanine preferring) and ASC (alanine, serine, cysteine) are sodium dependent and transport small neutral amino acids. Due to their bulky side chains the ^{18}F-labelled aromatic amino acids are preferably transported via the L-system. The modifications occurring due to the insertion of ^{18}F-fluorine are in most cases well-tolerated by this transport system. But in contrast to natural L-amino acids most fluorinated amino acids are not incorporated in proteins.

Nevertheless studies comparing [11C]MET and [18F]FET in brain tumour patients showed similar distribution patterns and similar tumour-to-blood ratios (e.g. [22]). An advantage of using unnatural instead of natural amino acids may be the improved metabolic stability of the first avoiding problems with metabolites which may decrease tumour specificity and complicate kinetic analysis. Moreover, animal studies suggest that [18F]FET, in contrast to [18F]FDG and also [11C]MET, is not accumulated in inflammatory tissue making it potentially superior for distinguishing neoplasm from inflammation [24]. The reason for the differences in the uptake of [18F]FET and [11C]MET in inflammatory tissue is not completely understood, yet. The authors discuss that the difference may be caused by a different expression of transport system subtypes.

[18F]FDOPA is a ^{18}F-labelled analogue of the naturally occurring L-DOPA and has been used extensively for evaluating the dopaminergic system in the brain. There is a physiological high uptake and retention of [18F]FDOPA in substancia nigra and striatum [25]. But it also shows high uptake in primary brain tumours due to amino acid transport. Current data suggest that FDOPA transport is mainly mediated by the L system [26]. In addition to brain tumour imaging, [18F]FDOPA has also been used for imaging extracranial tumours [27]. It was found that the enzyme aromatic amino acid decarboxylase (AADC), for which [18F]FDOPA is a substrate, is expressed in many tumours of neuroendocrine origin.

Hypoxia imaging

Available hypoxia imaging tracers

Tumour hypoxia is considered as an important factor for resistance to radiotherapy and appears to be an independent risk factor for tumour progression. Thus, imaging oxygenation of tumours is of great interest especially for radiation treatment.

At the moment, the most common PET tracers for imaging hypoxia are 1-[2-nitro-1-imidazolyl)-3-[^{18}F]fluoro-2-propanol ([^{18}F]FMISO), 1-(5-[^{18}F]fluoro-5-deoxy-α-D-arabinofuranosyl)-2-nitroimidazole ([^{18}F]FAZA) and [^{64}Cu]copper(II)-diacetyl-bis(N^4-methylthiosemicarbazone [^{64}Cu]ATSM (see also Table 2). Synthesis of the nitroimidazole derivatives [^{18}F]FMISO and [^{18}F]FAZA can be carried out via nucleophilic fluorination of 1-(2-nitro-1-imidazolyl)-2-O-tetrahydropyranyl-3-O-toluene-sulfonylpropane-diol and 1-α-D-(2,3-diacetyl-5-tosyloxy-arabinofuranosyl)-2-nitroimidazole, respectively. After ^{18}F-fluorination protection groups are removed and the corresponding product is isolated via RP-HPLC. Both tracers can be produced in high specific activity and radiochemical purity (see e.g. [28]). However, radiochemical yields are much higher for [^{18}F]FMISO (80%; decay corrected) than for [^{18}F]FAZA (20%; decay corrected).

Synthesis of [^{64}Cu]ATSM is straight forward. It can be produced by incubating cyclotron-produced ^{64}CuCl$_2$ in a buffer solution in the presence of H$_2$ATSM at room temperature within a few minutes [29]. After passing the reaction solution through a C18-SepPak cartridge the product can be obtained in high radiochemical purity. Due to the short incubation time and the loss of complex deprotection and purification steps synthesis of [^{64}Cu]ATSM is much easier and faster than synthesis of [^{18}F]FMISO and [^{18}F]FAZA. One disadvantage might be the long half-life of ^{64}Cu ($t_{1/2}$ = 12.7 h), which may result in higher radiation burden for the patient. Anyway, an investigational new drug application for [^{64}Cu]ATSM was recently approved by the FDA, paving the way for a multicenter trial validating the utility of this tracer, which may result in an FDA approval for routine clinical use.

Biological characteristics of hypoxia imaging tracer

[^{18}F]FMISO has a partition coefficient near unity indicating that it can unspecifically penetrate almost all cell membranes. Intracellular, nitroreductases can transfer an electron to the nitro group of the nitroimidazole. In normoxic cells this electron is rapidly transferred to oxygen and [^{18}F]FMISO changes back to its original structure allowing diffusion of the tracer out of the cell. When oxygen is lacking (threshold of the oxygen level is approx. 10 mm Hg), however, a second electron transfer reduces the nitroimidazole to a very reactive intermediate, which binds to proteins and RNA within the cell and therefore, becomes trapped intracellular (schematic uptake mechanism is found in Fig. 3). Thus, [^{18}F]FMISO uptake is inversely related to the intracellular partial pressure of oxygen [30]. The same mechanism mediates the accumulation of [^{18}F]FAZA by hypoxic cells. Due to the included sugar moiety [^{18}F]FAZA is more hydrophilic than [^{18}F]FMISO. This leads to a
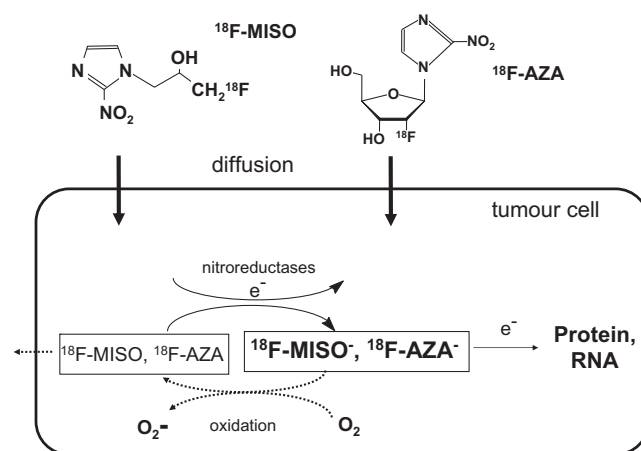

Fig. 3. Schematic presentation of [^{18}F]FMISO and [^{18}F]FAZA uptake mechanism: Both tracers enter the cell predominantly via unspecific diffusion. In the cell an electron is transferred by nitroreductases to the nitro group of the nitroimidazole ring. In normoxic cells this electron is rapidly transferred to oxygen and [^{18}F]FMISO and [^{18}F]FAZA, respectively changes back to its original structure allowing diffusion of the tracer out of the cell. In hypoxic cells no electron shift to oxygen is possible. In this case a second electron transfer reduces the nitroimidazole to a very reactive intermediate which binds to proteins and RNA within the cell and becomes trapped.

more rapid renal elimination of [^{18}F]FAZA and results in a higher contrast between hypoxic and normoxic tissues [31]. Anyway, the image quality in patient studies seems not to be this much better. Thus, at the moment most studies are carried out with the earlier established [^{18}F]FMISO. Anyway further studies including quantitative analysis of the PET-signals may demonstrate which compound is superior.

There are several proposed trapping mechanisms for [^{64}Cu]ATSM (for review see [32]). Most recent studies including chemical, electrochemical, spectroscopic and computational methods suggest a slightly revised trapping mechanism [33]. Although the mechanism of cellular-uptake is uncertain it is assumed that, based on the properties of [^{64}Cu]ATSM, cellular uptake is due to passive diffusion independent from the oxygenation status of the cell. In the cell, via an enzyme-mediated reduction, [Cu(I)ATSM]$^-$ is generated in normoxic as well as hypoxic cells. In normoxic cells, rapid and facile re-oxidation occurs resulting in the neutral Cu(II) starting complex [^{64}Cu]ATSM which can penetrate the cell membrane and thus, not only diffuse into but also out of the cell. In hypoxic cells, strongly depending on the pH, [Cu(I)ATSM]$^-$ is protonated, which results in the instable [Cu(I)-ATSMH] (in the absence of a proton source [Cu(I)ATSM]$^-$ is stable towards ligand dissociation). [Cu(I)-ATSMH] dissociates allowing interaction of Cu(I) with proteins within the cell leading to the final trapping products.

There are only very few studies which compare the capacities of [^{18}F]FMISO and [^{64}Cu]ATSM concerning monitoring the oxygenation status in the tumour. All these studies are carried out using murine tumour models. In one study using squamous cell carcinoma (SCCVII) bearing mice [^{64}Cu]ATSM uptake was unable to

Table 2
Summary of some characteristics of the mostly used hypoxia imaging PET tracers.

Tracer	Isotope	Half life	Average synthesis time[a] (min)	Average yield	Proposed uptake mechanism
FMISO	F-18	109.7 min	50–60	∼80% (decay corrected)	Second electron transfer to nitroimidazol-group under hypoxic conditions
FAZA	F-18	109.7 min	50	∼20% (decay corrected)	Second electron transfer to nitroimidazol-group under hypoxic conditions
Cu-ATSM	Cu-64	12.7 h	10–20[b]	∼95% (non decay corrected)[b]	Instability of Cu(I))-complex under hypoxic conditions

[a] Time for isotope production and lead time is not included.
[b] Estimated from the process described in Ref. [28].

predictably detect changes in hypoxia if oxygenation status was modulated whereas [18F]FMISO tumour uptake was more responsive to changes of the oxygenation status [34]. Another group [35] studied [18F]FMISO and [64Cu]ATSM uptake in rats bearing different tumours. They found for rats bearing an anaplastic prostate tumour (R3327-AT) a poor correlation between the intra-tumoural distribution if [18F]FMISO uptake 4 h p.i. is compared with [64Cu]ATSM uptake 2 h p.i. but a good correlation if [18F]FMISO uptake 4 h p.i. is compared with [64Cu]ATSM uptake 16 h p.i. This is explained with a significant temporal evolution of [64Cu]ATSM uptake between 0.5 and 20 h in this tumour type. In contrast, for rats bearing a human squamous cell carcinoma (FaDu) no differences were found. The early and the late [64Cu]ATSM microPET images were similar and in general concordant with the [18F]FMISO images. Altogether these data demonstrate the complexity of the accumulation mechanism of both tracers and indicate that further studies are needed for a final assessment.

Imaging of lipid metabolism

Available imaging probes

Choline was initially labelled with 11C-carbon, which results in the isotopic tracer. Synthesis of [11C]choline can be carried out by two different routes [36]. Both are based on the 11C-methylation of 2-(dimethylamino)-ethanol (DMAE) but uses either [11C]methyliodide or [11C]methyltriflate as precursor. Synthesis was carried out either in solution, fixed on cartridges or by loading the DMAE into a loop. Depending on the method used radiochemical yields up to 95% could be obtained. [11C]choline was found to visualize a variety of tumours including prostate cancer [37]. However, to benefit from the longer half-life 18F-labelled derivatives were developed. Labelling with 18F results in the analogue tracers [18F]fluoromethylcholine ([18F]FCH) and [18F]fluoroethylcholine ([18F]FECH; sometimes also abbreviated [18F]FCH making distinction as to which tracer is used in some studies difficult). In contrast to [11C]choline production, synthesis of [18F]FECH and [18F]FCH is a two-step process. For the synthesis of [18F]FECH [38] 2-[18F]fluoroethyl tosylate is generated via nucleophilic 18F-fluorination of 1,2-bis(toxyloxy)ethane. This is converted to [18F]FECH by dissolving 2-[18F]fluoroethyl tosylate in *N,N*-dimethylethanolamine. For this two-step synthesis the decay corrected radiochemical yield is approx. 46%. In the first step of the [18F]FCH synthesis [39] [18F]bromofluoromethane is produced via nucleophilic substitution of dibromomethane. [18F]bromofluoromethane can either be directly used for alkylation of *N,N*-dimethylethanolamine or after online conversion to [18F]fluoromethyl triflate resulting in radiochemical yields between 30% and 40%.

Radiolabelled acetate is another tracer especially used for prostate cancer imaging. Similarly to choline, the compound was labelled either with 11C resulting in the isotopic [11C]acetate ([11C]ACE) or with 18F resulting in the analogue tracer [18F]fluoroacetate ([18F]FAC). Synthesis of [11C]ACE is based on a Grignard reaction [40]. Thus, after production of [11C]CO2 the radioactive gas is bubbled through a methyl magnesium bromide solution resulting, after hydrolysis using phosphoric acid, in the desired product in radiochemical yields up to 70% [41]. [18F]FAC synthesis follows the "classical" nucleophilic 18F-fluorination pathway using ethyl *O*-mesylglycolate which is subsequently hydrolyzed with sodium hydroxide to the final product in radiochemical yields of approx. 55% [40].

Biological characteristics

In many cancers high levels of phosphorylcholine have been found, whereas in the corresponding normal tissue only low levels are found [42]. Phosphorylcholine is the first intermediate in the incorporation of choline into phospholipids by the Kennedy pathway [43]. However, whether the corresponding choline kinase reaction or an upstream transporter mainly determines tracer accumulation is currently not entirely clear. It has been demonstrated that the choline transport systems tolerate synthetic analogues. It seems that two methyl groups are essential and that the third methyl group can be replaced with longer alkyl groups [44]. Very similar results have been obtained by studying the substrate specificity of choline kinase for such analogues [45]. There it was found that besides the two methyl groups the hydroxyethyl group is also of importance. Again the third methyl group could be replaced by longer alkyl groups. All these data indicate that uptake mechanisms for [11C]choline, [18F]fluoromethylcholine, and [18F]fluoroethylcholine are quite similar [8] (schematic uptake mechanism is found in Fig. 4). However, uptake studies with PC-3 prostate cancer cells indicate higher uptake of [11C]choline and [18F]fluoromethylcholine compared with [18F]fluoroethylcholine after 2 h incubation at 37 °C [39]. In the clinical setting uptake usually plateaus within 10–20 min after injection indicating that the transport may be the rate determining step, which is confirmed by additional experimental studies suggesting that choline transport and not phosphorylation is the key step for choline uptake in cancer cells [8].

It is assumed that in the myocardium 11C-carbon labelled acetate ([11C]ACE) is quickly metabolized to [11C]CO2 via the tricarboxylic acid cycle, which is then rapidly released from the cells. In contrast, [11C]ACE has been shown to steadily accumulate in prostate cancer and other tumours. Thus, it is discussed that in cancer cells [11C]ACE enters the lipid synthesis and therefore, becomes trapped intracellularly. Fluoroacetate is a toxic compound found in the South African poison plant *Dichapetalum chymosum*. Similarly to acetate, fluoroacetate is a substrate for acetyl coenzyme A synthase, but with a lower specificity [46]. Toxicity is due to its conversion to fluorocitric acid, which is an inhibitor of the tricarboxylic acid cycle. Anyway, Ponde et al. [40] calculated that maximum [18F]FAC concentration in patients is 10^{-6} times the human LD_{50} and found in animal studies that uptake in prostate cancer is very similar to [11C]ACE. However, because of its lack of oxidative metabolism [18F]FAC shows a relatively slower clearance than [11C]ACE and is only rarely used in clinical settings.

Fig. 4. Schematic presentation of [18F]FECH and [11C]choline uptake mechanism: Both tracers are transported into the cell via choline transport systems. In the cell, choline kinase, phosphorylates the compounds resulting in the corresponding phosphorylcholine derivatives. These can further be phosphorylated and transferred to phoshatidylcholine derivatives which can finally be incorporated into the cell membrane. However, it is discussed that either the transport or the first phosphorylation is the rate determining step.

Imaging proliferation

Available imaging probes

Tumour cell proliferation has been studied with [^{11}C]thymidine and 3′-[^{18}F]fluoro-3′-deoxythymidine ([^{18}F]FLT), a thymidine analogue where the hydroxyl function in position 3′ is replaced by ^{18}F-fluorine [47]. Although imaging of tumour cell proliferation with [^{11}C]thymidine has been shown to be feasible in patients, its fast and complex metabolism and the resulting demands on the construction of corresponding input functions was an obstacle to wider acceptance as a PET radiopharmaceutical [48]. As a practical alternative [^{18}F]FLT has been developed.

Different approaches for the production of [^{18}F]FLT are described. They mainly differ in the use of the precursor, but have in common, that for the nucleophilic substitution reaction, an activation at position 3′ is necessary. For this purpose one strategy uses 2,3′-anhydrothymidine and the other 3′-O-nosylthymidine derivatives. Since hydroxyl groups are thought to decrease the nucleophilicity of the [^{18}F]fluoride all synthesis routes use 5′-protected derivatives (e.g. benzoyl or dimethoxytrityl). Grierson and Shields [49] described this by using 3-N-dimethoxybenzyl-5′-dimethoxytrityl-3′-O-nosylthymidine in a three step synthesis including nucleophilic substitution of the nosyl leaving group, removal of the protection groups by ceric ammonium nitrate and isolation of the final product by RP-HPLC. This synthesis allows production of [^{18}F]FLT within approx. 90 min in approx. 8% yield. Machulla et al. [50] used 5′-O-(4,4′-dimethoxytrityl)-2,3′-anhydrothymidine and could produce [^{18}F]FLT within 90 min in approx. 7% yield. Newer approaches use 3-N-Boc-1-[5-O-(4,4′-dimethoxytrityl)-3-O-nosyl-2-deoxy-β-D-lyxofuranosyl]thymidine [51] and can produce in a three step procedure including synthesis, deprotection (hydrochloric acid), neutralization (sodium hydroxid), and HPLC purification [^{18}F]FLT in approx. 60 min in 21 ± 4% yield (personal communications).

Biological characteristics of [^{18}F]FLT

[^{18}F]FLT enters the cell via nucleoside transporters and to a lesser extent via passive diffusion [48]. However, the rate-limiting step for [^{18}F]FLT uptake is the initial phosphorylation by thymidine kinase 1 [47] (schematic uptake mechanism is found in Fig. 5). Even further phosphorylation is possible but, based on the missing 3′-hydroxyl function, only negligible amounts are incorporated into the DNA. However, due to the negative charge of the phosphate group, it is unable to penetrate biological membranes and thus, is trapped inside the cell. There is some dephosphorylation via 5′-deoxynucleotidases, but the rate is relatively slow compared to the thymidine kinase activity. Thus, the accumulation of [^{18}F]FLT-phosphates forms the basis of [^{18}F]FLT-PET imaging.

Thymidine kinase activity is known to fluctuate during the cell cycle. It has been shown that high levels of thymidine kinase are observed during the S-phase [48], as well as in a number of rapidly proliferating and malignant cells, where enzyme expression is increased up to 15-fold with respect to normal cells.

Since uncontrolled proliferation represents a hallmark of cancer cells, there is great interest in imaging tumour cell proliferation, especially before and after therapeutic interventions [47]. However, in many common solid tumours only a rather low fraction of tumour cells is in S-phase. As a consequence, uptake of [^{18}F]FLT has been found to be markedly lower than that of [^{18}F]FDG in most solid tumours. This makes [^{18}F]FLT less-suited for tumour staging. However, it is expected that [^{18}F]FLT may play an important role in monitoring tumour response to therapy. Animal studies have repeatedly indicated that arrest of tumour cells in the G1 phase causes a rapid and marked decline in FLT uptake. Yet
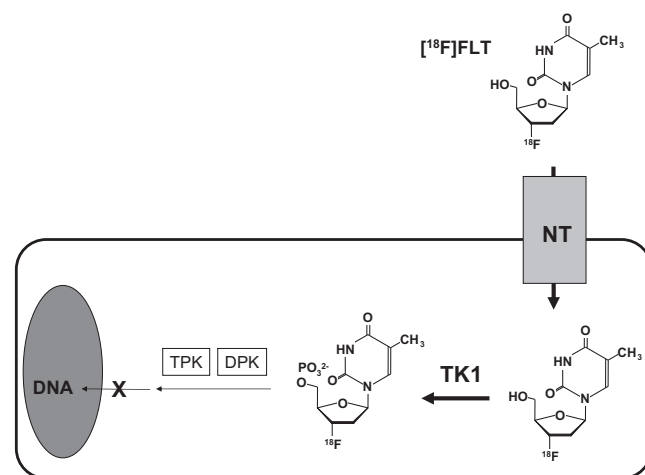
Fig. 5. Schematic presentation of [^{18}F]FLT uptake mechanism: [^{18}F]FLT enters the cell via Na$^+$-dependant active nucleoside transporters (NT) and to a lesser extent via passive diffusion. In the cell it is transformed to the monophosphate by the human thymidine kinase 1 (TK 1). Even further phosphorylation (via diphosphate kinase (DPK) and triphosphate kinase (TPK)) is possible but, based on the missing 3′-hydroxyl function, only negligible amounts are incorporated into the DNA. Thus, trapping is predominantly due to the negative charge of the phosphate group transferred under the catalysis of TK 1.

some drugs may cause a temporary increase in [^{18}F]FLT uptake. For example, chemotherapeutic agents that block thymidine synthesis have been shown to cause an activation of thymidine kinase activity and [^{18}F]FLT uptake. Further studies comparing [^{18}F]FLT with [^{18}F]FDG-PET including quantitative analysis will be important to determine the complementary advantage of both techniques in early cancer therapy response assessment.

Other imaging probes in clinical evaluation

RGD-peptides as angiogenesis marker

Angiogenesis is a complex multistep process involved in a variety of pathological processes including rheumatoid arthritis, diabetic retinopathy, psoriasis, restenosis and tumour growth [52]. Especially for the last a variety of drugs are currently developed and studied. Thus, imaging techniques allowing non-invasive monitoring of corresponding molecular processes will be of great interest for basic research as well as for planning and controlling corresponding anti-angiogenic therapies. One target structure involved in the angiogenic process is the integrin αvβ3, which mediates the migration of activated endothelial cells during vessel formation. It was found that peptides containing the amino acid sequence Arg-Gly-Asp (single letter code: RGD) bind with high affinity to this receptor (schematic binding mechanism is found in Fig. 6).

Meanwhile, a variety of radiolabelled RGD-peptides have been introduced for monitoring αvβ3 expression using nuclear medicine tracer techniques (for review see e.g. [52]). For imaging with PET peptides have been labelled with, ^{18}F-flourine, ^{68}Ga-gallium or ^{64}Cu-cupper. One class of RGD-peptides used already in clinical trials is based on the disulfide including double-bridged derivative ([^{18}F]AH111585) [53]. In an initial study including 7 breast cancer patients most of the lesions which have been detected with CT could also be identified using [^{18}F]AH111585. Moreover, it was found that [^{18}F]AH111585 is safe and metabolically stable.

Most intensively studied in preclinical as well as clinical settings is the ^{18}F-labelled glycosylated-cyclic pentapeptide [^{18}F]Galacto-RGD [54]. More than 100 patients were investigated including patients with malignant melanoma, glioblastoma, head
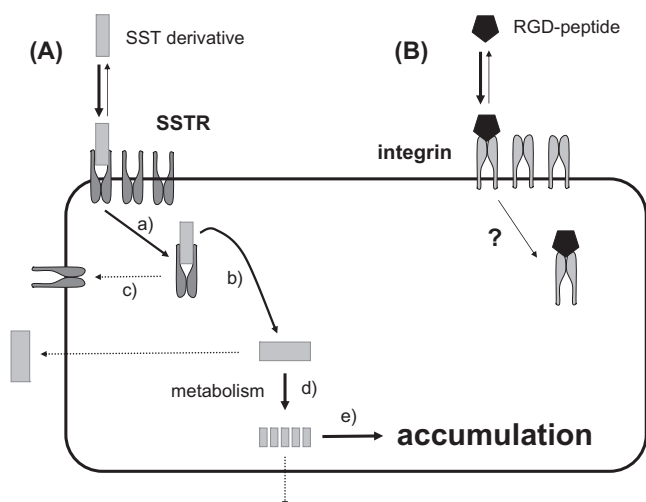
Fig. 6. Schematic presentation of uptake of radiolabelled-somatostatin derivatives and radiolabelled-RGD-peptides: (A) Somatostatin derivatives (e.g. radiolabelled DOTATOC and DOTATATE) bind to the somatosatin receptor (SSTR) and are internalized via endocytosis (a). After release of the tracer (b) the receptor can be recycled (c). The major amount of the radiolabelled somatostatin derivative is metabolized (d) resulting in fragments which can not penetrate the cell membrane (e). (B) Radiolabelled RGD-peptides bind with high affinity to the integrin (especially $\alpha v \beta 3$). It is discussed that the receptor ligand complex can also be internalized. However, at the moment corresponding studies are missing. In in vitro internalization assays only small amounts of activity are found inside the cell (see e.g. Ref. [69]). Thus, it is unclear if in vivo accumulation is mainly based on receptor-binding or internalization.

and neck cancer, breast cancer, sarcoma, non-small cell lung cancer and prostate cancer (see e.g. [55]). These studies demonstrated rapid, predominately renal tracer elimination, resulting in low background activity in almost all organs and thus, good tumour-to-background ratios. In one of these studies it has been demonstrated that tracer uptake correlates with $\alpha v \beta 3$ expression and, moreover, with vessel density of $\alpha v \beta 3$-positive vessels [55]. Metabolic stability was found high in blood samples up to 120 min after tracer injection. Tracer uptake in lesions showed great variances with SUV's ranging from 1.2 to 10.0. Moreover, great inter- as well as intra-individual heterogeneity in tracer uptake was found indicating great differences in receptor expression and thus, the importance of such imaging modalities for therapy planning and controlling. Comparison of [18F]FDG and [18F]Galacto-RGD uptake in non-small cell lung cancer but also in patients with other lesions demonstrate no correlation, confirming that different molecular mechanisms are monitored and indicating that [18F]Galacto-RGD-PET scans may supply additional helpful information about the tumour biology [56].

SSTR ligands in meningiomas

Meningiomas are the most common intracranial primary tumours, accounting for approx. 14–20% of all brain tumours in adults [57]. Surgical resection is the preferred treatment [58]. Postoperative-radiation therapy improves long-term local control and prevents tumour re-growth, especially after incomplete surgical removal. For target volume definition computed tomography and magnetic resonance imaging are the standard techniques. However, there are some limitations of these techniques for target delineation in infiltrative lesions [59]. Meningiomas show over-expression of a variety of receptors including the somatostatin-receptor subtype 2 (SSTR2) [60]. In contrast to [18F]FDG, somatostatin-receptor scintigraphy using PET showed very high meningioma-to-background ratios and may supply additional information allowing

more detailed target volume definition [61]. Somatostatin is ubiquitously distributed in the body and is an inhibitor of a variety of hormonal systems and physiological functions (schematic binding/uptake mechanism is found in Fig. 6). For the somatostatin receptor five subtypes are known. These are transmembrane domain G proteins which are over-expressed in many tumours including neuroendocrine, lung, and breast tumours [62].

A variety of radiolabelled somatostatin derivatives are described [63] including 18F- and 68Ga-labelled peptides for imaging with PET [64]. Labelling of peptides with 18F-fluorine is normally carried out via prosthetic groups implementing complex multistep processes. In contrast, labelling via 68Ga-gallium is a straightforward method producing the labelled peptide in a simple process allowing easy automatization for clinical routine production (e.g. [65]). An additional advantage is that 68Ga is produced in a commercially available generator system making its use independent from a cyclotron production. Thus, at the moment all routinely used radiolabelled somatostatin analogues for PET are labelled with 68Ga-gallium [61]. The most prominent labelling precursors are 1,4,7,10-tetraazacyclododecane-N,N′,N″,N‴-tetraacetic-acid-D-Phe^1-Tyr^3-octreotide (DOTATOC) and 1,4,7,10-tetraazacyclododecane-N,N′,N″,N‴-tetraacetic-acid-D-Phe^1-Tyr^3-octreotate (DOTATATE). Especially DOTATOC is used for diagnostic imaging with 68Ga-gallium. Two different production routes are possible. The differences are mainly found in the handling of the 68Ga-solution eluted from the generator. One strategy includes pre-concentration of the eluate using anion [66] or cation [67] exchange columns. The other approach uses fractionated elution [68]. The first approach eliminates possible 68Ge breakthrough in the pre-concentration step and is more flexible concerning reaction volume. The latter is much easier to handle but the elimination of possible 68Ge-released from the generator has to be guaranteed by additional steps. Anyway, for both production routes remote-controlled systems are commercially available allowing easy production of the corresponding 68Ga-labelled somatostatin derivatives.

References

[1] Rohren EM, Turkington TG, Coleman RE. Clinical applications of PET in oncology. Radiology 2004;231:305–32.

[2] Gregoire V, Haustermans K, Geets X, Roels S, Lonneux M. PET-based treatment planning in radiotherapy: a new standard? J Nucl Med 2007;48:68S–77S.

[3] Geets X, Daisne JF, Gregoire V, Hamoir M, Lonneux M. Role of 11-C-methionine positron emission tomography for the delineation of the tumor volume in pharyngo-laryngeal squamous cell carcinoma: comparison with FDG-PET and CT. Radiother Oncol 2004;71:267–73.

[4] Weber WA, Wester HJ, Grosu AL, Herz M, Dzewas B, Feldmann HJ, et al. O-(2-[18F]Fluoroethyl)-L-tyrosine and L-[methyl-11C]methionine uptake in brain tumours: initial results of a comparative study. Eur J Nucl Med 2000;27:542–9.

[5] Picchio M, Crivellaro C, Giovacchini G, Gianolli L, Messa C. PET-CT for treatment planning in prostate cancer. Q J Nucl Med Mol Imaging 2009;53:245–68.

[6] Padhani A. PET imaging of tumour hypoxia. Cancer Imaging 2006;6:S117–121.

[7] Bading JR, Shields AF. Imaging of cell proliferation: status and prospects. J Nucl Med 2008;49:64S–80S.

[8] Plathow C, Weber WA. Tumor cell metabolism imaging. J Nucl Med 2008;49:43S–63S.

[9] Yu S. Review of F-18-FDG synthesis and quality control. Biomed Imaging Interv J 2006;2:e57.

[10] Yamamoto T, Seino Y, Fukumoto H, Koh G, Yano H, Inagaki N, et al. Over-expression of facilitative glucose transporter genes in human cancer. Biochem Biophys Res Commun 1990;170:223–30.

[11] Arora KK, Fanciulli M, Pedersen PL. Glucose phosphorylation in tumor cells. Cloning, sequencing, and overexpression in active form of a full-length cDNA encoding a mitochondrial bindable form of hexokinase. J Biol Chem 1990;265:6481–8.

[12] Kubota R, Yamada S, Kubota K, Ishiwata K, Tamahashi N, Ido T. Intratumoral distribution of fluorine-18-fluorodeoxyglucose in vivo: high accumulation in macrophages and granulation tissues studied by microautoradiography. J Nucl Med 1992;33:1972–80.

[13] Buck AK, Schirrmeister H, Mattfeldt T, Reske SN. Biological characterisation of breast cancer by means of PET. Eur J Nucl Med Mol Imaging 2004;31:S80–7.

[14] Ido T, Wan CN, Fowler JS, Wolf AP. Fluorination with F2-2. A convenient synthesis of 2-FDG. J Org Chem 1977;42:2341–2.

[15] Bida GT, Satyamurthy N, Barrio JR. The synthesis of 2-[F-18]fluoro-2-deoxy-D-glucose using glycals: a reexamination. J Nucl Med 1984;25:1327–34.

[16] Hamacher K, Coenen HH, Stocklin G. Efficient stereospecific synthesis of no-carrier-added 2-[18F]-fluoro-2-deoxy-D-glucose using aminopolyether supported nucleophilic substitution. J Nucl Med 1986;27:235–8.

[17] Hawkins RA, Huang SC, Barrio JR, Keen RE, Feng D, Mazziotta JC, et al. Estimation of local cerebral protein synthesis rates with L-[1-11C]leucine and PET: methods, model, and results in animals and humans. J Cereb Blood Flow Metab 1989;9:446–60.

[18] Kubota K, Yamada K, Fukada H, Endo S, Ito M, Abe Y, et al. Tumor detection with carbon-11-labelled amino acids. Eur J Nucl Med 1984;9:136–40.

[19] Pruim J, Willemsen AT, Molenaar WM, van Waarde A, Paans AM, Heesters MA, et al. Brain tumors: L-[1-C-11]tyrosine PET for visualization and quantification of protein synthesis rate. Radiology 1995;197:221–6.

[20] McConathy J, Goodman MM. Non-natural amino acids for tumor imaging using positron emission tomography and single photon emission computed tomography. Cancer Metastasis Rev 2008;27:555–73.

[21] Del Fiore G, Schmitz P, Plenevaux A, Lemaire C, Aerts J, Luxen A. Fast routine production of l-[11C-methyl]methionine with Al2O3/KF in a disposable unit. J Labelled Compd Radiopharm 1995;37:746–8.

[22] Langen KJ, Hamacher K, Weckesser M, Floeth F, Stoffels G, Bauer D, et al. O-(2-[18F]Fluoroethyl)-L-tyrosine: uptake mechanisms and clinical applications. Nucl Med Biol 2006;33:287–94.

[23] Fuchtner F, Zessin J, Mading P, Wust F. Aspects of 6-[18F]fluoro-L-DOPA preparation. Deuterochloroform as a substitute solvent for Freon 11. Nuklearmedizin 2008;47:62–4.

[24] Rau FC, Weber WA, Wester HJ, Herz M, Becker I, Kruger A, et al. O-(2-[(18F]Fluoroethyl)-L-tyrosine (FET): a tracer for differentiation of tumour from inflammation in murine lymph nodes. Eur J Nucl Med Mol Imaging 2002;29:1039–46.

[25] Barrio JR, Huang SC, Phelps ME. Biological imaging and the molecular basis of dopaminergic diseases. Biochem Pharmacol 1997;54:341–8.

[26] Stout DB, Huang SC, Melega WP, Raleigh MJ, Phelps ME, Barrio JR. Effects of large neutral amino acid concentrations on 6-[F-18]Fluoro-L-DOPA kinetics. J Cereb Blood Flow Metab 1998;18:43–51.

[27] Sundin A, Garske U, Orlefors H. Nuclear imaging of neuroendocrine tumours. Best Pract Res Clin Endocrinol Metab 2007;21:69–85.

[28] Sorger D, Patt M, Kumar P, Wiebe LI, Barthel H, Seese A, et al. [18F]Fluoroazomycinarabinofuranoside (18FAZA) and [18F]Fluoromisonidazole (18FMISO): a comparative study of their selective uptake in hypoxic cells and PET imaging in experimental rat tumors. Nucl Med Biol 2003;30:317–26.

[29] Dehdashti F, Grigsby PW, Lewis JS, Laforest R, Siegel BA, Welch MJ. Assessing tumor hypoxia in cervical cancer by PET with 60Cu-labeled diacetyl-bis(N4-methylthiosemicarbazone). J Nucl Med 2008;49:201–5.

[30] Padhani AR, Krohn KA, Lewis JS, Alber M. Imaging oxygenation of human tumours. Eur Radiol 2007;17:861–72.

[31] Piert M, Machulla HJ, Picchio M, Reischl G, Ziegler S, Kumar P, et al. Hypoxia-specific tumor imaging with 18F-fluoroazomycin arabinoside. J Nucl Med 2005;46:106–13.

[32] Vavere AL, Lewis JS. Cu-ATSM: a radiopharmaceutical for the PET imaging of hypoxia. Dalton Trans 2007:4893–902.

[33] Holland JP, Barnard PJ, Collison D, Dilworth JR, Edge R, Green JC, et al. Spectroelectrochemical and computational studies on the mechanism of hypoxia selectivity of copper radiopharmaceuticals. Chemistry 2008;14:5890–907.

[34] Matsumoto K, Szajek L, Krishna MC, Cook JA, Seidel J, Grimes K, et al. The influence of tumor oxygenation on hypoxia imaging in murine squamous cell carcinoma using [64Cu]Cu-ATSM or [18F]Fluoromisonidazole positron emission tomography. Int J Oncol 2007;30:873–81.

[35] O'Donoghue JA, Zanzonico P, Pugachev A, Wen B, Smith-Jones P, Cai S, et al. Assessment of regional tumor hypoxia using 18F-fluoromisonidazole and 64Cu(II)-diacetyl-bis(N4-methylthiosemicarbazone) positron emission tomography: Comparative study featuring microPET imaging, Po2 probe measurement, autoradiography, and fluorescent microscopy in the R3327-AT and FaDu rat tumor models. Int J Radiat Oncol Biol Phys 2005;61:1493–502.

[36] Reischl G, Bieg C, Schmiedl O, Solbach C, Machulla HJ. Highly efficient automated synthesis of [(11)C]choline for multi dose utilization. Appl Radiat Isot 2004;60:835–8.

[37] Emonds KM, Swinnen JV, Mortelmans L, Mottaghy FM. Molecular imaging of prostate cancer. Methods 2009;48:193–9.

[38] Hara T, Kosaka N, Kishi H. Development of (18)F-fluoroethylcholine for cancer imaging with PET: synthesis, biochemistry, and prostate cancer imaging. J Nucl Med 2002;43:187–99.

[39] DeGrado TR, Baldwin SW, Wang S, Orr MD, Liao RP, Friedman HS, et al. Synthesis and evaluation of (18)F-labeled choline analogs as oncologic PET tracers. J Nucl Med 2001;42:1805–14.

[40] Ponde DE, Dence CS, Oyama N, Kim J, Tai YC, Laforest R, et al. 18F-Fluoroacetate: a potential acetate analog for prostate tumor imaging – in vivo evaluation of 18F-fluoroacetate versus 11C-acetate. J Nucl Med 2007;48:420–8.

[41] Moerlein SM, Gaehle GG, Welch MJ. Robotic preparation of Sodium Acetate C 11 Injection for use in clinical PET. Nucl Med Biol 2002;29:613–21.

[42] de Certaines JD, Larsen VA, Podo F, Carpinelli G, Briot O, Henriksen O. In vivo 31P MRS of experimental tumours. NMR Biomed 1993;6:345–65.

[43] Shindou H, Shimizu T. Acyl-CoA:lysophospholipid acyltransferases. J Biol Chem 2009;284:1–5.

[44] Deves R, Krupka RM. The binding and translocation steps in transport as related to substrate structure. A study of the choline carrier of erythrocytes. Biochim Biophys Acta 1979;557:469–85.

[45] Clary GL, Tsai CF, Guynn RW. Substrate specificity of choline kinase. Arch Biochem Biophys 1987;254:214–21.

[46] Patel SS, Walt DR. Substrate specificity of acetyl coenzyme A synthetase. J Biol Chem 1987;262:7132–4.

[47] Buck AK, Herrmann K, Shen C, Dechow T, Schwaiger M, Wester HJ. Molecular imaging of proliferation in vivo: positron emission tomography with [18F]fluorothymidine. Methods 2009;48:205–15.

[48] Barwick T, Bencherif B, Mountz JM, Avril N. Molecular PET and PET/CT imaging of tumour cell proliferation using F-18 fluoro-L-thymidine: a comprehensive evaluation. Nucl Med Commun 2009;30:908–17.

[49] Grierson JR, Shields AF. Radiosynthesis of 3′-deoxy-3′-[(18)F]fluorothymidine: [(18)F]FLT for imaging of cellular proliferation in vivo. Nucl Med Biol 2000;27:143–56.

[50] Machulla HJ, Blocher A, Kuntzsch M, Piert M, Wei R, Grierson JR. Simplified labeling approach for synthesizing 3′-deoxy-3′-[18F]fluorothymidine ([18F]FLT). J Radioanal Nucl Chem 2000;243:843–6.

[51] Martin SJ, Eisenbarth JA, Wagner-Utermann U, Mier W, Henze M, Pritzkow H, et al. A new precursor for the radiosynthesis of [18F]FLT. Nucl Med Biol 2002;29:263–73.

[52] Haubner R, Decristoforo C. Radiolabelled RGD peptides and peptidomimetics for tumour targeting. Front Biosci 2009;14:872–86.

[53] Kenny LM, Coombes RC, Oulie I, Contractor KB, Miller M, Spinks TJ, et al. Phase I trial of the positron-emitting Arg-Gly-Asp (RGD) peptide radioligand 18F-AH111585 in breast cancer patients. J Nucl Med 2008;49:879–86.

[54] Haubner R, Weber WA, Beer AJ, Vabuliene E, Reim D, Sarbia M, et al. PLoS Med 2005;2:e70.

[55] Beer AJ, Haubner R, Sarbia M, Goebel M, Luderschmidt S, Grosu AL, et al. Positron emission tomography using [18F]Galacto-RGD identifies the level of integrin alpha(v)beta3 expression in man. Clin Cancer Res 2006;12:3942–9.

[56] Beer AJ, Lorenzen S, Metz S, Herrmann K, Watzlowik P, Wester HJ, et al. Comparison of integrin alphaVbeta3 expression and glucose metabolism in primary and metastatic lesions in cancer patients: a PET study using 18F-galacto-RGD and 18F-FDG. J Nucl Med 2008;49:22–9.

[57] Norden AD, Drappatz J, Wen PY. Advances in meningioma therapy. Curr Neurol Neurosci Rep 2009;9:231–40.

[58] Campbell BA, Jhamb A, Maguire JA, Toyota B, Ma R. Meningiomas in 2009: controversies and future challenges. Am J Clin Oncol 2009;32:73–85.

[59] Gehler B, Paulsen F, Oksuz MO, Hauser TK, Eschmann SM, Bares R, et al. Radiat Oncol 2009;4:56.

[60] Henze M, Schuhmacher J, Hipp P, Kowalski J, Becker DW, Doll J, et al. PET imaging of somatostatin receptors using [68GA]DOTA-D-Phe1-Tyr3-octreotide: first results in patients with meningiomas. J Nucl Med 2001;42:1053–6.

[61] Khan MU, Khan S, El-Refaie S, Win Z, Rubello D, Al-Nahhas A. Clinical indications for Gallium-68 positron emission tomography imaging. Eur J Surg Oncol 2009;35:561–7.

[62] Froidevaux S, Eberle AN. Somatostatin analogs and radiopeptides in cancer therapy. Biopolymers 2002;66:161–83.

[63] Reubi JC, Maecke HR. Peptide-based probes for cancer imaging. J Nucl Med 2008;49:1735–8.

[64] Goldsmith SJ. Update on nuclear medicine imaging of neuroendocrine tumors. Future Oncol 2009;5:75–84.

[65] Decristoforo C, Knopp R, von Guggenberg E, Rupprich M, Dreger T, Hess A, et al. A fully automated synthesis for the preparation of 68Ga-labelled peptides. Nucl Med Commun 2007;28:870–5.

[66] Meyer GJ, Macke H, Schuhmacher J, Knapp WH, Hofmann M. 68Ga-labelled DOTA-derivatised peptide ligands. Eur J Nucl Med Mol Imaging 2004;31:1097–104.

[67] Asti M, De Pietri G, Fraternali A, Grassi E, Sghedoni R, Fioroni F, et al. Validation of (68)Ge/(68)Ga generator processing by chemical purification for routine clinical application of (68)Ga-DOTATOC. Nucl Med Biol 2008;35:721–4.

[68] Breeman WA, de Jong M, de Blois E, Bernard BF, Konijnenberg M, Krenning EP. Radiolabelling DOTA-peptides with 68Ga. Eur J Nucl Med Mol Imaging 2005;32:478–85.

[69] Decristoforo C, Hernandez Gonzalez I, Carlsen J, Rupprich M, Huisman M, Virgolini I, et al. 68 Ga- and 111In-labelled DOTA-RED peptides for imaging of avb3 integrin expression. Eur J Nucl Med Mol Imaging 2008;35:1507–15.

Review

PET/CT (and CT) instrumentation, image reconstruction and data transfer for radiotherapy planning

Bernhard Sattler [a,*], John A. Lee [b], Markus Lonsdale [c], Emmanuel Coche [d]

[a] Department of Nuclear Medicine, University Hospital Leipzig, Germany; [b] Molecular Imaging and Experimental Radiotherapy, Université catholique de Louvain, Brussels, Belgium; [c] Department of Clinical Physiology & Nuclear Medicine, Bispebjerg Hospital, Copenhagen, Denmark; [d] Radiology Department, Université Catholique de Louvain, Brussels, Belgium

ARTICLE INFO

ABSTRACT

The positron emission tomography in combination with CT in hybrid, cross-modality imaging systems (PET/CT) gains more and more importance as a part of the treatment-planning procedure in radiotherapy. Positron emission tomography (PET), as a integral part of nuclear medicine imaging and non-invasive imaging technique, offers the visualization and quantification of pre-selected tracer metabolism. In combination with the structural information from CT, this molecular imaging technique has great potential to support and improve the outcome of the treatment-planning procedure prior to radiotherapy. By the choice of the PET-Tracer, a variety of different metabolic processes can be visualized. First and foremost, this is the glucose metabolism of a tissue as well as for instance hypoxia or cell proliferation. This paper comprises the system characteristics of hybrid PET/CT systems. Acquisition and processing protocols are described in general and modifications to cope with the special needs in radiooncology. This starts with the different position of the patient on a special table top, continues with the use of the same fixation material as used for positioning of the patient in radiooncology while simulation and irradiation and leads to special processing protocols that include the delineation of the volumes that are subject to treatment planning and irradiation (PTV, GTV, CTV, etc.). General CT acquisition and processing parameters as well as the use of contrast enhancement of the CT are described. The possible risks and pitfalls the investigator could face during the hybrid-imaging procedure are explained and listed. The interdisciplinary use of different imaging modalities implies a increase of the volume of data created. These data need to be stored and communicated fast, safe and correct. Therefore, the DICOM-Standard provides objects and classes for this purpose (DICOM RT). Furthermore, the standard DICOM objects and classes for nuclear medicine (NM, PT) and computed tomography (CT) are used to communicate the actual image data created by the modalities. Care must be taken for data security, especially when transferring data across the (network-) borders of different hospitals.

Overall, the most important precondition for successful integration of functional imaging in RT treatment planning is the goal orientated as well as close and thorough communication between nuclear medicine and radiotherapy departments on all levels of interaction (personnel, imaging protocols, GTV delineation, and selection of the data transfer method).

© 2010 European Society for Therapeutic Radiology and Oncology and European Association of Nuclear Medicine. Published by Elsevier Ireland Ltd. All rights reserved. 96 (2010) 288–297

PET system characteristics

Positron Emission Tomography (PET), as an integral part of nuclear medicine imaging, is a non-invasive imaging technique offering the visualization and quantification of pre-selected tracer metabolism [1]. The design concepts of PET systems are discussed in detail in [2]. All commercial PET systems today come as a full-ring arrangement of detector blocks [3] or curved pixelar arrays [4], both covering an axial imaging range of up to 23 cm. The scintillators-of-choice are LSO, or LYSO, and GSO [5,6], offering a higher light output and shorter decay times, thus leading to overall improved count rate statistics compared to BGO-based PET systems. Over the past decade PET tomographs have become 3D-only [2], which is synonymous with a fivefold increase in volume sensitivity over conventional 2D-PET systems with inter-plane septa. State-of-the-art PET systems offer a point source sensitivity of ∼3% at a spatial resolution of ∼4 mm. Both values can be improved

* Corresponding author. Address: University Hospital Leipzig, Department of Nuclear Medicine, Liebigstrasse 18, 04103 Leipzig, Germany.
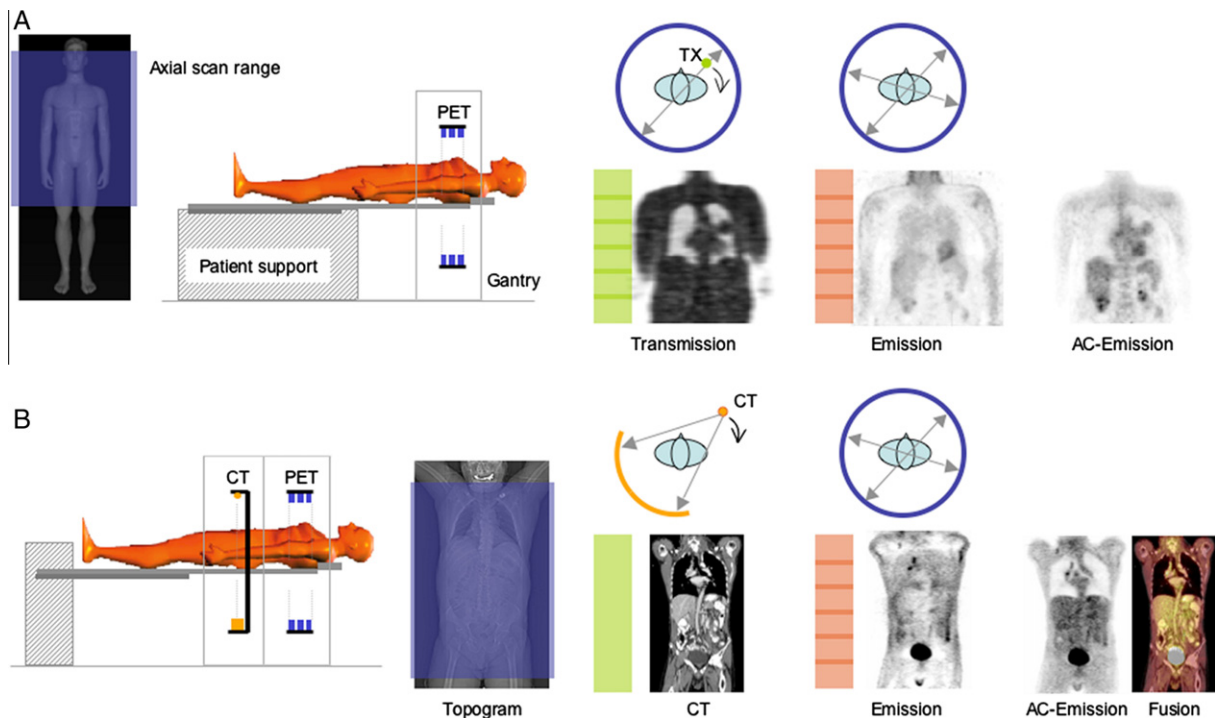E-mail address: bernhard.sattler@medizin.uni-leipzig.de (B. Sattler).

Fig. 1. PET (A) and PET/CT (B) system design and imaging protocol. (A) PET transmission and emission scanning are performed consecutively and stepwise for a pre-defined number of bed positions. The transmission data are used for attenuation and scatter correction (AC) of the emission data. Total scan time is about 30 min at 3/1 min for emission/transmission per bed and 7 bed positions. (B) In combined PET/CT imaging the standard PET transmission scan is replaced by a single, continuous spiral CT scan and the total examination time is shortened to about 20 min for the same co-axial scan range. The CT images are used for AC of the emission data. Courtesy Thomas Beyer, PhD (cmi-experts GmbH, Zurich, CH).

with dedicated brain-PET systems (5.6% and 2.1 mm, respectively), neither of these are, however, available in combined PET/CT systems.

Combined PET/CT have started to replace stand-alone PET devices [7]; today about 75% of all PET systems installed in Europe are PET/CT. Fig. 1 shows the design of combined PET/CT systems and the corresponding workflow. Standard PET/CT acquisition protocols will be discussed below. Here we limit the review to specific design concepts of the combined system.

All PET/CT systems for clinical use combine a whole-body PET and a standard, clinical multi-slice CT within a single gantry. Various design concepts exist (Fig. 2), all aiming at reducing footprint and bringing the PET and CT components as close together as possible. However, despite early efforts on a fully integrated emission-CT system [8] no fully integrated, single-detector PET/CT exists today. Thus, the centres of the fields-of-view of the CT and the PET are axially displaced by up to 85 cm. Still, by using a joint, dedicated patient-positioning system that is installed at the front of the PET/CT gantry, the patients can be positioned accurately and reproducibly for co-axial imaging ranges up to 195 cm. Reports on three-dimensional displacements between CT and PET along the co-axial imaging

range indicate a maximum displacement error of 0.5 mm [9]. Thus, combined PET/CT offers the best possible intra-patient co-registration of complementary anatomical and functional images.

Further considerations apply to PET/CT-guided radiation therapy planning (RTP). The patients scheduled for RTP can be positioned on a flat radiation therapy pallet that is mounted easily on the top of the PET/CT patient pallet (Fig. 3B). This allows employing additional positioning aids, such as a breast board, a pre-labeled vacuum lock for abdominal scans or a thermoplastic head mask, the same positioning means to be used during the actual radiation treatment of the patient (Fig. 3B). A dedicated RT laser system can be installed in front of the PET/CT gantry to ensure proper positioning of the patient based on the pre-defined markers (follow-up scans), or to define the isocentre if the patient is imaged pre-therapy on the PET/CT (Fig. 3A). Recently big-bore PET/CT systems have been introduced with an increased bore diameter adapted to more versatile radiation therapy treatment planning to ensure adequate and reproducible patient positioning using all standard RT-positioning aids during the diagnostic, pre-treatment PET/CT examination (Fig. 3D). Table 1 summarizes recent advances in PET technology that are available exclusively in combined PET/CT systems [7].

Fig. 2. Novel designs of PET/CT systems by the major vendors, fully integrating the time-of-flight technology and larger axial fields-of-view, improving the patient's comfort and thus providing a wider spectrum of applicability. Courtesy Thomas Beyer, PhD (cmi-experts GmbH, Zurich, CH).
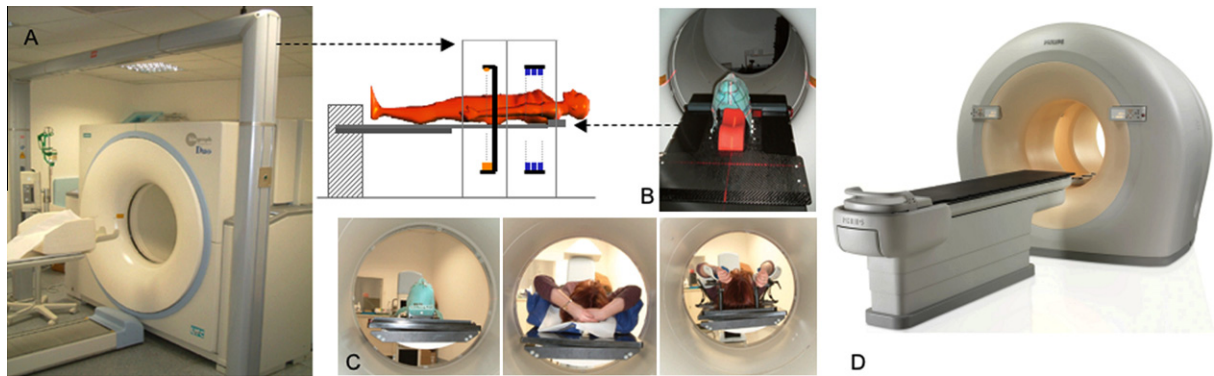
Fig. 3. PET/CT adaptations to radiation oncology applications. (A) RT laser bridge installation in front of the combined gantry, (B) patient support system with flat, carbon-fiber RT-pallet attached, (C) as in (B) with additional thermoplastic head restraint, vacuum lock bag and breast board (from left to right) and (D) dedicated, big-bore PET/CT with an 85-cm gantry opening (Philips Healthcare Systems). Courtesy Thomas Beyer, PhD (cmi-experts GmbH, Zurich, CH).

Table 1
Recent advances in PET technology and impact on PET/CT-guided patient management in radiation oncology.

Technical and methodological advance	Objective	Consequence	Importance for PET/CT-guided RTP
New crystal materials	LSO and LYSO replace BGO and GSO ↑ light output ↓ response/dead time	↓ scan time ↑ patient comfort	↓ involuntary motion artifacts ↑ diagnostic confidence
Fast detector electronics	Timing resolution < 600 ps; measure coincidence time differences (time-of-flight [95])	↑ signal-to-noise ratio in PET images (more prominent for large patients)	↑ diagnostic confidence
Smaller detector size	From 6×6 mm^2 to 4×4 mm^2 face area; improved spatial resolution	↓ partial volume effects ↑ quantification	↑ therapy response assessment ↑ diagnostic confidence
Retrospective correction for point spread function (PSF)	Account for variable image resolution inside active field-of-view	Gain uniform image resolution (<detector element size) ↑ image quality	↑ therapy response assessment ↑ diagnostic confidence
Extended axial field-of-view	Added additional layer of PET detectors in *z*-direction	↑ volume sensitivity ↓ scan time	↓ involuntary motion artifacts
Large bore diameter	Extending from 68 to 85 cm with corresponding increase in transverse FOV	Position patients in treatment-planning position; no truncation artifacts	↑ co-registration of planning PET/CT and treatment delivery
Gating	Respiratory and cardiac gating for CT and PET (synced) available	↓ motion artifacts ↑ co-registration accuracy and attenuation correction	↑ therapy planning

PET/CT acquisition and processing parameters

Standard PET/CT imaging protocol

Most PET/CT imaging protocols today involve so-called whole-body FDG-PET and CT examinations covering the same co-axial imaging range. CT images acquired during PET/CT will not be used only as a locator and for attenuation correction but – under appropriate boundary conditions – also as a diagnostic tool. The use of intravenous contrast medium in PET/CT optimizes the patient's imaging work-up, characterizes lesions and highlights occult lesions in some situations. Some findings such as pulmonary embolism will be discovered incidentally in approximately 4% of oncologic patients and probably missed if the examinations are not systematically reviewed by radiologists [10]. If a contrast-enhanced full dose CT is performed it should always be read by a radiologist or CT-trained nuclear medicine physician or a radiation oncologist. The CT part of the PET/CT, especially if carried out as diagnostic CT (high mAs, contrast media injection), requires specific skills in radiology. For this reason, in these cases, a final report performed side-by-side by the nuclear medicine physician and the radiologist is mandatory. International protocol guidelines were drafted by a consortium of experienced PET and PET/CT users [11] and are being adopted locally [12]. Recently, the EANM Guideline "FDG-PET and PET/CT: EANM procedure guidelines for tumour PET imaging: version 1.0" has been published [13]. These imaging guidelines are aimed at standardizing FDG-PET and -PET/CT imaging for general whole body imaging, which has been shown to be

superior in TNM staging when compared to stand-alone CT and PET imaging of the same co-axial imaging range [14]. This superiority, however, can be explored only when PET/CT image artifacts are minimized, and accurate quantification of CT and PET results following CT-based attenuation correction [15] is ensured. Therefore, all steps of the PET/CT-imaging procedure (patient preparation and positioning – scout scan – CT acquisition – PET acquisition – data processing and reconstruction – image analysis and reporting) have to be monitored and retrospective adjustments have to be considered where needed ([16,17], Tables 2 and 3). The software shipped with modern PET/CT systems often includes several reconstruction algorithms [18,19] and each of them involves many parameters and options, such as the data corrections, the reconstruction mode (2D, 3D to 2D rebinning, 3D), time-of-flight reconstruction [20–23] or classical sinogram-based reconstruction [18]. Data corrections for decay, scatter, attenuation, dead time, depth of interaction, non-colinearity should always be performed when they are applicable and available [24]. Reconstruction algorithms can be either analytic or iterative [18,19]. Thanks to their statistical approach, modern iterative reconstruction algorithms are less prone to artifacts than analytic reconstruction [18,25]. In contrast, quantification accuracy is still better with algebraic reconstruction [18,26]. The main parameters of reconstruction algorithms are the matrix size (or equivalently the voxel size) and the regularization scheme. The latter controls the signal-to-noise ratio of the images and encompasses the filter settings in analytic reconstruction (e.g., in filtered backprojection)

Table 2
CT acquisition recommendations (adapted from [46]).

Tumour location		Brain	Neck	Chest	Abdomen
Patient Preparation	Food cautions[a]	Diet (3 h)	Diet (3 h)	Diet (3 h)	Diet (3 h)
	Bowel opacification	No	No	Usually not[b]	500 ml water + 10 mL gastrografin (1 h before CT) or negative contrast agent
Patient position		Supine/head first	Supine/head first	Supine/head first	Supine/head first
Contrast medium injection	Contrast medium	300–350 mg l/mL	300–350 mg l/mL	300–350 mg l/mL	300–350 mg l/mL
	First injection	60 mL, 1 mL/s	60 mL, 1 mL/s	70 mL, 2 mL/s	120 mL, 2.5 mL/s
	Delay	3 min	3 min	–	–
	Second injection[c]	50 mL, 1.5 mL/s	50 mL, 1.5 mL/s	–	–
	Start of acquisition	End of snd injection	End of snd injection	35 s after 1st injection	70 s after first injection
CT acquisition parameters	Volume of investigation	Top of the vertex to C1	Skull base down to sternum	Lung apices down to the diaphragm	Diaphragm down to pubic symphysis
	Collimation[d]	$N \times 0.75$ mm	$N \times 1.5$ mm	$N \times 1.5$ mm	$N \times 1.5$ mm
	Slice thickness	3–5 mm	2–3 mm	3–5 mm	3–5 mm
	Slice increment	Continuous	Continuous	Continuous	Continuous
	Pitch[e]	1	1	1	1
	Rotation time	0.75–1 s	0.75–1 s	0.75–1 s	0.75–1 s
	mAs[f]	250	250–300	150	250
	X-ray tube voltage	120	120	120	120
	Resolution matrix	512×512	512×512	512×512	512×512
	FOV	240 mm	320 mm	500 mm	500 mm
	Reconstruction filter	Soft tissue	Soft tissue	Soft/lung tissue	Soft tissue

[a] Fasting prior the examination is not essential. It is recommended if intravenous contrast medium is given.
[b] Glass of gastrografin or water just before CT acquisition if oesophageal or upper GI tumour.
[c] Two injections are proposed: first for tissue impregnation, second for vessel opacification.
[d] N refers to the number of detectors: N = 16 if a 16-slice CT is employed.
[e] Pitch: a pitch > to 1 can be selected if the area of interest is too large to cover with the desired collimation.
[f] mAs: absolute values of mAs cannot be recommended in view of significant differences in operating characteristics between CT scanners. The values are given as indicators (from B-16 CT, Philips Medical Systems, OH, USA).

Table 3
FDG-oncology-PET/CT acquisition recommendations (adapted from [16]).

Body part	Whole body	Thorso	Head–neck	Brain
Patient preparation	No meals on day of PET, only tea without sugar, glucose level check, application of tracer (activity according to body weight-dependent reference values) 60–90 min prior to PET/CT scan, if needed usage of flat table top and fixation of the patient with fixation material (mask, fixator, see Fig. 4b and c) prepared by radiooncology staff			
Patient position	Supine	Supine	Supine	Supine
CT	Topogram, low-dose (for attenuation correction, anatomical landmarking) or full dose (attenuation correction, full diagnostic radiology reading) CT according to Table 2			
Beds positions	Number of beds according to CT-Topogram (up to 9 each), torso and legs separately 2–4 min per bed	Number of beds according to CT-Topogram (up to 9), 2–3 min per bed	Number of beds according to CT-Topogram (up to 3), 5–8 min per bed	One bed position according to CT-Topogram10 min
Matrix	128×128	128×128	256×256	128×128
Acquisition mode	3D, static	3D, static	3D, static	3D, static, dynamic[a]
Reconstruction	Iterative (2 iteration 8 subsets, 5 mm Gaussian or Hanning filter)	Iterative (2 iteration 8 subsets, 5 mm Gaussian or Hanning filter)	Iterative (4 iteration 8 subsets, 3 mm Gaussian or Hanning filter)	Iterative (10 iteration 16 subsets, 3–4 mm Hanning filter), zoom 1.5–2

[a] Some times it is necessary to follow the tracer kinetics in the brain. Thus, a dynamic protocol must be followed. The PET-acquisition protocol then consists of several time frames (f.i. 3 × 5 min) and starts earlier with respect to the number of frames. To yield a static image, the frames can be added (with decay correction) thereafter.

[18]. In iterative reconstruction algorithms, regularization is more complex and the signal-to-noise ratio depends on the number of iterations, the data fractionation (e.g., subsets in ordered subset expectation maximization [27]), and image smoothing (e.g., blob-based reconstruction [28,29] or Gaussian smoothing after each or all iterations). It is noteworthy that the reconstruction algorithm can influence the resolution of the images [30]. For instance, heavy smoothing blurs the images. The choice of a reconstruction algorithm and the adjustment of its parameters lead to a tradeoff that can influence the presence of artifacts, the signal-to-noise ratio, the resolution, the quantification accuracy, and the reconstruction time. Depending on the purpose of the images, it can be useful to optimize the reconstruction protocol. For instance, good quantification is important in SUV evaluation. Similarly, high resolution makes partial volume effect easier to correct for and is the key of accurate target delineation [31–35]. For heterogeneity assessment [36] and dose painting [37], a balance between high resolution and high signal-to-noise ratio must be found. The outcome of all these applications can be jeopardized by inappropriate or insufficiently optimized reconstruction settings. In any case, the best reconstruction protocol is of little help if the acquired data are of low quality. The signal-to-noise ratio of the image is indeed strongly conditioned by the acquisition duration, the tracer specificity, and the injected dose [38,39]. Motion blur can be addressed by performing gated acquisitions in modern PET/CT systems.

Unaccounted variations within the PET/CT-imaging procedure may lead to non-reproducible effects such as image distortions and biased tracer distribution. Various retrospective correction

algorithms exist, particularly to re-align images, however, at the expense of additional workload. Therefore, measures should be taken to optimize protocol parameters prospectively. For patients undergoing PET/CT-guided RTP this translates into considerations that follow later on.

CT-imaging parameters

At present, in numerous institutions, a low-dose non-enhanced CT is usually performed in order to provide anatomical landmarks for PET interpretation. To better explore the full capacities of spiral CT and to obviate the need for additional diagnostic contrast-enhanced CT, an optimal set-up of CT parameters is required [40–43]. This mandates the use of oral and intravenous contrast material as well as a CT image quality which proves diagnostically sufficient by radiology standards.

First, a scan projection radiograph or scout view will be performed in order to accurately plan the CT acquisition. It provides also a record of the location of images. In most clinical indications, the patient lies supine in a comfortable position with the knee flexed. Moreover, care should be taken that the patient lies identically to the way he/she does later on at the radio therapy accelerator if the CT will be used for treatment planning together with the PET-Data. Therefore, a special table top and fixation material identical to the ones used for fixation of the patient at the accelerator should be used. The patient should be mounted with arms down.

Thereafter, several CT imaging parameters have to be selected (Table 2) for CT acquisition: slice thickness, tube current and exposure time (mAs), tube voltage (kV), rotation time, pitch, field-of-view, reconstruction filter, and image matrix [44–46]. Normally, these combinations of parameters are preconfigured and comprised in protocols that can be selected by the operator. Recent PET/CT systems are equipped with multi-slice CT technology which can acquire up to 128 slices in a single rotation [47]. This faster scanning speed enables to get more and thinner slices than single-slice CT. In multi-slice CT, almost all different slice thicknesses can be obtained in routine by combining neighboring detectors, ranging from 0.5 to 10 mm. Two images per slice thickness should be routinely reconstructed since this improves diagnostic reliability and produces excellent multiplanar reconstructions and 3D images [45,48]. The mAs directly relates to the number of photons emitted in a X-ray beam, and therefore inversely to quantum noise. Increasing mAs will decrease quantum noise and increase in contrast resolution with higher dose to the patient and higher heat load on the tube anode. It has to be noted that doses delivered to the patient can be drastically reduced with a preserved image quality by using anatomical on-line tube dose modulation [49,50], resulting in an overall decrease in average tube current and in a lower mAs product per rotation. The kV reflects the energy spectrum of the photons the X-ray beam consists of. Beams of higher photon energy offer superior penetration through the patient so that a larger number of photons reach the detectors. Tube voltage is usually fixed at 120 kV for general applications. The rotation time is the time needed for the X-ray beam to complete one 360° revolution. The benefit of a longer revolution time is the higher mAs it can deliver, leading to increased contrast resolution. However, longer revolution times may also allow more patient motion and, thereby, leads to net loss in image quality. Rotation time is usually around 0.5–1 s for general purposes. The pitch in spiral scanning is the ratio of the patient's movement through the gantry during one 360° beam rotation relative to the beam collimation. The pitch can be defined as follows: pitch = patient (table) advancement per 360° gantry rotation/beam. For pitch > 1, the dose will be reduced compared with contiguous serial scanning. The performance of spiral CT with a pitch greater than 1.5 may imply lower and possibly insufficient diagnostic image quality due to reduced low contrast resolution [51,52]. During the image reconstruction process, the CT data will be passed through mathematical filter algorithms, each optimized for different body parts and tissue types. For example, a soft tissue algorithm may lead to smooth images while a bone algorithm will sharpen bone margins. The field-of-view is defined as the maximal diameter of the reconstructed image. Its value can be selected by the operator and generally lies between 24 and 50 cm. The image matrix relates to the number of pixels that forms the image grid. When the field-of-view is kept constant, increasing the matrix will lead to smaller individual pixels and therefore increased image details with a parallel increase of the weight of the images. The image matrix of 512×512 is usually selected for body imaging.

Contrast medium injection

The use of intravenous contrast media during CT examination is essential to analyse solid organs, assess vessels and delineate tumour invasion for treatment planning and organ delineation. The presence of contrast materials on CT images can cause problems in the attenuation correction of PET images. However, Malawi et al. [53] showed that i.v. contrast-enhanced CT scans can be used for attenuation correction in oncologic patients with minimal ef-

A   B

Fig. 4. Small cell lung carcinoma staging, contrast-enhanced CT (40 det. rows) according to the respective CT protocol (see Table 1); chest CT 35 s after contrast medium injection (arterial phase) with 120 kV, 200 mAs, 1 mm slices: last slices show slight heterogeneity of the liver parenchyma without any conspicuous lesion (a); abdominal CT 70 s after contrast medium injection (portal venous phase) with 120 kV, 108–200 mAs (dose modulation), 3 mm slices, same plane level: many hypodense lesions consistent with metastases (b).

fect on SUV in areas corresponding to low i.v. contrast media concentration. In regions of high contrast concentration, there was a significant increase in SUV; however, this increase was clinically insignificant in oncologic staging when these regions have background ^{18}F-FDG uptake. Importantly, the increase in SUV measurement in these areas would not have been misinterpreted as sites of metastases. Some investigators [54,55] have proposed CT correction methods to markedly reduce these artefacts. All intravenous contrast agents currently approved for CT contain iodine bound in a complex organic molecule. Ionic agents are now abandoned in favour of non-ionic agents [56,57]. The contrast medium is injected preferably with a power injector through a flexible catheter placed in the forearm. A central venous catheter or a porta-cath could also be used but the rate of injection will be adapted. A careful monitoring of the site of injection need to be performed in order to prevent extravasation in case of catheter misplacement or rupture of thin and fragile veins during injection. The volume, rate, delay time and concentration of contrast medium will be adapted to the organs (Fig. 4 and Table 2) [58–62]. The scan delay times are mean values which typically result in optimal opacification in patients with normal cardiac function. If possible, for chest and abdomen CT examinations, the patient should receive power injection with arms vertically above the shoulder with the palms of the hands on the face of the gantry during injection. This allows for uninterrupted passage of injected contrast medium through the axillary and subclavian veins at the thoracic outlet. Flushing the venous line with 30–40 mL of saline after contrast medium injection is recommended to decrease the risk of venous inflammation and prevent local phlebitis.

Oral and rectal opacification

The goal of the digestive opacification during a CT examination is twofold; first, to differentiate digestive structures from abnormal elements such as enlarged lymph nodes, fluid collections, extraluminal masses and second to analyse the lumen and the wall of digestive organs and detect eventually polyps, tumours or inflammatory disorders. For evaluation of gastro-intestinal tract, a positive [63,64] or negative oral contrast agents [65,66] such as water-like density contrast media could be given to the patient, prior the CT examination. Negative agents have the advantage of allowing for superior delineation of the bowel wall and the lumen and not interfere with image interpretation on PET [65,66]. Administration of contrast medium per rectum may be required for colon evaluation and some examinations of the pelvis.

Warnings

All enhanced CT examinations must be performed under the supervision of medical doctor. Reactions such as rash, urticaria, or bronchospasm have been estimated to occur in 0.004–0.7% and severe life-threatening anaphylactoid reactions to occur in between 1 in 10,000 and 1 in 300,000 [67,68]. For this reason, a rescue kit (adrenalin, anti-histaminic drugs, etc.) should be available in the close area of the site of injection. Minor disagreements such as sensation of warmth throughout the body and a metallic taste are sometimes observed shortly after the start of injection. Some nausea with vomiting efforts can occur but are rare with the use of non-ionic contrast agents. However, we recommend to perform CT examinations on an empty stomach which facilitates the study of the gastric wall and optimize oral preparation. Since contrast medium can impair the renal function by altering hemodynamics and by exerting direct toxic effects on tubular epithelial cells, it is therefore essential to identify patients at risk for induced contrast nephropathy [69–71]. Reduced renal function is the most important risk factor for contrast-induced nephropathy. The Contrast Media Safety Committee of the European Society of Urogenital Radiology (ESUR) [69] recommends measurements of serum creatinine (SCr) and calculations of the estimated glomerular filtration in patients with previously raised SCr [72], in patients taking Meformin [73], in patients [74] with a history suggesting the possibility of raised SCr (renal disease, renal surgery, proteinuria, diabetes mellitus, hypertension, gout, and recent intake of nephrotoxic drugs). Correct hydration (100 mL/oral fluid or intravenous normal saline 1 mL/kg/h), depending on the clinical situation, should be administrated starting 4 h before to 24 h after contrast medium injection. Reports of patients developing lactic acidosis following injection of iodinated contrast medium currently recommend that metformin should be stopped 48 h before and for 48 h after the administration of iodinated contrast media [75].

Since contrast medium contains some free iodide, contrast medium may induce thyrotoxicosis in patients with Graves' disease and thyroid autonomy [76]. This thyrotoxicosis is more relevant in patients with an associated cardiovascular risk and in the elderly. In this population, knowledge of thyroid function (at least TSH) before a contrast-enhanced study is helpful. All patients at risk should be monitored closely after the injection of iodinated contrast medium preferably by endocrinologists.

PET/CT for external RT planning

If it is known already that patients will receive external radiation therapy (i.e., primary staging completed) and PET/CT is used to define the active tumour and target volumes, then patients should be positioned for the PET/CT in the radiation treatment position. External positioning lasers (Fig. 3C) can help define the isocentre on PET/CT, which is referenced on the patient and transferred to the treatment plan. With the availability of an RT-certified pallet to which all standardized radiation treatment-positioning devices can be fitted, the patients can be repositioned on the treatment table.

However, PET/CT-guided treatment planning for lung cancer remains a challenge. Erdi and colleagues have demonstrated that respiration-induced misalignments between CT and PET data within a single PET/CT scan can lead to a significant underestimation of the standardized uptake value of the attenuation-corrected PET [77]. In the worst case scenario of maximum mismatches between CT (full inspiration) and PET (normal respiration that equals mid-expiration) lesions may disappear entirely on attenuation-corrected PET [78], although this effect remains infrequent.

Therefore, lung cancer patients require special adaptations to the PET/CT acquisition and treatment delivery. If external treatment is delivered during normal respiration then adequate verification of the PET/CT data appears sufficient to ensure an accurate representation of the target volume. In case of minimal PET–CT misalignment the mis-registration can be corrected retrospectively prior to a second attenuation correction using a linear or non-linear co-registration algorithm. Alternatively, the transmission data could be corrected manually to match the uncorrected emission data, and the CT-AC (CT-based attenuation correction of PET data) could be re-performed [79,80]. Finally, different gating schemes and tools are available to acquire CT transmission and PET emission data of the full respiratory cycle. Data for matching portions of the cycle can be extracted and used for further processing, thus maximizing the spatial–temporal match at the expense of reduced counts collected in the emission data. Clearly, PET/CT gating becomes mandatory in cases where external radiation treatment is delivered in gated mode as well. As of today, full inspiration PET/CT data cannot be acquired and matched to full-inspiration breath-hold treatment [81] delivery routinely.

PET/CT for therapy monitoring

In addition to the above-mentioned patient set-up and imaging considerations attention must be given to maintain similar pre-imaging conditions (blood glucose level, tracer distribution time, and uptake conditions). By adhering to standard set-up and imaging protocols, reproducible quantitative accuracy of PET/CT can be maintained and accurate therapy response assessment is feasible [82,83].

Alternative PET tracer imaging (hypoxia, thyroid and internal dosimetry)

Tracers other than FDG are being increasingly used in defining the active tumour volume. Examples for these tracers include, but are not limited to, ^{11}C-choline (prostate cancer), ^{64}Cu-ATSM, ^{18}F-FMISO and ^{18}F-FAZA (hypoxia imaging) and [124]I for thyroid cancer. While most tracers are labeled with radioisotopes that have a similar beta fraction as [18]F (FDG) some nuclides (e.g., [124]I, [86]Y) pose a challenge to the PET detection system and may have implications for calculating a dosimetry plan for internal radiation therapy planning [84]. PET quantification of impure positron emitters is the work in progress in several research and clinical institutions, but it is clear that the major pitfalls for both visual and quantitative target volume delineations are already being addressed today and that PET/CT is ready to be implemented in routine radiation oncology management.

Possible PET/CT pitfalls

Typical pitfalls in standard PET/CT imaging include motion-induced mis-registration, overestimation of PET activity following CT contrast administration and PET image artifacts in the vicinity of metal implants. Table 4 lists the sources of these artifacts, key studies and suggested solutions.

Data transfer, data format and data security

Today, radiation-treatment planning (RTP) is based mostly on anatomical image data [85]. Over the past decade, however, treatment plans have started to incorporate also functional image information, which represents various metabolic pathways [86]. Positron emission tomography (PET) and, more recently PET/CT, based on ^{18}F-FDG were shown to have a significant clinical impact on the diagnosis of a variety of cancers. While ^{18}F-FDG reveals increased glucose metabolism, other compounds can be used for more specific information, for example, to visualize and quantify hypoxia, cell proliferation and other characteristic features important for RTP [87].

The goal of functional imaging for radiation treatment planning is to add complementary information to anatomical imaging as anatomical imaging is known to be inadequate in certain imaging situations, such as in the differentiation of necrotic from active tumour volume. PET and PET/CT can serve as a source for delineation of metabolically active target volumes or gross tumour volume (GTV) [87].

There are several options concerning the platform on which these volumes of interest can be delineated:

GTV definition on the radiotherapy virtual simulation and treatment-planning environment

Here, the anatomical and biological imaging datasets are transferred to the virtual simulation or treatment-planning environment as DICOM datasets (objects) such as CT, PT and/or MR information object definition (IOD) [88,89]. Details about the capability of the sending and receiving systems can be found in the DICOM-conformance statements of the manufacturers of the systems involved (treatment-planning systems, virtual simulation systems). Systems need to be either IP networked or the image data are transferred on physical media to and from the other platform (Fig. 5) [90,91]. In case of a direct network transfer the systems must be configured with the TCP/IP-hostname (-address), application entity title (AET) and the TCP/IP-port number of each other to allow for data to be sent or received, respectively.

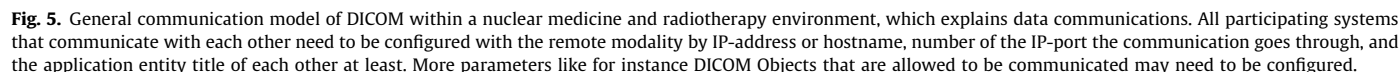*GTV definition on the nuclear medicine image-processing workstation*

In this case, the GTV is defined on the nuclear medicine image-processing workstation and transferred to the treatment-planning system as a set of regions of interest (ROI) forming a volume of interest (VOI) together with the DICOM image objects (CT, MR, PT) as described above. The GTV is typically transferred as a DICOM RT structure set as described in Supplement 11 to Part 3 of the DICOM-Standard [91]. Similar to the image data, the RT structure set can be transferred via a network connection or on physical media [90]. Within the RT environment the RT structure set serves as a source for creation of various other DICOM RT objects such as RT-Plan, RT-Dose, and RT-Image [91] that are communicated in the RT environment internally.

The data transfer between the nuclear medicine imaging and RT-planning modalities can also be facilitated through a hospital Picture Archiving and Communication System (PACS). Here, the prerequisite is that the PACS does support DICOM RT-IODs. This is frequently not the case in hospital environments, where RT and nuclear medicine departments often operate their own DICOM RT- (or NM-) Archive that directly communicates with the specific modalities and that is a client to the hospital PACS.

If the PET/CT is equipped with a dedicated RT laser system for marking the isocentre on the patient, the laser system should be directly connected to the RT virtual simulation system such that

Table 4
Sources of artifacts in standard FDG PET/CT imaging; consequences and solutions.

Pitfall	Artifact and consequence	Practical solution	Reference
Patient motion (muscle relaxation, coughing)	Local or global PET–CT mis-registration and potential translation through CT-AC into corrected PET image (bias)	Use positioning aids and adopt short scan times for higher patient comfort	[16,96]
Respiration	Prominent mis-registration in lower thorax	Use modified respiration protocol with breath hold in mid-expiration; respiratory gating of CT (and PET)	[97–99]
Large patient diameter	Truncation artifacts in areas exceeding the transverse field-of-view of the CT (50 cm) lead to masking of the AC-PET activity	Position arms of the patient above and below the head/neck for imaging the torso and neck, respectively; utilize the extended FOV reconstruction on the PET/CT	[100–102]
High-density CT contrast	Apparent focal or extensive hyper metabolism in lung apex (near subclavian vein) and stomach/colon due to overcorrection of CT-enhanced soft tissues in CT-AC	Acquire separate, low-dose CT for CT-AC only; modify IV contrast injection protocol; replace positive oral contrast medium with negative/water-based oral contrast	[103–110]
Non-removable metal implants	Beam hardening and scatter artifacts on CT that translate into combined over-/under-estimation on PET after CT-AC	Review the AC and non-AC images; correct CT images for metal artifacts prior to CT-AC (not routinely available)	[111–118]

Fig. 5. General communication model of DICOM within a nuclear medicine and radiotherapy environment, which explains data communications. All participating systems that communicate with each other need to be configured with the remote modality by IP-address or hostname, number of the IP-port the communication goes through, and the application entity title of each other at least. More parameters like for instance DICOM Objects that are allowed to be communicated may need to be configured.

the coordinates can be integrated seamlessly in the planning and simulation process. Usually this interface is realised on a ASCII-basis using a networked file system for proprietary data interchange.

Compared with anatomical imaging methods, the reason for integrating functional imaging in the GTV definition is its higher sensitivity and specificity for malignant tissues. Depending on which PET tracer is used and, thereby, what metabolic pathway is imaged, either the GTV or sub-volumes of it can be defined [86]. Besides manual delineation of target volumes on PET images there are several modes of automatic delineation of the different interrelated volumes that are with planning of radiotherapy (GTV, CTV, PTV, etc.). Most systems support a threshold-based method, where the actual VOIs can be defined with reference to the maximum specific uptake value (SUV) or maximum activity in a pre-defined VOI-mask. However, this method has drawbacks – especially if the signal-to-noise ratio is low. Hence, other methods of VOI-generation have been developed such as contrast-oriented methods [92,93] and gradient-based methods [94].

If data are transferred and first visualized there is a need for a visual assessment of correct transfer, i.e., check for correct orientation (left, right, anterior, and posterior) as well as for a complete number of images transferred. Most of the systems report messages in case of transfer or reception of incomplete datasets. These message boards are to be checked on a regular basis.

To ensure for security of the networked data interchange and the data itself, the data should be communicated only in a restricted, firewall-protected local area network (LAN). If the data need to be communicated across firewalls, virtual private network (VPN) tunnels or dedicated IP-Ports and an appropriate data encryption/decryption should be used. Be aware that the protection of patient-specific data is subject to regulatory issues that can vary significantly from country to country.

Overall, the most important precondition for successful integration of functional imaging in RT treatment planning is the goal orientated as well as close and thorough communication between nuclear medicine and radiotherapy departments on all levels of interaction (personnel, imaging protocols, GTV delineation, and selection of the data transfer method) [119–124].

Acknowledgements

References

[1] Gambhir SS et al. A tabulated summary of the FDG PET literature. J Nucl Med 2001;42:1S–93S.
[2] Townsend DW. From 3-D positron emission tomography to 3-D positron emission tomography/computed tomography: what did we learn? Mol Imaging Biol 2004;6:275–90.
[3] Casey ME, Nutt R. A multicrystal two-dimensional BGO detector system for PET. IEEE Trans Nucl Sci 1986;33:460–3.
[4] Karp JS et al. Performance standards in positron emission tomography. J Nucl Med 1991;12:2342–50.

[5] Karp JS. Is LSO the future of PET? Eur J Nucl Med 2002;29:1525–8.

[6] Nutt R. Is LSO the future of PET? Eur J Nucl Med 2002;29:1523–4.

[7] Townsend D. Multimodality imaging of structure and function. Phys Med Biol 2008;53:R1–R39.

[8] Hasegawa B et al. Description of a simultaneous emission–transmission CT system. Proc Soc Photo-Opt Instrum Eng (SPIE) 1990;1231:50–60.

[9] Geworski L et al. Verification of co-registration accuracy of PET/CT [Überprüfung der Co-Registrierung der PET/CT-Daten im Rahmen der Konstanzprüfung]. Nuklearmedizin 2008;47:A83–4.

[10] Gladish GW, Choe DH, Marom EM, Sabloff BS, Broemling LD, Munden RF. Incidental pulmonary emboli in oncology patients: prevalence, CT evaluation and natural history. Radiology 2006;240:246–55.

[11] Delbeke D et al. Procedure guideline for tumor imaging with ^{18}F-FDG PET/CT 1.0. J Nucl Med 2006;47:885–95.

[12] Krause B et al. FDG-PET/CT in oncology, German Guideline. Nuklearmedizin 2007;46:291–301.

[13] Boellaard R et al. EANM procedure guidelines for tumour PET imaging: version 1.0. Eur J Nucl Med Mol Imaging 2010;37:181–200.

[14] Antoch G et al. Accuracy of whole-body PET/CT for tumor staging in solid tumors: comparison with CT and PET in 260 patients. J Clin Oncol 2004;22:4357–68.

[15] Kinahan P, Hasegawa B, Beyer T. X-ray based attenuation correction for PET/CT scanners. Semin Nucl Med 2003;33:166–79.

[16] Beyer T et al. Acquisition protocol considerations for combined PET/CT imaging. J Nucl Med 2004;45:25S–35S.

[17] Boellard R et al. Standards for PET image acquisition and quantitative data analysis. J Nucl Med 2009;50:11S–20S.

[18] Defrise M, Kinahan PE, Michel C. Image reconstruction algorithms in PET. In: Valk PE, Bailey DL, Townsend DW, Maisey MN, editors. Positron emission tomography: basic science and clinical practice. Springer; 2004. p. 91–114.

[19] Alessio A, Kinahan P. PET image reconstruction. In: Henkin RE et al., editors. Nuclear medicine. Elsevier; 2006.

[20] Markham J, Mullani NA, Ter-Pogossian MM. Feasibility of time-of-flight reconstruction in positron emission tomography. J Nucl Med 1980;21:1095–7.

[21] Moses WW. Time of flight in PET revisited. IEEE Trans Nucl Sci 2003;50:1325–30.

[22] Conti M, Bendriem B, Casey M, Chen M, Kehren F, Michel C, et al. First experimental results of time of-flight reconstruction on an LSO PET scanner. Phys Med Biol 2005;50:4507–26.

[23] Watson CC. Image noise variance in 3D OSEM reconstruction of clinical time-of-flight PET. In: IEEE NSS MIC; 2006, M045.

[24] Meikle SR, Badawi RD. Quantitative techniques in PET. In: Valk PE, Bailey DL, Townsend DW, Maisey MN, editors. Positron emission tomography: basic science and clinical practice. Springer; 2004. p. 115–46.

[25] Wang CX, Snyder WE, Bilbro G, Santago P. Performance evaluation of filtered backprojection reconstruction and iterative reconstruction methods for PET images. Comput Biol Med 1998;28:13–25.

[26] Kappadath SC, Tinsu P, Erwin WD, Mawlawi O. Analysis of the dependence of PET/CT quantification on iterative reconstruction parameters. Nucl Sci Symp Conf Rec IEEE 2007;6:4406–9.

[27] Hudson HM, Larkin RS. Accelerated image reconstruction using ordered subsets of projection data. IEEE Trans Med Imaging 1994;13:601–9.

[28] Lewitt RM. Alternatives to voxels for image representation in iterative reconstruction algorithms. Phys Med Biol 1992;37:705–16.

[29] Matej S, Herman GT, Narayanan TK, Furie SS, Lewitt RM, Kinahan PE. Evaluation of task-oriented performance of several fully 3D PET reconstruction algorithms. Phys Med Biol 1994;39:355–67.

[30] Alessio A, Kinahan P, Lewellen T. Modeling and incorporation of system response functions in 3D whole body PET. IEEE Trans Med Imaging 2006;25:828–37.

[31] Daisne JF, Sibomana M, Bol A, Doumont T, Lonneux M, Grégoire V. Tri-dimensional automatic segmentation of PET volumes based on measured source-to-background ratios: influence of reconstruction algorithms. Radiother Oncol 2003;69:247–50.

[32] Kessler Jr RM, Ellis JR, Eden M. Analysis of emission tomographic scan data: limitations imposed by resolution and background. J Comput Assist Tomogr 1984;8:514–22.

[33] King MA, Long DT, Brill AV. SPECT volume quantitation: influence of spatial resolution, source size and shape, and voxel size. Med Phys 1991;18:1016–24.

[34] van Dalen JA, Hoffmann AL, Dicken V, Vogel WV, Wiering B, Ruers TJ, et al. A novel iterative method for lesion delineation and volumetric quantification with FDG PET. Nucl Med Commun 2007;28:485–93.

[35] Geets X, Lee J, Bol A, Lonneux M, Grégoire V. A gradient-based method for segmenting FDG-PET images: methodology and validation. Eur J Nucl Med Mol Imaging 2007;34:1427–38.

[36] Barbee D, Flynn R, Jaskowiak C, Jeraj R. Effects of PET reconstruction parameters on the delineation of heterogeneous target volumes. Med Phys 2006;33:2242–3.

[37] Tanderup K, Olsen DG, Grau C. Dose painting: art or science? Radiother Oncol Volume 2006;79:245–8.

[38] Bailey DL. Data acquisition and performance characterization in PET. In: Valk PE, Bailey DL, Townsend DW, Maisey MN, editors. Positron emission tomography: basic science and clinical practice. Springer; 2004. p. 69–90.

[39] Carney JPJ, Watson CC, Townsend DW. Optimization of the relative acquisition duration for PET/CT imaging in oncology. IEEE Nucl Sci Symp Conf Rec 2004;5:2910–4.

[40] Pfannenberg AC, Aschoff P, Brechtel K, Müller M, Bares R, Paulsen F, et al. Low dose non-enhanced CT versus standard dose contrast-enhanced CT in combined PET/CT protocols for staging and therapy planning in non-small cell lung cancer. Eur J Nucl Med Mol Imaging 2007;34:36–44.

[41] Kitajima K, Murakami K, Yamasaki E, Domeki Y, Kaji Y, Fukasawa I, et al. Performance of integrated FDG-PET/contrast-enhanced CT in the diagnosis of recurrent ovarian cancer: comparison with integrated FDG-PET/non-contrast-enhanced CT and enhanced CT. Eur J Nucl Med Mol Imaging 2008;35:1439–48.

[42] Tateishi U, Maeda T, Morimoto T, Miyake M, Arai Y, Kim EE. Non-enhanced CT versus contrast-enhanced CT in integrated PET/CT studies for nodal staging of rectal cancer. Eur J Nucl Med Mol Imaging 2007;34:1627–34.

[43] Pfannenberg AC, Aschoff P, Brechtel K, Müller M, Klein M, Bares R, et al. Value of contrast-enhanced multiphase CT in combined PET/CT protocols for oncological imaging. Br J Radiol 2007;80:437–45.

[44] Silverman PM, Kalender WA, Hazle JD. Common terminology for single and multislice helical CT. AJR Am J Roentgenol 2001;176:1135–6.

[45] Kalender WA. Computed tomography. 1st ed. Munich, Germany: Publicis MCD Verlag; 2000. p. 65–118.

[46] European Commission. European guidelines on quality criteria for computed tomography, EUR 16262EN. Luxembourg: Office for Official Publications of the European Communities, http://www.drs.dk/guidelines/ct/quality/htmlindex.htm; 2000.

[47] Teräs M, Tolvanen T, Johansson JJ, Williams JJ, Knuuti J. Performance of the new generation of whole-body PET/CT scanners: discovery STE and discovery VCT. Eur J Nucl Med Mol Imaging 2007;34:1683–92.

[48] Mahesh M. The AAPM/RSNA physics tutorial for residents: search for isotropic resolution in ct from conventional through multiple-row detector. Radiographics 2002;22:949–62.

[49] Kalender WA, Wolf H, Suess C, Gies M, Greess H, Bautz WA. Dose reduction in CT by on-line tube current control: principles and validation on phantoms and cadavers. Eur Radiol 1999;9:323–8.

[50] Gies M, Kalender WA, Wolf H, Suess C. Dose reduction in CT by anatomically adapted tube current modulation, I. Simulation studies. Med Phys 1999;26:2235–47.

[51] Brink JA, McFarland EG, Heiken JP. Helical/spiral computed body tomography. Clin Radiol 1997;52:489–503.

[52] Verdun FR, Meuli RA, Bochud FO, Imsand C, Raimondi S, Schnyder P, et al. Image quality and dose in spiral computed tomography. Eur Radiol 1996;6:485–8.

[53] Malawi O, Erasmus JJ, Munden RF, et al. Quantifying the effect of IV contrast media on integrated PET/CT: clinical evaluation. AJR Am J Roentgenol 2006;186:308–19.

[54] Bunyaviroch T, Turkington TG, Wong TZ, Wilson JW, Colsher JG, Coleman RE. Quantitative effects of contrast enhanced CT attenuation correction on PET SUV measurements. Mol Imaging Biol 2008;10:107–13.

[55] Büther F, Stegger L, Dawood M, Range F, Schäfers M, Fischbach R, et al. Effective methods to correct contrast agent-induced errors in PET quantification in cardiac PET/CT. J Nucl Med 2007;48:1060–8.

[56] Stockberger Jr SM, Hicklin JA, Liang Y, Wass JL, Ambrosius WT. Spiral CT with ionic and nonionic contrast material: evaluation of patient motion and scan quality. Radiology 1998;206:631–6.

[57] Valentine A, Jakobsen JA, Klaveness AJ. Iopentol (Imagopaque 350) compared with diatrizoate (Urografin 370) in cerebral CT, A clinical trial assessing immediate and late (7 days) adverse events and diagnostic information (visualization quality and Hounsfield unit measurements). Eur Radiol 1997;7:S145–8.

[58] Ho LM, Nelson RC, Delong DM. Determining contrast medium dose and rate on basis of lean body weight: does this strategy improve patient-to-patient uniformity of hepatic enhancement during multi-detector row CT? Radiology 2007;243:431–7.

[59] Goshima S, Kanematsu M, Kondo H, et al. Pancreas: optimal scan delay for contrast-enhanced multi-detector row CT. Radiology 2006;241:167–74.

[60] Chung YE, Kim KW, Kim JH, Lim JS, Oh YT, Chung JJ, et al. Optimal delay time for the hepatic parenchymal enhancement at the multidetector CT examination. J Comput Assist Tomogr 2006;30:182–8.

[61] Herman S. Computed tomography contrast enhancement principles and the use of high-concentration contrast media. J Comput Assist Tomogr 2004;28:S7–S11.

[62] Fleischmann D. Use of high-concentration contrast media in multiple-detector-row CT: principles and rationale. Eur Radiol 2003;13:M14–20.

[63] Megibow AJ, Bosniak MA. Diluted barium as contrast agent for abdominal CT. Am J Roentgenol AJR 1980;134:1273–4.

[64] Ott DJ, Gelfand DW. Gastrointestinal contrast agents. JAMA 1983;249:2380–4.

[65] Hausegger K, Reinprecht P, Kau T, Igerc I, Lind P. Clinical experience with a commercially available negative oral contrast medium in PET. CT. Rofo 2005;177:796–9.

[66] Antoch G, Kuehl H, Kanja J, Lauenstein TC, Schneemann H, Hauth E, et al. Dual-modality PET/CT scanning with negative oral contrast agent to avoid artifacts: introduction and evaluation. Radiology 2004;230:879–85.

[67] Webb JA. Prevention of acute reactions. In: Thomsen HS, editor. Contrast media safety issues and ESUR guidelines. Heidelberg-Berlin: Springer-Verlag; 2006. p. 11–7.

[68] Wang CL, Cohan RH, Ellis JH, Caoili EM, Wang G, Francis IR. Frequency, outcome and appropriateness of treatment of non-ionic iodinated contrast media reactions. Am J Roentgenol AJR 2008;191:409–15.

[69] Thomsen HS. European Society of Urogenital Radiology. European Society of Urogenital Radiology guidelines on contrast media application. Curr Opin Urol 2007;17:70–6.

[70] Thomsen HS, Morcos SK. Contrast-medium-induced nephropathy: is there a new consensus? A review of published guidelines. Eur Radiol 2006;16:1835–40.

[71] Thomsen HS, Morcos SK. ESUR. ESUR guidelines on contrast media. Abdom Imaging 2006;31:131–40.

[72] Hou SH, Bushinsky DA, Wish JB, et al. Hospital acquired renal insufficiency. Am J Med 1983;74:243–8.

[73] Nash K, Hafeez A, Hou S. Hospital-acquired renal insufficiency. Am J Kidney 2002;39:930–6.

[74] Solomon R. Contrast medium-induced acute renal failure. Kidney Int 1988;53:230–42.

[75] Thomsen HS. Non-Insulin dependent diabetes and contrast media. In: Thomsen HS, editor. Contrast media safety issues and ESUR guidelines. Heidelberg-Berlin: Springer-Verlag; 2006. p. 53–5.

[76] van der Molen AJ, Thomsen HS, Morcos SK. Contrast Media Safety Committee, European Society of Urogenital Radiology (ESUR). Effect of iodinated contrast media on thyroid function in adults. Eur Radiol 2004;14:902–7.

[77] Erdi YE et al. The CT motion quantitation of lung lesions and its impact on PET-measured SUVs. J Nucl Med 2004;45:1287–92.

[78] Osman MM et al. Clinically significant inaccurate localization of lesions with PET/CT: frequency in 300 patients. J Nucl Med 2003;44:240–3.

[79] Martinez-Möller A et al. Dual cardiac-respiratory gated PET: implementation and results from a feasibility study. Eur J Nucl Med Mol Imaging 2007;34:1447–54.

[80] Souvatzoglou M et al. Attenuation correction in cardiac PET/CT with three different CT protocols: a comparison with conventional PET. Eur J Nucl Med Mol Imaging 2007;34:1991–2000.

[81] Rosenzweig KE et al. The deep inspiration breath-hold technique in the treatment of inoperable non-small-cell lung cancer. Int J Radiat Oncol Biol Phys 2000;48:81–7.

[82] Weber W et al. Reproducibility of metabolic measurements in malignant tumors using FDG PET. J Nucl Med 1999;40:1771–7.

[83] Weber W. Use of PET for monitoring cancer therapy and for predicting outcome. J Nucl Med 2005;46:983–95.

[84] Jentzen W et al. Iodine-124 PET dosimetry in differentiated thyroid cancer: recovery coefficient in 2D and 3D modes for PET(/CT) systems. Eur J Nucl Med Mol Imaging 2008;35:611–23.

[85] Evans PM et al. Topical review: anatomical imaging for radiotherapy. Phys Med Biol 2008;53:R151–91.

[86] Nestle U et al. Topical review: biological imaging in radiation therapy: role of positron emission tomography. Phys Med Biol 2009;54:R1–R25.

[87] NEMA. DICOM Supplement 12, Addendum to part 3, positron emission tomography image objects, Final Text, 9, http://dicom.nema.org/; June 1996.

[88] NEMA. DICOM, Part 3, Information Object Definitions, http://dicom.nema.org; 2008.

[89] NEMA. DICOM Supplement 1, Addenda to part 10 on Directory, Media Storage Service Class and Data Dictionary, Final Text; February 26 1995.

[90] NEMA. DICOM, Part 10, Media Storage and File Format for Media Interchange, http://dicom.nema.org; 2008.

[91] NEMA. DICOM, Supplement 11, Addendum to part 3, Radiotherapy Objects, Final Text, http://dicom.nema.org/; 29 April 1997.

[92] MacManus MP, Hicks RJ. Where do we draw the line? Contouring tumors on positron emission tomography/computed tomography. Int J Radiat Oncol Biol Phys 2008;71:2–4.

[93] Nestle U et al. Comparison of different methods for delineation of ^{18}F-FDG PET-positive tissue for target volume definition in radiotherapy of patients with non-small cell lung cancer. J Nucl Med 2005;46:1342–8.

[94] Geets X et al. A gradient-based method for segmenting FDG-PET images: methodology and validation. Eur J Nucl Med Mol Imaging 2007;34:1427–38.

[95] Karp J et al. Benefit of time-of-flight in PET: experimental and clinical results. J Nucl Med 2008;49:462–70.

[96] Beyer T et al. Reduced motion artifacts in the head/neck region of whole-body PET/CT studies through the use of positioning aids. J Nucl Med 2004;45:428P.

[97] Beyer T et al. Respiration artifacts in whole-body ^{18}F-FDG PET/CT studies with combined PET/CT tomographs employing spiral CT technology with 1 to 16 detector rows. Eur J Nucl Med Mol Imaging 2005;32:1429–39.

[98] Beyer T et al. A limited breath-hold technique for improved image quality in multi-slice PET/CT exams. J Nucl Med 2003;44:274P–5P.

[99] Bettinardi V et al. An automatic classification technique for attenuation correction in positron emission tomography. Eur J Nucl Med 1999;26:447–58.

[100] Beyer T et al. Whole-body ^{18}F-FDG PET/CT in the presence of truncation artifacts. J Nucl Med 2006;47:91–9.

[101] Schaller S et al. An algorithm for virtual extension of the CT field of measurement for application in combined PET/CT scanners. Radiology 2002;225:497.

[102] Ohnesorge B et al. Efficient correction for CT image artifacts caused by objects extending outside the scan field-of-view. Med Phys 2000;27:39–46.

[103] Pfannenberg A et al. Low dose non-enhanced CT versus standard dose contrast-enhanced CT in combined PET/CT protocols for staging and therapy planning in non-small cell lung cancer. Eur J Nucl Med Mol Imaging 2007;34:36–44.

[104] Brechtel K et al. Optimized contrast enhanced CT protocols for diagnostic whole-body ^{18}F-FDG PET/CT: single-phase versus multi-phase CT imaging. J Nucl Med 2006;47:470–6.

[105] Strobel K, Thuerl C, Hany T. How much intravenous contrast is needed in FDG-PET/CT? Nuklearmedizin 2005;44:S32–7.

[106] Kuehl H, Antoch G. How much CT do we need for PET/CT? A radiologist's perspective. Nuklearmedizin 2005;44:S24–31.

[107] Hausegger K et al. Clinical experience with a commercially available negative oral contrast medium in PET/CT. Fortschr Roentgenstr 2005;177:796–9.

[108] Beyer T et al. Optimized IV contrast administration protocols for diagnostic PET/CT imaging. J Nucl Med 2005;46:429–35.

[109] Antoch G et al. Dual-modality PET/CT scanning with negative oral contrast agent to avoid artifacts: introduction and evaluation. Radiology 2004;230:879–85.

[110] Antoch G et al. Contrast-induced artifacts in dual-modality PET/CT: can a negative oral contrast agent solve the problem? J Nucl Med 2003;44:377P.

[111] Schäfers K, Raupach R, Beyer T. Combined ^{18}F-FDG-PET/CT imaging of the head and neck. An approach to metal artifact correction. Nuklearmedizin 2006;45:219–22.

[112] DiFilippo FP, Brunken RC. Do implanted pacemakers leads and ICD leads cause metal-related artifact in cardiac PET/CT? J Nucl Med 2005;46:436–43.

[113] Halpern BS et al. Cardiac pacemakers and central venous lines can induce focal artifacts on CT-corrected PET images. J Nucl Med 2004;45:290–3.

[114] Mahnken AH et al. A new algorithm for metal artifact reduction in computed tomography, in vitro and in vivo evaluation after total hip replacement. Invest Radiol 2003;38:769–75.

[115] Kamel EM et al. Impact of metallic dental implants on CT-based attenuation correction in a combined PET/CT scanner. Eur Radiol 2003;13:724–8.

[116] Goerres GW et al. Artifacts at PET and PET/CT caused by metallic hip prosthetic material. Radiology 2003;226:577–84.

[117] Goerres G, Schmid D, Eyrich G. Do hardware artefacts influence the performance of head and neck PET scans in patients with oral cavity squamous cell cancer? Dentomaxillofac Radiol 2003;32:365–71.

[118] Bujenovic S et al. Artifactual 2-deoxy-2-[^{18}F]fluoro-D-glucose localization surrounding metallic objects in a PET/CT scanner using CT-based attenuation correction. Mol Imaging Biol 2003;5:20–2.

[119] Grégoire V, Haustermans K, Geets X, Roels S, Lonneux M. PET-based treatment planning in radiotherapy: a new standard? J Nucl Med 2007;48:68S–77S.

[120] Mac Manus M, Hicks RJ, Everitt S. Role of PET–CT in the optimization of thoracic radiotherapy. J Thorac Oncol 2006;1:81–4.

[121] Hutchings M, Loft A, Hansen M, Berthelsen AK, Specht L. Clinical impact of FDG-PET/CT in the planning of radiotherapy for early-stage Hodgkin lymphoma. Eur J Haematol 2007;78:206–12.

[122] Jarritt PH, Carson KJ, Hounsell AR, Visvikis D. The role of PET/CT scanning in radiotherapy planning. Br J Radiol 2006;79:S27–35.

[123] Messa C, Di Muzio N, Picchio M, Gilardi MC, Bettinardi V, Fazio F. PET/CT and radiotherapy. Q J Nucl Med Mol Imaging 2006;50:4–14.

[124] Leong T, Everitt C, Yuen K, Condron S, Hui A, Ngan SY, et al. A prospective study to evaluate the impact of FDG-PET on CT-based radiotherapy treatment planning for oesophageal cancer. Radiother Oncol 2006;78:254–61.

Review

Patient setup for PET/CT acquisition in radiotherapy planning

Mary Coffey [a], Aude Vaandering [b,*]

[a] TCD School of Radiation Therapy, Trinity Centre for Health Science, Dublin, Ireland; [b] Department of Radiation Oncology, Cliniques Universitaires Saint-Luc, Belgium

ARTICLE INFO

ABSTRACT

PET/CT imaging modalities have been shown to be useful in the diagnosis, staging, and monitoring of malignant diseases. Its inclusion into the treatment planning process is now central to modern radiotherapy practice. However, it is essential to be cognisant of the factors that are necessary in order to ensure that the acquired images are consistent with the requirements for both treatment planning and treatment delivery.

Essential parameters required in image acquisition for radiotherapy planning and treatment include consistencies of table tops and the use of laser light for patient set-up. But they also include the accurate definition of the patient's initial positioning and the use of proper immobilization devices in the radiotherapy department. While determining this optimum set-up, patient psychological factors and limitations that may be due to the subsequent use of PET/CT for planning purposes need to be taken into account. Furthermore, patient set-up data need to be properly recorded and transmitted to the imaging departments. To ensure the consistency of patient set-up, the radiation therapist should ideally be directly involved in informing and positioning the patient on the PET/CT. However, a proper exchange of patient-related information can also be achieved by a close liaison between the two departments and by the use of clear detailed protocols per type of patient set-up and/or per localization of tumour site.

© 2010 European Society for Therapeutic Radiology and Oncology and European Association of Nuclear Medicine. Published by Elsevier Ireland Ltd. All rights reserved. 96 (2010) 298–301

Importance of correct patient set-up in radiotherapy treatment planning

The developments that have taken place, both in radiotherapy and diagnostic imaging equipment, have enabled a more precise approach to the treatment of malignant disease. This has led to the potential to deliver higher doses to tumour volumes while increasing normal tissue sparing and minimising the dose to critical organs at risk. The possible risk of second malignancy following radical radiotherapy emphasises the need for optimum accuracy in volume delineation and treatment delivery [1,2]. The technological advances in diagnostic imaging provide us with more detailed images than previously obtained and now also provide additional functional information.

Technological advances in radiotherapy include multileaf collimators and the incorporation of imaging modalities within the treatment room. With these advances, treatment volumes can now be designed to conform to the shape of the tumour and daily images of the treatment volume can be acquired before, during or after treatment delivery.

The developments in diagnostic imaging have enabled a more precise definition of the treatment volume by facilitating a more accurate definition of both the primary tumour and the secondary spread including lymph nodes. The integration of new imaging modalities into the actual treatment planning process has redefined volume delineation and is now central to modern radiotherapy practice. The use of CT and MRI is routine practice in many departments and increasingly PET is now also being used in this way [3]. The inclusion of PET allows functional imaging to be incorporated into the localization and planning process giving a further level of accuracy to the definition of the tumour volume and the individualization of treatment [4,5].

Key to maximising the potential benefits of these imaging technologies is an awareness of the factors that must be considered to ensure that the images acquired are consistent with the requirements for both treatment planning and treatment delivery[6].

Essential parameters required in image acquisition for radiotherapy planning and treatment

Of critical importance when delivering higher doses to the tumour volume is the tolerance level of normal tissue and this underpins the importance of accurate position reproducibility. This position is determined at the outset of the process and must be consistent throughout the treatment preparation and delivery.

---

* Corresponding author. Address: Department of Radiation Oncology, Cliniques Universitaires Saint-Luc, Avenue Hippocrate 10, B-1200 Brussels, Belgium.
  E-mail address: aude.vaandering@uclouvain.be (A. Vaandering).

The consistency and reproducibility of this position are core to accurate treatment delivery and many factors must be considered when PET or PET/CT images are to be acquired for treatment planning purposes. These factors include initial patient positioning, consistency of table tops, laser lights, and patient psychological factors [7–9]. Consistency of table tops, the use of laser lights and psychological factors are applicable to all patients and tumour sites, patient position and immobilisation are site dependent and will be considered in this context.

Initial patient positioning

The initial definition of the patient position and the ability to accurately reproduce this position on a daily basis are crucial for the accurate delivery of a course of treatment. The optimum patient position and the method of immobilisation are based on the clinical site, the extent of the tumour volume and the surrounding organs at risk. The physical status of the patient and the stage of disease need to be considered at the time of initial positioning as patient comfort is an important component of maintaining a stable reproducible position. Patients suffering from various co-morbidities may not be able to achieve and maintain the required position and this must be taken into account when determining the optimal patient positioning.

An important aspect of positioning and immobilisation is the clarity of the information given to the patient and the level of their understanding of the importance of maintaining their position. Trousers at thigh level, for instance, do not maintain patient modesty and will compromise both position stability and reproducibility. A comfortable arm position when patients are in a supine position helps to maintain stability and it has been found that placing the arms on the chest prevented the weight of the arms on the trunk and subsequent distortion of surface contours and marks [10]. In the case of the treatment of extremities, the patient position and the type of immobilisation device should be defined to distance the tumour site as far as possible from the trunk.

The patient should be positioned parallel to the table top with minimal rotation. Longitudinal and lateral reference ink or tattoo marks are used for accurate alignment and reproducibility. If the RT cannot attend with the patient during the imaging procedure the importance of these reference marks must be stressed to the imaging staff.

Table tops

Table tops on the treatment units are flat and narrow to facilitate rotation of the gantry. Table tops must be rigid to prevent sag under the patient weight. Mattresses are not used in radiotherapy to avoid patient-positional variation in the AP/PA direction as a result of variation in mattress depression. These conditions must be replicated in the PET or PET/CT and necessitate the introduction of a flat table top insert of equal width and flexibility into the PET or PET/CT table. The table top must be securely fitted to the PET/CT couch and must be consistent with the table tops in the treatment rooms and should allow registration or indexing of immobilisation devices. This may further reduce the effective size of the bore particularly with larger patients. When immobilisation devices are used in radiotherapy their exact position relative to the table top is registered for reproducibility. If possible registration of the immobilisation device to the table top should be enabled in the PET/CT. The couch coordinates can then be set and tracked in the Record and Verify System [11]. Clear, detailed instructions for storage and insertion of the couch top and registration of immobilisation devices should be prepared for the Nuclear Medicine staff.

Laser lights

Key to accurate reproducibility is alignment. For accurate patient positioning and alignment lateral and sagital lasers are used to ensure that the patient is straight/parallel on the treatment couch with no lateral rotation. This initial positioning is a critical component of the process and it is important that the images for treatment planning are acquired with the patient in the treatment position. The patient should be as comfortable as possible as this helps to maintain stability. A laser light system consistent with the treatment unit should be installed in the PET/CT unit. Quality assurance procedures on the laser lights should be carried out routinely by the staff of the radiotherapy department to ensure that consistency with the treatment room lasers is maintained. A simple protocol for checking the laser lights daily before use should be prepared for the Nuclear Medicine staff with alerts for variation levels that should be reported prior to scan acquisition.

Psychological impact

Particularly where the PET component bore is smaller than the CT the psychological impact on the patient must be considered. They will be required to remain still for a prolonged period of time in what may be a difficult and uncomfortable position in what quantifies a claustrophobic situation. Patient stability and reproducibility is directly related to comfort and a balance needs to be achieved. Patient movement including respiration results in artefacts on the acquired image and therefore a detailed explanation should be given to the patient prior to commencement of the scanning procedure. Artefacts will be introduced due to the variation in scan time between CT and PET image acquisition and careful patient preparation will keep this to a minimum.

Patient preparation should include information on the approximate time for the procedure, the size of the aperture through which the patient will pass, and the necessity for the patient to remain calm still and to breathe quietly and evenly during the scanning time. This is routine in the Nuclear Medicine department for any PET scanning procedure but, in addition, the patient should understand how this procedure fits into the overall plan of treatment and the importance of their cooperation. The patient should be assured that they will be observed at all times throughout the procedure and can indicate distress at any point.

Immobilisation devices

To achieve stability and reproducibility a wide range of immobilisation devices are used. These will be specific to the site to be treated. As previously mentioned, the patient should be in as comfortable a position as is feasible within the confines of accurate immobilisation. A balance must be achieved between the optimum immobilisation method, patient comfort and the ability to acquire images in the treatment position. Careful consideration should be given to the patient position and the type of immobilisation device used to ensure that it does not produce artefacts on the CT images [11,12]. This is particularly important for obese patients or patients suffering from articular fibrosis/arthrosis. Streak artefacts can arise when the patient's arms are placed alongside the body during the scanning procedure and the quality of acquired images can also be altered by the ingestion of certain oral contrast agents [13].

Where possible immobilisation aids should be patient specific and these should accompany the patient to the PET or PET/CT department. Where this is not the case a complete set of standard immobilisation material should at all time be accessible to the staff of the Nuclear Medicine or Diagnostic Imaging department consistent with that available within the radiotherapy department.

It is important to remember to update these when any changes are made. Clear guidelines on the careful storage and maintenance of these devices must be provided and the materials must be checked regularly by the staff of the radiotherapy department. If any of the material disappears or is damaged the radiotherapy department needs to be promptly informed.

Limiting factors in image acquisition for radiotherapy planning and treatment

Contrast material

Contrast material is frequently used in radiotherapy scan acquisition to define areas or volumes of specific concern. The use of contrast can be contraindicated in PET/CT acquisition due to attenuation variance. Recent studies have shown that contrast agents can be used without compromising image quality but modifications may be required to avoid artefacts in the PET images [14]. Discussion with the Nuclear Medicine staff should take place prior to scan acquisition to achieve optimum image quality with the necessary radiotherapy-related information.

PET/CT bore size

A significant limiting factor impacting on acquisition of images in the treatment position is the size of the bore and the scan field of view. The gantry of the treatment unit is free standing and rotates around the patient at an FSD appropriate to the delivery of the prescribed dose. For CT, MRI and PET the aperture size is fixed and was traditionally too small for treatment planning purposes. CT simulators are now generally available with aperture sizes up to 85 cm and wider scan field of view thus facilitating imaging in the treatment position and the ability to accurately contour the patient outline for treatment planning. The increased scan field of view does result in very small increases in noise levels of the scans and the dose to the patient but with little diagnostic or clinical impact [8]. Aperture size in PET or PET/CT units is generally smaller and will not facilitate image acquisition in the actual treatment position and modifications must be made. If the CT scan field of view is limited this may also affect the acquisition of the patient contour as the full extent of the patient skin may not be visible on the CT image. Where separate PET and CT units are used it is recommended that the CT images are acquired first. In addition, images should be acquired as close to each other in time as is feasible to minimise normal physiological changes [15]. This would be relevant where the PET/CT or CT was located in the diagnostic imaging department and not modified for radiotherapy use. These modifications will need to be considered when the treatment plan is prepared. If a radiation therapist does not accompany the patient it is essential that the Nuclear Medicine staff understand the importance of contour acquisition as part of the radiotherapy process.

Staff involved in image acquisition

In a majority of institutions, the PET or PET/CT scanner is located in the Nuclear Medicine department with defined access allocated to the radiotherapy department. For most patients the implementation of the prescription in terms of the treatment technique, the position and immobilisation method and any specific requirements such as bladder or bowel filling protocols, are defined as part of the pre-treatment procedures within the radiotherapy department.

Patient marking in radiotherapy is core to reproducibility and must be carried out with absolute accuracy. The radiation therapists are familiar with marking protocols and the importance of ensuring that reference points/lines or field outlines are marked exactly with clean fine lines. The need for this level of care and attention is rarely appreciated outside of the radiotherapy department. This usually precedes the acquisition of treatment planning PET/CTs. Due to the differing aims of the imaging, radiation therapists are more aware of the importance of initial set-up and the time that must be given to this stage of the process than diagnostic staff. Ideally, to ensure the consistency of patient set-up protocols, the radiation therapist should also be directly involved in informing and positioning the patient during scan acquisitions on the PET/CT. Department time planning should incorporate the allocated radiotherapy department time in the PET/CT unit.

Where this is not possible a close liaison between the two departments is essential in order to ensure the proper exchange of patient-related information. Clear, detailed protocols for each site including the positioning and immobilisation must be present in the Nuclear Medicine department and updated consistently with the department protocols.

The dose delivered to the patient as part of the imaging procedure is less of a concern in the context of radiotherapy and for the CT component it is important that scan acquisition is not compromised by diagnostic dose concerns. Concerns have been raised relating to staff doses when positioning patients for PET scanning for radiotherapy purposes, but a study by Kearns et al. demonstrated that doses received are well below normal parameters for staff [16].

Excellent communication between the staff of the two departments is essential and the Nuclear Medicine staff should fully understand the importance of the factors identified above in the acquisition of images for treatment planning and delivery. Regular meetings to update protocols and discuss any issues that might arise should be scheduled.

Recording and transmission of set-up data

As previously mentioned a close liaison must exist between the radiotherapy department and the PET/CT department to reduce errors in patient position. In all cases, through the use of written and photographic documentation, the initial patient set-up should be accurately recorded by the RTs. These should include clear details on the type of immobilisation method and aids used, the nature and localization of the skin markings and other patient-related factors such as oxygen need, level of pain, etc. These documents should accompany the patient from the radiotherapy department to the imaging department and should be carefully reviewed by the staff. Conversely, it is of utmost importance, that the Nuclear Medicine staff contacts the RTs if they do encounter problems in setting up the patient and all difficulties should be carefully noted in the patient's documentation.

Site specific scan acquisition

The scout images obtained prior to scanning can be very useful in evaluating patient position and will allow for any changes to be made prior to image acquisition. Where a radiation therapist cannot accompany the patient, the importance of this component of the procedure and how it can be used to confirm patient position for treatment should be explained to the Nuclear Medicine staff.

In addition to general protocols relating to image acquisition, patient positioning and care of the immobilisation material, site-specific protocols should be available clearly outlining the additional requirements for that site. There should be defined and clear protocols per type of patient set-up and/or per localization of tumour site. These protocols should be readily available to the Nuclear Medicine staff if the radiation therapist is not accompanying the patient, either electronically or in paper form, and should ideally include photographic documentation particularly if patient set-up is complex.

Head and neck region

Organ motion is virtually absent in the head and neck region so daily patient set-ups can be reproduced accurately when care and attention is paid to the preparation of immobilisation devices. Swallowing can significantly alter the tumour position and affect the image resolution and must be considered. In this region high

doses are frequently delivered and there are many organs at risk to be considered. Most patients are immobilized by some form of neck support (standard neck supports, frames, vacuum bags . . .) in addition to a head/neck cast which can be in the form of aquaplast or thermoplastic mask [17–20]. These devices are initially rigid but they become pliable when placed in warm water, allowing them to conform to the contour of the treated area and to be fixed to the treatment table with various fixation points. Five point fixation should be used where shoulder movement must be restricted and the immobilisation device must be indexed to the table top. Neck supports must be rigid and maintained in good condition. A range of supports must be available in the Nuclear Medicine department and these must be clearly labelled to avoid errors.

Upper thoracic region: Lung, oesophagus and breasts

Breathing artefacts are a factor of single slice CT systems. This can be beneficial if the patient is to be subsequently treated with free breathing but multi-slice scanners will give better quality DRRs and are more applicable if gating is to be used in treatment delivery. Artefacts are also introduced by the time variance between CT and PET image acquisition. When CT and PET images are acquired separately a mismatch in anatomy at the apex or close to the lower lung and diaphragm region can occur due to patient breathing pattern during acquisition. Gating should be considered during image acquisition to minimise artefacts arising as a result of variations in the breathing cycle over time [21–23].

Various immobilization techniques are used such as vacuum bags and masks which conform to and fix the patient's upper body [24]. While, immobilization techniques such as T-bars or wing boards facilitate positioning of the arms above the head for treatment. With the large bore scanners this position can be replicated but where the bore size is limited position modifications will have to be made. The treatment position must be replicated as far as possible within the limitations and a system of fiducial markers might be considered for accurate image co-registration [25].

Pelvic region: prostate, rectum and cervix

Patient positioning for pelvic irradiation includes care with the position of the extremities to avoid excess dose delivery to areas of tissue folds such as the groins or buttock crease. Positioning the legs to achieve maximum stability while minimising tissue folds may not be achievable with the restriction of bore size. This must be taken into consideration, particularly in the lower pelvic region. Simple knee and foot fixation methods have been shown to be equally effective for stability of the pelvis region, and should be feasible to use in most settings [26].

To reduce dose to the small bowel, some patients need to be positioned in the prone on a belly board [27]. However, this may not be possible particularly when the bore size is limited.

Prostate patients are frequently treated with a full bladder and this is contraindicated during scan acquisition as voiding immediately prior to the scan minimises the radioactivity accumulation in the urinary bladder. Furthermore, it might be necessary to use endo-rectal balloons, contrast-embedded tampons or other radioopaque material during CT mage acquisitions but which may alter PET images [28]. These factors must thus be carefully considered as part of the entire planning process.

Conclusion

Accurate positioning and immobilisation is core to treatment delivery and in ideal circumstances a radiation therapist should always accompany the patient to the Nuclear Medicine department.

Where this is not possible, as much information as possible should be provided to the staff of the Nuclear Medicine department so that they fully understand the importance of the factors described in this section.

References

[1] Trott KR. Can we reduce the incidence of second primary malignancies occurring after radiotherapy? Radiother Oncol 2009;91:1–3.
[2] Tubiana M. Can we reduce the incidence of second primary malignancies occurring after radiotherapy? A critical review. Radiother Oncol 2009;91:4–15 [discussion 11–13].
[3] Budiharto T, Musat E, Poortmans P, et al. Profile of European radiotherapy departments contributing to the EORTC Radiation Oncology Group (ROG) in the 21st century. Radiother Oncol 2008;88:403–10.
[4] MacManus M, Nestle U, Rosenzweig KE, et al. Use of PET and PET/CT for radiation therapy planning: IAEA expert report 2006–2007. Radiother Oncol 2009;91:85–94.
[5] Olsen DR, Thwaites DI. Now you see it. . . Imaging in radiotherapy treatment planning and delivery. Radiother Oncol 2007;85:173–5.
[6] Gregoire V. Is there any future in radiotherapy planning without the use of PET: unraveling the myth. Radiother Oncol 2004;73:261–3.
[7] Ford EC, Herman J, Yorke E, Wahl RL. 18F-FDG PET/CT for image-guided and intensity-modulated radiotherapy. J Nucl Med 2009;50:1655–65.
[8] Parker W, Patrocinio H, Podgorsak EB, editors. Radiation oncology physics: a handbook for teachers and students. Vienna: International Atomic Energy Agency; 2005.
[9] Zaidi H, Vees H, Wissmeyer M. Molecular PET/CT imaging-guided radiation therapy treatment planning. Acad Radiol 2009;16:1108–33.
[10] Griffiths SE, Craig A, Abraham M. Radiographer roles and risk management in radiotherapy, and a UK survey. J Radiother Pract 2006;5:137–46.
[11] Mutic S. The simulation process in the determination and definition of the treatment volume and treatment planning, in technical basis of radiation therapy: practical clinical applications. Berlin: Springer Verlag; 2006.
[12] Mutic S, Palta JR, Butker EK, et al. Quality assurance for computed-tomography simulators and the computed-tomography-simulation process: report of the AAPM Radiation Therapy Committee Task Group No. 66. Med Phys 2003;30:2762–92.
[13] Levitt SH, Purdy JA, Perez CA, Vijayakumar S. Technical basis of radiation therapy: practical clinical application. 4th ed. Berlin: Springer Verlag; 2008.
[14] Otero HJ, Yap JT, Patak MA, et al. Evaluation of low-density neutral oral contrast material in PET/CT for tumor imaging: results of a randomized clinical trial. AJR Am J Roentgenol 2009;193:326–32.
[15] Paulino AC. PT–CT in radiotherapy treatment planning. USA: Saunders Elsevier; 2008.
[16] Kearns WT, Urbanic JJ, Hampton CJ, et al. Radiation safety issues with positron-emission/computed tomography simulation for stereotactic body radiation therapy. J Appl Clin Med Phys 2008;9:2763.
[17] Bentel GC, Marks LB, Hendren K, Brizel DM. Comparison of two head and neck immobilization systems. Int J Radiat Oncol Biol Phys 1997;38:867–73.
[18] Bentel GC, Marks LB, Sherouse GW, Spencer DP. A customized head and neck support system. Int J Radiat Oncol Biol Phys 1995;32:245–8.
[19] Saw CB, Yakoob R, Enke CA, Lau TP, Ayyangar KM. Immobilization devices for intensity-modulated radiation therapy (IMRT). Med Dosim 2001;26:71–7.
[20] Verhey LJ. Immobilizing and positioning patients for radiotherapy. Semin Radiat Oncol 1995;5:100–14.
[21] McNair HA, Brock J, Symonds-Tayler JRN, et al. Feasibility of the use of the Active Breathing Coordinator (ABC) in patients receiving radical radiotherapy for non-small cell lung cancer (NSCLC). Radiother Oncol 2009;93:424–9.
[22] Guckenberger M, Krieger T, Richter A, et al. Potential of image-guidance, gating and real-time tracking to improve accuracy in pulmonary stereotactic body radiotherapy. Radiother Oncol 2009;91:288–95.
[23] Han K, Cheung P, Basran PS, et al. A comparison of two immobilization systems for stereotactic body radiation therapy of lung tumors. Radiother Oncol 2010;95:103–8.
[24] Hurkmans CW, Remeijer P, Lebesque JV, Mijnheer BJ. Set-up verification using portal imaging; review of current clinical practice. Radiother Oncol 2001;58:105–20.
[25] MacManus M, Leong T. Review: incorporating PET information into radiation therapy planning. Biomed Imaging Interv J 2007;3:e4.
[26] Haworth A, Kearvell R, Greer PB, et al. Assuring high quality treatment delivery in clinical trials – results from the Trans-Tasman Radiation Oncology Group (TROG) study 03.04 "RADAR" set-up accuracy study. Radiother Oncol 2009;90:299–306.
[27] O'Neill L, Armstrong J, Buckney S, et al. A phase II trial for the optimisation of treatment position in the radiation therapy of prostate cancer. Radiother Oncol 2008;88:61–6.
[28] Smeenk RJ, Teh BS, Butler EB, van Lin EN, Kaanders JH. Is there a role for endorectal balloons in prostate radiotherapy? A systematic review. Radiother Oncol 2010;95:277–82.

Review

Segmentation of positron emission tomography images: Some recommendations for target delineation in radiation oncology

John A. Lee *

Centre for Molecular Imaging and Experimental Radiotherapy (IMRE 5469), Université catholique de Louvain, Brussels, Belgium

ARTICLE INFO

ABSTRACT

Positron emission tomography can be used in radiation oncology for the delineation of target volumes in the treatment planning stage. Numerous publications deal with this topic and the scientific community has investigated many methodologies, ranging from simple uptake thresholding to very elaborate probabilistic models. Nevertheless, no consensus seems to emerge. This paper reviews delineation techniques that are popular in the literature. Special attention is paid to threshold-based techniques and the caveats of this methodology are pointed out by formal analysis. Next, a simple model of positron emission tomography is suggested in order to shed some light on the difficulties of target delineation and how they might be eventually overcome. Validation aspects are considered as well. Finally, a few recommendations are gathered in the conclusion.

© 2010 European Society for Therapeutic Radiology and Oncology and European Association of Nuclear Medicine. Published by Elsevier Ireland Ltd. All rights reserved. 96 (2010) 302–307

Positron emission tomography (PET) [1,2] is increasingly used in radiation oncology, at several stages of the treatment. Before the treatment, it serves in the disease diagnosis and staging (see e.g., [3–5]). PET images can also be involved in the treatment planning [6–9]. During the treatment, PET can assess the tumour response (see e.g., [10–12]). After the treatment, PET can be used in the patient follow-up, in order to detect recurrences (see e.g., [13]). This paper mainly focuses on the treatment planning part, which typically involves the delineation of several volumes on X-ray computed tomography (CT) images. These volumes are for instance the patient body, the organs at risk (e.g., eyes, salivary glands, spinal cord, etc.), and the target volumes (the primary tumour, invaded lymph nodes, and metastases). The functional information conveyed by PET has been proved useful for the definition of target volumes in the literature [6]. In practice, the most straightforward integration of PET images into the data flow of current treatment planning systems consists in (i) drawing volumes based on the PET images, (ii) transposing these volumes on CT images after registration. The second step has been significantly simplified thanks to the advent of combined PET/CT systems [14]. On the other hand, the delineation step keeps raising many questions, in spite of the vast literature dedicated to this topic (see e.g., [15–18] and references therein). A recurrent issue is the lack of accuracy of the proposed delineation methods [17,19], with respect to the high quality standards of nowadays radiation oncology. Any error in the delineation could potentially lead to a suboptimal probability of loco-regional control of the disease or to an increased toxicity of the treatment. Progress of modern irradiation techniques, which can produce high dose gradient, obviously makes this issue even more critical.

This paper first goes through a review of the main classes of delineation methodologies. Next, we concentrate on several aspects of the most popular of them, namely threshold-based delineation. Validation issues are also briefly discussed. Finally, some recommendations and conclusions are suggested.

From delineation to segmentation

The delineation of target volumes on PET images can obviously be done by hand with an appropriate computer interface. The major drawback of this approach is the variability of the resulting contours [15]. Because of their modest resolution [1], PET images look blurred and the human eye cannot easily distinguish the boundaries of the target. An additional difficulty is related to display settings (windowing level and width). Changing the colour scale or saturation can dramatically change the perception of volumes in the images. Hence, manual delineation of targets on PET images requires a lot of expertise and strict guidelines for the display device, and remains largely operator-dependent.

If PET/CT images are available, the physician can reduce the delineation variability by looking at the fusion of the registered

* Address: Centre for molecular imaging and experimental radiotherapy (IMRE 5469), Université catholique de Louvain, Avenue Hippocrate 55/5469, B-1200 Brussels, Belgium.
  E-mail address: john.lee@uclouvain.be

images [20,21]. Superimposed images supposedly allow the physician to combine information conveyed by both modalities. PET images can help the physician to include or exclude some regions of the images. On the other hand, CT images can provide anatomic boundaries for PET-positive regions. One might naturally wonder whether the boundary seen at the anatomic modality really corresponds to the boundary of the PET-positive tissue. This question is largely discussed in the literature (see e.g., [17,21–23]) and is beyond the scope of this paper. Another approach to reducing the variability of the delineation consists in relying on automatic or semi-automatic segmentation methods. Letting the computer do the job is an obvious way to ensure consistency and reproducibility, at least for fully automatic methods. In practice, target delineation is achieved by segmentation of the image [24]. This technical term refers to the action of splitting an image into non-overlapping regions that are meaningful with respect to the image semantics, i.e., there is an agreement between the regions and the underlying depicted objects. Segmentation can also be cast within a statistical framework as an unsupervised classification problem [24]. This means that one gets a data set, consisting of several items (e.g., pixels), and one wants to give a label to each item with some level of certainty.

Review of automatic delineation methodologies

Image segmentation can be achieved in various ways. The simplest method consists in considering each pixel independently and to determine its class label by looking solely at its value. This turns out to be equivalent to building the image histogram and to split it into several parts thanks to one or several thresholds. In a binary problem (e.g., with two classes: target and non-target), one threshold is sufficient.

Thresholding can be refined in several ways. The simplest and most common approach is hard-thresholding and consists in a binary decision: any voxel with an uptake higher than the threshold value belongs to the target. Alternatively, hard thresholds can be replaced with probabilistic modelling [25], that is, "soft thresholding". The histogram is then approximated by a mixture of several probability density functions, one for each class. Parameters of the densities can be adjusted using the expectation–maximization algorithm [26]. This approach allows the user to balance the rates of false positives and false negatives.

Another refinement is provided by clustering methods [27]. Schematically, clustering aims at gathering items with similar properties, e.g., pixels with close values. Clustering generalizes thresholding to more than two regions or to multivalued pixels and it can thus be useful when the target is surrounded by several other regions such as healthy tissues, air, inflammation, etc., which all have a different uptake. Multivalued pixels are encountered in dynamic PET images: each pixel is associated with a time activity curve and takes several values during the course of the acquisition [28]. Clustering is also particularly useful in multimodal segmentation [29]. Like thresholding, clustering can entail hard boundaries (e.g., K-means [25]) as well as soft or probabilistic ones (e.g., fuzzy K-means [27]) or mixtures of multivariate distributions ([25]).

Most of the above-mentioned methods make their decisions without taking into account the structure of the image and the spatial relationships between pixels. Only pixel values are used to identify regions. Accounting for this structure can be achieved in various ways. For instance, one can feed a clustering algorithm with multivalued pixels, composed of the genuine pixel value plus combinations of adjacent pixels [30,31]. The image processing community can also provide us with segmentation methods that work directly on the image and fully exploit its spatial structure. Such methods are for instance active contours (deformable contours that stick to high gradient zones) [29,32,33], the watershed transform (flooding simulation on a gradient magnitude image) [34,35], or hidden Markov random fields (generalization of soft clustering that takes into account the spatial structure of the image) [36,37]. In contrast to thresholding, these methods provide more flexibility, at the expense of a bigger complexity and a larger number of parameters to be tuned in many cases.

Nevertheless, the capability of a delineation technique to take into account the interdependences between neighbouring pixels is not a guarantee of success. Resolution blur generates indeed a specific type of interdependences, whose correct modelling is the key to delineation accuracy. In this respect, methods that explicitly account for resolution blur in their model (see e.g., [35]) are likely to outperform those in which interdependences are not directly related to resolution blur. The former methods are closely related to state-of-the-art PVE correction techniques [38] and typically involve a deblurring step that is achieved with a deconvolution algorithm [39,40]. They also show a great versatility and can be adapted to different PET systems in a straightforward and principled way. For instance, the method described in [35] has been used with various systems in [12,28].

Thresholding in question

As a matter of fact, thresholding is an old [41] but still very popular automatic method of segmenting PET images (see e.g., [15,17,18,42–47] and references therein). As the goal is to separate a region with high uptake from a background with lower uptake, the idea of an intensity threshold naturally emerges. It is both intuitive to understand and easy to implement: all pixels having an intensity that is lower than the threshold are labeled as non-target whereas those with a higher intensity are considered to belong to the target region. In order to avoid disconnected regions, region-growing [24] algorithms can refine the process. Their purpose is to avoid speckled regions, by considering the neighbourhood of each pixel in addition to its own value. If a pixel has an intensity that classifies it in region A whereas the majority of its neighbours are in region B, it will be seen as an outlier and swallowed by region B. Region-growing thus improves the robustness of thresholding against statistical noise. The implementation of thresholding raises several questions about the threshold value. The literature suggests many answers. If the images are appropriately normalized, e.g., expressed in standardized uptake value [48], then the threshold can be an absolute value (e.g., SUV = 2.5 [15,17,18,49]). The threshold can otherwise be specified in a relative way, with respect to lower and/or upper landmarks; these can be for instance the average uptake in the background and the maximum value inside the target [50–52]. The average background uptake is sometimes subtracted from the maximum target uptake [46,53–55]. As to the threshold, it can be a single, fixed percentage in all cases or its value can be adaptive [17], that is, specific to each situation. A value of approximately 40 percent of the maximum value in the target region is often mentioned for methods with a fixed threshold [41,56]. Adaptive methods often rely on calibrated curves that give the threshold as a function of some variable such as the source-to-background ratio [52,57,58]. This approach makes these methods applicable to a broader range of cases. In particular, it tends to increase their robustness against partial volume effect (PVE) [38,52].

Many threshold-based delineation techniques found in the literature still rely on an empiric methodology. Phantom images are acquired with objects of various shapes and sizes and measurements are collected. These are for instance the average background uptake, the maximum uptake inside the objects, and of course the threshold that allows the objects to be delineated as exactly as possible. Next, regression is carried on in order to obtain the threshold as a function of the measured quantities. After regression,

performing the same measurements on any new object leads to an approximation of the optimal threshold. In this methodology, nothing guarantees that the measured quantities are optimal or even meaningful. In addition, this methodology is not easily transposable from one PET system to another, as it does not clearly identify how key parameters such as the resolution [59] of the images influence the delineation result [52]. A more principled approach to the problem should actually focus on those important parameters. Blur caused by the low resolution of PET image is likely to account for the difficulty of target delineation. Several publications have pursued this line of investigation, in both SPECT [60,61] and PET [46] literatures. Briefly, the principle is as follows. Resolution blur can be simulated by convolving sharp images with a Gaussian function that approximates the point-spread function (PSF) [59] of the considered PET system. This mathematical tool allows us to visualize how blur actually distorts the contours of the depicted objects. It has been used in simple configurations such as spherical objects, with uniform uptakes both inside and outside. In this case, the threshold curve can be analytically determined and even the cold wall of the spheres can be modelled [46,62].

Simulations as described above convey much information. For instance, they show that the optimal threshold depends on the size, shape, and uptake of the object to be delineated [61]. By 'optimal' it is meant that the threshold can be adjusted in such a way that the delineated volume matches the true object volume. Unfortunately, the relationship between the threshold and the object properties is difficult to establish. The conditions to obtain an accurate delineation, that is, an exact (or very close) correspondence between the delineated and true contours are very strict. From the formal analysis given in [46,61,62], one can conclude the following: considering an object whose largest diameter is less than ten times the image resolution, given as the full width at half maximum (FWHM) of the PSF, there exists a single threshold value that allows the true contours of the object to be accurately recovered if and only if (i) the object is spherical, (ii) the uptake is uniform inside and outside the object, and (iii) the PSF is isotropic and constant over the whole field of view. As a corollary, the same analysis [46] tells that (i) the threshold must be expressed as a percentage with 0% being the background uptake and 100% being the maximum target uptake and (ii) the optimal threshold depends on the ratio given by the sphere radius divided by the PSF FWHM. The resulting curve is illustrated in Fig. 1. For small spheres, a high

threshold (>50%) compensates for the typical uptake loss that is related to PVE [38]. For mid-sized spheres, PVE is negligible but edges are still heavily smoothed, requiring a low threshold. For large spheres, both PVE and resolution blur become negligible and the threshold converges on the intuitive value of 50%. Incidentally, thresholds ranging from 35 to 45% correspond to radius/FWHM ratios that are typical of mid-sized tumours (diameter of less than 4 cm) imaged with conventional PET systems (smoothed/filtered images having a FWHM PSF of 4–7 mm). Hence this provides a theoretical justification to thresholds about 40% that are applied to smoothed images in the literature [46].

The above model shows that the delineation problem is circular already in a very simple configuration. The threshold that gives the contour of the spherical volume, and thus its radius, depends on a ratio that involves itself the unknown radius. Therefore, the threshold should be determined in an iterative way [46]. Successive trials can help to find out an agreement between the assumed ratio (radius/FWHM), the corresponding threshold, and the resulting radius. Eventually, accurate threshold-based delineation turns out to be difficult in simple cases. If any of the above-mentioned conditions (sphericity, uniformity, etc.) is not satisfied, then the situation gets even worse and the true object contour cannot be exactly recovered (see Fig. 2). In real cases, delineation accuracy of thresholding (in terms of contours, not volumes) is thus likely to be low, because noise and reproducibility issues come as additional difficulties. This rather discouraging situation is confirmed empirically in numerous studies (see comparisons and references in [17–19,42–45], for instance).

Validation issues

The purpose of validation is basically to check that the considered delineation method is applicable to a broad range of cases with a reasonable accuracy. Quality and pertinence of validation thus depends on (i) the set of images it involves and (ii) the quality criteria it uses to assess the discrepancy between the obtained result and the desired one.

Several types of images can be used in validation. Computer-generated images are typically useful in the primary steps of validation, as a proof of concept [35,46,61]. They can be produced in a straightforward way by a two-step model of the considered PET
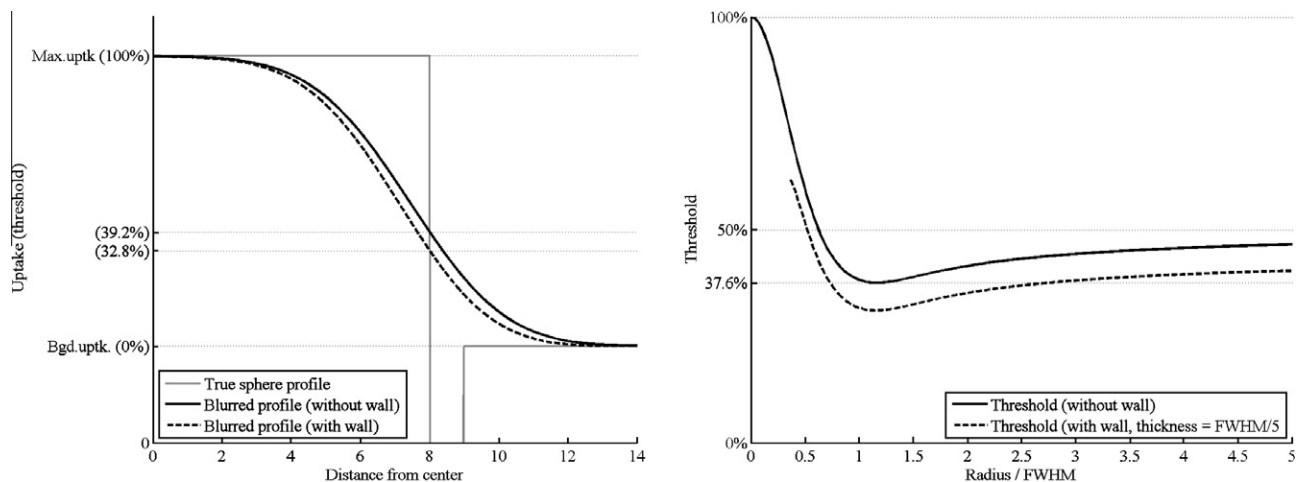

Fig. 1. Threshold-based delineation of spherical objects. The left diagram considers a sphere with a radius of 8 mm and a 1 mm-thick wall. The uptake is four times higher inside the sphere than outside; it is null within the wall. Three profiles are shown: the true uptake (infinitely high resolution, i.e., zero PSF FWHM), the blurred profile (Gaussian isotropic PSF with FWHM = 5 mm) when the cold wall is neglected, and the blurred profile (same resolution) when the wall is taken into account. The right diagram shows the threshold that allows the exact delineation of a sphere in a blurred image. The PSF is assumed to be Gaussian and isotropic. The threshold is expressed as a percentage of the maximum uptake after subtraction of the background activity. A mathematical analysis reveals that the threshold varies with respect to the ratio given by the sphere radius divided by the PSF FWHM. Two curves are drawn, depending on whether the sphere wall is taken into account or not.
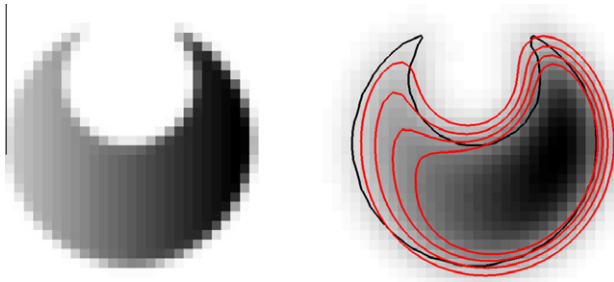
Fig. 2. Effect of resolution blur on threshold-based delineation. The object to be delineated consists of two intersecting spheres having radii equal to 13 and 7 mm. Uptake is zero everywhere except in the part of the large sphere that does not intersect with the small one. Uptake is non-uniform and grows linearly from left to right. The same slice of the three-dimensional object is depicted twice, with 1 mm^3 voxels. On the left, resolution is high (PSF FWHM no larger than 1 mm); on the right, the resolution is lower and representative of a modern PET system (Gaussian PSF with an isotropic FWHM of 5 mm). The blurred image of the object is delineated five times. The black curve is the true contour of the object (7.786 ml), whereas the red ones correspond to thresholds respectively equal to 20% (9.971 ml), 30% (7.747 ml), 40% (5.954 ml), and 50% (4.421 ml) of the maximum uptake. As can be seen, a threshold of 30% delineates the object with nearly the right volume but with an important mismatch. No single threshold value is actually able to accurately recover the true object contour. The above toy example illustrates only two difficulties, namely a non-uniform uptake and a non-spherical shape. Accuracy would further decrease with a smaller object, heterogeneous background uptake, larger voxels, statistical noise, and/or object motion.

system. In this model, sharp images are first convolved with the PSF of the PET system and some noise is added afterwards [35]. A more principled method of generating artificial images consists in simulating the imaged objects and the PET system with a Monte Carlo approach [63,64]. This provides raw data (e.g., sinograms [59]), from which images can be reconstructed [65] using the PET system's software. This second method is obviously much more convincing but is more difficult to implement.

Another type of images that is often used in validation stems from phantom experiments (see e.g., [41,46,52,66]). Like artificial images, phantom images have the advantage that the experimenter can easily measure the true object properties (volume, contours, etc.) and compare them to those obtained by delineation. In this respect, it is noteworthy that phantoms usually contain plastic walls that separate compartments with different tracer concentrations. Though thin, these walls have a non-negligible impact on the images and should be accounted for [35,46,55,62]. Compared to artificial images, phantoms do not require complex software simulations. Limitations rather come from the hardware. Objects mimicking realistic tumours with complex shapes and heterogeneous tracer concentrations prove difficult to make.

The ultimate validation step usually involves patient images. They raise many issues. They can be difficult to obtain, for financial, logistic, as well as ethical reasons. More importantly, the ground truth behind these images is nearly out of reach. In order to measure the tumour volume and its contours, the physician needs to acquire images with another modality than PET (e.g., CT) and/or to surgically extract the tumour [12,23,67,68]. Both ways are paved with difficulties. Comparing PET with another modality can raise registration and patient repositioning issues. Moreover, nothing guarantees that the alternative modality conveys trustworthy and/or relevant information. For instance, comparing PET to CT or magnetic resonance relies on the questionable assumption that the tumor contours look the same with all three modalities. Any proof of this hypothesis would at the same time reduce the interest of PET. The literature rather points in the opposite direction (see e.g., [12,23]). As to surgical specimens, difficulties are numerous and various as well. Once extracted, the surgical specimen can de-

form and/or loose volume. Further deformation can occur during freezing, slicing, scanning, 3D reassembly, and registration. Finally, contours that are manually drawn by an anatomopathologist are subject to the usual questions of variability and relevance (as compared to PET).

Starting from the validation material as described above, various figures of merit can assess the results of delineation techniques. The simplest criterion is to compare the volume of the delineated target with its true value. The volume difference, however, proves to be too mild a criterion: strict volume equality does not guarantee that delineated and true contours match. Volume differences should at least be analysed in terms of bias and variance, in order to distinguish systematic over- or underestimation from a lack of precision.

In fact, segmentation results should ideally be further evaluated with volume overlap measures, such as Dice's similarity index [69,70]. This index allows false positive and false negative (or equivalently, sensitivity and specificity) to be summarized in a single quantity. When the comparison with reference contours involves a registration step, mismatch measures tend to underrate delineation results as they are sensitive to registration inaccuracies as well. Many other volume comparison criteria exist, such as Hausdorff's contour-to-contour distances, barycenter distance, shape characterization, etc. They usually do not offer the intuitive simplicity of overlap measures.

From a statistical point of view, validation is the last step of a model fitting process and it aims at confirming that the considered model is appropriate with respect to the available data [71]. In the case of PET-based delineation, data consists of inputs, i.e., the images, and outputs, i.e., the target contours. Similarly, the segmentation method corresponds to the model that processes the input to produce the desired output. Statistical models can be characterized by their complexity, which roughly amounts to the number of parameters that need to be calibrated using data. For instance, the shape parameters of a curve that gives an uptake threshold with respect to a source-to-background ratio fall in this category. They are specific to the considered segmentation method and their value is 'learnt' from pre-segmented phantom images. On the other hand, a parameter such as the resolution of a PET image has a meaning by its own and it can be measured directly and independently of any image segmentation. This allows us to distinguish methods that need a calibration (e.g., [41,57,52]) from those that do not (e.g., [35,46]).

When a calibration is necessary, the available data for which the ground truth is assumed to be known must be split in two parts: the calibration set and the validation set. In many publications, calibration data consists of contoured phantom images whereas patient images are kept for validation (see e.g., [41,46,52]). From a statistical point of view, if the true contours are known for patient images, then it is actually better to mix phantom and patient data in both calibration and validation sets, provided calibration data are not reused in the validation step. Blending prevents the model from overfitting, that is, performing very well with calibration data and poorly with validation data. Ideally, the size of the calibration and validation sets should be as large as possible, especially when the model includes many parameters to be adjusted.

Summary and conclusions

Accuracy of automatic target delineation is directly conditioned by image quality [61,72]. Therefore, image acquisition and reconstruction are as important as the delineation technique itself. Increasing the acquisition duration or the tracer dose can contribute to improving the signal-to-noise ratio of the image (the larger amount of collected data reduces the statistical uncertainty in the reconstructed image). These requirements must naturally be put in

the balance with patient comfort and financial cost. Breathing and other patient movements should be carefully addressed e.g., thanks to PET acquisitions with respiratory gating [73]. Motion blur significantly complicates the delineation task.

Image reconstruction should be achieved with modern iterative algorithms, which are less prone to artifacts [64]. Beside the signal-to-noise ratio, resolution appears as another important factor in the quality of delineation [46,61]. The lower the resolution is, the stronger the object edges are blurred and distorted, making accurate delineation very difficult. Although the underlying physical process of PET limits the resolution of the images, the reconstruction has a non-negligible impact. For the purpose of image segmentation, reconstruction protocols should avoid heavy smoothing [52,65] and include resolution recovery techniques [74–76]. Obtaining higher quality images usually increases the reconstruction time. If properly designed, delineation techniques can cope with noisy images, though they are not visually pleasant. As a simple way to improve the resolution of images, Gaussian post-reconstruction smoothing can be replaced with more elaborate denoising tools, such as edge-preserving tools [35].

As to the delineation technique itself, it would be hazardous to give precise recommendations. Uptake thresholding is simple to implement but relies on very strong assumptions, namely, target sphericity, uptake uniformity inside and outside the target, and isotropy of the PET system PSF [61,46]. Results for small, heterogeneous, or non-spherical tumours are often disappointing. Theory tells that the background uptake should be subtracted and that the threshold should be a fraction of the maximum activity measured inside the target [46]. The curves in Fig. 1 show that a fixed and identical threshold applied to all targets is not appropriate, especially for small ones. As the optimal threshold depends on a ratio that involves the target size, its value should be determined in an iterative way [46]. In practice, the above described technique suffers from several shortcomings. Estimating the average uptake in the background in a user-independent way can be difficult. Similarly, the measured maximum uptake inside the target tends to overestimate the true maximum due to noise. On the other hand, averaging a few pixels around the maximum leads to an underestimation for small objects. Eventually, the iterative search for the optimal threshold can fail to converge to the right value in difficult cases (non-spherical target and/or non-uniform uptake). In brief, even the best threshold-based segmentation methods suffer from significant shortcomings that counterbalance the intuitive simplicity of their principle.

Delineation methods that stem from another paradigm than thresholding are usually more complex. Some of these methods rely on less restrictive assumptions and are thus more robust than thresholding when tumours are small and/or heterogeneous. On the other hand, their requirements in terms of image quality can be higher: they are more sensitive to noise and artefacts. It is certainly too soon to indicate a non-threshold-based delineation technique that would stand out against all other proposals. However, likely candidates should be based on a model that directly address the issue of resolution blur, as this turns out to be the main impediment toward accurate delineation. Most of the published methods also suffer from validation weaknesses. The most prominent shortcomings are the small size and low quality of the validation sets. Patient data in particular are difficult to collect and to process. Methods should also be calibrated and validated with images coming from different PET systems, in order to clearly identify the relationships that bind the method parameters to those of the considered PET systems. This would also favour the dispersion of the methods across the scientific community. In the current situation, results are difficult to reproduce and researchers are often tempted to propose a new method that eventually shows the same weaknesses. This ambient tendency toward 'yapetism' (yet another

PET image segmentation method) explains the multitude of methods found in the literature. In spite of the accomplished work, the most reliable and robust delineation method remains to be found. It will probably emerge naturally once large, shared, and high-quality validation data sets will be available among research teams.

References

[1] Valk PE, Bailey DL, Townsend DW, Maisey MN. Positron emission tomography: basic science and clinical practice. Springer; 2004.

[2] Wahl RL, Buchanan JW. Principles and practice of positron emission tomography. Lippincott Williams & Wilkins; 2002.

[3] Czernin J, Allen-Auerbach M, Schelbert HR. Improvements in cancer staging with PET/CT: literature-based evidence as of september 2006. J Nucl Med 2007;48:78S–88S.

[4] Schrevens L, Lorent N, Dooms C, Vansteenkiste J. The role of PET scan in diagnosis, staging, and management of non-small cell lung cancer. Oncologist 2004;9:633–43.

[5] Bassi MC, Turri L, Sacchetti G, et al. FDG-PET/CT imaging for staging and target volume delineation in preoperative conformal radiotherapy of rectal cancer. Int J Radiat Oncol Biol Phys 2008;70:1423–6.

[6] Grégoire V, Haustermans K, Geets X, Roels S, Lonneux M. PET-based treatment planning in radiotherapy: a new standard? J Nucl Med 2007;48:68S–77S.

[7] Ford EC, Herman J, Yorke E, Wahl RL. 18F-FDG PET/CT for image-guided and intensity-modulated radiotherapy. J Nucl Med 2009;50:1655.

[8] MacManus M, Nestle U, Rosenzweig KE, et al. Use of PET and PET/CT for radiation therapy planning: IAEA expert report 2006–2007. Radiother Oncol 2009;91:85–94.

[9] Öllers M, Bosmans G, van Baardwijk A, et al. The integration of PET–CT scans from different hospitals into radiotherapy treatment planning. Radiother Oncol 2008;87:142–6.

[10] Geets X, Tomsej M, Lee JA, et al. Adaptive biological image-guided IMRT with anatomic and functional imaging in pharyngolaryngeal tumors: impact on target volume delineation and dose distribution using helical tomotherapy. Radiother Oncol 2007;85:105–15.

[11] Feng M, Kong F, Gross M, Fernando S, Hayman JA, Ten Haken RK. Using fluorodeoxyglucose positron emission tomography to assess tumor volume during radiotherapy for non-small-cell lung cancer and its potential impact on adaptive dose escalation and normal tissue sparing. Int J Radiat Oncol Biol Phys 2009;73:1228–34.

[12] Roels S, Slagmolen P, Nuyts J, et al. Biological image-guided radiotherapy in rectal cancer: challenges and pitfalls. Int J Radiat Oncol Biol Phys 2009;75:782–90.

[13] Langenhoff BS, Oyen WJG, Jager GJ, et al. Efficacy of fluorine-18-deoxyglucose positron emission tomography in detecting tumor recurrence after local ablative therapy for liver metastases: a prospective study. J Clin Oncol 2002;20:4453–8.

[14] Kinahan P, Schmitz R, Alessio A. The physics of PET/CT scanners. In: Lin E, Alavi A, editors. PET and PET/CT: a clinical guide. Thieme; 2006. p. 3–14.

[15] Nestle U, Kremp S, Schaefer-Schuler A, et al. Comparison of different methods for the delineation of 18F-FDG PET-positive tissue for target volume definition in radiotherapy of patients with non-small-cell lung cancer. J Nucl Med 2005;46:1342–8.

[16] Drever L, Roa W, McEwan A, Robinson D. Comparison of three image segmentation techniques for target volume delineation in positron emission tomography. J Appl Clin Med Phys 2007;8:93–109.

[17] Schinagl DA, Vogel WV, Hoffmann AL, van Dalen JA, Oyen WJ, Kaanders JH. Comparison of five segmentation tools for 18F-fluorodeoxy-glucose-positron emission tomography-based target volume definition in head and neck cancer. Int J Radiat Oncol Biol Phys 2007;69:1282–9.

[18] Vees H, Senthamizhchelvan S, Miralbell R, Weber DC, Ratib O, Zaidi H. Assessment of various strategies for 18F-FET PET-guided delineation of target volumes in high-grade glioma patients. Eur J Nucl Med 2009;36:182–93.

[19] Yaremko B, Riauka T, Robinson D, et al. Thresholding in PET images of static and moving targets. Phys Med Biol 2005;50:5969–82.

[20] Riegel AC, Berson AM, Destian S, et al. Variability of gross tumor volume delineation in head-and-neck cancer using CT and PET/CT fusion. Int J Radiat Oncol Biol Phys 2006;65:726–32.

[21] Guido A, Fuccio L, Rombi B, et al. Combined 18F-FDG-PET/CT imaging in radiotherapy target delineation for head-and-neck cancer. Int J Radiat Oncol Biol Phys 2009;73:759–63.

[22] Paulino AC, Koshy M, Howell R, Schuster D, Davis LW. Comparison of CT- and FDG-PET-defined gross tumor volume in intensity modulated radiotherapy for head-and-neck cancer. Int J Radiat Oncol Biol Phys 2005;61:1385–92.

[23] Daisne J-F, Duprez T, Weynand B, et al. Tumor volume in pharyngolaryngeal squamous cell carcinoma: comparison at CT, MR imaging, and FDG-PET and validation with surgical specimen. Radiology 2004;233:93–100.

[24] Pham DL, Xu C, Prince JL. Current methods in medical image segmentation. Annu Rev Biomed Eng 2000;2:315–37.

[25] McLachlan GJ, Peel D. Finite mixture models. Wiley; 2000.

[26] Dempster AP, Laird NM, Rubin DB. Maximum likelihood from incomplete data via the EM algorithm. J Royal Stat Soc Ser B (Methodol) 1977;39:1–38.

[27] Jain AK, Murty MN, Flynn PJ. Data clustering: a review. ACM Comput Surv 1999;31:264–323.

[28] Janssen M, Aerts H, Ollers M, et al. Tumor delineation based on time activity curve differences assessed with dynamic fluorodeoxyglucose positron emission tomography computed tomography in rectal cancer patients. Int J Radiat Oncol Biol Phys 2008;73:456–65.

[29] El Naqa I, Yang D, Apte A, et al. Concurrent multimodality image segmentation by active contours for radiotherapy treatment planning. Med Phys 2007;34:4738–49.

[30] Noordam JC, Van Den Broek WHAM. Multivariate image segmentation based on geometrically guided fuzzy c-means clustering. J Chemometrics 2002;16:1–11.

[31] Cai W, Chen S, Zhang D. Fast and robust fuzzy c-means clustering algorithms incorporating local information for image segmentation. Pattern Recognit 2007;40:825–38.

[32] Kass M, Witkin A, Terzopoulos D. Snakes: active contour models. Int J Comput Vision 1988;1:321–31.

[33] Hua L, Thorstad WL, Biehl KJ, et al. A novel PET tumor delineation method based on adaptive region-growing and dualfront active contours. Med Phys 2008;35:3711–21.

[34] Roerdink JBTM, Meijster A. The watershed transform: definitions, algorithms and parallelization strategies. Fundam Inform 2001;41:187–228.

[35] Geets X, Lee JA, Bol A, Lonneux M, Grégoire V. A gradient-based method for segmenting FDG-PET images: methodology and validation. Eur J Nucl Med 2007;34:1427–38.

[36] Marroquin JL, Santana EA, Botello S. Hidden Markov measure field models for image segmentation. IEEE Trans PAMI 2003;25:1380–7.

[37] Chen JL, Gunn SR, Nixon MS, Gunn RN. Markov random field models for segmentation of PET images. Lecture Notes Comput Sci 2001;2082: 468–74.

[38] Soret M, Bacharach SL, Buvat I. Partial-volume effect in PET tumor imaging. J Nucl Med 2007;48:932–45.

[39] Kirov AS, Piao JZ, Schmidtlein CR. Partial volume effect correction in PET using regularized iterative deconvolution with variance control based on local topology. Phys Med Biol 2008;53:2577–91.

[40] Boussion N, Cheze Le Rest C, Hatt M, Visvikis D. Incorporation of wavelet-based denoising in iterative deconvolution for partial volume correction in whole-body pet imaging. Eur J Nucl Med 2009;36:1064–75.

[41] Erdi YE, Mawlawi O, Larson SM, et al. Segmentation of lung lesion volume by adaptive positron emission tomography image thresholding. Cancer 1997;80:2505S–9S.

[42] Greco C, Nehmeh SA, Schöder H, et al. Evaluation of different methods of 18F-FDG-PET target volume delineation in the radiotherapy of head and neck cancer. Am J Clin Oncol 2008;31:439–45.

[43] Schinagl DAX, Hoffmann AL, Vogel WV, et al. Can FDG-PET assist in radiotherapy target volume definition of metastatic lymph nodes in head-and-neck cancer? Radiother Oncol 2009;91:95–100.

[44] Yu W, Fu X-L, Zhang Y-J, et al. GTV spatial conformity between different delineation methods by 18FDG PET/CT and pathology in oesophageal cancer. Radiother Oncol 2009;93:441–6.

[45] Wang H, Vees H, Miralbell R, et al. 18F-fluorocholine PET-guided target volume delineation techniques for partial prostate re-irradiation in local recurrent prostate cancer. Radiother Oncol 2009;93:220–5.

[46] van Dalen JA, Hoffmann AL, Dicken V, et al. A novel iterative method for lesion delineation and volumetric quantification with FDG PET. Nucl Med Commun 2007;28:485–93.

[47] Vauclin S, Doyeux K, Hapdey S, Edet-Sanson A, Vera P, Gardin I. Development of a generic thresholding algorithm for the delineation of 18FDG-PET-positive tissue: application to the comparison of three thresholding models. Phys Med Biol 2009;54:6901–16.

[48] Thie JA. Understanding the standardized uptake value, its methods, and implications for usage. J Nucl Med 2004;45:1431–4.

[49] Wang D, Schultz CJ, Jursinic PA, et al. Initial experience of FDG-PET/CT-guided IMRT of head-and-neck carcinoma. Int J Radiat Oncol Biol Phys 2006;65:143–51.

[50] Yaremko B, Riauka T, Robinson D, Murray B, McEwan A, Roa W. Threshold modification for tumour imaging in non-small-cell lung cancer using positron emission tomography. Nucl Med Commun 2005;26:433–40.

[51] Ciernik IF, Huser M, Burger C, Davis JB, Szekely G. Automated functional image-guided radiation treatment planning for rectal cancer. Int J Radiat Oncol Biol Phys 2005;62:893–900.

[52] Daisne J-F, Sibomana M, Bol A, Doumont T, Lonneux M, Grégoire V. Tri-dimensional automatic segmentation of PET volumes based on measured source-to-background ratios: influence of reconstruction algorithms. Radiother Oncol 2003;69:247–50.

[53] Ciernik IF, Dizendorf E, Baumert BG, et al. Radiation treatment based on an integrated computer-assisted positron emission tomography (PET/CT): a feasibility study. Int J Radiat Oncol Biol Phys 2003;57:853–63.

[54] Davis JB, Reiner B, Huser M, Burger C, Szekely G, Ciernik IF. Assessment of (18)F PET signals for automatic target volume definition in radiotherapy treatment planning. Radiother Oncol 2006;80:43–50.

[55] Drever L, Robinson DM, McEwan A, Roa W. A local contrast based approach to threshold segmentation for pet target volume delineation. Med Phys 2006;33:1583–94.

[56] Biehl KJ, Kong F-M, Dehdashti F, et al. 18F-FDG PET definition of gross tumor volume for radiotherapy of non-small cell lung cancer: Is a single standardized uptake value threshold approach appropriate? J Nucl Med 2006;47:1808–12.

[57] Black QC, Grills IS, Kestin LL, et al. Defining a radiotherapy target with positron emission tomography. Int J Radiat Oncol Biol Phys 2004;60:1272–82.

[58] Brambilla M, Matheoud R, Secco C, Loi G, Krengli M, Inglese E. Threshold segmentation for PET target volume delineation in radiation treatment planning: the role of target-to-background ratio and target size. Med Phys 2008;35:1207–13.

[59] Bailey DE. Data acquisition and performance characterization in PET. In: Valk PE, Bailey DL, Townsend DW, Maisey MN, editors. Positron emission tomography: basic science and clinical practice. Springer; 2004. p. 69–90.

[60] Kessler RM, Ellis Jr JR, Eden M. Analysis of emission tomographic scan data: limitations imposed by resolution and background. J Comput Assist Tomogr 1984;8:514–22.

[61] King MA, Long DT, Brill AB. SPECT volume quantitation: influence of spatial resolution, source size and shape, and voxel size. Med Phys 1991;18:1016–24.

[62] Hofheinz F, Dittrich S, Pötzsch C, Hoff J. Effects of cold sphere walls in PET phantom measurements on the volume reproducing threshold. Phys Med Biol 2010;55:1099–113.

[63] Stute S, Tylski P, Grotus N, Buvat I. LuCaS: Efficient Monte Carlo simulations of highly realistic PET tumor images. Nuclear Science Symposium Conference Record. IEEE. 2008; p. 4010–12.

[64] Nehmeh SA, El-Zeftawy H, Greco C, et al. An iterative technique to segment PET lesions using a Monte Carlo based mathematical model. Med Phys 2009;36:4803–9.

[65] Defrise M, Kinahan PE, Michel C. Image reconstruction algorithms in PET. In: Valk PE, Bailey DL, Townsend DW, Maisey MN, editors. Positron emission tomography: basic science and clinical practice. Springer; 2004. p. 91–114.

[66] Ford EC, Kinahan PE, Hanlon L, et al. Tumor delineation using PET in head and neck cancers: threshold contouring and lesion volumes. Med Phys 2006;33:4280–8.

[67] Wong WL, Hussain K, Chevretton E, et al. Validation and clinical application of computer-combined computed tomography and positron emission tomography with 2-[18F]fluoro-2-deoxy-D-glucose head and neck images. Am J Surg 1996;172:628–32.

[68] Stroom J, Blaauwgeers H, van Baardwijk A, et al. K. Feasibility of pathology-correlated lung imaging for accurate target definition of lung tumors. Int J Radiat Oncol Biol Phys 2007;69:267–75.

[69] Dice LR. Measures of the amount of ecologic association between species. Ecology 1945;26:297–302.

[70] Zou KH, Warfield SK, Bharatha A, et al. Statistical validation of image segmentation quality based on a spatial overlap index. Acad Radiol 2004;11:178–89.

[71] Kohavi R. A study of cross-validation and bootstrap for accuracy estimation and model selection. Proc 14th Int Jt Conf Art Intell 1995;2:1137–43.

[72] Christian N, Lee JA, Bol A, De Bast M, Jordan B, Grégoire V. The limitation of PET imaging for biological adaptive-IMRT assessed in animal models. Radiother Oncol 2009;91:101–6.

[73] Nehmeh SA, Erdi YE, et al. Effect of respiratory gating on quantifying PET images of lung cancer. J Nucl Med 2002;43:876–81.

[74] Alessio A, Kinahan P, Lewellen T. Modeling and incorporation of system response functions in 3D whole body PET. IEEE Trans Med Imaging 2006;25:828–37.

[75] Panin V, Ren F, Michel C, Casey M. Fully 3-D PET reconstruction with system matrix derived from point source measurements. Phys Med Biol 2006;50:4507–26.

[76] Reader AJ. The promise of new PET image reconstruction. Phys Med 2008;24:49–56.

Review

Quantitative analysis of PET studies

Wolfgang A. Weber *

Department of Nuclear Medicine, University Hospital Freiburg, Germany

ARTICLE INFO

ABSTRACT

Quantitative analysis can be included relatively easily in clinical PET-imaging protocols, but in order to obtain meaningful quantitative results one needs to follow a standardized protocol for image acquisition and data analysis. Important factors to consider are the calibration of the PET scanner, the radiotracer uptake time and the approach for definition of regions of interests. Using such standardized acquisition protocols quantitative parameters of tumor metabolism or receptor status can be derived from tracer kinetic analysis and simplified approaches such as calculation of standardized uptake values (SUVs).

© 2010 European Society for Therapeutic Radiology and Oncology and European Association of Nuclear Medicine. Published by Elsevier Ireland Ltd. All rights reserved. 96 (2010) 308–310

Rationale for quantitative analysis of PET scans

For staging of malignant tumors PET scans are assessed visually and focally increased FDG-uptake not explained by the normal biodistribution of FDG is considered to be suspicious for metastatic disease. In a similar way PET scans may be read for radiation treatment planning, e.g., if PET is used for detection of lymph node metastases. However, quantitative analysis of the PET signal frequently becomes necessary, when PET scans are performed for the biological characterization of the tumor tissue in order to define subvolumes within a tumor mass or in order to assess the prognosis of a patient. In this context, quantitative analysis of the PET images permits objective comparisons between an individual case and data in the literature. Quantitative analysis can also differentiate unspecific binding of a tracer from specific accumulation by the studied biological process. Finally, quantification of the PET signal can facilitate observer-independent algorithms for automatic delineation of target volumes.

After appropriate image acquisition, reconstruction and scanner calibration PET images are inherently quantitative as every pixel of the image represents an activity concentration (Bq/ml). Factors that influence the accuracy of the measured activity concentrations are briefly discussed in this section and in more detail in Section 7 "PET image reconstruction, segmentation and thresholding". The focus of this chapter is on the next steps in quantification which aim to derive a biologically relevant quantitative signal from the activity concentrations measured by the PET scanner. Another important issue related to quantitative analysis of PET scans is standardization of PET image acquisition and analysis, which ensures that the results obtained at one site can be reproduced at other centers. EANM guidelines for standardization of PET imaging have been published recently [1].

Fundamentally three major biologic factors determine the uptake of a PET tracer by the tumor tissue. First the specific interaction of the imaging probe with the targeted process, e.g., the metabolic rate of glucose. This signal is, however, more or less confounded by the second factor, the unspecific accumulation of the tracer, i.e., uptake by passive diffusion or due to an increased extracellular volume. Both specific and unspecific uptakes are dependent on the amount of tracer injected and its clearance from the blood pool. The goal of quantitative analysis is to determine the specific uptake of the tracer from the total tracer uptake measured by the PET scanner.

Different PET tracers vary significantly in their specific and unspecific tumor uptakes as well as in their distribution and clearance. The approach for quantitative data analysis is therefore dependent on the individual tracer studied. Since FDG is by the most commonly used tracer for oncologic PET studies, this chapter focuses on the analysis of FDG-PET scan. Yet several of the principles discussed are also valid for other PET tracers.

Factors influencing quantitative measurements of tumor glucose utilization by FDG-PET

Quantification of tumor metabolic activity by FDG-PET is complicated by the fact that several factors [2] other than tumor glucose use have an impact on the FDG-signal. Partial volume

* Address: Department of Nuclear Medicine, University Hospital Freiburg, Hugstetterstr. 55, 79106 Freiburg, Germany.
E-mail address: wolfgang.weber@uniklinik-freiburg.de

effects can cause a marked underestimation of the true activity concentration within a tumor. For a spherical lesion with a diameter equivalent to 1.5 times the spatial resolution of the PET scanner at full width half maximum (FWHM) the measured maximum activity concentration is only about 60% of the true activity concentration. The mean activity concentration is even lower, about 30% of the true activity concentration. Only when the diameter of the lesion is about four times higher than the spatial resolution of the scanner, the difference between the peak measured activity concentration and the true activity concentration will be less than 5% [3]. In clinical studies the spatial resolution of the reconstructed images is in the range of 5 mm. This means that there is a marked underestimation of tumor FDG-uptake in tumors up to a size of 2 cm. Furthermore, the activity concentration may be considerably underestimated even in large tumors due to heterogeneous FDG-uptake.

In addition to these principal physical limitations of PET imaging, the definition of regions of interest affects the results of quantitative measurements of tumor FDG-uptake. Due to partial volume effects the mean measured tumor FDG-uptake will decrease, when the size of the region of interest used to define the tumor is increased. On the other hand, image noise will lead to larger random errors of the measured tracer uptake, when the size of the region of interest is decreased. Boellaard et al. [4] reported that these factors may cause an increase or decrease of the measured tracer uptake by at least 50%.

Furthermore, it must be considered that FDG-uptake of malignant tumors is time dependent. In most tumors tracer uptake increases for at least 90 min after injection of FDG [5,6]. Thus FDG-uptake will generally be considerably higher at later than at earlier time points. In gastric cancer, e.g., a 50% increase in tumor FDG-uptake has been observed from 40 to 90 min post-injection [6].

Plasma glucose levels have a significant influence on tumor FDG-uptake, since FDG and glucose compete for glucose transport and phosphorylation by hexokinase [7]. Therefore, FDG-uptake in diabetic patients tends to be lower than in non-diabetic patients, because plasma glucose levels are frequently elevated in this group of patients at the time of the PET scan.

Finally, FDG is not chemically identical to glucose. This means that FDG and glucose differ in their rates of phosphorylation, transport and distribution volume in a tissue. The correction factor, known as the "lumped constant" (LC), has been determined for normal brain tissue and current estimates range from 0.65 to 0.89 [8]. In malignant tumors the LC is generally unknown. Accordingly tumor FDG-uptake rates can always be only an approximation of tumor glucose utilization.

Approaches for quantitative analysis of PET scans

The FDG concentration measured by the PET scanner in a tissue is a sum of three components: (1) phosphorylated intracellular FDG, (2) unphosphorylated, intracellular FDG, and (3) unphosphorylated, intravascular FDG. Only the first component, the amount of phosphorylated FDG is directly related to the metabolic activity of the tumor cells. Static measurements of FDG-uptake, which cannot differentiate between these three components, are therefore not necessarily a measure of glucose metabolic rates. As recently reviewed in detail [9] there are numerous approaches to overcome these limitations of static imaging and to quantify tumor glucose metabolism. The two main approaches are (i) non-linear regression analysis with a two tissue compartment models and (ii) simplified tracer kinetic approaches such as Patlak–Gjedde analysis. Both approaches require dynamic PET studies of the tumor region lasting about 60 min. During this period only one bed position (about 15 cm axial field of view) can be imaged. Thus, only one tumor le-

sion can be assessed and additional scans are required for tumor staging. Because of this limitation dynamic scans are only rarely used in clinical PET studies.

Instead, tumor FDG-uptake is frequently quantified by so-called standardized uptake values or (SUVs). Only one PET scan at a fixed time post-injection is necessary to calculate SUVs according to the following formula.

$$SUV = \frac{c}{D} bw.$$

In this formula c is the tumor activity concentration measured by the PET scanner (Bq/ml), D is the injected dose (Bq) and bw is the body weight in grams.

The activity concentration in the tumor is divided by the injected dose in order to correct for the fact that different patients are injected with slightly different amounts of radioactivity for PET imaging. The multiplication with the body weight serves as a first order correction for differences in the whole body distribution of FDG. In a patient with a body weight of 50 kg the average activity concentration in the body immediately after injection will be two times higher than that in a patient with a body weight of 100 kg. By multiplying with the body weight this effect is eliminated. However, the distribution volume of FDG does obviously depend not only on patients' body weight, but also on the body composition. SUVs of malignant tumors tend to be significantly higher in obese patients, since the FDG concentration in adipose tissue is significantly smaller than in the remaining body. Accordingly, the distribution volume of FDG per kg body weight is smaller in obese than in non-obese patients, so multiplying with body weight leads to incorrectly high SUVs [10]. SUVs normalized by body surface or lean body mass have been shown to provide more reliable estimates of FDG metabolic rates in obese patients [10,11].

Overall, however, several studies have shown that SUVs are quite well correlated with more sophisticated parameters derived from tracer kinetic analysis [9,12]. This indicates that in highly metabolically active tumors contribution of unphosphorylated intracellular and intravascular FDG can be ignored when imaging is performed sufficiently late after tracer injection (i.e., about 60 min p.i.). In tumors with low metabolic activity, however, the contribution of unphosphorylated FDG to the PET signal can be significant and SUVs may therefore overestimate the metabolic activity of the tumor tissue [13].

An alternative simplified approach for quantitative analysis is the calculation of tumor/background ratios. While these ratios are easy to calculate and do not require a cross-calibration of the PET scanner and the dose calibrator, their use is associated with several problems. Dividing by the activity concentration in the reference tissue increases the statistical noise of the measurements, especially when tissues with low FDG (e.g., resting skeletal muscle) are used as reference tissues. Furthermore, tumor/background ratios are more dependent on the uptake time than SUVs, as FDG continues to be accumulated in the tumor, while it is continuously washed out from most normal tissues (e.g., liver).

Errors in SUV calculation

Although calculation of SUVs is straightforward, a number of errors may occur in clinical practice [14]. Frequent sources of error are listed in Table 1. Paravenous injection of FDG will decrease the amount of tracer that is available for uptake by the tumor and will incorrectly decrease the measured SUVs. If the injected activity is not decay corrected for the time between injection and imaging (uptake period), SUVs will be markedly underestimated. After a typical uptake period of 1 h approximately 30% of the injected activity has decayed. This means that tumor SUVs will be

Table 1
Common sources of errors in the measurement of SUVs.

Error	Effect on tumor SUV
Paravenous FDG injection, residual activity in the syringe	Incorrectly low SUV because less FDG is available to be taken up by the tumor
No decay correction of the injected activity	Incorrectly low SUV
Incorrect cross-calibration of scanner and dose calibrator	Incorrectly low or high SUV, depending on the error of the calibration factor
Body weight of the patient incorrect	The higher the body weight the higher the SUV
Different approaches to define regions of interest (e.g., 75% and 50% isocontours)	The larger the region of interest the lower the SUV
Patient movement	Incorrectly low SUV due to blurring of the tumor
Variable uptake period (time between injection and imaging)	The longer the uptake period, the higher the SUV

underestimated by a factor of approximately 1.5 if the injected activity is not decay corrected.

The interval between FDG injection and imaging (uptake period) is perhaps the most critical parameter. As described above, the activity concentration in malignant increases for at least 90 min after injection of FDG. Thus, it is difficult to compare SUVs that are measured at different times after injection. Therefore, every effort should be made to keep the range of variations of the uptake below 10 min. In clinical practice this requires careful planning of the time of FDG injection and start of scanning.

If one follows a strict protocol for data acquisition and analysis SUVs represent a fairly stable parameter that can be measured with rather high reproducibility. A series of studies have indicated that the standard error of repeated SUV measurements is about 10% [15–21].

References

[1] Boellaard R, O'Doherty MJ, Weber WA, Mottaghy FM, Lonsdale MN, Stroobants SG, et al. FDG PET and PET/CT: EANM procedure guidelines for tumour PET imaging: version 1.0. Eur J Nucl Med Mol Imaging 2010;37:181–200.

[2] Thie JA. Understanding the standardized uptake value, its methods, and implications for usage. J Nucl Med 2004;45:1431–4.

[3] Geworski L, Knoop BO, de Cabrejas ML, Knapp WH, Munz DL. Recovery correction for quantitation in emission tomography: a feasibility study. Eur J Nucl Med 2000;27:161–9.

[4] Boellaard R, Krak NC, Hoekstra OS, Lammertsma AA. Effects of noise, image resolution, and ROI definition on the accuracy of standard uptake values: a simulation study. J Nucl Med 2004;45:1519–27.

[5] Hamberg LM, Hunter GJ, Alpert NM, Choi NC, Babich JW, Fischman AJ. The dose uptake ratio as an index of glucose metabolism: useful parameter or oversimplification? J Nucl Med 1994;35:1308–12.

[6] Stahl A, Ott K, Schwaiger M, Weber WA. Comparison of different SUV-based methods for monitoring cytotoxic therapy with FDG PET. Eur J Nucl Med Mol Imaging 2004;31:1471–8.

[7] Torizuka T, Clavo AC, Wahl RL. Effect of hyperglycemia on in vitro tumor uptake of tritiated FDG, thymidine, L-methionine and L-leucine. J Nucl Med 1997;38:382–6.

[8] Wu HM, Bergsneider M, Glenn TC, Yeh E, Hovda DA, Phelps ME, et al. Measurement of the global lumped constant for 2-deoxy-2-[18F]fluoro-D-glucose in normal human brain using [15O]water and 2-deoxy-2-[18F]fluoro-D-glucose positron emission tomography imaging. A method with validation based on multiple methodologies. Mol Imaging Biol 2003;5:32–41.

[9] Krak NC, Hoekstra OS, Lammertsma AA. Measuring response to chemotherapy in locally advanced breast cancer: methodological considerations. Eur J Nucl Med Mol Imaging 2004;31:S103–11.

[10] Zasadny KR, Wahl RL. Standardized uptake values of normal tissues at PET with 2-[fluorine-18]-fluoro-2-deoxy-D-glucose: variations with body weight and a method for correction. Radiology 1993;189:847–50.

[11] Kim CK, Gupta NC. Dependency of standardized uptake values of fluorine-18 fluorodeoxyglucose on body size: comparison of body surface area correction and lean body mass correction. Nucl Med Commun 1996;17:890–4.

[12] Weber WA, Petersen V, Schmidt B, Tyndale-Hines L, Link T, Peschel C, et al. Positron emission tomography in non-small-cell lung cancer: prediction of response to chemotherapy by quantitative assessment of glucose use. J Clin Oncol 2003;21:2651–7.

[13] Huang SC. Anatomy of SUV. Standardized uptake value. Nucl Med Biol 2000;27:643–6.

[14] Weber WA. Use of PET for monitoring cancer therapy and for predicting outcome. J Nucl Med 2005;46:983–95.

[15] Jacene HA, Leboulleux S, Baba S, Chatzifotiadis D, Goudarzi B, Teytelbaum O, et al. Assessment of interobserver reproducibility in quantitative 18F-FDG PET and CT measurements of tumor response to therapy. J Nucl Med 2009;50:1760–9.

[16] Velasquez LM, Boellaard R, Kollia G, Hayes W, Hoekstra OS, Lammertsma AA, et al. Repeatability of 18F-FDG PET in a multicenter phase I study of patients with advanced gastrointestinal malignancies. J Nucl Med 2009;50:1646–54.

[17] Nahmias C, Wahl LM. Reproducibility of standardized uptake value measurements determined by 18F-FDG PET in malignant tumors. J Nucl Med 2008;49:1804–8.

[18] Minn H, Zasadny KR, Quint LE, Wahl RL. Lung cancer: reproducibility of quantitative measurements for evaluating 2-[F-18]-fluoro-2-deoxy-D-glucose uptake at PET. Radiology 1995;196:167–73.

[19] Hoekstra CJ, Hoekstra OS, Stroobants SG, Vansteenkiste J, Nuyts J, Smit EF, et al. Methods to monitor response to chemotherapy in non-small cell lung cancer with 18F-FDG PET. J Nucl Med 2002;43:1304–9.

[20] Kamibayashi T, Tsuchida T, Demura Y, Tsujikawa T, Okazawa H, Kudoh T, et al. Reproducibility of semi-quantitative parameters in FDG-PET using two different PET scanners: influence of attenuation correction method and examination interval. Mol Imaging Biol 2008;10:162–6.

[21] Weber WA, Ziegler SI, Thodtmann R, Hanauske AR, Schwaiger M. Reproducibility of metabolic measurements in malignant tumors using FDG PET. J Nucl Med 1999;40:1771–7.

Review

Detection and compensation of organ/lesion motion using 4D-PET/CT respiratory gated acquisition techniques

Valentino Bettinardi [a,d,*], Maria Picchio [a,d], Nadia Di Muzio [b], Luigi Gianolli [a], Maria Carla Gilardi [a,c,d], Cristina Messa [c,d,e,f]

[a] Nuclear Medicine; [b] Radiotherapy, San Raffaele Scientific Institute, Milan, Italy; [c] Center for Molecular Bioimaging, University of Milano-Bicocca, Milan, Italy; [d] Institute for Bioimaging and Molecular Physiology, National Research Council, Milan, Italy; [e] Nuclear Medicine, San Gerardo Hospital, Monza, Italy; [f] L.A.T.O., HSR-Giglio, Cefalù, Italy

ABSTRACT

Purpose: To describe the degradation effects produced by respiratory organ and lesion motion on PET/CT images and to define the role of respiratory gated (RG) 4D-PET/CT techniques to compensate for such effects.
Methods: Based on the literature and on our own experience, technical recommendations and clinical indications for the use of RG 4D PET/CT have been outlined.
Results: RG 4D-PET/CT techniques require a state of the art PET/CT scanner, a respiratory monitoring system and dedicated acquisition and processing protocols. Patient training is particularly important to obtain a regular breathing pattern. An adequate number of phases has to be selected to balance motion compensation and statistical noise. RG 4D PET/CT motion free images may be clinically useful for tumour tissue characterization, monitoring patient treatment and target definition in radiation therapy planning.
Conclusions: RG 4D PET/CT is a valuable tool to improve image quality and quantitative accuracy and to assess and measure organ and lesion motion for radiotherapy planning.
© 2010 European Society for Therapeutic Radiology and Oncology and European Association of Nuclear Medicine. Published by Elsevier Ireland Ltd. All rights reserved. 96 (2010) 311–316

Integrated positron emission tomography/computed tomography (PET/CT) imaging with the use of [^{18}F]fluorodeoxyglucose (FDG) is a widely established imaging technique with major indications in oncology for staging, re-staging and monitoring response to therapy. FDG-PET/CT is also used in radiation oncology for target volume definition and treatment strategy, taking full advantage of the state of the art technology. As an example, intensity modulated radiation therapy (IMRT) allows highly accurate conformal treatments. PET biological information (biological target volume, BTV) being integrated with the anatomical information provided by CT (gross tumor volume, GTV) may accurately characterize the tumor tissue to be treated [1–6]. However, an important source of image degradation in both CT and PET is represented by organ movements, mainly due to cardiac and respiratory motion, affecting: (i) image quality and quantitative accuracy for diagnostic purposes and (ii) the ability to define accurate target volumes in radiation oncology. Whereas cardiac motion has important local effects on the heart itself and on areas proximal to the heart, respiratory motion affects the imaging for the majority of the body extent, from the thorax to the abdomen (including heart, lungs, liver, pancreas and kidneys). It has been reported that organ displacements of about 5, 5 and 20 mm may occur in anterior–posterior, left–right and superior–inferior directions, during normal breathing [7,8].

In CT imaging, organs' motion can produce inaccurate information about the size, shape and volume of the anatomical region under examination [9,10]. To avoid motion artefacts, most of the CT clinical protocols are performed in breath-holding condition. This procedure is easily accomplished in CT, because of the short duration of CT scans (few seconds), particularly when the latest generation multi-slice CT scanners are used.

Conversely, breath-holding is not feasible in PET, due to the long acquisition time needed to complete a whole body PET study (1–3 min/field of view × 6–8 fields of view). PET studies, performed in free breathing condition, are thus affected by motion artefacts, resulting in image degradation effects. As a result of motion, the radioactivity of a concentrated source (lesion) appears smeared over the volume of displacement, causing a loss of image contrast (thus of lesion detectability), an underestimation of the tracer uptake (radioactivity concentration, as measured by standardized uptake value – SUV), and an overestimation of the lesion volume [11–13].

Furthermore, when using integrated PET/CT tomographs, to combine anatomical CT and functional PET information, the temporal mismatch between the short (few seconds) CT and the long (minutes) PET scans may generate a spatial misalignment

* Corresponding author. Address: Nuclear Medicine, San Raffaele Scientific Institute, Milan, Italy.
E-mail address: valentino.bettinardi@hsr.it (V. Bettinardi).

between CT and PET data. This misalignment is responsible for artefacts in the reconstructed PET images, when CT is used for attenuation correction [14–16].

The limitations in PET image quality and quantitative accuracy caused by motion explain the growing interest in studying the effects of breathing and in developing methods to control and compensate for the degradation effects related to motion. To this regard, one of the most recent technological progresses of integrated PET/CT systems is related to the development of respiratory gated (RG) 4D-PET/CT acquisition techniques. The RG 4D-PET/CT techniques, by synchronizing PET and CT acquisition to the patient's respiratory cycle, represents an innovative methodology for accurate imaging of tumors, particularly those located in the thorax and in the upper abdomen, where organ/lesion motion is relevant. The aim of RG 4D-PET/CT techniques is, in fact, to produce "motion free" and well-matched PET and CT images corresponding to specific phases of the patient's respiratory cycle [17,18]. The RG 4D-PET/CT techniques might have a great impact on: (i) clinical diagnostic applications, where the goal is the detection and the accurate metabolic characterization of lesions affected by respiratory movements and (ii) radiation therapy, where the goal is to assess, the true volume of the tumor and its real motion, to obtain an accurate target delineation and, in general, a more accurate and personalized definition of the treatment plan [7,19–24].

RG 4D-PET/CT: technical aspects

There are three essential tools required to perform RG 4D-PET/CT studies. These are:

 (i) an integrated PET/CT system;
 (ii) a respiratory monitoring system to detect and record a signal representative of the patient's respiratory cycle, synchronized to 4D-CT and 4D-PET data acquisition;
 (iii) acquisition and processing protocols dedicated to RG 4D-PET/CT studies.

Integrated PET/CT system

State of the art PET/CT systems have to be characterized by powerful hardware and dedicated software, to process the large amount of data, as those produced in an RG 4D-PET/CT study. Furthermore, for RT applications: (i) additional external lasers have to be installed in the PET/CT room, to reproduce the same spatial reference system as in radiation therapy, (ii) a flat patient table has to be available, to reproduce the same setting of the patient as during radiation treatment, and (iii) the gantry bore should be wide ($\geqslant 70$ cm), to allow the use of patient's positioning/immobilization devices specifically designed for radiation therapy applications.

Respiratory monitoring system

Several devices can be used as respiratory monitoring systems [25], based on different physical principles:

– *pressure sensor:* it consists of an elastic belt containing a load-cell (sensor) that can be fastened around the patient's abdomen or thorax. With respiratory movements the belt tightens producing a change of the pressure inside the belt, which is detected and measured by the load-cell;
– *spirometry system:* it measures the respiratory flow of air incoming and out-coming from the lungs;
– *strain-gauge belt:* it measures the volumetric expansion of the chest as a change of either resistance or voltage of an electric transducer (e.g. piezoelectric element);

– *temperature sensor:* it measures the temperature of the air incoming and out-coming from the nose during breathing;
– *opto-electronic system:* it detects, by using optical methods (e.g. infrared light), the movements of one or more markers positioned either on the chest or on the abdomen of the patient.

It is important to note that among the different respiratory monitoring systems, only the spirometry system reveals the patient's breathing pattern through a signal directly associated to patient's respiration, whereas all other respiratory monitoring systems detect the breathing pattern through an indirect measurement of the patient's breathing signal (e.g. expansion of the chest, abdomen motion).

Respiratory monitoring systems, during both 4D-CT and 4D-PET scans, should allow:

 (i) detection and registration of the patient's breathing curve;
 (ii) detection and registration of whether the X-ray beam is On/Off;
 (iii) generation of a trigger signal at the beginning of each new breathing cycle;
 (iv) generation of a trigger signal when the breathing curve crosses a specified threshold;
 (v) conversion of the measured breathing signal in a real time breathing curve to be synchronized with the acquisition system.

RG 4D-PET/CT: acquisition and processing protocols

Once the synchronization between patient's breathing curve and acquisition system is established, RG 4D-PET/CT data can be acquired either in a prospective or in a retrospective mode [26–28]. In the prospective mode data are addressed to a selected respiratory phase during acquisition, whereas in the retrospective mode data are sorted to the appropriate respiratory phase by post-processing after acquisition.

4D-CT

In the prospective 4D-CT technique, data are selectively acquired during a time window within the breathing cycle, corresponding to a specific respiratory phase. The time window is defined by a pre-established threshold: during each breathing cycle over the CT scan, data acquisition starts and stops when the respiratory curve triggers the established threshold. The most commonly used respiratory phases for prospective 4D-CT acquisitions are those corresponding to end-expiration or end-inspiration. In particular, with respect to organ/lesion motion, end-expiration usually represents the most stable condition within the whole breathing cycle. When using the prospective 4D-CT technique, the anatomical volume is depicted in a single respiratory phase, corresponding to a specific moment of the breathing cycle, without information on the whole respiratory motion of the organ/lesion under examination.

Prospective 4D-CT protocols are commonly used, independently from the association with PET or 4D-PET, for RT applications performed in gated mode over the same phase (e.g. end-expiration or end-inspiration).

The retrospective 4D-CT technique requires the acquisition of data at each table position (over the same anatomical region) for the duration of at least one complete patient's breathing cycle. Once reconstructed the 4D-CT images are sorted in a number of phases (e.g. 10), each representative of the anatomical volume in a specific moment of the patient's breathing cycle. Conversely to the prospective technique, the retrospective 4D-CT technique, by producing a set of images representative of the whole breathing cycle, allows the detection of the complete organ/lesion motion during respiration.

In a retrospective 4D-CT scan, the dose delivered to the patient is higher than that in a prospective 4D-CT scan or in a conventional helical CT scan, using the same acquisition parameters (e.g. kVp, mA).

RG 4D-CT data acquisition, both prospective and retrospective, can be performed by either the helical or the cine scanning mode [26–28]. When 4D-CT helical scan mode is used, the acquisition parameters (translation speed, gantry rotation time, pitch factor) must be properly set, in order to guarantee that each portion of the body is imaged throughout the whole breathing cycle (complete sampling), and no anatomical slice in the final reconstructed volume is missed.

In the 4D-CT cine scan mode, a step and shoot technique is adopted: the X-ray tube rotates (very fast) repeatedly around the patient in the same axial position for a time lasting at least for one complete patient's breathing cycle. The X-ray beam is then automatically turned off, the table is moved into the next adjacent axial position, and this process is repeated until the whole anatomical region of interest is fully covered. Acquisition time for each axial position is normally prolonged for 0.5–1 s, with respect to the patient's average breathing cycle, to account for possible variability in the length of the patient's respiratory cycles.

4D-PET

RG 4D-PET studies are preferentially recorded in the 3D acquisition mode, in either the prospective frame or the retrospective list acquisition mode.

The prospective frame mode requires the a priori definition of the number and duration of the phases into which each breathing cycle is divided and data are sorted during acquisition. At the end of the PET scan, data are reconstructed in a set of images corresponding to the different phases of a representative patient's breathing cycle.

By using the retrospective list mode acquisition, data are recorded event by event with their spatial and temporal information. At the end of the scan, 4D-PET raw data are processed (unlisted) and reconstructed into a number of new datasets (4D-PET phase) corresponding to the phases of the 4D-CT study.

The prospective frame acquisition mode has the advantage of a limited disk space required to store 4D data. However, due to the much higher flexibility in data processing allowed by the retrospective list acquisition mode, the prospective frame mode is currently very seldom used.

In order to perform accurate attenuation correction of the 4D-PET study, 4D-PET phases should be corrected for attenuation using the phase-matched 4D-CT data, warranting PET–CT accurate spatial registration and temporal synchronization. For this purpose, 4D-CT must be recorded in retrospective mode.

Gating schemes

Once acquired, 4D-CT and 4D-PET data are sorted and binned according to a gating scheme to create the corresponding 4D-PET/CT dataset. Different types of gating schemes are possible. All these gating schemes divide each breathing cycle into the same number of gates, either in time or in amplitude [29–32]:

- Time-based with equal gates: within each breathing cycle each gate has equal time width.
- Time-based with variable gates: the time width of the gates varies proportionally to the length of each breathing cycle.
- Amplitude-based with equal gates: each gate has the same height with respect to the amplitude of the respiratory signal.
- Amplitude-based with variable gates: the height of each gate varies with respect to the amplitude of the respiratory signal.

The choice of the best gating scheme, to be used in the sorting of 4D-PET/CT data, depends on the characteristics of the patient's breathing pattern. Although time-based methods are most commonly used in clinical PET/CT systems, mainly for their simpler implementation, amplitude-based methods are reported to provide more accurate results [29–32].

RG 4D-PET/CT: technical recommendations

Patient preparation

A condition required to obtain a valuable RG 4D-PET/CT study is the regularity of patients' respiration and their compliance during the time of the scan. For this purpose, it is suggested to well train the patient prior to RG 4D-PET/CT examination, by explaining the purpose of the study and by describing the steps of the procedure. Training is very important in radiation therapy applications, where respiration regularity is crucial, in particular when respiratory gated RT is used. To help the patient in this task, also considering that gating techniques usually increase the overall scanning time, audio and/or video coaching techniques can be used [33]. Although it may cause constraints to patient's normal breathing pattern, the use of a coaching technique assists the patient in maintaining a regular and reproducible breathing pattern. It is thus important to find the coaching technique less affecting the normal breathing pattern of the patient [33]. Furthermore, if a coaching technique is used during the RG 4D-PET/CT study, the same coaching technique has to be used during the RT treatment sessions.

RG 4D-PET/CT: acquisition and processing protocols

4D-CT

As mentioned above, 4D-CT acquired using a retrospective protocol, despite the higher radiation dose, is preferable as it allows detection of the complete organ/lesion motion and the attenuation correction of PET images with CT phase-matched images.

4D-CT at low dose (120–140 kVp and 30–90 mA, depending on patient's size and weight) may be performed in lung studies. When 4D-CT scan has to be performed with the concomitant injection of contrast media, acquisition protocols have to be optimized to the specific organ/tumor under examination (e.g. liver, pancreas), to obtain images of diagnostic quality [34,35].

Once reconstructed, the whole 4D-CT image set has to be sorted in a number of phases, each representative of the anatomical volume in a specific moment of the patient's breathing cycle. Higher the number of phases in which the breathing cycle is divided, better the time sampling and thus the description of the tumor motion. The number of phases used to sort a 4D-CT study is usually 10 [36–41].

Once generated, the 4D-CT phases can be used for target volume definition (TVD). The contour of the target in each of 4D-CT phases represents the GTV in different moments of the patient's breathing cycle. The combination of the GTVs gives the internal target volume (ITV) representing the volume of space encompassing the motion of the tumor due to the patient's respiration.

A further data processing of 4D-CT images, to be used for TVD of lung cancer, consists in the generation of maximum intensity projections (MIP) or an averaged (AVE) set of CT images. Briefly, in an MIP image each voxel reflects the greatest density values throughout all the 4D-CT phases, while in an AVE image each voxel is obtained as the arithmetic mean among the 4D-CT phases.

The use of MIP or AVE images has been proposed (for lung cancer) to reduce the workload of contouring multiple target volumes. In fact, it should be done for each of the 4D-CT phases, generated in the data processing of a 4D-CT study. Main differences between MIP or AVE images can be seen at the edges of the tumor where,

due to the motion, AVE images show blurred edges. Due to this effect, the contouring of AVE images may underestimate the volume of space encompassing the tumor motion [38,42].

Furthermore, MIP and AVE images have to be carefully evaluated in all the regions where the background and the tumor present similar Hounsfield numbers (e.g. tumors located closed to the diaphragm, nodal volumes in the mediastinum). Finally, both MIP and AVE images may be used only for lung studies [37,38].

4D-PET

Counts collected during a 4D-PET scan are subdivided among the image phases representative of a respiratory cycle. The number of phases has to be sufficiently high to produce motion-free or almost motion-free images. A main limitation in 4D-PET is thus represented by the statistical noise in the individual phases. As a result, the total acquisition time of the 4D-PET scan has to be longer than that of conventional (non-4D) scans in order to collect enough counts to balance statistical noise and motion compensation in each image phase. 4D-PET studies should be performed in 3D list mode, to take full advantage of the higher sensitivity of the 3D acquisition mode as well as of the retrospective data post-processing protocols flexibility. The suggested number of phases is six, as this represents a good compromise between statistical noise and motion compensation [20,32,43–45]. The acquisition time for an RG 4D-PET (per single FOV) can be estimated as the product of the time per bed position, in a conventional PET scan, and the established number of phases. In a 4D PET/CT study, the number of 4D CT and 4D PET phases has to be the same.

Noise control in 4D-PET is also important to allow quantitative or semi-quantitative (SUV) assessment of radioactivity concentration.

RG 4D-PET/CT: clinical indications

A general recommendation for the use of clinical RG 4D-PET/CT is the appropriate selection of patients to be referred for such procedure. A regular breathing pattern and a good patient collaboration are essential components for a valuable achievement of the whole procedure. These aspects are particularly relevant when RG 4D-PET/CT is performed to plan radiotherapy treatment. In fact, the patient's breathing pattern during RG 4D-PET/CT is supposed to be the same as during RT treatment, thus providing target volume definition accurately representative of organ and lesion motion. The rationale for the clinical use of the RG 4D-PET/CT technique relies on its capability to: (i) improve image quality in terms of lesion/background contrast; (ii) improve quantification accuracy in the estimation of the radiotracer uptake, and (iii) assess and measure organ/lesion motion. RG 4D-PET/CT provides useful information primarily in all those clinical situations where a high mobility of the target due to respiration is expected (thorax and in the upper abdomen regions). Furthermore, RG 4D-PET/CT may also be useful in those conditions where the target presents low mobility. In such cases, the use of RG 4D-PET/CT provides an objective measure of the low motion, allowing a reduction of internal target motion margins.

The following clinical indications can be envisaged:

Tumor tissue characterization

RG 4D-PET/CT techniques are particularly useful when small lesions located in regions affected by respiratory movements are under evaluation, both in the staging and the re-staging phases. In fact, as a result of the improved image quality (better lesion/background contrast), motion-free images obtained by the RG 4D-PET/CT technique provide a higher clinical confidence in the assessment and characterization of the lesion.

Table 1
RG 4D-PET/CT indications for radiotherapy applications.

Tumor location	Disease phase	Inclusion criteria
Lung	Primary cancer Recurrence Metastases	No surgical indication Small lesions ($\leqslant$50 mm) Limited number of lesions ($\leqslant$5)
Liver	Primary cancer Metastases	No surgical indication Limited number of lesions ($\leqslant$5)
Pancreas	Primary cancer Recurrence	No surgical indication
Adrenal gland	Metastases	Small lesions ($\leqslant$50 mm)

Response to therapy and follow-up

Taking advantage of the more accurate quantification of the tracer uptake, RG 4D-PET/CT techniques could be suggested in evaluating the response to treatment and in monitoring oncological patients during follow-up, by a comparative quantification of the metabolic activity of the lesion, usually performed by means of SUV changes.

Target definition in radiation therapy planning

The true assessment of the target movements, as provided by RG 4D-PET/CT techniques, allows the personalization of the target volume definition, particularly with respect to its motion characteristics. The potential reduction of the final planning target volume (PTV) may allow an increased dose delivery to the target and better sparing of the surrounding healthy tissues [35,46–49]. Clinical indications are summarized in Table 1.

In conventional radiation therapy planning, the gross tumor volume (GTV) drawn on CT images is expanded to clinical target volume (CTV) to account for the possible presence of sub-clinical disease around the lesion, then to internal target volume (ITV) to account for the possible movement of the lesion during treatment (in particular, due to patient's respiration), and finally to the PTV to also account for errors in the set-up of the patient. The expansion margins are in general standardized depending on the type and position of the tumor. When metabolic PET information are available, the biological target volume (BTV) drawn on the PET images is combined to GTV for better characterization of the lesion and the resulting target volume is expanded as previously described [47] .

When 4D-PET/CT images are used for TVD and RT treatment planning, the following procedure to define PTV is suggested:

– sum of the 4D-PET phases to generate a single PET dataset;
– draw the BTV over the resulting high statistics PET images, taking advantage of the low statistical noise for an accurate definition of the edges of the tumor. Being derived from the sum of the phases, the BTV also represents the volume of space encompassing the metabolic active part of the tumor, accounting for its motion during respiration (ITV$_{BTV}$);
– draw GTV on individual CT phases;
– expand GTV to CTV for every phase (only for primary cancer);
– the convolution (Boolean union) of the resulting CTVs defines the ITV$_{CTV}$;
– ITV$_{BTV}$ and ITV$_{CTV}$ can then be combined (Boolean union) to obtain the "anatomical/functional" ITV;
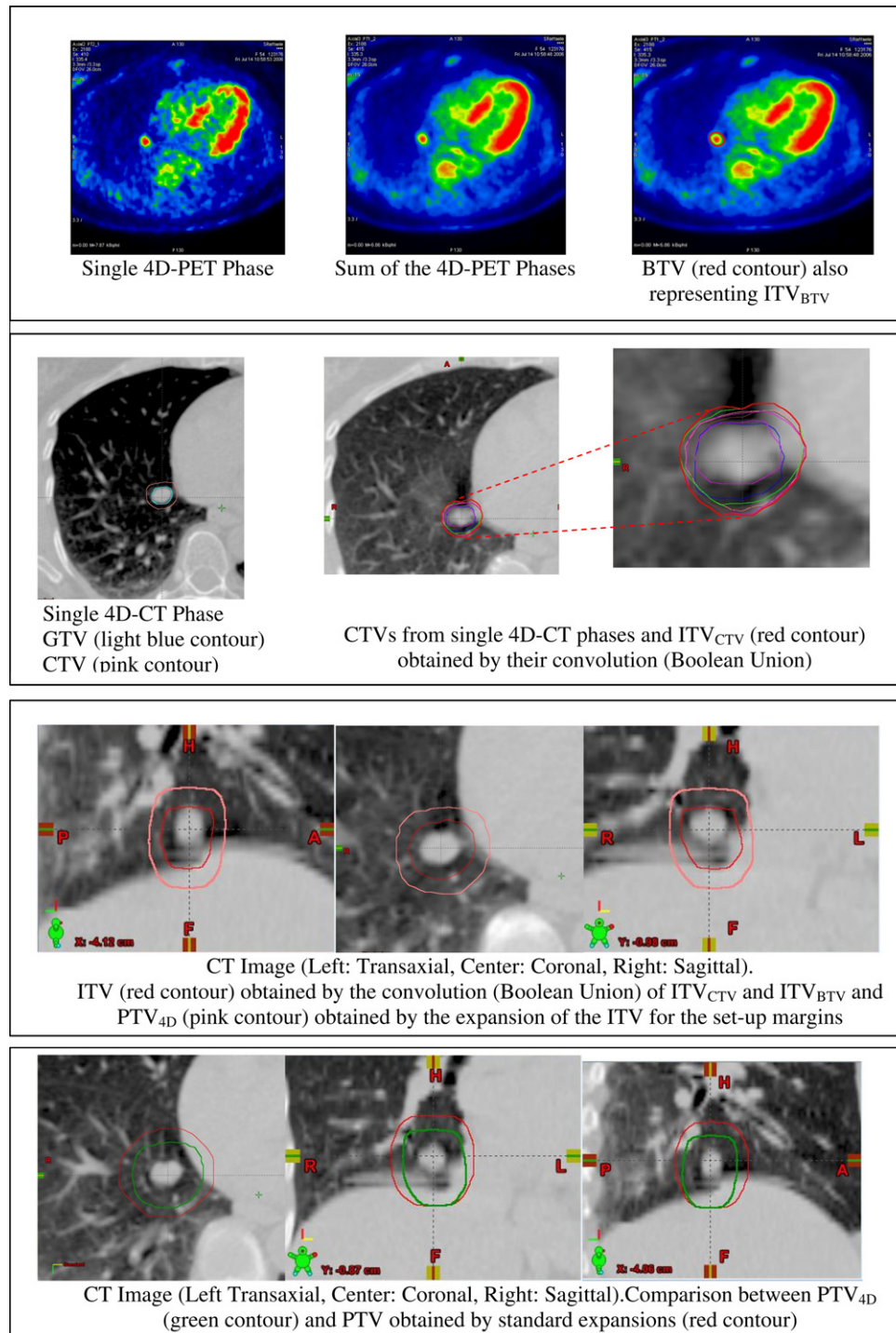– finally, expansions for set-up margins are added to ITV, to generate PTV$_{4D}$.

Fig. 1. describes the main steps of the procedure and shows how PTV$_{4D}$, which accounts for personalized motion information, is smaller than standard PTV, obtained by conventional planning expansions.

Fig. 1 describes the main steps of the procedure and shows how PTV$_{4D}$, which accounts for personalized motion information, is smaller than standard PTV, obtained by conventional planning expansions.

Conclusions

RG 4D-PET/CT seems to be a valuable tool in improving diagnostic performance of PET/CT and better defining the target volume for radiation therapy. However, its real benefit in routine clinical setting and its possible impact on patient management have not been established yet. In order to bring this technique into the normal workflow of a diagnostic imaging department, simple procedures for scanner setting, fast acquisition protocols and powerful reconstruction-processing algorithms are needed.

Today, technical improvements and optimization of the acquisition and processing protocols are making the routine clinical use of the RG 4D-PET/CT technique possible, with minimal increase in

time and in patient radiation dose, compared to conventional (non-4D) PET/CT studies.

It is likely that in the near future, a whole body PET/CT protocol that includes RG 4D-PET/CT will be recommended for routine clinical application in oncological studies, as well as in radiation therapy applications, according to specific clinical indications, as envisaged in this document.

With respect to radiation therapy, the objective measure and compensation of the movements of the target will provide a patient-specific ITV definition which may reduce the internal margins and hence the overall PTV. This approach may result in a more effective RT treatment with less side effects.

References

[1] MacManus M, Nestle U, Rosenzweig KE, et al. Use of PET and PET/CT for radiation therapy planning: IAEA expert report 2006–2007. Radiother Oncol 2009;91:85–94.

[2] Abramyuk A, Tokalov S, Zophel K, et al. Is pre-therapeutical FDG-PET/CT capable to detect high risk tumor subvolumes responsible for local failure in non-small cell lung cancer? Radiother Oncol 2009;91:399–404.

[3] Aerts HJ, van Baardwijk AA, Petit SF, et al. Identification of residual metabolic-active areas within individual NSCLC tumors using a pre-radiotherapy (18)fluorodeoxyglucose-PET–CT scan. Radiother Oncol 2009;91:386–92.

[4] Petit SF, Aerts HJ, van Loon JG, et al. Metabolic control probability in tumour subvolumes or how to guide tumour dose redistribution in non-small cell lung cancer (NSCLC): an exploratory clinical study. Radiother Oncol 2009;91:393–8.

[5] Vorwerk H, Beckmann G, Bremer M, et al. The delineation of target volumes for radiotherapy of lung cancer patients. Radiother Oncol 2009;91:455–60.

[6] Grosu AL, Piert M, Weber WA, et al. Positron emission tomography for radiation treatment planning. Strahlenther Onkol 2005;181:483–99.

[7] Keall PJ, Mageras GS, Balter JM, et al. The management of respiratory motion in radiation oncology report of AAPM Task Group 76. Med Phys 2006;33:3874–900.

[8] Brandner ED, Wu A, Chen H, et al. Abdominal organ motion measured using 4D CT. Int J Radiat Oncol Biol Phys 2006;65:554–60.

[9] Chen GT, Kung JH, Beaudette KP. Artefacts in computed tomography scanning of moving objects. Semin Radiat Oncol 2004;14:19–26.

[10] Sureshbabu W, Mawlawi O. PET/CT imaging artefacts. J Nucl Med Technol 2005;33:156–61 [quiz 63–4].

[11] Nehmeh SA, Erdi YE, Ling CC, et al. Effect of respiratory gating on quantifying PET images of lung cancer. J Nucl Med 2002;43:876–81.

[12] Nehmeh SA, Erdi YE, Ling CC, et al. Effect of respiratory gating on reducing lung motion artifacts in PET imaging of lung cancer. Med Phys 2002;29:366–71.

[13] Erdi YE, Nehmeh SA, Pan T, et al. The CT motion quantitation of lung lesions and its impact on PET-measured SUVs. J Nucl Med 2004;45:1287–92.

[14] Osman MM, Cohade C, Nakamoto Y, Wahl RL. Respiratory motion artefacts on PET emission images obtained using CT attenuation correction on PET–CT. Eur J Nucl Med Mol Imaging 2003;30:603–6.

[15] Pan T, Mawlawi O, Nehmeh SA, et al. Attenuation correction of PET images with respiration-averaged CT images in PET/CT. J Nucl Med 2005;46:1481–7.

[16] Mawlawi O, Pan T, Macapinlac HA. PET/CT imaging techniques, considerations, and artefacts. J Thorac Imaging 2006;21:99–110.

[17] Nehmeh SA, Erdi YE, Pan T, et al. Four-dimensional (4D) PET/CT imaging of the thorax. Med Phys 2004;31:3179–86.

[18] Boucher L, Rodrigue S, Lecomte R, Benard F. Respiratory gating for 3-dimensional PET of the thorax: feasibility and initial results. J Nucl Med 2004;45:214–9.

[19] Underberg RW, Lagerwaard FJ, Slotman BJ, Cuijpers JP, Senan S. Benefit of respiration-gated stereotactic radiotherapy for stage I lung cancer: an analysis of 4DCT datasets. Int J Radiat Oncol Biol Phys 2005;62:554–60.

[20] Park SJ, Ionascu D, Killoran J, et al. Evaluation of the combined effects of target size, respiratory motion and background activity on 3D and 4D PET/CT images. Phys Med Biol 2008;53:3661–79.

[21] Li G, Citrin D, Camphausen K, et al. Advances in 4D medical imaging and 4D radiation therapy. Technol Cancer Res Treat 2008;7:67–81.

[22] Berman AT, Rengan R. New approaches to radiotherapy as definitive treatment for inoperable lung cancer. Semin Thorac Cardiovasc Surg 2008;20:188–97.

[23] van der Geld YG, Senan S, de Koste JR, et al. Evaluating mobility for radiotherapy planning of lung tumors: a comparison of virtual fluoroscopy and 4DCT. Lung Cancer 2006;53:31–7.

[24] Zhao B, Yang Y, Li T, et al. Image-guided respiratory-gated lung stereotactic body radiotherapy: which target definition is optimal? Med Phys 2009;36:2248–57.

[25] Nehmeh SA, Erdi YE. Respiratory motion in positron emission tomography/computed tomography: a review. Semin Nucl Med 2008;38:167–76.

[26] Keall PJ, Starkschall G, Shukla H, et al. Acquiring 4D thoracic CT scans using a multislice helical method. Phys Med Biol 2004;49:2053–67.

[27] Pan T, Lee TY, Rietzel E, Chen GT. 4D-CT imaging of a volume influenced by respiratory motion on multi-slice CT. Med Phys 2004;31:333–40.

[28] Pan T. Comparison of helical and cine acquisitions for 4D-CT imaging with multislice CT. Med Phys 2005;32:627–34.

[29] Wink N, Panknin C, Solberg TD. Phase versus amplitude sorting of 4D-CT data. J Appl Clin Med Phys 2006;7:77–85.

[30] Abdelnour AF, Nehmeh SA, Pan T, et al. Phase and amplitude binning for 4D-CT imaging. Phys Med Biol 2007;52:3515–29.

[31] Dawood M, Buther F, Lang N, Schober O, Schafers KP. Respiratory gating in positron emission tomography: a quantitative comparison of different gating schemes. Med Phys 2007;34:3067–76.

[32] Dawood M, Buther F, Stegger L, et al. Optimal number of respiratory gates in positron emission tomography: a cardiac patient study. Med Phys 2009;36:1775–84.

[33] Kini VR, Vedam SS, Keall PJ, et al. Patient training in respiratory-gated radiotherapy. Med Dosim 2003;28:7–11.

[34] Beddar AS, Briere TM, Balter P, et al. 4D-CT imaging with synchronized intravenous contrast injection to improve delineation of liver tumors for treatment planning. Radiother Oncol 2008;87:445–8.

[35] Mancosu P, Bettinardi V, Passoni P, et al. Contrast enhanced 4D-CT imaging for target volume definition in pancreatic ductal adenocarcinoma. Radiother Oncol 2008;87:339–42.

[36] Underberg RW, Lagerwaard FJ, Cuijpers JP, et al. Four-dimensional CT scans for treatment planning in stereotactic radiotherapy for stage I lung cancer. Int J Radiat Oncol Biol Phys 2004;60:1283–90.

[37] Underberg RW, Lagerwaard FJ, Slotman BJ, Cuijpers JP, Senan S. Use of maximum intensity projections (MIP) for target volume generation in 4DCT scans for lung cancer. Int J Radiat Oncol Biol Phys 2005;63:253–60.

[38] Bradley JD, Nofal AN, El Naqa IM, et al. Comparison of helical, maximum intensity projection (MIP), and averaged intensity (AI) 4D CT imaging for stereotactic body radiation therapy (SBRT) planning in lung cancer. Radiother Oncol 2006;81:264–8.

[39] Muirhead R, McNee SG, Featherstone C, Moore K, Muscat S. Use of maximum intensity projections (MIPs) for target outlining in 4DCT radiotherapy planning. J Thorac Oncol 2008;3:1433–8.

[40] Park K, Huang L, Gagne H, Papiez L. Do maximum intensity projection images truly capture tumor motion? Int J Radiat Oncol Biol Phys 2009;73:618–25.

[41] Xi M, Liu MZ, Zhang L, et al. How many sets of 4DCT images are sufficient to determine internal target volume for liver radiotherapy? Radiother Oncol 2009;92:255–9.

[42] Ehler ED, Tome WA. Lung 4D-IMRT treatment planning: an evaluation of three methods applied to four-dimensional data sets. Radiother Oncol 2008;88:319–25.

[43] Pevsner A, Nehmeh SA, Humm JL, Mageras GS, Erdi YE. Effect of motion on tracer activity determination in CT attenuation corrected PET images: a lung phantom study. Med Phys 2005;32:2358–62.

[44] Vines DC, Keller H, Hoisak JD, Breen SL. Quantitative PET comparing gated with nongated acquisitions using a NEMA phantom with respiratory-simulated motion. J Nucl Med Technol 2007;35:246–51.

[45] Mancosu P, Sghedoni R, Bettinardi V, et al. 4D-PET data sorting into different number of phases: a NEMA IQ phantom study. J Appl Clin Med Phys 2009;10:2917.

[46] Rietzel E, Liu AK, Doppke KP, et al. Design of 4D treatment planning target volumes. Int J Radiat Oncol Biol Phys 2006;66:287–95.

[47] Hof H, Rhein B, Haering P, et al. 4D-CT-based target volume definition in stereotactic radiotherapy of lung tumours: comparison with a conventional technique using individual margins. Radiother Oncol 2009;93:419–23.

[48] D'Souza WD, Nazareth DP, Zhang B, et al. The use of gated and 4D CT imaging in planning for stereotactic body radiation therapy. Med Dosim 2007;32:92–101.

[49] Wang L, Hayes S, Paskalev K, et al. Dosimetric comparison of stereotactic body radiotherapy using 4D CT and multiphase CT images for treatment planning of lung cancer: evaluation of the impact on daily dose coverage. Radiother Oncol 2009;91:314–24.

Review

Physical radiotherapy treatment planning based on functional PET/CT data

Daniela Thorwarth [a,*], Xavier Geets [b], Marta Paiusco [c]

[a] Section for Biomedical Physics, University Hospital for Radiation Oncology, Tübingen, Germany; [b] Department of Radiation Oncology, St-Luc University Hospital, Brussels, Belgium;
[c] Medical Physics Department, Arcispedale Santa Maria Nuova, Reggio Emilia, Italy

ARTICLE INFO

ABSTRACT

Positron emission tomography (PET) provides molecular information about the tumor microenvironment in addition to anatomical imaging. Hence, it seems to be highly beneficial to integrate PET data into radiotherapy (RT) treatment planning. Functional PET images can be used in RT planning following different strategies, with different orders of complexity. In a first instance, PET imaging data can be used for better target volume delineation. A second strategy, dose painting by contours (DPBC), consists of creating an additional PET-based target volume which will then be treated with a higher dose level. In contrast, dose painting by numbers (DPBN) aims for a locally varying dose prescription according to the variation of the PET signal. For both dose painting approaches, isotoxicity planning strategies should be applied in order not to compromise organs at risk compared to conventional modern RT treatment.

In terms of physical dose painting treatment planning, several factors that may introduce limitations and uncertainties are of major importance. These are the PET voxel size, uncertainties due to image acquisition and reconstruction, a reproducible image registration, inherent biological uncertainties due to biological and chemical tracer characteristics, accurate dose calculation algorithms and radiation delivery techniques able to apply highly modulated dose distributions. Further research is necessary in order to investigate these factors and their influence on dose painting treatment planning and delivery thoroughly.

To date, dose painting remains a theoretical concept which needs further validation. Nevertheless, molecular imaging has the potential to significantly improve target volume delineation and might also serve as a basis for treatment alteration in the future.

© 2010 European Society for Therapeutic Radiology and Oncology and European Association of Nuclear Medicine. Published by Elsevier Ireland Ltd. All rights reserved. 96 (2010) 317–324

In the last decade radiation therapy (RT) has gone through a technological innovation. Advanced techniques such as conventional and helical intensity modulated radiation therapy (IMRT), and proton/ion therapy, allow highly conformal dose distributions. Combined with IGRT, they significantly improve the accuracy of radiation dose delivery. Furthermore, IMRT brings the opportunity to voluntarily deliver heterogeneous dose prescriptions within the target or to multiple targets. Adaptive radiation therapy (ART) was initially defined as "the explicit inclusion of the temporal changes in anatomy during the imaging, planning, and delivery of RT" [1], but this concept could easily be extended to the integration of temporal modifications of the tumor biology occurring during fractionated radiotherapy. The identification of such biological changes might help in adjusting radiation intensity or fields and/or altering the RT regimen, at the time when further treatment optimizations are still possible. This raises the question how to guide the optimal dose distribution. In this regard it was suggested that functional positron emission tomography (PET) imaging might be of additional value. Together with anatomical computed tomography (CT) and magnetic resonance imaging (MRI), PET offers valuable data for tumor and sensitive structures [2].

Integrating molecular imaging information as obtained from PET into RT treatment planning might be highly beneficial for the patient in terms of improved target volume definition and characterization [3–10].

For clinical PET imaging, most often the tracer [18F]Fluorodeoxyglucose (FDG) is used which allows to examine tumor metabolism [11–14]. For individual RT adaptation other specific PET biomarkers such as tracers for tumor hypoxia and proliferation might be of interest [15–21]. Tumor hypoxia can be visualized using different PET tracers such as [18F]Fluoromisonidazole (FMISO) [16], [18F]Fluoroazomycin (FAZA) [15] and Cu-ATSM [17]. In contrast, tumor proliferation can be imaged with [18F]Fluorothymidine (FLT) [22].

Molecular imaging can be used in radiotherapy treatment planning (RTP) with different intentions and levels of complexity:

* Corresponding author. Address: Section for Biomedical Physics, University Hospital for Radiation Oncology, Hoppe-Seyler-Str. 3, 72076 Tübingen, Germany.
E-mail addresses: daniela.thorwarth@med.uni-tuebingen.de (D. Thorwarth), xavier.geets@uclouvain.be (X. Geets), marta.paiusco@asmn.re.it (M. Paiusco).

(1) PET may be used as any other anatomic imaging modality to define a gross target volume (GTV) which has to be identified using a proper segmentation algorithm [11,23]. This PET-based volume will modify the GTV delineated on CT if an abnormal uptake is found outside that volume. A potential impact of PET is an increased size of the high dose planning target volume (PTV) mainly from additional inclusion of metastatic lymph nodes missed on CT or the reduction of the low-dose PTV due to the exclusion of negative lymph nodes [24,25]. In addition to target selection, additional PET data can also have a high impact on target volume delineation, by either increasing or decreasing the size of the primary GTV [12–14].

(2) The PET signal might also be used to define a subvolume in a CT-derived GTV [26]. In this case the aim of biological image-guided radiotherapy is to modify the dose to particular regions identified by functional imaging, also referred to as dose painting by contours (DPBC). Since the target dose is often restricted by surrounding organs at risk (OAR), the idea is to enhance the tumor control rate by increasing the prescribed dose only to the functional subvolume within the tumor as these regions are considered to be more radioresistant than the rest of the tumor. DPBC can be realized either by giving a simple dose boost to the functional volume during the whole treatment or only to certain fractions or by redistributing the integral dose according to this functional information.

(3) Furthermore, the functional PET image might be used to gradually shape the dose according to the voxel intensities [27–30]. This concept, dose painting by numbers (DPBN), is currently investigated by a number of academic centers. To date DPBN remains a theoretical concept.

PET/CT-based radiotherapy planning has been extensively studied during the last years. Cases are reported in which FDG PET [27], FMISO PET [17] or FAZA PET [15] imaging have been used for guiding therapy and for hypoxia-directed IMRT. Several authors have shown the theoretical feasibility of a dose escalation to the PET-based hypoxic GTV which might improve the loco-regional control without exceeding the normal tissue tolerance [16,18,19,31–34]. The only clinical dose painting trial so far has been reported by Madani et al. [33]. The trial has demonstrated the feasibility of FDG PET imaging for focused dose escalation.

However, PET imaging has some important drawbacks. One of the main limitations for biological image-guided radiotherapy is the limited spatial resolution of 5–7 mm and the related partial volume effects [35,36]. This results in an underestimation of activity and an overestimation of the size of small objects. This effect becomes even more important when PET is used for dose painting in subvolumes of the tumor as these are likely to have small diameters of only a few millimeters. One possible solution which has been proposed recently is to apply a recovery technique during image reconstruction [37,38]. In addition to the limited inherent resolution of PET, the reconstruction algorithms introduce signal noise. Hence an accurate definition of the geometric tumor extension is very difficult. Different segmentation methods have been suggested [11,23] to find a standardized delineation method but the issue is still under investigation and needs more validation studies.

Recently, a few studies were published where the temporal and spatial stability of PET signals before the start of RT were investigated from multiple examinations [20,39,40]. For a potential clinical realization of dose painting in the future, spatial and temporal stability of PET images are major requirements. Even with the advent of PET/CT, image registration is not an outdate problem. It is necessary to take into account that the acquisition times for PET

and CT are different, which can lead to misregistration effects caused by patient movement or breathing motion. In some institutions, the CT used for treatment planning is acquired separately from the PET/CT which requires subsequent image registration. In that case, in order to guarantee the reproducibility of patient positioning, laser localization, positioning aids such as masks and vacuum pillows, and a flat tabletop are necessary.

Dose painting strategies

Dose painting by contours

A first concept of integrating functional image information into treatment planning has been proposed in 2000 by Ling et al. [26]. According to this strategy, a functional PET image acquired before the start of therapy is used to delineate an additional sub-region of the PTV which shows the respective functional characteristics. This functional part of the target volume may be defined as the metabolically active volume in the GTV as assessed by an FDG PET scan [28,41] or the hypoxic fraction of the tumor imaged with dedicated hypoxia PET tracers such as FMISO [20], FAZA [15] and Cu-ATSM [21]. Dose painting by contours (DPBC) consists of applying a higher, homogeneous dose to the functional part of the PTV. The rationale for this strategy is to overcome the specific local radioresistance induced by the functional abnormality as assessed from the PET data. A major requirement for the definition of a functional PTV is the temporal and spatial stability of the respective PET images [20].

DPBC can either be realized by prescribing additional dose to the functional parts of the PTV [21] or by dose redistribution which basically means to escalate the dose to a sub-region of the PTV while keeping the mean dose to the whole PTV constant [42]. In general, treatment application and also planning for DPBC can be realized using the simultaneous integrated boost (SIB) technique. Cautious decisions have to be taken considering the question of a safety margin around the functional subvolumes. In addition, the resulting dose distribution (DD) will present with steep dose gradients. Those finite gradient regions should be carefully placed within the PTV during the planning process. One possible strategy would be a combination of positioning errors and location of the dose gradient. In other words, placing the dose gradient outside the PET-based functional target volume may have synergistic effects considering the eventual patient motion during RT.

Figure 1 shows an example of an HNC patient where FDG PET/CT was used in order to delineate the PTV of first order (PTV66). In this case, three different GTV areas were identified: the central primary tumor mass (GTV66$_C$), a lymph node on the right (GTV66$_R$) as well as on the left side (GTV66$_L$). Each of those volumes was delineated automatically with three different techniques, a 40% isocontour technique (GTV66$_{40\%}$), a 50% isocontour (GTV66$_{50\%}$), and a signal-to-background-based algorithm (GTV66$_{SB}$). The respective PTVs were generated by extending the clinical target volume (CTV) by 3 mm, whereas the CTV resulted from a 5 mm extension of the GTV. The treatment plan has been optimized for the volumes drawn with a 50% PET signal intensity threshold (PTV66$_{R50\%}$, PTV66$_{L50\%}$, PTV66$_{C50\%}$, PTV60$_{50\%}$). The planning system Eclipse vs. 8.1 was used for radiation treatment planning with the pencil beam (PB) dose engine. The resulting dose distribution (DD) as shown in Figure 1 was then evaluated for the three different sets of PET-based PTVs by comparing the corresponding dose volume histograms (DVHs). Table 1 summarizes the DVH statistics as well as the different volume sizes in detail. It was observed that the level of dose coverage did not vary significantly for all the three delineation techniques. The results suggest that the choice of employed threshold value is not so crucial for small volumes, which may be different for larger PET-based target volumes.
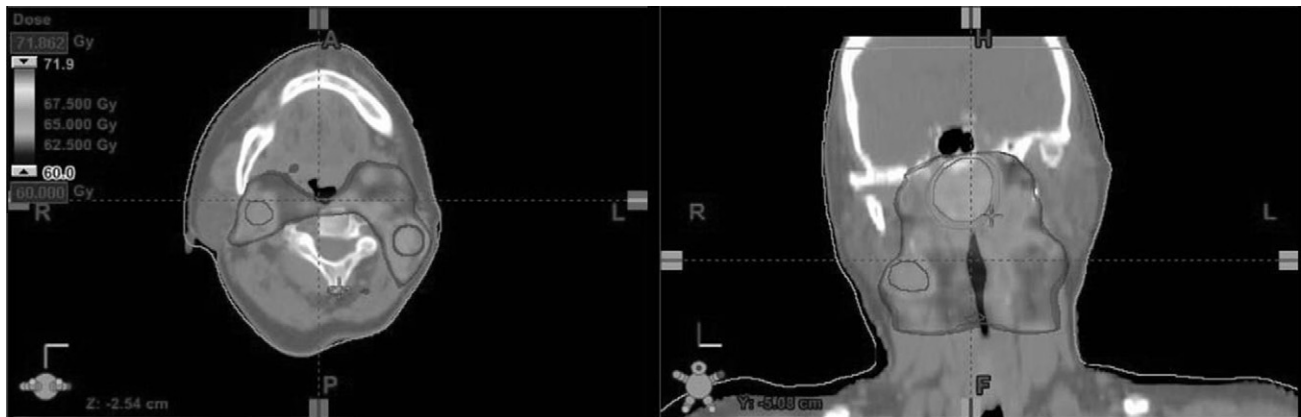
Fig. 1. Example of an HNC patient where GTVs were delineated on the basis of an [18F]-FDG PET/CT scan using different techniques. The figure shows the DD resulting from a plan optimization using the GTVs contoured with the 50% isocontour technique.

Table 1
Dose–volume histogram (DVH) details and volumes of the PTVs automatically delineated with different techniques corresponding to the example case presented in Fig. 1.

	Vol [cc]	$D_{95\%}$	$V_{100\%}$ (%)	D_{min}	D_{max}	D_{mean}
PTV66$_{R\_50\%}$	6.2	66.0	95	63.3	67.7	66.7
PTV66$_{R\_40\%}$	7.9	65.0	77	63.0	67.7	66.5
PTV66$_{R\_SB}$	8.4	65.0	77	62.8	67.7	66.4
PTV66$_{L\_50\%}$	6.8	66.4	99	65.4	68.5	67.4
PTV66$_{L\_40\%}$	8.6	65.4	90	62.9	68.5	67
PTV66$_{L\_SB}$	8.6	65.4	90	62.9	68.5	67
PTV66$_{C\_50\%}$	23.9	66.8	99	62.5	71.8	67.9
PTV66$_{C\_40\%}$	34.0	64.8	85	55.7	71.8	67.3
PTV66$_{C\_SB}$	37.9	63.7	76	54.2	71.8	66.9
PTV60$_{50\%}$	270.8	61	99	52.7	68.8	63.3
PTV60$_{40\%}$	258.7	61	99	52.7	68.5	63.2
PTV60$_{SB}$	258.7	61	99	52.7	68.5	63.2

Especially in cases where the target volumes are located close to tissue inhomogeneities, as for example in the lung region, the dose calculation algorithms used during the planning process have to be chosen carefully as they may influence clinical results. Published data show that the accuracy of dose calculation depends strongly on the performance of the calculation algorithm used [43]. Moreover, the treatment technique which is available for irradiation has a major influence on the dose gradients and hence the dose painting DD. Two recent planning studies compared the potential of IMRT, helical tomotherapy (HTT) and intensity modulated proton therapy (IMPT) for dose painting [44,45]. In both studies, it was found that proton therapy is able to deliver highly irregular DDs with steep gradients while sparing the OARs to a higher level than IMRT and HTT. Nevertheless, compared to the biological and also the geometrical uncertainties, the potential of IMRT and HTT for dose painting is comparable to that of IMPT. Moreover, modern IMRT equipments such as small multi-leaf-collimators (MLCs) in combination with dynamic sequencing techniques (dMLC) are able to fulfill the specific criteria of dose painting in terms of steep gradients and highly modulated doses.

Nevertheless, to date most dose painting prescriptions are chosen arbitrarily, no recommendations for the level of dose escalation have been published yet. Only a few centers report on clinical dose painting studies [33], whereas most groups published only theoretical planning studies [15,18,19,21,41]. Hence, DPBC is technically feasible but the clinical benefit of this technique has still to be proven by clinical trials.

For a clinical use of dose painting, isotoxicity planning approaches are very important in order to compare the treatment plans to conventional IMRT plans and also to evaluate the risks for the OARs. Figure 2 shows an example of a DPBC IMRT plan where the FDG-based volume was prescribed 110% of the regular PTV dose, i.e. 77 Gy to the metabolically active volume instead of 70 Gy to the PTV of first order (PTV70). In comparison, a conventional IMRT plan is shown for the same case. For both plans, the DD as well as the dose volume histogram (DVH) is presented in Fig. 2. OARs are not compromised when escalating the dose to this level.

Dose painting by numbers

In contrast to the previously discussed DPBC strategy, Alber et al. [28] and Bentzen [29] proposed a much more sophisticated concept of DPBN. While DPBC uses only binary information derived from the PET image, i.e. a contour that has been delineated using a dedicated segmentation method [11,23], DPBN intends to deliver spatially varying doses according to the specific functional characteristics of the tumor. This can be realized by shaping the dose according to either the local voxel intensity values of the PET image or a functional map, which has been derived from the PET data by applying a mathematical prescription function [46] (Table 2).

To date, several groups have demonstrated the theoretical feasibility of DPBN by extensive planning studies [30,41,47,48], whereas a clinical realization of this concept has not yet been reported which is due to huge technical and also clinical requirements. Most of the planning studies used arbitrary dose levels, which seems to be crucial for a potential clinical use of DPBN.

DPBN intends to assign inhomogeneous doses to the PTV. As a consequence, homogeneous dose coverage of the PTV is no longer a quality criterion for a treatment plan. New tools for plan quality evaluation are necessary. In this context, Alber et al. [28] have proposed to use the effective dose volume histogram (eDVH). These eDVHs are cumulative histograms – similar to regular DVHs – and show the fractional tumor volume which receives at least a certain percentage of the prescribed dose. Such DVH transformation allows for an objective evaluation of the target coverage in the case of inhomogeneous prescriptions.

Figure 3 shows an example of a DPBN treatment plan for an HNC patient based on dynamic FMISO PET [41].

Limitations and uncertainties

For dose painting treatment planning in general, a number of different factors in terms of errors and uncertainties will have a
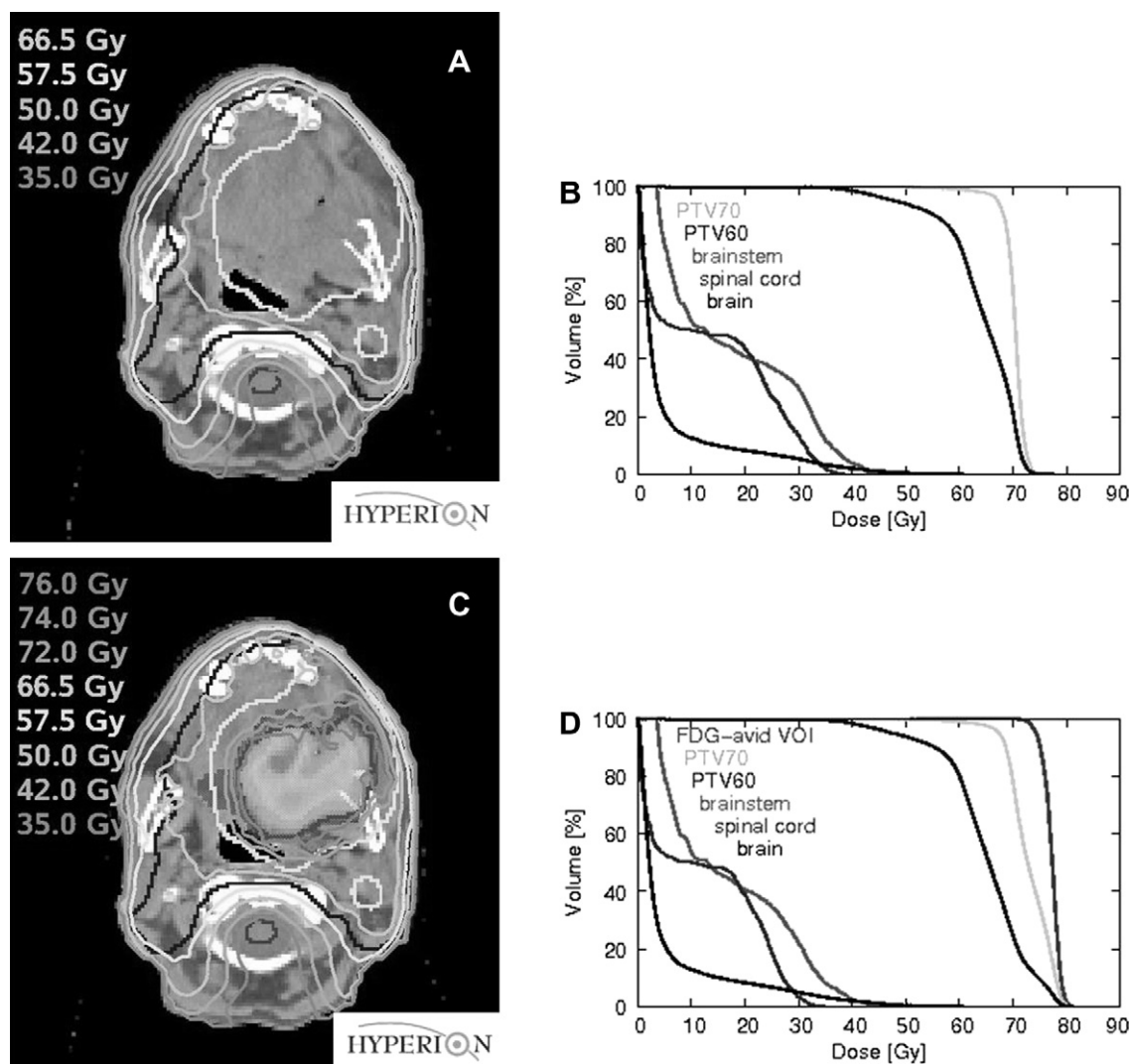
Fig. 2. Conventional HNC IMRT plan in comparison to a DPBC IMRT plan with a 10% dose escalation to the FDG-PET avid volume under isotoxicity conditions. These treatment plans were created with the planning system Hyperion in a realistic treatment setting for an Elekta Synergy S with sliding window delivery technique (dMLC). (A) DD conventional IMRT plan and (B) corresponding DVH. (C) DD DPBC IMRT plan, (D) DVH DPBC plan. Volumes of interest (VOIs): FDG PET-avid VOI, PTV70, brainstem (green, not visible on this slice), spinal cord (magenta) and brain (black, not visible on this slice).

major influence on the quality and also the realizability of treatment planning and delivery.

The very limited resolution of the PET image of approximately 5–7 mm is crucial for dose painting [49]. For objects smaller than the resolution limit of the PET system, there will be a reduction of the detected PET signal intensity due to partial volume effects. As a consequence, the true activity of a small tumor lesion will be underestimated and at the same time its size will be overestimated. Further uncertainties can be introduced into the PET signal already at the time of image acquisition and reconstruction [50]. Here, standardized protocols which have to be chosen very carefully are of major importance for the overall image quality. Consequentially, non-protocol compliance in terms of tracer injection, image acquisition, data reconstruction and also data transfer and manipulation can be sources of errors and uncertainties when using those PET images for potential dose painting.

Furthermore, there are inherent biological uncertainties related to the tracer used for PET imaging. Currently, the most commonly used PET tracer is the metabolic biomarker FDG, nevertheless, also other tracers such the hypoxia biomarkers FMISO and FAZA, or the proliferation marker FLT, might be used for dose painting (see also [51]). In this context, also tracer pharmacokinetics is an important

issue to be considered. For tracers where active transport mechanisms in the tissue exist, such as FDG and receptor binding tracers, the PET signal will be stable after a certain time and presents with a high signal-to-background ratio (SBR). In contrast, hypoxia tracers are not subject to active transport. Here, the distribution in the tissue is purely diffusive. Due to the resulting low SBRs, delineation of functional areas is very difficult which requires imaging time points several hours after injection. Dynamic imaging may be a method to study the tissue characteristics of such tracers in more detail, but then kinetic modeling to evaluate the data is necessary which may also be quite error prone [52]. Additionally, patient motion is an inherent problem in PET imaging as the duration of data acquisition is in general in the order of 15–30 min.

Also the dose calculation algorithm used for treatment planning is an important factor for the quality of the treatment plan as well as the treatment modality available for radiation delivery.

Uncertainties related to the above-mentioned problems are the limiting factors for all kinds of dose painting approaches. It is a whole chain of factors being important for the quality of the treatment plan which is always as weak as the weakest point. This means that improvements for only one of those factors, e.g. the PET resolution, will not noticeably affect the planning result when

Table 2
Guidelines for kick reading. Short summary of the most important points of these guidelines.

	Important factors for treatment planning
PET-based GTV delineation	• PET image quality and reconstruction
	• Image registration
DPBC	• PET image quality and reconstruction
	• Image registration
	• Automatic algorithm for delineation of the PET-based region which will be prescribed for higher doses
	• Dose escalation or redistribution?
	• Level of dose escalation?
	• Isotoxicity planning approach!
	• Accurate dose calculation algorithm (Monte Carlo)
	• High precision delivery technique (Small MLC, Tomotherapy, Protons)
	• Daily on-board position verification
DPBN	• PET image quality and reconstruction
	• Quantification of PET necessary
	• Temporal and spatial stability of PET image data
	• Image registration!
	• Calibration of prescription function to outcome data
	• Dose escalation or redistribution?
	• Isotoxicity planning approach!
	• Accurate dose calculation algorithm (Monte Carlo)
	• New tool for evaluation of treatment plans: eDVH
	• High precision delivery technique (Small MLC, Tomotherapy, Protons)
	• Daily on-board position verification

the physical dose gradients which depend mostly on the ability of the treatment machine to apply small treatment fields remain unchanged. Moreover, as the size of the calculation grid used for treatment planning defines the 'resolution' of the dose matrix, small voxels have to be used when integrating high-resolution functional images into planning.

When aiming for DPBC based on PET imaging, the delineation method which is used for contouring is crucial. Here, different methods of varying complexity are described and discussed in the literature [11,23], which have to be chosen carefully depending on the tracer used, the examined tumor site and several other factors which are in more detail discussed in [50].

Especially for DPBN, but also for DPBC, a reliable quantification of PET images is necessary to extract the relevant tissue properties, such as metabolism, clonogenic cell density, hypoxia, proliferation and vascularization, from the respective PET data. It may even be necessary to acquire a multiparametric set of functional image data in order to derive a more detailed picture of the underlying tumor tissue properties. Multiparametric imaging can either be achieved by combination of different functional imaging modalities, i.e. PET and magnetic resonance imaging (MRI) [53], or by a dynamic PET acquisition which allows to determine a set of different tissue parameters [54]. A further requirement for the use of functional image data for DPBN is a direct relation of the functional tissue parameters to therapy outcome. Several studies could show that tumor hypoxia as assessed from FMISO PET scans has a prognostic value for radiation therapy outcome [55–57]. Also for the proliferation data imaged with FLT PET first studies could show a positive correlation of PET data and clinical outcome [58,59]. Only when a positive correlation between quantitative PET parameters and therapy outcome is established, a functional relationship of local tumor control and functional tissue characteristics can be derived [30,60]. This TCP function represents the mathematical prescrip-
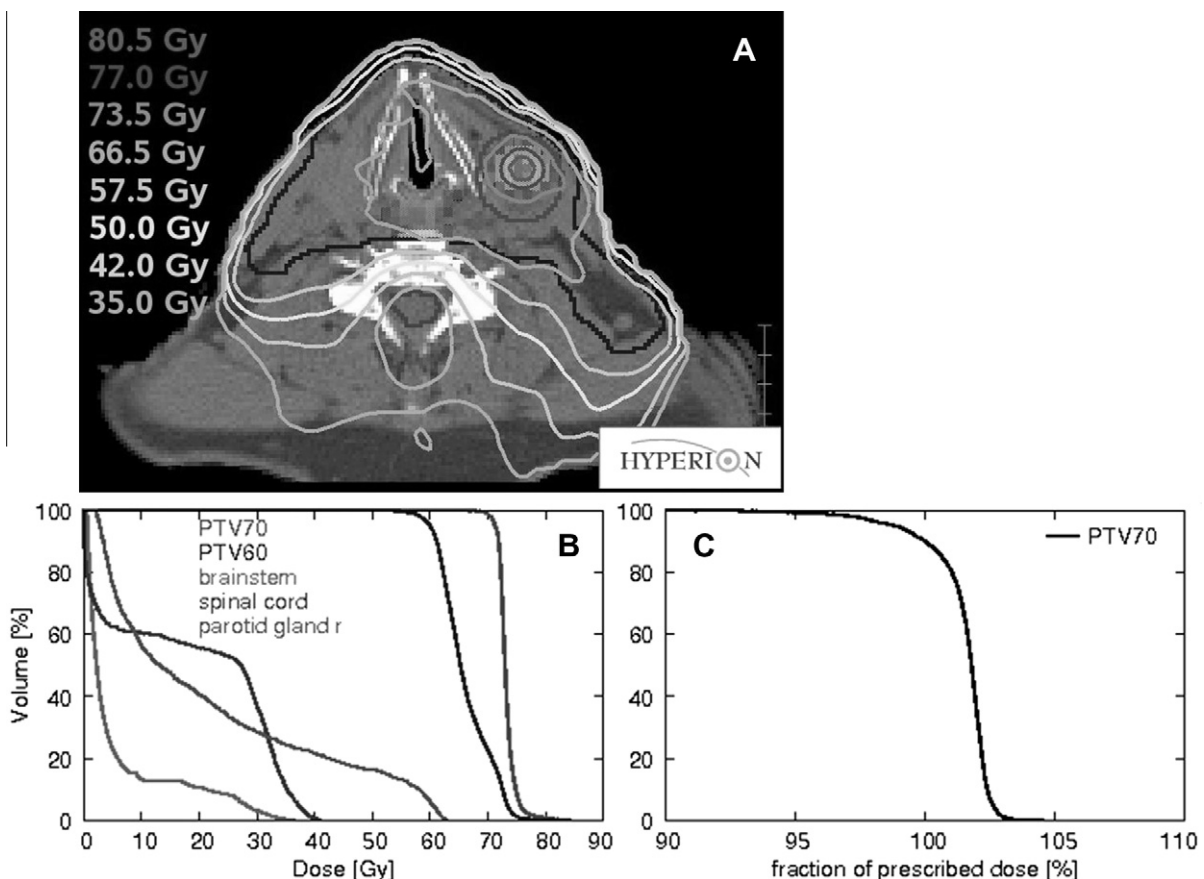

Fig. 3. DPBN IMRT plan for a larynx cancer patient with hypoxic lymph node. (A) DPBN IMRT DD. The dose escalation map derived from a dynamic [18F]FMISO PET scan is overlaid to the planning CT. (B) Corresponding DVH and (C) eDVH, evaluating the planned dose as a function of the prescribed dose, for the PTV70.

tion function that associates a certain radiation dose to a precisely defined voxel intensity in the functional image [46].

As a consequence, the prescription function used to translate PET signal intensities into local dose prescriptions meant to compensate for differences in radiation resistance is also subjected to uncertainties. Strategies on how to handle these uncertainties and potential resulting errors in the treatment plan still have to be investigated in the future.

Finally, temporal and spatial stability of the PET data before and also throughout the treatment course are of major importance for dose painting in general. Both dose painting approaches, DPBC and DPBN, may apply extremely high doses to small sub-regions of the tumor. Hence, patient movement or temporal instabilities of the PET images are crucial [20,39]. As these questions have not been answered yet, dose painting is to be applied only in clinical trials before it can be introduced into clinical practice.

Recommendations

As prerequisites for the integration of functional PET/CT images into RTP, different technical aspects concerning patient positioning, image acquisition, image fusion, dose calculation, and also available treatment techniques have to be considered. These technical requirements have to be carefully reviewed, independent of the integration level of the PET data – either for a more reliable delineation of the PTV or as a basis for DPBC or DPBN.

If the PET/CT data exist as image information in addition to a dedicated planning CT, a reproducible way of image fusion in the treatment planning system (TPS) has to be guaranteed [61]. Most commercially available TPS does not allow for deformable registration and, moreover, the standard patient positioning for routine diagnostic PET/CT examinations is different from radiotherapy patient positioning. Hence, it is recommended to acquire PET/CT data that will be used as a basis for RTP in treatment position [62]. This very sensitive aspect of image registration could be avoided by using PET/CT directly for simulation.

Moreover, the PET images which are used for RTP purposes have to be of high quality. Hence, image acquisition procedures [49] as well as reconstruction algorithms and post-filtering techniques [50] used have to follow pre-defined protocols in order to guarantee high levels of reproducibility.

Especially when aiming for a dose escalation in eventually very small volumes which may be located near tissue inhomogeneities, the performance of the dose calculation algorithm is of major importance. Recent studies showed that the choice of the dose calculation method may influence clinical results [43]. Hence, for dose painting treatment planning high accuracy of the dose engine is required, which can only be guaranteed by a Monte Carlo-based dose calculation.

For a clinical realization of PET-based dose painting, treatment techniques which are able to generate small radiation fields are necessary in order to achieve high dose gradients. State of the art RT treatment equipments such as small multi-leaf collimators used in combination with dynamic delivery techniques and intensity modulated proton therapy (IMPT) constitute the technical basis for a clinical use of sophisticated dose painting strategies [44,45].

Finally, high-quality position verification is needed when treating patients with PET-based dose escalation concepts. As high doses may be delivered to small regions with functional abnormality, geometrical accuracy of the RT treatment has to be assessed carefully using daily on-board imaging techniques.

To date, the use of FDG PET in order to delineate the GTV most accurately is the standard of care only in a few indications. Neither DPBC to functional subvolumes of the PTV nor DPBN is clinically established yet. For both DPBC and DPBN, so far only theoretical feasibility could be shown. For a clinical application, there is not enough evidence yet. Geometrical, biological, and imaging uncertainties are still too high.

Future research issues

The practical integration of molecular imaging into RT treatment planning is subjected to a large number of limitations and uncertainties. Most of the factors mentioned above and their consequences for practical dose painting have to be investigated in the near future.

Further studies are necessary in order to assess the levels of dose escalation needed for both DPBC and DPBN. To date, most planning studies used arbitrary dose prescriptions. On the one hand side, the dose load of the OARs is a limiting factor for the applicable dose escalation level whereas the dose levels necessary to reach higher tumor control rates can only be addressed by clinical studies.

Methodologies for a clinical applicability of DPBN strategies have to be developed in the near future. The robustness of DPBN plans with reference to errors in the PET image, image registration, treatment planning and also positioning during treatment has to be investigated. Moreover, when tracers beyond FDG are used to map functional characteristics of the tumor, the temporal and spatial behaviors of those agents before and during the course of radiotherapy treatment have to be studied before using them as a basis for dose painting [20,39]. In addition, quantification of PET data is a very important and promising issue in the context of DPBN. Without a reliable quantification of functional tissue parameters, DPBN is not possible.

In terms of individual adaptation of the radiation dose to functional tissue properties such as hypoxia and proliferation, correlation studies have to be carried out in order to assess the potential geographical correlation between local PET image parameters and individual therapy failure [63–66]. Only a complete analysis of the patterns of failure with regard to the respective biological imaging technique can verify or falsify the basic hypothesis of dose painting, which is an increase in TCP by higher levels of dose in regions with higher levels of radiation resistance induced by functional tissue abnormalities.

As the technical feasibility of dose painting could be shown by several investigators [15,20,25,40,41], the challenge is now to design clinical studies in order to prove the impact of dose painting treatments on individual therapy success.

In the next years, challenging new tracers may become available to image a variety of different tissue properties such as hypoxia, proliferation, vascularization, apoptosis and even EGFR/VEGF-expression with clinical PET/CT machines. In terms of physical treatment planning, it may be beneficial to use functional PET imaging not only for better tumor control purposes but also to assess functional characteristics or loss of function of certain OARs as an input for a more realistic, biological treatment planning.

Conclusion

Individual adaptation of RT based on functional PET imaging is possible and highly promising. So far, only the theoretical feasibility of DPBC and DPBN could be shown.

Biological ART offers new opportunities to modify in depth the way in which the treatment plan is designed and the dose is delivered, in better accordance with the radiobiology of solid cancers. Although very promising, several issues have still to be addressed in well-designed studies, and additional efforts should be paid at the development of more sensitive and specific tracers, tracer quantification, accurate segmentation tools, and at the improvement of PET image quality.

Acknowledgements

References

[1] Keall P. 4-Dimensional computed tomography imaging and treatment planning. Semin Radiat Oncol 2004;14:81–90.
[2] Boellard R, O'Doherty MJ, Weber WA, et al. FDG PET and PET/CT: EANM guidelines for tumour PET imaging: version 1.0. Eur J Nucl Med Mol Imaging 2010;37:181–200.
[3] MacManus M, Nestle U, Rosenzweig KE, et al. Use of PET and PET/CT for radiation therapy planning: IAEA expert report 2006–2007. Radiother Oncol 2009;91:85–94.
[4] Nestle U, Weber W, Hentschel M, Grosu AL. Biological imaging in radiation therapy: role of positron emission tomography. Phys Med Biol 2009;54:R1–R25 [review].
[5] Ford EC, Herman J, Yorke E, Wahl RL. 18F-FDG PET/CT for image-guided and intensity-modulated radiotherapy. J Nucl Med 2009;50:1655–65 [review].
[6] Zaidi H, Vees H, Wissmeyer M. Molecular PET/CT image-guided radiotherapy treatment planning. Acad Radiol 2009;16:1108–33 [review].
[7] Yu W, Fu X-L, Zhang Y-J, et al. GTV spatial conformity between different delineation methods by 18FDG PET/CT and pathology in esophageal cancer. Radiother Oncol 2009;93:441–6.
[8] Muijs CT, Schreurs LM, Busz DM, et al. Consequences of additional use of PET information for target volume delineation and radiotherapy dose distribution for esophageal cancer. Radiother Oncol 2009;93:447–53.
[9] de Figueiredo BH, Barret O, Demeaux H, et al. Comparison between CT- and FDG-PET-defined target volumes for radiotherapy planning in head-and-neck cancers. Radiother Oncol 2009;93:479–82.
[10] Wang H, Vees H, Miralbell R, et al. 18F-fluorocholine PET-guided target volume delineation techniques for partial prostate re-irradiation in local recurrent prostate cancer. Radiother Oncol 2009;93:220–5.
[11] Geets X, Tomsej M, Lee JA, et al. Adaptive biological image-guided IMRT with anatomic and functional imaging in pharyngo-laryngeal tumours: impact on target volume delineation and dose distribution using helical tomotherapy. Radiother Oncol 2007;85:105–15.
[12] Nestle U, Walter K, Achmidt S, et al. 18F deoxyglucose positron emission tomography (FDG-PET) for the planning of radiotherapy in lung cancer: high impact in patients with atalectasis. Int J Radiat Oncol Biol Phys 1999;44:593–7.
[13] Geets X, Daisne JF, Tomsej M, et al. Impact of the type of imaging modality on target volume delineation and dose distribution in pharyngo-laryngeal squamous cell carcinoma: comparison between pre and per-treatment studies. Radioter Oncol 2006;78:291–7.
[14] Douglas JG, Stelzer KJ, Mankoff DA, et al. [18-F] fluorodeoxyglucose positron emission tomography for targeting radiation dose escalation for patients with glioblastoma multiforme: clinical outcomes and patterns of failure. Int J Radiat Oncol Biol Phys 2006;64:886–91.
[15] Grosu AL, Souvatzoglou M, Röper B, et al. Hypoxia imaging with FAZA-PET and theoretical consideration with regard to dose painting for individualization of radiotherapy in patients with head and neck cancer. Int J Radiat Oncol Biol Phys 2007;69:541–51.
[16] Lee NY, Mechalakos J, Nemeh S, et al. Fluorine-18 labeled fluoromisonidazole positron emission and computed tomography guided intensity modulated radiotherapy for head and neck cancer; a feasibility study. Int J Radiat Oncol Biol Phys 2008;70:2–13.
[17] Rajendran JG, Hendrickson KRG, Spence AM, et al. Hypoxia imaging directed radiation treatment planning. Eur J Nucl Med Mol Imaging 2006;33:S44–53.
[18] Seppälä J, Seppänen M, Arponen E, Lindholm P, Minn H. Carbon-11 acetate PET/CT based dose escalated IMRT in prostate cancer. Radiother Oncol 2009;93:234–40.
[19] Pinkawa M, Attieh C, Piroth MD, et al. Dose-escalation using intensity-modulated radiotherapy for prostate cancer–evaluation of the dose distribution with and without 18F-choline PET-CT detected simultaneous integrated boost. Radiother Oncol 2009;93:213–9.
[20] Lin Z, Mechalakos J, Nehmeh S, et al. The influence of changes in tumor hypoxia on dose-painting treatment plans based on [18F]-FMISO positron emission tomography. Int J Radiat Oncol Biol Phys 2008;70:1219–28.
[21] Chao KS, Bosch WR, Mutic S, et al. A novel approach to overcome hypoxic tumor resistance. Cu-ATSM guided intensity modulated radiation therapy. Int J Radiat Oncol Biol Phys 2001;49:1171–82.
[22] Barwick T, Bencherif B, Mountz JM, Avril N. Molecular PET and PET/CT imaging of tumour cell proliferation using F-18 fluoro-L-thymidine: a comprehensive evaluation. Nucl Med Commun 2009;30:908–17.
[23] Schaefer A, Kremp S, Hellwig D, Rübe C, Kirsch CM, Nestle U. A contrast-oriented algorithm for FDG-PET-based delineation of tumour volumes for the radiotherapy of lung cancer: derivation from phantom measurements and validation in patient data. Eur J Nucl Med Mol Imaging 2008;35:1989–99.
[24] Esthappan J, Chaudhari S, Santanam L, et al. Prospective clinical trial of positron emission tomography/computed tomography image-guided intensity modulated radiation therapy for cervical carcinoma with positive para-aortic lymph nodes. Int J Radiat Oncol Biol Phys 2008;72:1134–9.
[25] Schinagl DAX, Hoffmann AL, Vogel WV, et al. Can FDG-PET assist in radiotherapy target volume definition of metastatic lymph nodes in head-and-neck cancer? Radiother Oncol 2009;91:95–100.
[26] Ling CC, Humm J, Larson S, et al. Towards multidimensional radiotherapy (MD-CRT): biological imaging and biological conformality. Int J Radiat Oncol Biol Phys 2000;47:551–60.
[27] Vanderstraeten B, Duthoy W, De Gersem W, et al. [18F]fluoro-deoxy-glucose positron emission tomography ([18F]FDG-PET) voxel intensity based intensity modulated radiation therapy (IMRT) for head and neck cancer. Radiother Oncol 2006;79:249–58.
[28] Alber M, Paulsen F, Eschmann SM, Machulla HJ. On biologically conformal boost dose optimization. Phys Med Biol 2003;48:N31–5.
[29] Bentzen SM. Theragnostic imaging for radiation oncology: dose-painting by numbers. Lancet Oncol 2005;6:112–7.
[30] Petit SF, Aerts HJWL, van Loon JGM, et al. Metabolic control probability in tumour subvolumes or how to guide tumour dose redistribution in non-small cell lung cancer (NSCLC): An exploratory clinical study. Radiother Oncol 2009;91:393–8.
[31] Wang D, Schultz CJ, Jursinic PA, et al. Initial experience of FDG-PET/CT guided IMRT of head and neck carcinoma. Int J Radiat Oncol Biol Phys 2006;65:143–51.
[32] Popple RA, Ove R, Shen S. Tumour control probability for selective boosting of hypoxic subvolumes, including the effect of reoxygenation. Int J Radiat Oncol Biol Phys 2002;54:921–7.
[33] Madani I, Duthoy W, Derrie C, et al. Positron emission tomography guided focal dose escalation using intensity modulated radiotherapy for head and neck cancer. Int J Radiat Oncol Biol Phys 2007;68:126–35.
[34] Van der Wel A, Nijsten S, Hochstenbag M, et al. Increased therapeutic ratio by FDG-PET-CT planning in patients with clinical CT stage N2/N3 M0 non small cell lung cancer (NSCLC): a modeling study. Int J Radiat Oncol Biol Phys 2005;61:648–54.
[35] Soret M, Bacharacj SL, Buvat I, et al. Partial volume effect in PET tumor imaging. J Nucl Med 2007;48:932–45.
[36] Busk M, Horsman MR, Overgaard J. Resolution in PET hypoxia imaging: voxel size matters. Acta Oncol 2008;47:1201–10.
[37] Reader AJ. The promise of a new PET image reconstruction. Phys Med 2008;24:49–56.
[38] Christian N, Lee JA, Bol A, et al. The limitation of PET imaging for biological adaptive-IMRT assessed in animal models. Radiother Oncol 2009;91:101–6.
[39] Nehmeh SA, Lee NY, Schröder H, et al. Reproducibility of intratumor distribution of 18F-fluoromisonidazole in head and neck cancer. Int J Radiat Oncol Biol Phys 2008;70:235–42.
[40] Sovik A, Malinen E, Skogmo HK, Bentzen SM, Bruland OS, Olsen DR. Radiotherapy adapted to spatial and temporal variability in tumor hypoxia. Int J Radiat Oncol Biol Phys 2007;68:1496–504.
[41] Thorwarth D, Eschmann SM, Paulsen F, Alber M. Hypoxia dose painting by numbers: a planning study. Int J Radiat Oncol Biol Phys 2007;68:291–300.
[42] Søvik A, Malinen E, Olsen DR. Strategies for biologic image-guided dose escalation: a review. Int J Radiat Oncol Biol Phys 2009;73:650–8.
[43] Vanderstraeten B, Reynaert N, Paelinck L, et al. Accuracy of patient dose calculation for lung IMRT: A comparison of Monte Carlo, convolution/superposition, and pencil beam computations. Med Phys 2006;33:3149–58.
[44] Flynn RT, Bowen SR, Bentzen SM, Rockwell Mackie T, Jeraj R. Intensity-modulated X-ray (IMXT) versus proton (IMPT) therapy for theragnostic hypoxia-based dose painting. Phys Med Biol 2008;53:4153–67.
[45] Thorwarth D, Soukup M, Alber M. Dose painting with IMPT, helical tomotherapy and IMXT: a dosimetric comparison. Radiother Oncol 2008;86:30–4.
[46] Bowen SR, Flynn RT, Bentzen SM, Jeraj R. On the sensitivity of IMRT dose optimization to the mathematical form of a biological imaging-based prescription function. Phys Med Biol 2009;54:1483–501.
[47] Vanderstraeten B, De Gersem W, Duthoy W, De Neve W, Thierens H. Implementation of biologically conformal radiation therapy (BCRT) in an algorithmic segmentation-based inverse planning approach. Phys Med Biol 2006;51:N277–86.
[48] Rickhey M, Koelbl O, Eilles C, Bogner L. A biologically adapted dose-escalation approach, demonstrated for 18F-FET PET in brain tumours. Strahlenther Onkol 2008;184:536–42.
[49] Sattler B, Lee JA, Lonsdale M, Coche E. PET/CT (and CT) instrumentation, image reconstruction and data transfer for radiotherapy planning. Radiother Oncol 2010;96:288–97.
[50] Lee JA. Segmentation of positron emission topography images: Some recommendations for target delineation in radiation oncology. Radiother Oncol 2010;96:302–7.
[51] Haubner R. PET radiopharmaceuticals in radiation treatment planning – Synthesis and biological characteristics. Radiother Oncol 2010;96:280–7.
[52] Wang W, Georgi JC, Nehmeh SA, et al. Evaluation of a compartmental model for estimating tumor hypoxia via FMISO dynamic PET imaging. Phys Med Biol 2009;54:3083–99.
[53] Dirix P, Vandevaceye V, De Keyzer F, Stroobants S, Hermans R, Nuyts S. Dose painting in radiotherapy for head and neck squamous cell carcinoma: value of repeated functional imaging with 18F-FDG, 18F-fluoromisonidazole, diffusion-

weighted MRI, and dynamic contrast-enhanced MRI. J Nucl Med 2009;50:1020–7.

[54] Thorwarth D, Eschmann SM, Paulsen F, Alber M. A kinetic model for dynamic [18F]-Fmiso PET data to analyse tumour hypoxia. Phys Med Biol 2005;50:2209–24.

[55] Hicks RJ, Rischin D, Fisher R, Binns D, Scott AM, Peters LJ. Utility of FMISO PET in advanced head and neck cancer treated with chemoradiation incorporating a hypoxia-targeting chemotherapy agent. Eur J Nucl Med Mol Imaging 2005;32:1284–91.

[56] Rajendran JG, Schwartz DL, O'Sullivan J, et al. Tumor hypoxia imaging with [18-F] fluoromisonidazole positron emission tomography in head and neck cancer. Clin Cancer Res 2006;12:5435–41.

[57] Eschmann SM, Paulsen F, Reimold M, et al. Prognostic impact of hypoxia imaging with 18F-fluoromisonidazole PET in non-small cell lung cancer and head and neck cancer. J Nucl Med 2005;46:253–60.

[58] Troost EG, Vogel WV, Merkx MA, et al. 18F-FLT PET do not discriminate between reactive and metastatic lymph nodes in primary head and neck cancer patients. J Nucl Med 2007;48:726–35.

[59] Troost EG, Bussink J, Hoffmann AL, Boerman OC, Oyen WJ, Kaanders JH. 18F-FLT PET/CT for early response monitoring and dose escalation in oropharyngeal tumors. J Nucl Med 2010;51:866–74.

[60] Thorwarth D, Eschmann SM, Paulsen F, Alber M. A model of reoxygenation dynamics of head-and-neck cancer based on serial 18F-fluoromisonidazole

positron emission tomography investigations. Int J Radiat Oncol Biol Phys 2007;68:515–21.

[61] Malandrain G. Guidelines for the use of PET/CT in radiotherapy treatment planning. Image registration. Radiother Oncol 2010; in press.

[62] Hwang AB, Bacharach SL, Yom SS, et al. Can positron emission tomography (PET) or PET/computed tomography (CT) acquired in a nontreatment position be accurately registered to a head-and-neck radiotherapy planning CT? Int J Radiat Oncol Biol Phys 2009;73:578–84.

[63] Aerts HJWL, van Baardwijk AAW, Petit SF, et al. Identification of residual metabolic-active areas within individual NSCLC tumours using a pre-radiotherapy 18Fluorodeoxyglucose-PET-CT scan. Radiother Oncol 2009;91:386–92.

[64] Soto DE, Kessler ML, Piert M, Eisbruch A. Correlation between pretreatment FDG-PET biological target volume and anatomical location of failure after radiation therapy for head and neck cancers. Radiother Oncol 2008;89: 13–8.

[65] Brouwer J, de Bree R, Comans EFI, et al. Improved detection of recurrent laryngeal tumor after radiotherapy using 18FDG-PET as initial method. Radiother Oncol 2008;87:217–20.

[66] Gillham C, Zips D, Pönisch F, et al. Additional PET/CT in week 5–6 of radiotherapy for patients with stage III non-small cell lung cancer as a means of dose escalation planning? Radiother Oncol 2008;88:335–41.

Review

PET for radiation treatment planning of brain tumours

Anca-L. Grosu [a,*], Wolfgang A. Weber [b]

[a] Department of Radiation Oncology, University of Freiburg, Germany; [b] Department of Nuclear Medicine, University of Freiburg, Germany

ARTICLE INFO

ABSTRACT

AA-PET (MET-PET and FET-PET) can be used for gross tumour volume (GTV) delineation in brain gliomas and for the differentiation between treatment-related changes (pseudo-progression, pseudo-regression) and residual/recurrent tumour. There are some data showing that MET-PET and (DOTATOC)-PET can be used for GTV delineation in meningiomas and glomus tumours. The role of PET in the visualization of the biological characteristics of the tumours: proliferation (FLT-PET), hypoxia (FMISO-PET) and angiogenesis/peptide expression (RGD-PET) should be investigated in future studies.
© 2010 European Society for Therapeutic Radiology and Oncology and European Association of Nuclear Medicine. Published by Elsevier Ireland Ltd. All rights reserved. 96 (2010) 325–327

In brain tumours, treatment planning and the evaluation of local response to therapy are usually based on magnetic resonance imaging (MRI) and computed tomography (CT). Although these investigations show the anatomy of the brain with high accuracy, contrast enhancement or hyperintensity on T2- or flair-MRI are not tumour specific. Tumour tissue can also be located in the areas with iso-intense appearance. Moreover, after surgery, radiation, chemotherapy etc. treatment-related changes, such as blood–brain-barrier (BBB) disturbance or edema, in general cannot be differentiated from viable tumour tissue.

New concepts such as pseudo-progression or pseudo-remission were introduced for brain gliomas, underscoring the fact that conventional MRI is insufficient for the visualization of tumour tissue after therapy [1]. New MRI methods such as diffusion and perfusion MRI are promising; however, histopathological data validating the sensitivity and specificity are scarce. Hence, routine integration of diffusion or perfusion MRI in radiation treatment planning is premature. MRI spectroscopy has a long tradition but, unfortunately, the method remains relatively laborious and has a low resolution. Therefore, there is an urgent need for new imaging approaches to increase accuracy in tumour delineation for high precision radiotherapy.

Imaging the biological and molecular characteristics of tumour tissue by positron emission tomography (PET) is an interesting approach to improve treatment planning for high precision radiotherapy. In the first part of this chapter we will discuss the role of amino acid (AA)-PET for gross tumour volume (GTV) delineation in brain gliomas, metastases and benign cranial tumours such as meningiomas and glomus tumours. In the second part, we will focus on tracers used to visualize biological properties of tumours such as hypoxia, proliferation or expression of peptide/protein on the cell membrane.

Gross tumour volume delineation: AA-PET

Brain gliomas

[11]C-labelled methionine (MET), ^{123}I-labelled alpha-methyl-tyrosine (IMT) and ^{18}F-labelled O-(2) fluoroethyl-L-tyrosine (FET) are the most important radio-labelled AA used in the diagnosis of brain tumours. These three tracers were shown to have a very similar uptake intensity and distribution in brain tumours [2–4]. Currently available AA-PET tracers are accumulated by L and A amino acid transporters. Tumour cells take up radio-labelled AA at a high rate, while there is only a relatively low uptake in normal cerebral tissue. They are independent from BBB disturbance.

The higher sensitivity and specificity of AA-PET in the diagnosis of gliomas in comparison to CT and MRI was demonstrated in many clinical trials. Summarizing the data from the literature between 1983 and 2008, we identified, 45 trials including 1721 patients, which investigated the role of MET-PET in the diagnosis of gliomas. Eleven studies including 706 patients were based on PET/MRI/CT stereotactic biopsies. Between 2000 and 2008, 12 trials including 361 patients evaluated the role of FET-PET in the diagnosis of brain gliomas. In three studies with 126 patients, the results were based on PET/MRI/CT stereotactic biopsies. All these studies have shown that the specificity of MET-PET and FET-PET for malignant gliomas was significantly higher (85–95%) in comparison to

* Corresponding author. Address: Department of Radiation Oncology, Albert Ludwigs University Freiburg, Robert Koch Str. 3, Freiburg 79106, Germany.
E-mail addresses: anca.grosu@uniklinik-freiburg.de (Anca-L. Grosu), wolfgang.weber@uniklinik-freiburg.de (W.A. Weber).

Table 1
Differentiation of radiation necrosis and tumour recurrence by amino acid PET or SPECT.

Author	N	Technique	Sensitivity (%)	Specificity (%)
Rachinger	45	FET-PET	94 (29/31)	93 (13/14)
		MRI[a]	97(30/31)	50 (7/14)
Tsuyuguch	21	MET-PET	78 (7/9)	100 (12/12)
Samnick	78	IMT-SPECT	94 (62/66)	100 (12/12)

[a] Contrast enhancement in T1-weighted images after administration of gadolinium-DTPA [13].

Table 2
Accuracy of amino acid PET for brain tumour delineation in comparison with histologic evaluation.

Author	N[a]	Technique	Sensitivity[b] (%)	Specificity[b] (%)
Braun	32	MET-PET	87 (26/30)	75 (3/4)
Pirotte	32	MET-PET	100 (61/61)	100 (9/9)
Kracht	30	MET-PET	87 (87/100)	89 (16/18)
Pauleit	31	FET-PET	93[c]	94[c]
		MRI[d]	96	53

[a] Number of patients.
[b] Based on analysed lesions or biopsies.
[c] Total of 52 samples, 26 positive for tumour tissue. Sensitivity and specificity were calculated from fitted receiver operator characteristic (ROC) curve.
[d] Combined analysis of non-enhanced T1-weighted sequences, Gd-enhanced sequences and FLAIR sequences [13].

MRI, which has a high sensitivity but a lower specificity (ca. 50%) (Tables 1 and 2).

The similarity between MET- and FET-PET for tumour visualization was demonstrated in a few studies [2,3]. We investigated 42 patients with gliomas and metastases on the same day with MET- and FET-PET. We found an almost identical sensitivity and specificity of both tracers [4]. Furthermore, the intensity of tracer uptake and the extension of gliomas with FET-PET were closely correlated with the extension with MET-PET. Thus, these studies indicate that the results of MET-PET can be extrapolated to FET-PET.

The higher diagnostic accuracy of AA-PET is the rationale for using this technique in target volume delineation of gliomas, since AA-PET can also provide information regarding tumour extension (Fig. 1). In a series of clinical studies, marked differences between AA-PET or SPECT and MRI in GTV delineation for radiation treatment planning have been demonstrated [5–9]. In 39 patients with high-grade gliomas imaged postoperatively, tumour contrast enhancement in MRI and MET uptake corresponded in only 13% of the patients. On average 13 ml (33%) of the tumour volume defined on MET-PET demonstrated no contrast enhancement on MRI [9].

Lee et al. [10] have demonstrated that increased uptake on MET-PET obtained before radiation therapy and temozolomide was associated with the site of subsequent failure in newly diagnosed glioblastoma. Weber et al. [11] assessed the failure pattern observed after FET planning after chemo- and radiotherapy for high-grade glioma. The target mismatch-survival data suggested that using FET-PET planning may counteract the possibility of biological target volume-related progression, which may have a detrimental effect on survival.

In a small study, patients with recurrent gliomas lived significantly longer when AA-PET or single photon emission tomography (AA-SPECT) were integrated in target volume delineation. Median survival of patients who underwent AA-PET or -SPECT based radiation treatment was 4.5 months longer than that of patients who underwent CT/MRI based radiation treatment [12].

In contrast, FDG-PET for GTV delineation which was systematically analysed by Gross et al. [14] was shown to be of limited value. In 18 patients with malignant brain gliomas, the tumour volume defined by PET was compared with the tumour volume defined by PET/MRI fusion images. Only in a few patients, additional information was derived from FDG-PET for radiation treatment planning because of the low contrast between viable tumour and normal brain tissue, although FDG uptake is regionally related to anaplastic areas.

Other tumours

There are some data in the literature showing that AA-PET could be of interest in the differentiation between recurrent tumours and treatment-related changes in brain metastases treated with stereotactic radiotherapy/radiosurgery [4].

In meningiomas, the GTV is routinely delineated using the contrast enhancement areas on CT and MRI, and bone windowing on CT. Meningiomas can infiltrate the region of sella, cavernous sinus, orbit, tentorium, falx cerebri and the dura mater. It may be difficult to define tumour extension because contrast enhancement in
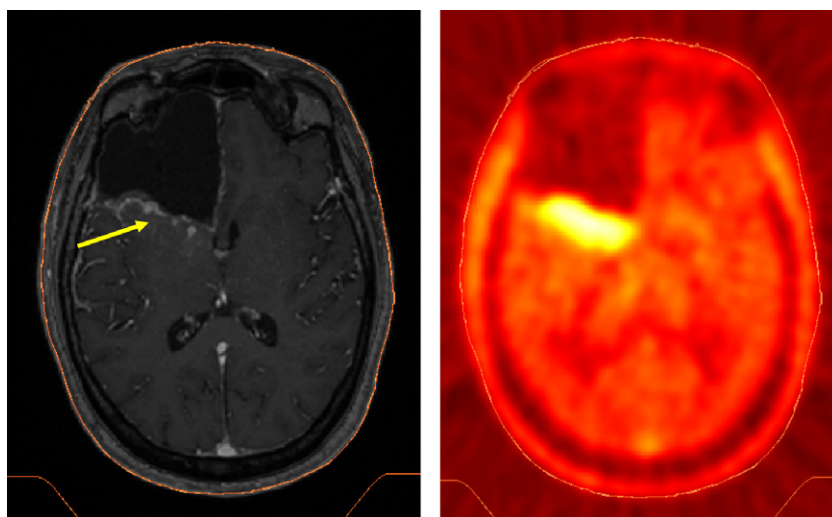

Fig. 1. Glioblastoma WHO IV two weeks after surgery. The contrast enhancement on T1-MRI with gadolinium (yellow row) can be treatment related (BBB disturbance after surgery) or can be due to residual tumour in this region. T1-MRI alone can not differentiate between treatment-related changes and residual tumour. MET-PET (MRI/PET coregistration) shows a high tracer uptake in this area, typically for residual tumour. This has consequences for the GTV delineation in radiation treatment planning process.

normal tissues may be comparable to that of the tumour itself in these regions. Using MET-PET/CT-fused images, meningioma borders can be delineated more accurately with respect to normal tissue [8,15,16]. The inter-observer variability in the GTV and PTV definition can be significantly reduced [15]. Similar observations were made using [68 Ga] -labelled DOTA (0)-D-Phe (1)-Tyr (3)-Octreotide (DOTATOC)-PET [17,18]. Gluc-Lys[(18)F]-TOCA- or DOTATOC-PET were also used in the GTV delineation for stereotactic radiotherapy in glomus tumours [19].

Visualization of tumour biology: FLT-PET, FMISO-PET and RGD-PET

Proliferation of tumour cells is the basic mechanism for malignant growth. [^{18}F]-Fluorine labelled thymidine analogue 3′-deoxy-3′-[^{18}F]-fluorothymidine (FLT) is retained in the cell after phosphorylation by thymidine kinase 1, whose levels correlate with cell proliferation. The kinetics of FLT uptake in malignant gliomas correlates with cell proliferation measured by Ki-67 [20].

The first data showing that malignant gliomas have a different level of oxygenation using FMISO-PET were published many years ago [21]. However, the real impact of hypoxia imaging in the diagnosis and treatment of high-grade gliomas is unclear and still under investigation.

The $\alpha v \beta 3$ integrin is an important receptor for cell adhesion and is involved in tumour-induced angiogenesis and metastasis. The expression of $\alpha v \beta 3$ integrin can be visualized with F18-labelled RDG-containing glycopeptide, which binds to the $\alpha v \beta 3$ receptor [22]. $\alpha v \beta 3$ integrin is blocked by cilengitide, a new drug under investigation in the treatment of high-grade gliomas.

The intensity modulated radiotherapy (IMRT) combined with a treatment plan based on biological imaging could be used for individualised, i.e. customised radiation therapy. This approach has been named *dose painting*. However, this new treatment approach will generate a new set of problems and questions such as: What are the dynamics of the visualized biological processes? How many biological investigations are necessary during the treatment and when? Which radiation treatment schedules have to be applied? Prospective clinical trails and experimental studies should supply the answer to these questions.

Conflicts of interest notification

The authors declare that they have no conflict of interest.

References

[1] Brandsma D, Stalpers L, Taal W, et al. Clinical features, mechanisms, and management of pseudoprogression in malignant gliomas. Lancet Oncol 2008;9:453–61.

[2] Langen KJ, Jarosch M, Muhlensiepen H, et al. Comparison of fluorotyrosines and methionine uptake in F98 rat gliomas. Nucl Med Biol 2003;30:501–8.

[3] Weber WA, Wester HJ, Grosu AL, et al. O-2(18F)Fluoroethyl-L-tyrosine and L-(methyl-11C)-methionine uptake in brain tumors: initial results of a comparative study. Eur J Nucl Med 2000;27:542–9.

[4] Grosu AL, Weber WA, Riedl E et al. An interindividual comparison of O-(2-[18F]Fluoroethyl)-L-tyrosine (FET) and L-[methyl-11C]methionine (MET) PET in patients with brain gliomas and metastases. Int J Radiat Oncol Biol Phys 2010;doi:10.1016/j.ijrobp.2010.07.022.

[5] Grosu AL, Weber WA, Feldmann HJ, et al. First experience with I-123-alpha-methyl-tyrosine SPECT in the 3-D radiation treatment planning of brain gliomas. Int J Rad Oncol Biol Phys 2000;47:517–27.

[6] Weber WA, Dick S, Reidl G, et al. Correlation between postoperative 3-(123I)-Iodo-L-alpha-methyltyrosine uptake and survival in patients with gliomas. J Nucl Med 2001;42:1144–50.

[7] Grosu AL, Feldmann HJ, Dick S, et al. Implications of IMT-SPECT for postoperative radiation treatment planning in patients with gliomas. Int J Rad Oncol Biol Phys 2002;54:842–54.

[8] Grosu AL, Lachner R, Wiedenmann N, et al. Validation of a method for automatic fusion of CT- and C11-methionine-PET datasets of the brain for stereotactic radiotherapy using a LINAC. First clinical experience. Int J Rad Oncol Biol Phys 2003;56:1450–63.

[9] Grosu AL, Weber AW, Riedel E, et al. L-(Methyl-11C) methionine positron emissions tomography for target delineation in resected high grade gliomas before radiation therapy. Int J Rad Oncol Biol Phys 2005;63:64–74.

[10] Lee IH, Piert M, Gomez-Hassan D, et al. Association of 11C-methionine PET uptake with the site of failure after concurrent temozolomide and radiation for primary glioblastoma multiforme. Int J Rad Oncol Biol Phys 2009;73:479–85.

[11] Weber DC, Casanova N, Zilli T, et al. Recurrence pattern after [(18)F]fluoroethyltyrosine-positron emission tomography-guided radiotherapy for high-grade glioma: a prospective study. Radiother Oncol 2009;93:586–92.

[12] Grosu AL, Weber WA, Franz M, et al. Re-Irradiation of recurrent high grade gliomas using amino-acids-PET(SPECT)/CT/MRI image fusion to determine gross tumor volume for stereotactic fractionated radiotherapy. Int J Rad Oncol Biol Phys 2005;63:511–9.

[13] Weber WA, Grosu AL, Czernin J. Technology insight: advances in molecular imaging and an appraisal of PET/CT scanning. Nat Clin Pract Oncol 2008;5:160–70.

[14] Gross MW, Weber WA, Feldmann HJ, et al. The value of F-18-fluorodeoxyglucose PET for the 3-D radiation treatment planning of malignant gliomas. Int J Radiat Oncol Biol Phys 1998;41:989–95.

[15] Grosu AL, Weber WA, Astner S, et al. 11C-Methionine PET improves the target volume delineation of meningiomas treated with stereotactic fractionated radiotherapy. Int J Rad Oncol Biol Phys 2006;66:339–44.

[16] Astner ST, Dobrei-Ciuchendea M, Essler M, et al. Effect of 11C-methionine-positron emission tomography on gross tumor volume delineation in stereotactic radiotherapy of skull base meningiomas. Int J Radiat Oncol Biol Phys. 2008;72:1161–7.

[17] Milker-Zabel S, Zabel-du Bois A, Henze M, et al. Improved target volume definition for fractionated stereotactic radiotherapy in patients with intracranial meningiomas by correlation of CT, MRI, and [68Ga]-DOTATOC-PET. Int J Radiat Oncol Biol Phys 2006;65:222–7.

[18] Gehler B, Paulsen F, Öksüz MÖ, et al. [^{68}Ga]-DOTATOC-PET/CT for meningioma IMRT treatment planning. Radiat Oncol 2009;4:56.

[19] Astner ST, Bundschuh RA, Beer AJ, et al. Assessment of tumor volumes in skull base glomus tumors using Gluc-Lys[(18)F]-TOCA positron emission tomography. Int J Radiat Oncol Biol Phys 2009;73:1135–40.

[20] Ullrich R, Backes H, Li H, et al. Glioma proliferation as assessed by 3′-fluoro-3′-deoxy-L-thymidine positron emission tomography in patients with newly diagnosed high-grade glioma. Clin Cancer Res 2008;14:2049–55.

[21] Valk PE, Mathis CA, Prados MD, et al. Hypoxia in human gliomas: demonstration by PET with fluorine-18-fluoromisonidazole. J Nucl Med 1992;33:2133–7.

[22] Beer AJ, Grosu AL, Carlsen J, et al. Feasibility of (18F)Galacto-RGD PET for imaging of $\alpha v \beta 3$ expression on noevasculature in patients with squamous cell carcinoma of head and neck. Clin Cancer Res 2007;13:6610–6.

Review

Clinical evidence on PET–CT for radiation therapy planning in head and neck tumours

Esther G.C. Troost [a,*], Dominic A.X. Schinagl [a], Johan Bussink [a], Wim J.G. Oyen [b], Johannes H.A.M. Kaanders [a]

[a] Department of Radiation Oncology; and [b] Department of Nuclear Medicine, Radboud University Nijmegen Medical Centre, Institute of Oncology, The Netherlands

ARTICLE INFO

ABSTRACT

The potential benefits of positron emission tomography (PET) imaging for the management of head and neck tumours are increasingly being recognized. Integrated PET–CT has found its way into the practice of radiation oncology providing both functional and anatomical tumour information for treatment planning and the implications for clinical practice are currently being investigated. First, it has been demonstrated that ^{18}F-fluorodeoxyglucose ([18]FDG)-PET can improve the accuracy of gross tumour volume delineation for radiation therapy planning. Next, PET using [18]FDG or more specific tracers may facilitate dose escalation to radioresistant tumour subvolumes. Finally, PET can provide tumour characterization prior to and during radiotherapy, facilitating adaptive radiotherapy and other tailored treatment strategies. Although these are promising prospects, unresolved issues remain and these applications are not yet ready for introduction into routine clinical practice.

© 2010 European Society for Therapeutic Radiology and Oncology and European Association of Nuclear Medicine. Published by Elsevier Ireland Ltd. All rights reserved. 96 (2010) 328–334

High-precision radiotherapy for head and neck tumours

Intensity-modulated radiation therapy (IMRT) revolutionized radiation therapy in the 1990s. IMRT is based on the use of numerous radiation beams with optimized non-uniform intensities resulting from inverse treatment planning. The algorithm for beam fluence calculations is guided by dose–volume objectives for the target volume and organs at risk delineated by the radiation oncologist. IMRT can thus achieve much better conformity than conventional radiotherapy techniques. In head and neck cancer, this technique facilitates boosting of the primary tumour while reducing the dose to normal tissues, such as the salivary glands and swallowing structures [1–3]. Due to the highly conformal dose distribution and steep dose gradients used in IMRT, knowledge about the localization and boundaries of the primary tumour and of the cervical lymph node metastases is of increasing importance. PET provides biological tumour information complementary to anatomical information obtained by computed tomography (CT) or magnetic resonance imaging (MRI). PET may therefore facilitate selection and delineation of the primary head and neck tumour and lymph node metastases. Furthermore, PET provides a basis to shape the radiation dose according to the tumour's metabolic activity and to adapt the treatment plan during irradiation.

[18]FDG-PET

Selection of radiotherapy target volumes

Imaging of the primary tumour

Numerous studies have assessed the value of ^{18}F-fluorodeoxyglucose ([18]FDG) PET(-CT) for imaging of primary squamous cell carcinomas of the head and neck and for undifferentiated nasopharyngeal tumours. Summarizing the most recent and largest studies on all tumour sites, an overall sensitivity of 93–100%, a specificity of 90–100% and an accuracy of 94–98% have been reported [4–9]. However, as stand-alone PET has not been proven superior to conventional imaging modalities (CT or MRI), it is currently not recommended for routine diagnostic imaging of primary head and neck cancer. With the wide introduction of combined PET–CT facilities, these conclusions may need to be revised in the coming years (Table 1).

Detection of the unknown primary tumour

Some patients present with an enlarged neck mass harbouring metastatic squamous cell carcinoma of unknown origin. In most cases, the standard work-up – thorough physical examination, panendoscopy with blind biopsies and CT and/or MRI – reveals the primary tumour. In some cases, however, the primary tumour may be too small to be detected or it may escape notice due to an inaccessible location. In this situation, [18]FDG-PET detects the primary tumour in about 25% of the cases [10,11]. A therapeutic benefit attributed to [18]FDG-PET was observed in 25% of the patients

* Corresponding author. Address: Department of Radiation Oncology, Radboud University Nijmegen Medical Centre, Institute of Oncology, PO Box 9101, 6500 HB Nijmegen, The Netherlands.
 E-mail address: e.troost@rther.umcn.nl (E.G.C. Troost).

Table 1
Summary of available data on the use of PET–CT in radiotherapy planning.

Tumour site/pathology/tracer	Target volume selection	Target volume delineation	Isodose distribution	Adaptive treatment	Patient outcome
HNSCC and [18]FDG	Limited (lymph nodes) or no use (primary tumour) of [18]FDG. Potential benefit for unknown primary tumour	Potentially interesting for primary tumour GTV using automatic segmentation. Decision aid for lymph nodes	Preliminary study indicating more conformed [18]FDG-PET-based plans	Promising preliminary data. No routine use yet	No prospective data available comparing CT-based and [18]FDG-PET-based plans
Undifferentiated NPC	No use of [18]FDG (primary tumour)	No data available	No data available	No data available	No data available
HNSCC and [18]FMISO	Three successful theoretical studies on selection of subvolume	Three successful theoretical studies on delineation of subvolume	Theoretical study indicating an increased TCP with same toxicity	No data available	Prognostic and predictive value shown in small clinical studies
HNSCC and [18]FLT	Limited (primary tumour) and no use (lymph nodes) of [18]FLT	No data available	One theoretical planning study on dose escalation to [18]FLT subvolume	One study on oropharyngeal tumours	Results on prognostic value awaited

HNSCC, head and neck squamous cell carcinoma; [18]FDG, ^{18}F-fluorodeoxyglucose; GTV, gross tumour volume; NPC, nasopharyngeal carcinoma; [18]FMISO, ^{18}F-fluoromisonidazole; TCP, tumour control probability; [18]FLT, 3'-deoxy-3'-^{18}F-fluorothymidine.

either because of identification of the primary tumour or detection of previously unrecognized distant metastases. A multidisciplinary expert panel therefore concluded that the use of [18]FDG-PET is beneficial if conventional imaging findings are negative in identifying the primary tumour [12]. Positive PET findings should, if possible, be confirmed by biopsy because of the risk of false-positive results.

Identification of cervical lymph node metastases

A meta-analysis recently summarized the available literature on the use of [18]FDG-PET for the assessment of the cervical lymph node status in squamous cell carcinomas of the head and neck [13]. Overall, the sensitivity and specificity of [18]FDG-PET were slightly higher compared to those of conventional imaging modalities, but direct comparison revealed no statistically significant differences. In studies exclusively enrolling patients without clinically apparent cervical lymph node metastases, the sensitivity was only 50% and not better than conventional imaging methods, specifically ultrasound with fine needle cytology. The threshold for detecting lymph nodes with a very low tumour burden is insufficient to allow identification of these nodes. Recently, a multi-centre study on 233 head and neck cancer patients prospectively compared therapeutic decisions based on conventional work-up (CT and MRI) with those additionally performing a whole-body [18]FDG-PET scan [14]. Functional imaging resulted in up- or down-staging of the lymph node status in 10% of patients (upstage in 16 patients and downstage in 7 patients). However, the detection on metastatic or additional disease had a greater impact on patient management.

There is limited information about the value of [18]FDG-PET for the identification of lymph node metastases in nasopharyngeal tumours. Chang et al. performed a retrospective analysis on 95 nasopharyngeal cancer patients and found little discrepancy between MRI and [18]FDG-PET for neck node staging [15]. In patients with advanced nodal disease, [18]FDG-PET may reveal distant metastases missed by all other conventional imaging modalities.

In summary, for head and neck cancer, there is insufficient evidence to support the routine clinical application of [18]FDG-PET in the pre-treatment identification of lymph node metastases. Thus, ultrasound-guided fine needle aspiration cytology remains the gold standard.

Delineation of radiation therapy target volume

Radiation target volume delineation is primarily based on anatomical information. A thorough physical examination of the head and neck is the basis for assessment of tumour extensions, especially for superficially spreading mucosal tumours, and for detection of metastatic cervical lymph nodes. CT- and MR-imaging provide important complementary information depicting distorted anatomy and regions of abnormal contrast enhancement. MRI achieves a better soft-tissue contrast and is therefore the preferred imaging modality for oral cavity and oropharyngeal carcinomas.

As discussed, the value of [18]FDG-PET for staging of the primary tumour and cervical lymph nodes is still controversial. However, in the meantime the incorporation of [18]FDG-PET data for radiation treatment purposes is performed in an increasing number of patients.

There are several potential advantages with the use of [18]FDG-PET: reduction of inter-observer variability in gross tumour volume (GTV) delineation, reduction of the size of the GTV, identification of tumour extensions that were missed by CT or MRI, and the possibility of identifying parts of the GTV potentially requiring an additional radiation dose. Drawbacks in the use of [18]FDG-PET are: the limited spatial resolution, the lack of a standardized method of signal segmentation, and false-positive [18]FDG-PET readings caused by inflammation.

Primary tumour

A reduction of the inter-observer variability has frequently been demonstrated when incorporating [18]FDG-PET in GTV delineation of non-small cell lung cancer [16,17]. Albeit less consistent, this was also observed in head and neck cancer patients [18,19].

A reduction in the size of the GTV has been demonstrated in a landmark study by Daisne et al. comparing the role of co-registered CT, MRI and [18]FDG-PET in GTV delineation of laryngeal cancer in patients scheduled for laryngectomy [20]. [18]FDG-PET was closest to depict the true tumour volume when compared to the reference surgical specimen. All modalities overestimated the extension of the tumour, with an average of 29%, 65% and 89% for [18]FDG-PET, CT and MRI, respectively. However, all three imaging modalities, including [18]FDG-PET, failed to identify a small fraction of the macroscopic tumour (approximately 10%), mainly superficial mucosal extensions.

The GTV derived from [18]FDG-PET is highly dependent on the method of PET signal segmentation. Daisne et al. used a variable threshold adaptive to the signal-to-background ratio [21]. Simple visual interpretation generally yields larger volumes but is very susceptible to the window-level settings of the images and is highly operator dependent [19,22,23]. This is why more objective methods such as isocontouring based on a chosen standardized uptake value (SUV) were explored, e.g. of 2.5, or thresholds acquired through phantom experiments such as a fixed threshold of the

maximum tumour signal intensity (40% or 50%) or a variable threshold adaptive to the signal-to-background ratio [18,21,24,25].

A recent study in 78 head and neck cancer patients compared five commonly used methods of ^{18}FDG-PET signal segmentation. It showed that the volume and the shape of the resulting GTV were influenced heavily by the choice of the segmentation tool [26]
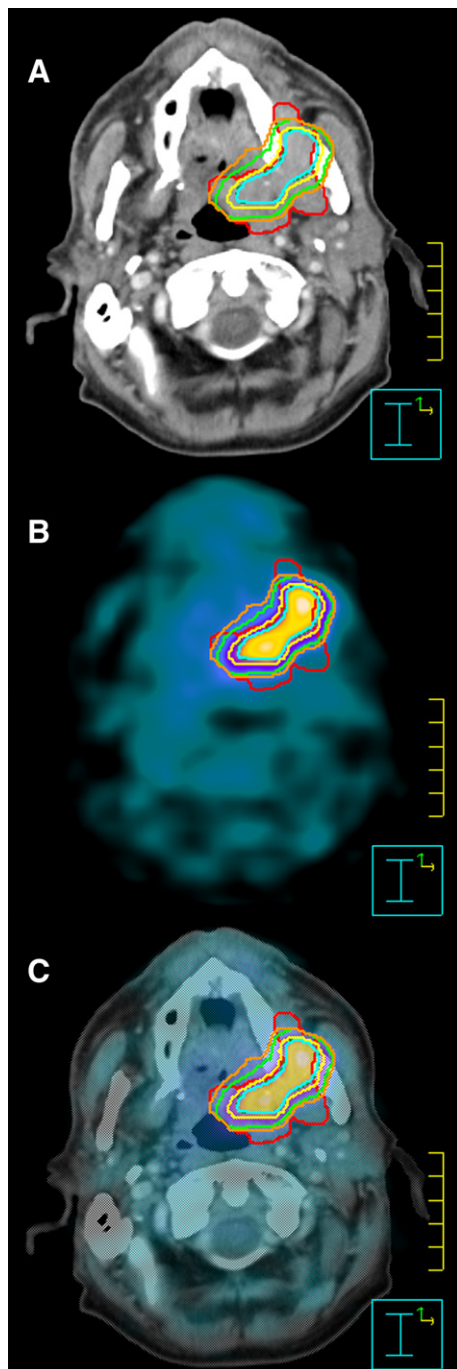

Fig. 1. Planning CT scan (A), corresponding ^{18}FDG-PET scan (B) and fusion image (C) from a patient with a cT4N2cM0 oropharyngeal carcinoma show differences in target volume definition. Indicated are gross tumor volume (GTV) delineated on CT (GTV$_{CT}$; red) and PET-based GTVs obtained by visual interpretation (GTV$_{VIS}$; light green), using a fixed threshold of 40% (GTV$_{40\%}$; yellow) and 50% (GTV$_{50\%}$; blue) of the maximum signal intensity, applying an adaptive threshold based on the signal-to-background ration (GTV$_{SBR}$; dark green, largely covered by GTV$_{50\%}$ in blue) and applying an isocontour of a standardized uptake value (SUV) of 2.5 (GTV$_{SUV}$; orange). The respective volumes ranged from 15.1 cm^3 (GTV$_{50\%}$) to 59.7 cm^3 (GTV$_{SUV}$).

(Fig. 1). All automated segmentation methods resulted in significantly smaller GTVs than the GTVs based on clinical information and CT, whereas visual interpretation of the PET signal yielded volumes closer to those of CT-based GTV delineation [26] (Fig. 2). This study also revealed that, depending on the segmentation tool used, in a large proportion of the patients (29–64%) more than 20% of the ^{18}FDG-PET-based GTV was located outside the GTV based on clinical information and CT. This suggests that tumour could be identified by ^{18}FDG-PET that was missed using the standard methods of GTV delineation. However, in the absence of histologic validation it remains unclear in what percentage of cases this might be caused by peri-tumoral inflammation, resulting in a false-positive reading of the ^{18}FDG-PET signal.

In recent years, promising segmentation tools have been developed taking into account the underlying PET physics. Geets et al. have published a gradient-based segmentation tool based on watershed transform and hierarchical cluster analysis [27]. van Dalen and co-workers developed an iterative background-subtracted relative-threshold level (RTL) method [28]. Although both groups validated their new tools, broader experience implementing these in the research setting is compulsory.

Cervical lymph node metastases

In head and neck cancer, delineation studies incorporating ^{18}FDG-PET have mostly concentrated on the primary tumour. CT-based delineation of metastatic lymph nodes usually is less prone to error due to better discrimination from the surrounding fatty tissue. This can be more difficult in cases with large, matted nodes. ^{18}FDG-PET might be helpful in these situations, although one should be aware of the caveat of ^{18}FDG-PET negative necrotic parts. A recent publication by Schinagl et al. showed that the segmented cervical lymph node volumes again depended on the segmentation tool applied [29]. The potential value of ^{18}FDG-PET may further be in the decision-making whether marginally enlarged lymph nodes should be included in the boost volume and to which dose levels these nodes should be treated.

It can be concluded that ^{18}FDG-PET can provide important complementary information for radiotherapy planning in head and neck cancer. The GTV may be reduced which can facilitate the sparing of nearby normal structures and allow dose escalation to relatively small boost volumes. Furthermore, ^{18}FDG-PET may identify
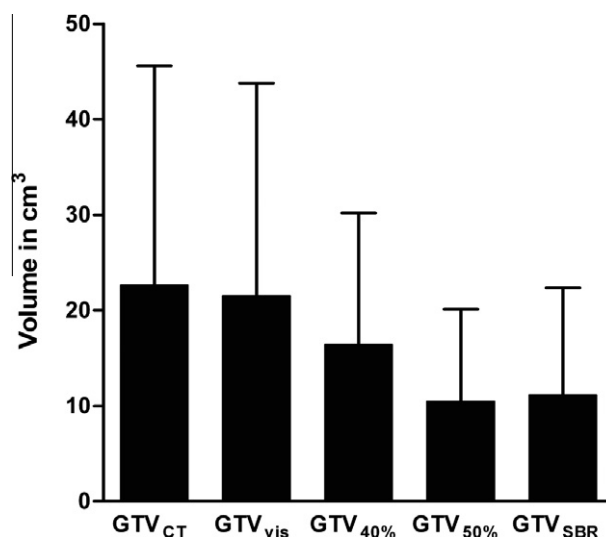

Fig. 2. Mean absolute gross tumor volumes (GTV) obtained after segmentation of the ^{18}FDG-PET signal in 78 head and neck cancer patients using the various methods described in Fig. 1. Error bars indicate SD of the mean. Reprinted from [26] with permission.

areas of tumour spread not recognized by anatomical imaging, which can potentially improve the accuracy of GTV definition. However, to address the clinical value of these concepts, additional histologic validation studies and properly designed clinical studies for the evaluation of local tumour control and radiation-induced toxicity are necessary before [18]FDG-PET can be used safely in routine daily practice.

Dose escalation based on [18]FDG-PET

The metabolic activity detected by [18]FDG may be indicative of tumour cell density. Therefore, [18]FDG-PET can be used to direct dose escalation to [18]FDG-avid subvolumes of the tumour applying either uniform or voxel intensity-based dose escalation [3,30,31]. Schwartz et al. were the first to deliver a uniform escalated dose of 75 Gy in a theoretical planning study involving 20 patients with head and neck cancer [30]. Vanderstraeten et al. applied voxel-intensity-based dose escalation, whereby the [18]FDG signal intensity in the PET voxel is proportionally related to the dose described to that voxel; that is, the higher the PET signal, the higher the prescribed dose [31]. The feasibility of dose escalation using a uniform dose distribution was demonstrated in a phase I clinical trial including 41 head and neck cancer patients, delivering doses up to 77.5 Gy, partly in 3 Gy fractions employing IMRT with simultaneous integrated boost (SIB) [32]. Data on treatment outcome applying this approach are still pending.

One study has addressed the possibility of adaptive image-guided radiotherapy based on repetitive [18]FDG-PET imaging. The results of this study are discussed in the section 'Adaptive radiation treatment planning based on repetitive [18]FDG-PET'.

Initial clinical results after [18]FDG-PET–CT guided IMRT planning

Recently, retrospective studies addressed the impact of integration of [18]FDG-PET–CT data into IMRT planning on clinical treatment outcome. A case-control study compared 45 patients with stage IV-A pharyngeal carcinomas treated with [18]FDG-PET–CT-based IMRT with a historical matched cohort receiving three-dimensional conformal radiotherapy without [18]FDG-PET [33]. The 2-year overall survival and event-free survival rates of patients treated with [18]FDG-PET–CT-based IMRT were 91% and 80%, and significantly better than for the control group. A similar study reported 2-year overall survival and disease-free survival rates of 83% and 71%,respectively, for 42 patients with head and neck cancer of various stage and subsites [34]. Toxicity profiles in this second study were reported as favourable.

Although encouraging, the results of these studies must be interpreted cautiously because they suffer from a number of flaws including small and heterogeneous patient populations, short follow-up, and use of historical controls. Furthermore, it remains unclear from both studies whether the suggested improvements in tumour control must be attributed to improved radiotherapy techniques, or the introduction of [18]FDG-PET–CT or to other factors.

Adaptive radiation treatment planning based on repetitive [18]FDG-PET

Thus far, only one proof of concept study on ten patients with pharyngo-laryngeal squamous cell carcinomas has addressed the impact of adaptive radiation treatment planning in the head and neck [35]. The patients were repetitively imaged using contrast-enhanced CT, MRI and dynamic [18]FDG-PET before the start of treatment and then once weekly during week 2–5. GTVs were delineated in CT and MRI, and segmented on PET using the gradient-based segmentation method [27]. Furthermore, the clinical target volume (CTV), planning target volume (PTV) and organs at risk (i.e., parotid glands, spinal cord, oral cavity) were defined and treatment plans calculated using the SIB IMRT approach. The GTVs delineated from functional imaging were at all times significantly smaller than those defined on anatomical imaging. During the course of treatment, the CTVs and PTVs progressively decreased; at 45 Gy the mean volumes had decreased by 51% and 48%, respectively. However, these findings did not translate into significantly reduced average doses to the organs at risk.

This adaptive treatment planning approach combined with highly conformal dose delivery poses the possibility of dose escalation impacting on tumour control. However, clinical trials need to first address the safety of this approach and assess the possible improvement in outcome.

Hypoxia PET

Selection and delineation of hypoxic tumour subvolumes

Hypoxia is a common feature in head and neck tumours adversely affecting treatment response and prognosis [36–38]. With the increasing use of IMRT, there is great interest in identifying
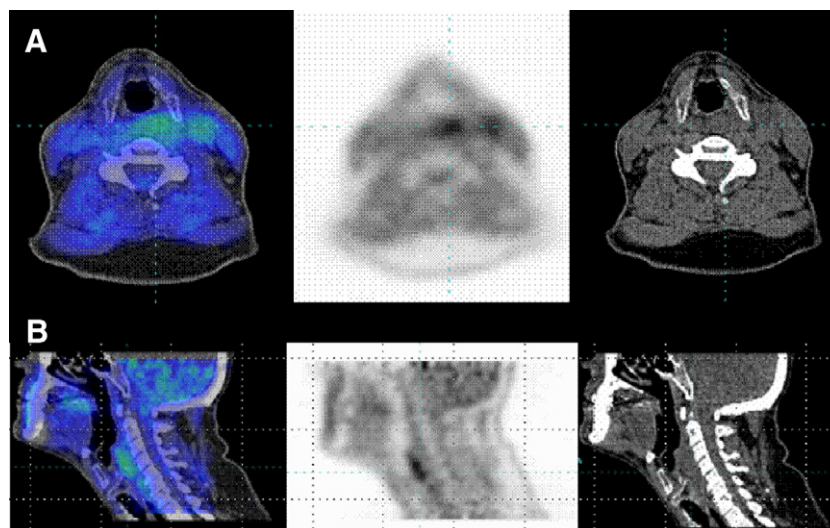

Fig. 3. Fused [18]FMISO-PET–CT (left column), [18]FMISO-PET (middle column) and CT scan (right column) of a patient with a cT3N2bMo supraglottic laryngeal tumour. Images were obtained 4 h after injection of 408 MBq [18]FMISO and are shown in coronal (A) and sagittal (B) view. These images were acquired on a Siemens Biograph HiRez and are courtesy of Dr. S. Welz.

and delineating hypoxic tumour subvolumes for selective escalation of the radiation dose as a method to circumvent hypoxia-induced radioresistance.

^{60}Cu(II)-Diacetyl-bis(N^4-methylthiosemicarbazone) (^{60}Cu-ATSM) was the first hypoxia-related PET tracer for which the potential use of a selective boost to the hypoxic subvolume was illustrated [39]. Partly due to its limited specificity, especially if imaging is performed at relatively short intervals after its administration, this compound did not find its way in larger scale clinical studies.

^{18}F-Fluoromisonidazole (^{18}FMISO) is a nitroimidazole PET tracer that has been extensively used for the detection of hypoxia in various tumour sites, such as the head and neck. First attempts were made to delineate a biological target volume based on ^{18}FMISO-PET [40–42] (Fig. 3). Lee et al. defined the hypoxic subvolume as voxels with an ^{18}FMISO tumour-to-blood activity ratio $\geqslant$1.3 encompassed by the GTV delineated CT and ^{18}FDG-PET [40]. Rajendran et al. also defined one hypoxic subvolume within the gross tumour volume defined on CT and ^{18}FDG-PET [41]. Finally, Thorwarth et al. determined hypoxic voxels based on dynamic ^{18}FMISO-PET imaging. The voxels' different degree of hypoxia served as basis for a map of locally varying dose-escalation factors allowing spatially variant doses [42].

Although all three approaches successfully defined hypoxic subvolumes, the relatively long time for ^{18}FMISO diffusion and uptake hinders quantification of hypoxia.

^{18}F-Fluoroerythronitroimidazole (^{18}FETNIM), ^{18}F-fluoroazomycin arabinoside (^{18}FAZA) and ^{18}F-2-(2-nitroimidazol-1-yl)-N-(3,3,3-trifluoropropyl)-acetamide (^{18}F-EF3) are new generation nitroimidazoles. Souvatzoglou et al. proved ^{18}FAZA-PET to be suitable for clinical use in head and neck tumours [43]. Subsequently, Grosu et al. defined hypoxic subvolumes of different size and distribution based on ^{18}FAZA-uptake exceeding the background muscle uptake by 50% or more [44]. Based on positive findings regarding the ^{18}FAZA reproducibility, the authors stated that these subvolumes could theoretically be used as biologic target volume for radiation treatment planning [44,45].

A phase I study using ^{18}F-EF3 has shown the tracer to be safe in head and neck patients, but the number of tumours visualized was disappointingly low [46].

Although the initial findings on subvolume definition incorporating various hypoxic PET tracers are promising, the data have to be interpreted cautiously because the number of theoretical datasets studied was limited.

Dose escalation based on hypoxia PET

Apart from identification and delineation of hypoxic volumes, theoretical planning studies have escalated the dose to these biological target volumes [40–42]. Two theoretical planning studies proved the feasibility of dose escalation to the ^{18}FMISO-PET detected hypoxic subvolume using IMRT [40,41]. In a third study, Thorwarth et al. compared conventional IMRT planning with dose painting by numbers based on dynamic ^{18}FMISO-PET data [42]. Applying this approach, the tumour control probability could potentially be increased while maintaining the same level of toxicity.

Experience with dose escalation based on hypoxic PET tracers other than ^{18}FMISO is limited. Only Grosu et al. proved the theoretical feasibility of dose escalation to 80.5 Gy on ^{18}FAZA positive tumour subvolumes [44].

The employment of radiation dose escalation based on hypoxia PET in practice awaits early clinical testing.

Clinical outcome and adaptive treatment based on hypoxia PET

Over the past few years, ^{18}FMISO-PET was found to have both prognostic and possibly also predictive value in various small studies on head and neck cancer patients [47–50]. In three clinical studies, the degree of hypoxia visualized on ^{18}FMISO-PET prior to treatment significantly correlated with locoregional failure [47,49, 50]. Rather surprising, Lee et al. recently reported excellent local and regional control rates (100% and 95%, respectively) despite the fact that 18 of the twenty patients studied had evidence of hypoxia in the primary tumour and/or metastatic lymph nodes on the pre- or mid-treatment ^{18}FMISO-PET scans [48]. However, based on the reported 100% local control rate, no firm conclusions regarding the prognostic value of ^{18}FMISO-PET could be drawn. Rischin et al. published data supporting also predictive value of ^{18}FMISO [49]. Advanced stage head and neck cancer patients were treated with radiotherapy and concurrent chemotherapy alone or combined with a hypoxic cytotoxin. Patients with hypoxic tumours treated with the additional hypoxic cytotoxin developed significantly less local failures compared to patients treated with chemoradiation alone [49].

Interestingly, high uptake of the new nitroimidazole ^{18}FETNIM was also associated with a trend towards poor overall survival in head and neck tumours [51].

Although hypoxic subvolumes or voxels can be identified, no studies on adaptive radiotherapy planning have been performed yet. One of the reasons for this is that pre-clinical studies on head and neck xenograft tumour lines found tumour cell hypoxia to be a highly dynamic process both in location and time [52]. This probably influences results of non-invasive *in vivo* imaging, ultimately affecting patient selection for treatment modification, subvolume definition for dose escalation, adaptive radiotherapy planning and tumour response evaluation.

The large temporal fluctuations of the tumour oxygenation status before and during treatment have been shown in a study on ^{18}FMISO reproducibility (strong correlation in only 46% of the patients studied) [53]. In a subsequent study, Lin et al. assessed the effect of these changes in a theoretical planning study on seven head and neck cancer patients undergoing IMRT [54]. They found that although spatial changes occurred in the majority of patients, the equivalent uniform dose to the hypoxic volume could still be significantly increased using dose-painting IMRT (from 70 to 80 Gy).

In summary, a number of hypoxic or hypoxia-related PET tracers are available that are able to identify hypoxic tumour subvolumes. However, before these can be clinically implemented for patient selection, dose escalation or adaptive radiotherapy, additional study is required. Unresolved issues include: limited spatial resolution; further knowledge about the influence of changes in the oxygenation status before and during treatment; and questions about radiation dose levels required to effectively eliminate these radioresistant subpopulations.

Other PET tracers

False-positive readings due to tracer uptake in inflammatory tissue or reactive lymph nodes are the major limitation of ^{18}FDG-PET in oncology. Therefore, PET tracers that more specifically image DNA-, protein- or lipid-synthesis are currently being developed and tested.

Tumour cell proliferation adversely affects radiation treatment outcome and prognosis. 3′-Deoxy-3′-^{18}F-fluorothymidine (^{18}FLT) is a tracer reflecting DNA-synthesis and is not influenced by peritumoral inflammation [55]. This promising compound was shown to be useful for imaging primary tumours but not for the detection of metastatic lymph nodes of head and neck cancer due to a high rate of false-positive findings caused by ^{18}FLT uptake in the germinal centres of reactive lymph nodes [56,57]. Recently, our group assessed the value of repetitive ^{18}FLT-PET–CT imaging regarding

volumetric and signal changes in ten oropharyngeal cancer patients undergoing (chemo)radiation [58]. All patients underwent combined anatomical and functional imaging before treatment, and in the second and the fourth week of (chemo)radiation. It was found that the GTV on CT decreased significantly between the second and third CT scan, but not in the initial phase of treatment. In contrast to this, the [18]FLT-PET signal calculated as SUV already decreased significantly before the second PET scan. However, due to the rapid decline in [18]FLT-PET signal intensity, the applied PET segmentation methods resulted in unsatisfactory volumes during treatment and were thus not useful for adaptive radiotherapy planning [58].

O-2-^{18}F-Fluoroethyl-L-tyrosine ([18]FET) and L-methyl-^{11}C-methionine (^{11}C-MET) are amino acids used to visualize cellular amino acid uptake or protein synthesis. [18]FET may be useful in differentiating tumour from inflammatory tissue, but for ^{11}C-MET, high uptake in the normal tissues was found [59,60].

1-^{11}C-acetate (^{11}C-ACE) may be a biomarker for the anabolic pathway metabolism in cancer tissues. The use of ACE-PET for tumour volume delineation resulted in 51% larger volumes than obtained with [18]FDG-PET [61]. The biological information provided by ACE-PET needs to be further evaluated.

Finally, non-invasive methods to assess the uptake and biodistribution of biological modifiers will be of great value to direct new targeted therapies, such as antibodies against the epidermal or vascular endothelial growth factor receptors (EGFR, VEGFR). Radiolabelled antibodies and small molecules for PET imaging are currently being developed and tested in pre-clinical and early clinical studies [62–66].

In conclusion, PET tracers imaging specific biological tumour characteristics offer potential for tailor-made radiation therapy. However, they remain in the research arena until proper clinical validation.

General conclusions and future prospects

1. [18]FDG-PET is not recommended for the routine diagnostic work-up and staging of head and neck cancer, except in case of cervical metastases from an unknown primary tumour. In the setting of the unknown primary tumour, it may be beneficial if conventional imaging modalities fail to identify the tumour.
2. [18]FDG-PET can improve the accuracy of gross tumour volume delineation. Automatic tools for tumour delineation reduce intra- and inter-observer variability and are therefore recommended. Validation of the various threshold- and gradient-based segmentation methods is mandatory before they can be safely applied in clinical practice.
3. [18]FDG-PET can facilitate boost planning and dose escalation to smaller volumes. The feasibility of this approach is under investigation in phase I-II clinical trials. Proof of concept has been demonstrated for adaptive [18]FDG-PET-guided radiotherapy. Clinical testing is awaited.
4. PET tracers imaging specific biological tumour characteristics remain in the research arena until clinical validation.

Conflict of interest

The authors declare no conflict of interest.

Acknowledgements

References

[1] Feng FY, Kim HM, Lyden TH, et al. Intensity-modulated radiotherapy of head and neck cancer aiming to reduce dysphagia: early dose–effect relationships for the swallowing structures. Int J Radiat Oncol Biol Phys 2007;68:1289–98.
[2] Kam MK, Leung SF, Zee B, et al. Prospective randomized study of intensity-modulated radiotherapy on salivary gland function in early-stage nasopharyngeal carcinoma patients. J Clin Oncol 2007;25:4873–9.
[3] Kapanen M, Collan J, Saarilahti K, Heikkonen J, Kairemo K, Tenhunen M. Accuracy requirements for head and neck intensity-modulated radiation therapy based on observed dose–response of the major salivary glands. Radiother Oncol 2009;93:109–14.
[4] Gordin A, Golz A, Daitzchman M, et al. Fluorine-18 fluorodeoxyglucose positron emission tomography/computed tomography imaging in patients with carcinoma of the nasopharynx: diagnostic accuracy and impact on clinical management. Int J Radiat Oncol Biol Phys 2007;68:370–6.
[5] King AD, Ma BB, Yau YY, et al. The impact of ^{18}F-FDG PET/CT on assessment of nasopharyngeal carcinoma at diagnosis. Br J Radiol 2008;81:291–8.
[6] Ng SH, Yen TC, Liao CT, et al. ^{18}F-FDG PET and CT/MRI in oral cavity squamous cell carcinoma: a prospective study of 124 patients with histologic correlation. J Nucl Med 2005;46:1136–43.
[7] Ng SH, Chan SC, Yen TC, et al. Staging of untreated nasopharyngeal carcinoma with PET/CT: comparison with conventional imaging work-up. Eur J Nucl Med Mol Imaging 2009;36:12–22.
[8] Schoder H, Yeung HW, Gonen M, Kraus D, Larson SM. Head and neck cancer: clinical usefulness and accuracy of PET/CT image fusion. Radiology 2004;231:65–72.
[9] Sigg MB, Steinert H, Gratz K, Hugenin P, Stoeckli S, Eyrich GK. Staging of head and neck tumors: [^{18}F]fluorodeoxyglucose positron emission tomography compared with physical examination and conventional imaging modalities. J Oral Maxillofac Surg 2003;61:1022–9.
[10] Johansen J, Buus S, Loft A, et al. Prospective study of [18]FDG-PET in the detection and management of patients with lymph node metastases to the neck from an unknown primary tumor. Results from the DAHANCA-13 study. Head Neck 2008;30:471–8.
[11] Rusthoven KE, Koshy M, Paulino AC. The role of fluorodeoxyglucose positron emission tomography in cervical lymph node metastases from an unknown primary tumor. Cancer 2004;101:2641–9.
[12] Fletcher JW, Djulbegovic B, Soares HP, et al. Recommendations on the use of ^{18}F-FDG PET in oncology. J Nucl Med 2008;49:480–508.
[13] Kyzas PA, Evangelou E, Denaxa-Kyza D, Ioannidis JP. ^{18}F-Fluorodeoxyglucose positron emission tomography to evaluate cervical node metastases in patients with head and neck squamous cell carcinoma: a meta-analysis. J Natl Cancer Inst 2008;100:712–20.
[14] Lonneux M, Hamoir M, Reychler H, et al. Positron emission tomography with [^{18}F]fluorodeoxyglucose improves staging and patient management in patients with head and neck squamous cell carcinoma: a multicenter prospective study. J Clin Oncol 2010;28:1190–5.
[15] Chang JT, Chan SC, Yen TC, et al. Nasopharyngeal carcinoma staging by (18)F-fluorodeoxyglucose positron emission tomography. Int J Radiat Oncol Biol Phys 2005;62:501–7.
[16] Schinagl DA, Kaanders JH, Oyen WJ. From anatomical to biological target volumes: the role of PET in radiation treatment planning. Cancer Imaging 2006;6:S107–16.
[17] Steenbakkers RJ, Duppen JC, Fitton I, et al. Reduction of observer variation using matched CT-PET for lung cancer delineation: a three-dimensional analysis. Int J Radiat Oncol Biol Phys 2006;64:435–48.
[18] Ciernik IF, Dizendorf E, Baumert BG, et al. Radiation treatment planning with an integrated positron emission and computer tomography (PET/CT): a feasibility study. Int J Radiat Oncol Biol Phys 2003;57:853–63.
[19] Riegel AC, Berson AM, Destian S, et al. Variability of gross tumor volume delineation in head-and-neck cancer using CT and PET/CT fusion. Int J Radiat Oncol Biol Phys 2006;65:726–32.
[20] Daisne JF, Duprez T, Weynand B, et al. Tumor volume in pharyngolaryngeal squamous cell carcinoma: comparison at CT, MR imaging, and FDG PET and validation with surgical specimen. Radiology 2004;233:93–100.
[21] Daisne JF, Sibomana M, Bol A, Doumont T, Lonneux M, Gregoire V. Tri-dimensional automatic segmentation of PET volumes based on measured source-to-background ratios: influence of reconstruction algorithms. Radiother Oncol 2003;69:247–50.
[22] Heron DE, Andrade RS, Flickinger J, et al. Hybrid PET–CT simulation for radiation treatment planning in head-and-neck cancers: a brief technical report. Int J Radiat Oncol Biol Phys 2004;60:1419–24.
[23] Nishioka T, Shiga T, Shirato H, et al. Image fusion between [18]FDG-PET and MRI/CT for radiotherapy planning of oropharyngeal and nasopharyngeal carcinomas. Int J Radiat Oncol Biol Phys 2002;53:1051–7.
[24] Nestle U, Kremp S, Schaefer-Schuler A, et al. Comparison of different methods for delineation of ^{18}F-FDG PET-positive tissue for target volume definition in radiotherapy of patients with non-small cell lung cancer. J Nucl Med 2005;46:1342–8.

[25] Paulino AC, Koshy M, Howell R, Schuster D, Davis LW. Comparison of CT- and FDG-PET-defined gross tumor volume in intensity-modulated radiotherapy for head-and-neck cancer. Int J Radiat Oncol Biol Phys 2005;61:1385–92.

[26] Schinagl DA, Vogel WV, Hoffmann AL, van Dalen JA, Oyen WJ, Kaanders JH. Comparison of five segmentation tools for ^{18}F-fluoro-deoxy-glucose-positron emission tomography-based target volume definition in head and neck cancer. Int J Radiat Oncol Biol Phys 2007;69:1282–9.

[27] Geets X, Lee JA, Bol A, Lonneux M, Gregoire V. A gradient-based method for segmenting FDG-PET images: methodology and validation. Eur J Nucl Med Mol Imaging 2007;34:1427–38.

[28] van Dalen JA, Hoffmann AL, Dicken V, et al. A novel iterative method for lesion delineation and volumetric quantification with FDG PET. Nucl Med Commun 2007;28:485–93.

[29] Schinagl DA, Hoffmann AL, Vogel WV, et al. Can FDG-PET assist in radiotherapy target volume definition of metastatic lymph nodes in head-and-neck cancer? Radiat Oncol 2009;91:95–100.

[30] Schwartz DL, Ford EC, Rajendran J, et al. FDG-PET/CT-guided intensity modulated head and neck radiotherapy: a pilot investigation. Head Neck 2005;27:478–87.

[31] Vanderstraeten B, Duthoy W, De Gersem W, De Neve W, Thierens H. [18]fluoro-deoxy-glucose positron emission tomography ([18]FDG-PET) voxel intensity-based intensity-modulated radiation therapy (IMRT) for head and neck cancer. Radiother Oncol 2006;79:249–58.

[32] Madani I, Duthoy W, Derie C, et al. Positron emission tomography-guided, focal-dose escalation using intensity-modulated radiotherapy for head and neck cancer. Int J Radiat Oncol Biol Phys 2007;68:126–35.

[33] Rothschild S, Studer G, Seifert B, et al. PET/CT staging followed by intensity-modulated radiotherapy (IMRT) improves treatment outcome of locally advanced pharyngeal carcinoma: a matched-pair comparison. Radiat Oncol 2007;2:22.

[34] Vernon MR, Maheshwari M, Schultz CJ, et al. Clinical outcomes of patients receiving integrated PET/CT-guided radiotherapy for head and neck carcinoma. Int J Radiat Oncol Biol Phys 2008;70:678–84.

[35] Geets X, Tomsej M, Lee JA, et al. Adaptive biological image-guided IMRT with anatomic and functional imaging in pharyngo-laryngeal tumors: impact on target volume delineation and dose distribution using helical tomotherapy. Radiother Oncol 2007;85:105–15.

[36] Brizel DM, Sibley GS, Prosnitz LR, Scher RL, Dewhirst MW. Tumor hypoxia adversely affects the prognosis of carcinoma of the head and the neck. Int J Radiat Oncol Biol Phys 1997;38:285–9.

[37] Hoogsteen IJ, Marres HA, van der Kogel AJ, Kaanders JH. The hypoxic tumour microenvironment, patient selection and hypoxia-modifying treatments. Clin Oncol (R Coll Radiol) 2007;19:385–96.

[38] Yaromina A, Thames H, Zhou X, et al. Radiobiological hypoxia, histological parameters of tumour microenvironment and local tumour control after fractionated irradiation. Radiother Oncol 2010;96:116–22.

[39] Chao KS, Bosch WR, Mutic S, et al. A novel approach to overcome hypoxic tumor resistance: Cu-ATSM-guided intensity-modulated radiation therapy. Int J Radiat Oncol Biol Phys 2001;49:1171–82.

[40] Lee NY, Mechalakos JG, Nehmeh S, et al. Fluorine-18-labeled fluoromisonidazole positron emission and computed tomography-guided intensity-modulated radiotherapy for head and neck cancer: a feasibility study. Int J Radiat Oncol Biol Phys 2008;70:2–13.

[41] Rajendran JG, Hendrickson KR, Spence AM, Muzi M, Krohn KA, Mankoff DA. Hypoxia imaging-directed radiation treatment planning. Eur J Nucl Med Mol Imaging 2006;33:44–53.

[42] Thorwarth D, Eschmann SM, Paulsen F, Alber M. Hypoxia dose painting by numbers: a planning study. Int J Radiat Oncol Biol Phys 2007;68:291–300.

[43] Souvatzoglou M, Grosu AL, Roper B, et al. Tumour hypoxia imaging with [18]FAZA PET in head and neck cancer patients: a pilot study. Eur J Nucl Med Mol Imaging 2007;34:1566–75.

[44] Grosu AL, Souvatzoglou M, Roper B, et al. Hypoxia imaging with FAZA-PET and theoretical considerations with regard to dose painting for individualization of radiotherapy in patients with head and neck cancer. Int J Radiat Oncol Biol Phys 2007;69:541–51.

[45] Beck R, Roper B, Carlsen JM, et al. Pretreatment ^{18}F-FAZA PET predicts success of hypoxia-directed radiochemotherapy using tirapazamine. J Nucl Med 2007;48:973–80.

[46] Mahy P, Geets X, Lonneux M, et al. Determination of tumour hypoxia with [(18)F]EF3 in patients with head and neck tumours: a phase I study to assess the tracer pharmacokinetics, biodistribution and metabolism. Eur J Nucl Med Mol Imaging 2008;35:1282–9.

[47] Eschmann SM, Paulsen F, Reimold M, et al. Prognostic impact of hypoxia imaging with ^{18}F-misonidazole PET in non-small cell lung cancer and head and neck cancer before radiotherapy. J Nucl Med 2005;46:253–60.

[48] Lee N, Nehmeh S, Schoder H, et al. Prospective trial incorporating pre-/mid-treatment [18F]-misonidazole positron emission tomography for head-and-neck cancer patients undergoing concurrent chemoradiotherapy. Int J Radiat Oncol Biol Phys 2009;75:101–8.

[49] Rischin D, Hicks RJ, Fisher R, et al. Prognostic significance of [18F]-misonidazole positron emission tomography-detected tumor hypoxia in patients with advanced head and neck cancer randomly assigned to chemoradiation with or without tirapazamine: a substudy of Trans-Tasman Radiation Oncology Group Study 98.02. J Clin Oncol 2006;24:2098–104.

[50] Thorwarth D, Eschmann SM, Scheiderbauer J, Paulsen F, Alber M. Kinetic analysis of dynamic ^{18}F-fluoromisonidazole PET correlates with radiation treatment outcome in head-and-neck cancer. BMC Cancer 2005;5:152.

[51] Lehtio K, Eskola O, Viljanen T, et al. Imaging perfusion and hypoxia with PET to predict radiotherapy response in head-and-neck cancer. Int J Radiat Oncol Biol Phys 2004;59:971–82.

[52] Ljungkvist AS, Bussink J, Kaanders JH, et al. Hypoxic cell turnover in different solid tumor lines. Int J Radiat Oncol Biol Phys 2005;62:1157–68.

[53] Nehmeh SA, Lee NY, Schroder H, et al. Reproducibility of intratumor distribution of (18)F-fluoromisonidazole in head and neck cancer. Int J Radiat Oncol Biol Phys 2008;70:235–42.

[54] Lin Z, Mechalakos J, Nehmeh S, et al. The influence of changes in tumor hypoxia on dose-painting treatment plans based on ^{18}F-FMISO positron emission tomography. Int J Radiat Oncol Biol Phys 2008;70:1219–28.

[55] Shields AF, Grierson JR, Dohmen BM, et al. Imaging proliferation in vivo with [F-18]FLT and positron emission tomography. Nature Med 1998;4:1334–6.

[56] Cobben DC, van der Laan BF, Maas B, et al. ^{18}F-FLT PET for visualization of laryngeal cancer: comparison with ^{18}F-FDG PET. J Nucl Med 2004;45:226–31.

[57] Troost EG, Vogel WV, Merkx MA, et al. ^{18}F-FLT PET does not discriminate between reactive and metastatic lymph nodes in primary head and neck cancer patients. J Nucl Med 2007;48:726–35.

[58] Troost EG, Bussink J, Hoffmann AL, Boerman OC, Oyen WJ, Kaanders JH. ^{18}F-FLT PET/CT for early response monitoring and dose escalation in oropharyngeal tumors. J Nucl Med 2010;51:866–74.

[59] Geets X, Daisne JF, Gregoire V, Hamoir M, Lonneux M. Role of 11-C-methionine positron emission tomography for the delineation of the tumor volume in pharyngo-laryngeal squamous cell carcinoma: comparison with FDG-PET and CT. Radiother Oncol 2004;71:267–73.

[60] Pauleit D, Stoffels G, Schaden W, et al. PET with O-(2-^{18}F-fluoroethyl)-L-tyrosine in peripheral tumors: first clinical results. J Nucl Med 2005;46:411–6.

[61] Sun A, Sorensen J, Karlsson M, et al. 1-[11C]-Acetate PET imaging in head and neck cancer – a comparison with ^{18}F-FDG-PET: implications for staging and radiotherapy planning. Eur J Nucl Med Mol Imaging 2007;34:651–7.

[62] Aerts HJ, Dubois L, Perk L, et al. Disparity between in vivo EGFR expression and [89]Zr-labeled cetuximab uptake assessed with PET. J Nucl Med 2009;50:123–31.

[63] Cai W, Chen K, He L, Cao Q, Koong A, Chen X, et al. Expression in xenograft-bearing mice using ^{64}Cu-labeled cetuximab, a chimeric anti-EGFR monoclonal antibody. Eur J Nucl Med Mol Imaging 2007;34:850–8.

[64] Nagengast WB, de Vries EG, Hospers GA, et al. In vivo VEGF imaging with radiolabeled bevacizumab in a human ovarian tumor xenograft. J Nucl Med 2007;48:1313–9.

[65] Niu G, Li Z, Xie J, Le QT, Chen X. PET of EGFR antibody distribution in head and neck squamous cell carcinoma models. J Nucl Med 2009;50:1116–23.

[66] Wang JQ, Gao M, Miller KD, Sledge GW, Zheng QH. Synthesis of [^{11}C]Iressa as a new potential PET cancer imaging agent for epidermal growth factor receptor tyrosine kinase. Bioorg Med Chem Lett 2006;16:4102–6.

Review

PET scans in radiotherapy planning of lung cancer ☆

Dirk De Ruysscher [a,*], Carl-Martin Kirsch [b]

[a] Department of Radiation Oncology (MAASTRO Clinic), Maastricht University Medical Center, The Netherlands; [b] Department of Nuclear Medicine, Saarland University Medical Center, Homburg, Germany

ARTICLE INFO

ABSTRACT

Especially for non-small cell lung cancer, FDG-PET has in the majority of the patients led to the safe decrease of radiotherapy volumes, enabling radiation-dose escalation and, experimentally, redistribution of radiation doses within the tumor. In limited-disease small cell lung cancer, the role of FDG-PET is emerging.

© 2010 European Society for Therapeutic Radiology and Oncology and European Association of Nuclear Medicine. Published by Elsevier Ireland Ltd. All rights reserved. 96 (2010) 335–338

Radiotherapy is a key treatment modality in the curative treatment of patients with both non-small cell lung cancer (NSCLC) and small cell lung cancer (SCLC). Recent progress in combined modality treatments incorporating radio-chemotherapy, with or without surgery, as well as the technical advances in radiation delivery, has led to significant improvements in treatment outcomes. Careful staging and patient selection are important to achieve the maximal chance of long-term survival with acceptable side effects. Similarly, accurate delineation of target volumes is crucial for preventing geographical misses. An incorrect definition of the gross tumor volume (GTV) (i.e. detectable tumor) or clinical target volume (CTV) (tumor plus a margin for microscopic extension) is a source of systematic errors, which can lead to under-treatment and reduce the probability of tumor control.

As the overwhelming majority of the relevant clinical work has been done with [18F]deoxyglucose (FDG), which is moreover the only PET radiopharmaceutical that is widely available, in the rest of this section, by PET, FDG-PET is meant unless otherwise stated.

In contrast with diagnostic questions, which basically go down to dichotomous outcomes, that is, cancer yes/ no, in radiotherapy, also the volume and shape of the tumor volumes are of importance. Moreover, uncertainties, for example due to tumor movements, should be tackled.

Although covered in other sections, it should directly be stressed that as with any other imaging and therapeutic modality, PET in radiotherapy *must* also be calibrated thoroughly as well as used in strict clinical protocols. Indeed, the influence of technical factors in the measurement of the Standardized Uptake Value cannot be overemphasized. Volume assessment with PET is crucially dependent on technical factors and huge mistakes can only be avoided by sticking to well-established protocols [1]. Moreover, patients should be placed in a treatment planning position on the PET-(CT) scan, which implies strict protocols that should be adhered to in different departments.

Non-small cell lung cancer (NSCLC)

Target volume selection

Many studies have investigated the specificity and sensitivity of CT scans vs. FDG-PET-(CT) scans. For the evaluation of indeterminate lung lesions, the sensitivity and specificity ranged in five studies from 79% to 96% and from 40% to 83% (reviewed in Ref. [2]). The main limitations of FDG-PET in the evaluation of lung nodules are due to an increased uptake of FDG in inflammatory sites leading to a reduction of the specificity. Nevertheless, the sensitivity is about 90%, which is very high.

For mediastinal lymph node staging, the role of FDG-PET scan is very well established. While the sensitivity of CT is 56%, for FDG-PET, this is 83% for all stages, 91% when the CT scan shows enlarged lymph nodes, and 70% for normal-sized lymph nodes. The specificity for CT is 81%, for FDG-PET for all stages 89%, with enlarged nodes 70%, and with normal-appearing lymph nodes on

---

☆ Guidelines for the use of PET in radiotherapy planning A. Chiti (EANM) and V. Grégoire (ESTRO).

* Corresponding author. Address: Maastricht University Medical Center, Department of Radiation Oncology (MAASTRO Clinic), GROW Research Institute, Maastricht, The Netherlands.

E-mail addresses: dirk.deruysscher@maastro.nl (D. De Ruysscher), carl.m.kirsch @uniklinikum-saarland.de (C.-M. Kirsch).

CT 94% (reviewed in Ref. [2]). These results should be viewed in perspective with the current golden standard, mediastinoscopy. The specificity is 100%, but the sensitivity is 78% for all stages, 82% when the CT scan shows enlarged lymph nodes, and 42% for normal-sized lymph nodes.

In conclusion, the major role of FDG-PET is due to its very high negative predictive value (>90%) for the detection of mediastinal lymph nodes. It should be noted that these favorable results only hold true when no chemotherapy was administered, for chemotherapy markedly reduced the accuracy of FDG-PET-CT scans [3].

Accurate identification of nodal metastases is crucial for planning curative radiotherapy, particularly as the routine elective nodal irradiation is no longer recommend in NSCLC [4]. In several planning studies, it was shown that PET or PET-CT influences the GTV [5,6]. The PET volumes were in general smaller than with CT, thus leading to a decreased radiation exposure of the lungs and the esophagus sufficiently as to allow for radiation-dose escalation [7,8]. A prospective clinical trial using this approach reported isolated nodal failures in only 1 of 44 patients [9] (Fig. 1). These results were subsequently confirmed in another, similar prospective study from the Netherlands Cancer Institute [10], but not in a US retrospective series [11]. The latter may be due to the absence of a clearly defined PET-delineation protocol. This underscores the absolute pre-requisite of a well-established protocol before PET-based tumor definition may be introduced into clinical practice [6,12]. Moreover, clinicians need to update these protocols on a regular basis as much research is ongoing in this field, which will result in ever-improving the current state-of-the-art.

Although PET-defined mediastinal radiotherapy fields appear to be safe, because of a false-positive rate of approximately 30%, depending on the patient population, ideally, pathological confirmation of PET-positive mediastinal nodes should be obtained by mediastinoscopy or endoscopic ultrasound-guided fine needle aspiration (EUS-FNA).

If selective nodal irradiation is done, be it for the whole radiotherapy treatment or only after an elective part, FDG-PET-based radiotherapy planning is the method of choice, because of the reproducible higher accuracy of PET over CT. Obviously, all other diagnostic information, including findings at bronchoscopy, mediastinoscopy, endoscopic ultrasound, and others, should be taken into account.

Although this approach is safe from the point of view of the small proportion of isolated nodal failures, more studies to demonstrate the benefit of this policy are needed.

Target volume delineation

At present, FDG-PET scans offer little additional advantage over CT or MRI scans for staging of the primary tumor because of its lack of precise anatomical localization. The spatial resolution of modern CT scanners (typically about 1 mm) is far superior to that of current PET scanners (6–8 mm), – which is considerably compromised by respiratory motion in real life – so that the extra gain with fusion is expected not be large, unless PET scans can reliably address tumor delineation caused by atelectasis or intra-tumor heterogeneity. However, PET did show a remarkably good correlation with pathology and patient data [12–14] (illustrated in Fig. 2).

Moreover, PET scans reduced the inter-observer variability compared to CT alone [15]. Integrated PET-CT scans further improved delineation variability [16]. The next step is to use the PET signal to construct an automatic delineation of the tumor [12] and to offer the radiation oncologist a solution that only needs contour editing. This method was on its turn to be less prone to variability than PET-CT [12].

As PET acquisition takes several minutes, tumor motion due to respiration or cardiac action results in PET 'GTV's' that incorporate at least some effects of this motion. Respiration-gated PET acquisition techniques have been developed [17,18] and are at present evaluated in clinical studies.

Dose distribution comparison

Many studies have investigated radiation dose distributions based on CT or on FDG-PET (reviewed in Ref. [4]). All of them showed a significant decrease of the irradiated volumes when FDG-PET-based radiotherapy planning was used. This was obvious in the case of atelectasis, where PET enables the differentiation between tumor and collapsed lung. Also nodal volumes decreased in over 80% of the patients, thus theoretically allowing radiation-dose escalation with the same toxicity or decreasing normal tissue exposure for radiation with the same tumor dose. This strategy is still experimental. Optimal PET acquisition is crucial [19].

Clinical outcome comparison

No randomized phase III trial has been reported comparing PET with CT planning. However, PET scans have shown to detect distant metastases in up to 30% of the patients with stage III NSCLC who were M0 with conventional staging [19,20]. This clearly affects patient outcome for it spares toxic therapy in individuals who will not benefit from it.

The incorporation of PET into radiotherapy planning has as previously shown the potential to allow radiation-dose escalation without increasing side effects, this is because of the reduction of radiation fields [7,8]. In a large phase II trial, it was shown that this pre-requisite is indeed true [21]. Whether this radiation dose increase will ultimately lead to higher cure rates is a matter of current research.

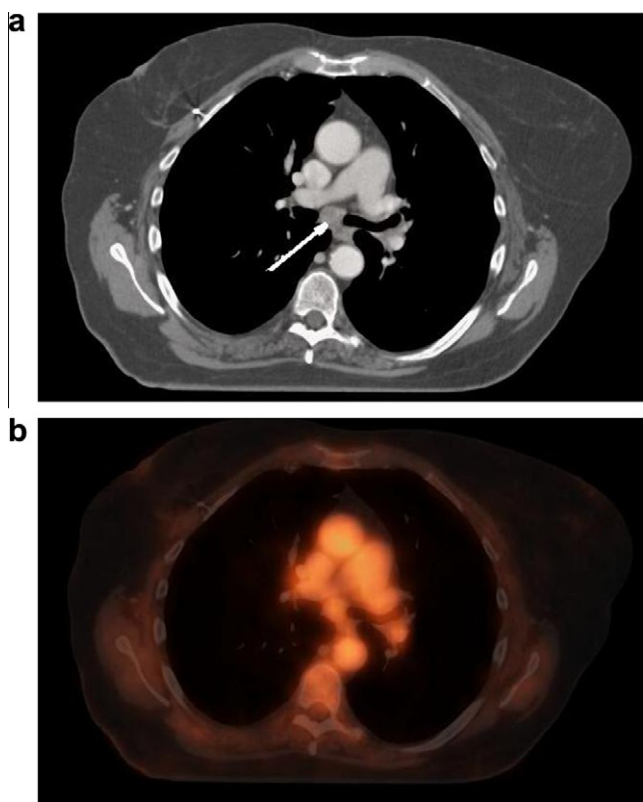**Fig. 1.** Axial view of ^{18}FDG-PET-CT with contrast. CT shows an enlarged subcarinal node (level 7, diameter of 1.9 cm, white arrow), while PET shows no FDG uptake in level 7. This finding influences the delineation of the nodal target volume.
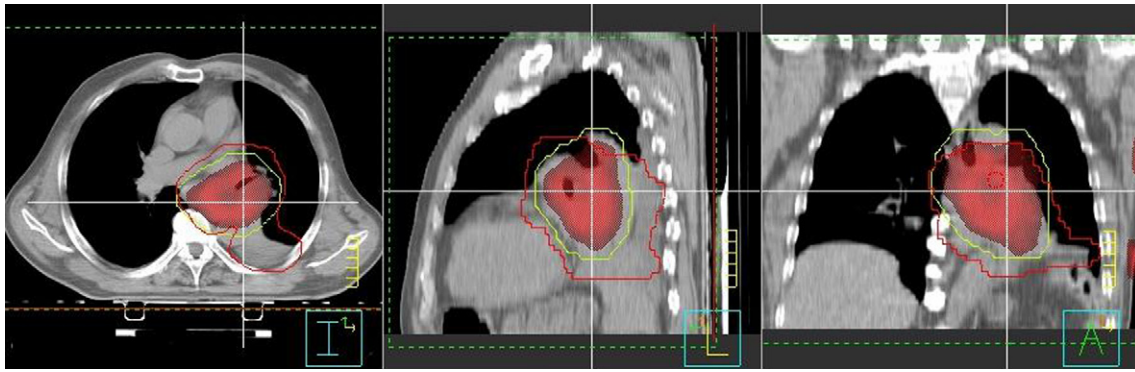
Fig. 2. Radiotherapy planning using CT and PET derived 3D information: the yellow line shows the GTV as derived form PET plus an 8 mm expansion; the red line represents the CT-derived GTV + 8 mm expansion. Please note: (a) the general shrinkage of the GTV using PET and (b) the missing part of the GTV using CT (red line) in the sagittal view (image in the middle) as compared to the PET-derived GTV (yellow line) still containing tumor. Yellow line, GTV (derived from FDG-PET) + 8 mm expansion. Red line, GTV (derived from CT) + 8 mm expansion.

Experimentally, PET scans may also allow the identification of therapy-resistant areas within the tumor that could be given a higher radiation dose and hence lead to a better outcome [22–24].

Adaptive treatment

Significant changes of FDG uptake in the primary lung tumor during a course of radiotherapy have been described [16]. Although in most patients a decrease was observed, in about 15% FDG uptake increased dramatically. Most of these patients have a very bad prognosis. Further research may incorporate early FDG-PET scans early during treatment for treatment adaptation [25].

Limited-disease small-cell lung cancer (LD-SCLC)

Target volume selection

Although many studies have investigated the specificity and sensitivity of CT scans vs. FDG-PET-(CT) scans for the staging of small cell lung cancer, its role has not been clearly established [26–31]. In general, though, the accuracy for detection mediastinal lymph nodes is higher with PET than with CT.

Although after CT-based radiotherapy planning, isolated nodal recurrences may be seen in over 10% of the patients, in a prospective study selective nodal irradiation based on PET scans proved to result in only 3% of isolated nodal failures [32].

Target volume delineation

No studies have been performed investigating target volume delineation based on PET for small cell lung cancer.

Dose distribution comparison

In one study, FDG-PET changed radiotherapy fields in 25% of patients with limited-stage small cell lung cancer [33]. Both increases and decreases of the volumes were found.

Clinical outcome comparison

No randomized studies are available comparing PET with CT planning. In the only prospective study in which the nodal volumes were defined on the basis of FDG-PET, only 3% isolated nodal failures were observed, and the incidence of severe esophagitis was only half of expected [32].

Adaptive treatment

No studies have been described on adaptive treatment in small cell lung cancer.

Other tracers than FDG

Hypoxia

Visualizing and quantifying hypoxia is of obvious importance, for hypoxia is related to resistance for radio- and chemotherapy and the early occurrence of distant metastases. PET scans suitable for hypoxia detection would also enable the selection of patients for hypoxic cell sensitizers. Many PET tracers have been investigated, including ^{18}F-misonidazole, (62)Cu-diacetyl-bis(N(4)-methylthiosemicarbazone (^{62}Cu-ATSM), and 1-alpha-D-(5-deoxy-5-[(18)F]-fluoroarabinofuranosyl)-2-nitroimidazole (^{18}F-FAZA) [34]. At present, it is unclear as which one is the most suitable in clinical practice, and this is the subject of intensive ongoing research.

It should nevertheless be stressed that although FDG uptake is increased in hypoxic tumor regions, FDG is not a hypoxia marker. Indeed, the uptake of FDG and hypoxia markers dissociates both in animal models and in clinical trials, with spatial mismatching probably being more pronounced in SCLC than in NSCLC [35,36].

Proliferation

Many tracers are correlated with cell proliferation, but the measurement of thymidine kinase 1 with (18)F-fluoro-L-thymidine (^{18}F-FLT) has been studied the most extensively [37]. This tracer is from a diagnostic point of view less accurate than FDG for the staging of NSCLC, but it may give interesting information on early tumor response to chemotherapy or chemo-radiation [38]. This and other tracers may therefore enter clinical practice in the future [39].

Conclusions

For NSCLC, FDG-PET scans allow more thorough staging, thus avoiding unnecessary treatments. It reduces radiation treatment volumes because of the avoidance of mediastinal lymph nodes that are PET negative and hence reduces toxicity with the same radiation dose or enables radiation-dose escalation with the same toxicity. Data are also encouraging for small cell lung carcinoma.

More research is needed to assess the effect of PET on survival.

PET also reduces inter-observer variability for delineating tumors and opens perspective for more automated delineation parts

in radiation planning, as well as innovative radiation treatment delivery.

Using diagnostic PET-CT scans for radiotherapy treatment planning is attractive, for it saves time and resources. However, the disadvantages are the influence of time delay between the diagnosis and referral for radiotherapy on tumor volume and tracer uptake, the effects of induction systemic therapy on FDG uptake, the differences in patient position and immobilization devices between diagnostic and therapeutic sets, calibration and SUV measurement issues, and breathing (4D) information that has now become standard in radiotherapy treatment for lung cancer and is not regularly available from diagnostic images. Although many issues can be solved, especially breathing and positioning differences support the use of a new PET-CT scan specifically designed for radiotherapy planning [39].

Although FDG has been extremely useful for lung cancer radiotherapy and new applications still emerge, new tracers are of interest, for they may be more specific for tumor characteristics such as proliferation and hypoxia. These tracers are at present in use in clinical investigations.

References

[1] Boellaard R, Oyen WJ, Hoekstra CJ, et al. The Netherlands protocol for standardisation and quantification of FDG whole body PET studies in multi-centre trials. Eur J Nucl Med Mol Imaging 2008;35:2320–33.

[2] Hellwig D, Baum RP, Kirsch C. FDG-PET, PET/CT and conventional nuclear medicine procedures in the evaluation of lung cancer: a systematic review. Nuklearmedizin 2009;48:59–69.

[3] Dooms C, Verbeken E, Stroobants S, et al. Prognostic stratification of stage IIIA-N2 non-small-cell lung cancer after induction chemotherapy: a model based on the combination of morphometric-pathologic response in mediastinal nodes and primary tumor response on serial 18-fluoro-2-deoxy-glucose positron emission tomography. J Clin Oncol 2008;26:1128–34.

[4] Senan S, De Ruysscher D, Giraud P, et al. Literature-based recommendations for treatment planning and execution in high-precision radiotherapy in lung cancer. Radiother Oncol 2004;71:139–46.

[5] Nestle U, Kremp S, Grosu AL. Practical integration of [18F]-FDG-PET and PET-CT in the planning of radiotherapy for non-small cell lung cancer (NSCLC): the technical basis, ICRU-target volumes, problems, perspectives. Radiother Oncol 2006;81:209–25.

[6] Nestle U, Schaefer-Schuler A, Kremp S, et al. Target volume definition for 18F-FDG PET-positive lymph nodes in radiotherapy of patients with non-small cell lung cancer. Eur J Nucl Med Mol Imaging 2007;34:453–62.

[7] van Der Wel A, Nijsten S, Hochstenbag M, et al. Increased therapeutic ratio by 18F-DG-PET-CT planning in patients with clinical CT stage N2/N3 M0 non-small cell lung cancer (NSCLC): a modelling study. Int J Radiat Oncol Biol Phys 2005;61:648–54.

[8] De Ruysscher D, Wanders S, Minken A, et al. Effects of radiotherapy planning with a dedicated combined PET-CT-simulator of patients with non-small cell lung cancer on dose limiting normal tissues and radiation dose-escalation: results of a prospective study. Radiother Oncol 2005;77:5–10.

[9] De Ruysscher D, Wanders S, van Haren E, et al. Selective mediastinal node irradiation on basis of the FDG-PET scan in patients with non-small cell lung cancer: a prospective clinical study. Int J Radiat Oncol Biol Phys 2005;62:988–94.

[10] Belderbos JS, Heemsbergen WD, De Jaeger K, et al. Final results of a Phase I/II dose escalation trial in non-small-cell lung cancer using three-dimensional conformal radiotherapy. Int J Radiat Oncol Biol Phys 2006;66:126–34.

[11] Sura S, Greco C, Gelblum D, et al. (18)F-Fluorodeoxyglucose positron emission tomography-based assessment of local failure patterns in non-small-cell lung cancer treated with definitive radiotherapy. Int J Radiat Oncol Biol Phys 2008;70:1397–402.

[12] Nestle U, Kremp S, Schaefer-Schuler A, et al. Comparison of different methods for delineation of 18F-FDG PET-positive tissue for target volume definition in radiotherapy of patients with non-small cell lung cancer. J Nucl Med 2005;46:1342–8.

[13] van Baardwijk A, Bosmans G, Boersma L, et al. PET-CT-based auto-contouring in non-small-cell lung cancer correlates with pathology and reduces interobserver variability in the delineation of the primary tumor and involved nodal volumes. Int J Radiat Oncol Biol Phys 2007;68:771–8.

[14] Stroom J, Blaauwgeers H, van Baardwijk A, et al. Feasibility of pathology-correlated lung imaging for accurate target definition of lung tumors. Int J Radiat Oncol Biol Phys 2007;69:267–75.

[15] Schaefer A, Kremp S, Hellwig D, et al. A contrast-oriented algorithm for FDG-PET-based delineation of tumour volumes for the radiotherapy of lung cancer: derivation from phantom measurements and validation in patient data. Eur J Nucl Med Mol Imaging 2008;35:1989–99.

[16] MacManus M, Nestle U, Rosenzweig KE, et al. Use of PET and PET/CT for radiation therapy planning: IAEA expert report 2006–2007. Radiother Oncol 2009;91:85–94.

[17] Nehmeh SA, Erdi YE, Rosenzweig KE, et al. Reduction of respiratory motion artifacts in PET imaging of lung cancer by respiratory correlated dynamic PET: methodology and comparison with respiratory gated PET. J Nucl Med 2003;44:1644–8.

[18] Grgic A, Nestle U, Schaefer-Schuler A, et al. FDG-PET-based radiotherapy planning in lung cancer: optimum breathing protocol and patient positioning – an intraindividual comparison. Int J Radiat Oncol Biol Phys 2009;73:103–11.

[19] Hicks RJ, Kalff V, MacManus MP, et al. 18F-FDG PET provides high-impact and powerful prognostic stratification in staging newly diagnosed non-small cell lung cancer. J Nucl Med 2001;42:1596–604.

[20] MacManus MP, Hicks RJ, Matthews JP, et al. High rate of detection of unsuspected distant metastases by PET in apparent stage III non-small-cell lung cancer: implications for radical radiation therapy. Int J Radiat Oncol Biol Phys 2001;50:287–93.

[21] van Baardwijk A, Wanders S, Boersma L, et al. Mature results of an individualized radiation dose prescription study based on normal tissue constraints in stage I–III non-small cell lung cancer. J Clin Oncol 2010;28:1380–6.

[22] Aerts HJ, Bosmans G, van Baardwijk AA, et al. Stability of (18)F-deoxyglucose uptake locations within tumor during radiotherapy for NSCLC: a prospective study. Int J Radiat Oncol Biol Phys 2008;71:1402–7.

[23] Aerts HJ, van Baardwijk AA, Petit SF, et al. Identification of residual metabolic-active areas within individual NSCLC tumours using a pre-radiotherapy (18)fluorodeoxyglucose-PET-CT scan. Radiother Oncol 2009;91:386–92.

[24] van Baardwijk A, Bosmans G, Dekker A, et al. Time trends in the maximal uptake of FDG on PET scan during thoracic radiotherapy in relation to metabolic response. A prospective study in locally advanced non-small cell lung cancer patients. Radiother Oncol 2007;82:145–52.

[25] Brink I, Schumacher T, Mix M, et al. Impact of [18F]FDG-PET on the primary staging of small-cell lung cancer. Eur J Nucl Med Mol Imaging 2004;31:1614–20.

[26] Fischer BM, Mortensen J, Langer SW, et al. A prospective study of PET/CT in initial staging of small-cell lung cancer: comparison with CT, bone scintigraphy and bone marrow analysis. Ann Oncol 2007;18:338–45.

[27] Niho S, Fujii H, Murakami K, et al. Detection of unsuspected distant metastases and/or regional nodes by FDG-PET in LD-SCLC scan in apparent limited-disease small-cell lung cancer. Lung Cancer 2007;57:328–33.

[28] Pandit N, Gonen M, Krug L, et al. Prognostic value of [18F]FDG-PET imaging in small cell lung cancer. Eur J Nucl Med Mol Imaging 2003;30:78–84.

[29] Shen YY, Shiau YC, Wang JJ, et al. Whole-body 18F-2-deoxyglucose positron emission tomography in primary staging small cell lung cancer. Anticancer Res 2002;22:1257–64.

[30] Kamel EM, Zwahlen D, Wyss MT, et al. Whole-body (18)F-FDG PET improves the management of patients with small cell lung cancer. J Nucl Med 2003;44:1911–7.

[31] van Loon J, De Ruysscher D, Wanders R, et al. Selective nodal irradiation on basis of 18FDG-PET scans in limited disease small cell lung cancer: a phase II trial. Int J Radiat Oncol Biol Phys 2010;77:329–36.

[32] van Loon J, Offermann C, Bosmans G, et al. (18)FDG-PET based radiation planning of mediastinal lymph nodes in limited disease small cell lung cancer changes radiotherapy fields: a planning study. Radiother Oncol 2008;87:49–54.

[33] Mees G, Dierckx R, Vangestel C, et al. Molecular imaging of hypoxia with radiolabelled agents. Eur J Nucl Med Mol Imaging 2009;36:1674–86.

[34] Christian N, Lee JA, Bol A, et al. The limitation of PET imaging for biological adaptive-IMRT assessed in animal models. Radiother Oncol 2009;91:101–6.

[35] Lohith TG, Kudo T, Demura Y, et al. Pathophysiologic correlation between 62Cu-ATSM and 18F-FDG in lung cancer. J Nucl Med 2009;50:1948–53.

[36] van Waarde A, Elsinga PH. Proliferation markers for the differential diagnosis of tumor and inflammation. Curr Pharm Des 2008;14:3326–39.

[37] Everitt S, Hicks RJ, Ball D, et al. Imaging cellular proliferation during chemo-radiotherapy: a pilot study of serial (18)F-FLT positron emission tomography/computed tomography imaging for non-small-cell lung cancer. Int J Radiat Oncol Biol Phys 2009;75:1098–104.

[38] Nestle U, Weber W, Hentschel M, et al. Biological imaging in radiation therapy: role of positron emission tomography. Phys Med Biol 2009;54:R1–R25.

[39] Ollers M, Bosmans G, van Baardwijk A, et al. The integration of PET-CT scans from different hospitals into radiotherapy treatment planning. Radiother Oncol 2008;87:142–6.

Radiotherapy and Oncology

Review

Clinical evidence on PET-CT for radiation therapy planning in gastro-intestinal tumors

Maarten Lambrecht, Karin Haustermans *

Department of Radiation Oncology, Leuvens Kankerinstituut, University Hospitals Leuven, Belgium

ARTICLE INFO

ABSTRACT

A large number of histological and anatomically distinct malignancies originate from the gastro-intestinal (GI) tract. Radiotherapy (RT) plays an increasing role in the multimodal treatment of most of these malignancies. The proximity of different organs at risk such as the kidneys, the spinal cord and the small bowel and the potential toxicity associated with combined treatment modalities make accurate target volume delineation imperative. The ability of positron emission tomography (PET) imaging to visualize a so-called 'biological target volume' (BTV) may be helpful in this respect. Currently the most widely used tracer for diagnosis, staging, restaging and response assessment is [18F]Fluoro-deoxyglucose (FDG). Promising preliminary results in esophageal, pancreatic and anorectal cancers and colorectal liver metastasis suggest that FDG-PET might provide us with additional information useful in target volume delineation. Poor image resolution and a low sensitivity for lymph node detection currently obstructs its widespread implementation. Moreover, validation in large prospective trials and the pathological validation of the correct tumor volume is still lacking. In hepatocellular carcinoma (HCC) and gastric adenocarcinoma there is currently little evidence for the use of FDG-PET in target delineation. However more extensive research is warranted before the true value of FDG-PET in these sites can be assessed. Also other tracers are constantly being developed and investigated. Up to now however none of these tracers has found its way into the daily practice of target volume delineation.

© 2010 European Society for Therapeutic Radiology and Oncology and European Association of Nuclear Medicine. Published by Elsevier Ireland Ltd. All rights reserved. 96 (2010) 339–346

The gastro-intestinal (GI) tract gives rise to a wide variety of anatomically and histologically very distinct malignancies. This heterogeneity is expressed through differences in clinical behavior and sensitivity to ionizing radiation. In esophageal, anal and rectal cancer the role of radiotherapy (RT) in the multimodal treatment is well established [1–3]. In gastric cancer, pancreatic cancer and adenocarcinoma of the gastro-esophageal junction (GEJ) this role is more controversial [4–6]. In adenocarcinomas of the colon or gastro-intestinal stromal tumors (GIST) the role of RT in a curative setting is negligible. During the last decade, the widespread implementation of stereotactic body radiotherapy (SBRT), proton irradiation, intensity modulated RT (IMRT), intensity modulated arc therapy (IMAT) and 3D-brachytherapy enable us to deliver the dose more conformally around the tumor volume. This allows us to increase the dose on the tumor while maintaining or even reducing the dose on the organs at risk (OAR). This prospect is very appealing in GI cancers considering the often weakened patient population, the high doses needed for tumor control and the proximity of several organs prone to serious radiation toxicity (liver,

kidneys, lung, …). Accurate target volume (TV) definition and delineation, profound knowledge of the behavior of the tumor and healthy tissues during RT and a better understanding of the interaction between ionizing radiation and chemotherapy and/or biological-targeted therapies are essential hurdles to cross before we can fully exploit the potential of our technical abilities. Functional imaging with positron emission tomography (PET) might help resolve some problems. PET-imaging provides us with biological information of the tumor. To date the most commonly used tracer in tumors of the gastro-intestinal tract is [18F]Fluorodeoxyglucose (FDG). This tracer accumulates in tissues with a high metabolic turnover and is currently widely used for diagnosis, early response assessment and (re-)staging [7–15]. Other commonly used PET tracers under investigation are [18F]Fluorothymidine (FLT) and [18F]Fluoromisonidazole (FMISO). FLT enters the DNA synthesis salvage pathway and thus images DNA synthesis and cellular proliferation [16]. FMISO on the other hand selectively binds to hypoxic cells and is used to image hypoxia in tumoral regions [17].

The use of PET for TV definition and delineation in GI tract tumors is only recently being investigated. But interest is rapidly growing [18]. With this review we aim to give an overview of the current rationale and evidence of the value of PET and its

* Corresponding author. Address: Department of Radiation Oncology, Leuvens Kankerinstituut, University Hospitals Leuven, Herestraat 49, 3000 Leuven, Belgium.
E-mail address: karin.haustermans@uz.kuleuven.be (K. Haustermans).

different tracers for TV definition in esophageal, GE junction, gastric, pancreatic, hepatic, rectal and anal cancer.

Cancer of the esophagus and the gastro-esophageal junction

FDG-PET

Malignancies of the esophagus present themselves either as squamous cell cancer (SCC) or as adenocarcinoma (AC) [19]. Both cellular types avidly accumulate FDG in their cells and malignant deposits can be adequately detected by FDG-PET [11]. When considering neoadjuvant or definitive (chemo-)RT for esophageal cancer assessment of the full extent of the tumor and its malignant nodes is necessary for adequate radiation delivery to the tumor and sparing of the OAR.

A study by Mamede et al. reported a significant positive correlation between FDG-PET-based tumor lengths and pathological findings in 17 patients [20]. The best correlation was estimated for a SUV-threshold of two standard deviations. Similar results were found by Zhong et al. in a study on 36 patients [21]. They concluded that a noninvasive PET-based delineation of the superior and inferior extent of viable tumor involvement is accurate and that the addition of FDG-PET to the planning process improves the accuracy of the delineation process. The exact cut-off value however still remains up for debate. In an attempt to find the optimal threshold, Yu et al. compared five FDG-PET/CT-based lengths with the pathological gross tumor volume (GTV) length [22]. Although an optimal SUV-based threshold was obtained, the conformity index for the GTVs was unsatisfactorily low and concluded that the information provided by PET and CT should be considered complementary when delineating the GTV. An important remark is that the above mentioned studies all used a threshold-based delineation method. There is some evidence, although not in esophageal cancer, that a gradient-based or a signal to background-based delineation method might be more reproducible [23,24]. Also the effect of organ motion due to respiration on the PET acquisition warrants further investigation. The value of FDG-PET to determine the regional extent of the disease has been investigated in a few studies. Vrieze et al. investigated the additional value of FDG-PET on clinical target volume (CTV) delineation in 30 patients with an advanced esophageal carcinoma [25]. In 47% of the patients discordances were found in the detection of the pathological lymph nodes between CT, endoscopic ultrasound (EUS) and FDG-PET. In 8 patients, 9 lymph node regions were found with pathologic nodes on conventional imaging only. In 3 of these patients the influence of FDG-PET findings would have led to a decrease of the irradiated volume. In 6 patients, 8 lymph node regions were found with a normal CT/EUS and pathologic nodes on FDG-PET. In three of these patients (10%) the influence of the FDG-PET would have led to an enlargement of the irradiated volume. The authors therefore concluded that due to its low sensitivity the irradiated volume should not be reduced based on a negative FDG-PET in a region with suspect nodes on other investigations. The high specificity of FDG-PET on the other hand supports enlarging the irradiated volume based on a positive FDG-PET in a region without suspected lymph nodes on CT and/or EUS. Similarly Shimizu et al. investigated FDG-PET/CT and EUS in 20 patients who received radical surgery for SCC of the esophagus. They found that the detection rate of subclinical lymph node metastasis did not improve with the addition of PET [26]. This is to be expected when considering the limited spatial resolution of FDG-PET compared to CT. Continuous improvements in PET resolution might in the future overcome these problems.

The consequences of FDG-PET-based TV delineation on the radiation dose distribution were assessed in three studies. In the study by Leong et al. they found that in 5 out of 16 patients (31%) FDG-

PET-avid disease was excluded from the planning target volume (PTV) if the TV delineation was based on CT only [27]. No significant differences in doses to OAR were seen when FDG-PET information was added to the treatment-planning process. These findings are in contrast with Moureau-Zabotto et al. who found that changes in treatment plans based on the FDG-PET resulted in significant changes in doses to OAR's with an increase in lung V_{20} in 13 patients and a decrease in 12 patients [28]. Muijs et al. compared the addition of FDG-PET on the CT-based TV delineation [29]. They found that TV's based solely on CT might exclude PET-avid disease and that the addition of PET in radiation planning might result in clinically important changes in normal tissue complication probability (NTCP). Although these findings are very interesting, these studies only have a limited number of patients; they use different methods for defining CTV and PTV and lack pathological validation. In conclusion, there are no data available showing that the use of FDG-PET/CT has improved the patient outcome (Table 1). Its low sensitivity makes reduction of the TV potentially dangerous, while its high specificity makes enlarging the TV based on PET findings advisable.

GE junction tumors are AC, and its definition and optimal treatment are subject to a lot of debate [19,30–32]. FDG-PET has been established and validated in several studies as a surrogate marker that allows the prediction of response and prognosis in FDG-avid tumors [33–35]. The role of FDG-PET in the TV delineation of GE junction tumors is unclear as there is only limited evidence available. Furthermore in the latest TNM classification the Siewert classification has been abandoned and gastro-esophageal tumors are now classified as esophageal or stomach cancer based on the epicentre of the tumor and the presence of an extension in the esophagus or not [30,36]. Whether or not PET findings can be transposed in a similar way needs further investigation.

Other tracers

One study verified the FLT and FDG-PET/CT GTV-delineations with pathologic examination in 22 patients with SCC of the thoracic esophagus [37]. A fixed standardized uptake value (SUV) of 1.4 on FLT-PET/CT and a SUV of 2.5 for FDG-PET gave good approximations of the pathologic tumor length. The differences in the bilateral lung volume receiving $\geqslant 20$ Gy, heart volume receiving $\geqslant 40$ Gy, and the maximal dose received by the spinal cord between FLT and FDG was not significant. However, the values for the mean lung dose, bilateral lung volume receiving $\geqslant 5$, $\geqslant 10$, $\geqslant 30$, $\geqslant 40$, and $\geqslant 50$ Gy, the mean heart dose, and heart volume receiving $\geqslant 30$ Gy using FLT-PET/CT-based planning were significantly lower than those using FDG-PET/CT.

This study only shows the feasibility of an FLT-based GTV delineation compared to FDG. Furthermore the provided fixed thresholds are not reproducible. In other words, this is no evidence that FLT-based TV delineation might actually result in a better target coverage compared to conventional treatment planning.

Gastric cancer

The role of RT in gastric cancer remains unclear. Evidence provided by a large US group study (INT-0116) showed a favorable impact on survival by adding chemo-RT in AC of the stomach and GE junction [38].

Generally FDG-PET isn't considered an accurate imaging technique in gastric cancer. Lack of FDG avidity, low spatial resolution and the high physiological FDG uptake in the normal gastric wall results in a low sensitivity for detection of both the primary tumor and the lymph node metastasis (34–60%) [39–41]. The higher specificity compared to CT and a better positive predictive value for

Table 1
Summary of available data on the use of PET-CT in radiotherapy planning.

Tumor site	Tracer	Target definition	Target volume delineation	Effect on dose distribution	Patient outcome
Esophagus	FDG	Use for detection of primary tumor and metastatic disease. Limited sensitivity for detection lymph nodes	Several studies show a good correlation between FDG-PET and pathology-based tumor lengths	Contradictory data from two small studies without pathological validation	Several studies suggest prognostic and predictive value of metabolic imaging with FDG-PET
	FLT	No data available	One study showed that FLT-PET/CT gave good approximation of the tumor length	One theoretical study showed significant difference with FDG-PET in lung and heart dose	No data available
Adenocarcinoma of the GE junction	FDG	No separate data available	No separate data available	No separate data available	Several trials suggest prognostic and predictive value of metabolic imaging with FDG-PET
Gastric cancer	FDG	Low sensitivity for primary tumor and lymph nodes	No data available	No data available	Several studies suggest prognostic and predictive value of metabolic imaging with FDG-PET in case of FDG-avid tumors
	FLT	One study reports on higher sensitivities with FLT than FDG-PET for primary tumor detection	No data available	No data available	No data available
Adenocarcinoma of the pancreas	FDG	Accurate detection of primary tumor and distant metastasis	Has been used in a few studies, however the additional value remains under investigation	No data available	Several prospective trials suggest prognostic and predictive value of metabolic imaging with FDG-PET
Liver-HCC	FDG	Low sensitivities in tumor detection. Although some studies suggest better sensitivity in poorly differentiated HCC	No data available, no benefit is expected	No data available, no benefit is expected	No data available, no benefit is expected
	^{11}C-Acetate	Two studies report higher sensitivities compared to FDG. Accumulate preferably in well differentiated and larger tumors	No data available	No data available	No data available
	FCH	Small study showed high detection rate	No data available	No data available	No data available
Liver-metastases	FDG	Detection rated dependent on primary tumor histology. High sensitivity in for detection of metastases from colorectal cancer	One retrospective study showed larger local progression rate in case of incomplete PET/CT CTV coverage	No data available	
Rectal Cancer	FDG	High sensitivity for detection of primary tumor and metastases. Less sensitive in lymph node assessment	Small clinical studies support its use in GTV delineation. Only one correlated with pathology	No data available	Several clinical studies report on the predictive power of sequential FDG-PET during and after neoadjuvant treatment
	FLT	Limited studies show high detection rate in patients with rectal cancer. Although generally with lower uptake than FDG	Two small studies report a potential use for GTV delineation	No data available	No data available
	FMISO	No data available	Lack of reproducibility makes it unfit for GTV delineation	No data available	No data available
Anal Cancer	FDG	Part of standard pre-treatment workup. Higher sensitivity than CT	One retrospective study reported it is safe to omit PET-negative lymph nodes from high dose GTV	No data available	Post treatment FDG-PET/CT is predictive for response and long-term clinical outcome

FDG: ^{18}F-fluorodeoxyglucose; FLT: ^{18}F-fluorothymidine; FCH: ^{18}F-fluorocholine; FMISO: ^{18}F-fluoromisonidazole; GE: gastro-esophageal, PET: positron emission tomography; GTV: gross tumor volume; CTV: clinical target volume; CT: computed tomography.

lymph node metastasis compared to CT leads to the belief that the combination of FDG-PET with CT might result in a better lymph node staging [42]. More research is necessary to validate this statement.

FDG-PET might be used for the prediction of response to neoadjuvant treatment [43,44]. Better patient selection, improvements in PET-CT and pathology validation studies however are urgently needed. A study by Herrmann et al. indicated that imaging gastric cancer with the proliferation marker FLT is feasible. Forty-five patients with histologically proven locally advanced gastric cancer underwent FLT- and FDG-PET. All patients showed focal FLT uptake in the primary tumor while 14 primary tumors were negative for FDG-uptake, resulting in a sensitivity of 100% and 69% respectively [45]. These results need to be confirmed and so far no quantitative correlation with pathology nor assessment of lymph nodes was done.

Pancreatic cancer

The role of RT in the treatment of unresectable AC of the pancreas is unclear although it is frequently included in the multimodal therapeutic strategy [5,46,47]. Higher irradiation doses might result in better local control but the dose is limited by small bowel, liver, gastric and duodenal toxicity. New techniques such as stereotactic body RT (SBRT) with concurrent chemotherapy are being investigated to safely escalate the dose on the tumor [48–50]. Pancreatic tumors in general are FDG-avid and FDG-PET parameters have been shown to be of prognostic value for both progression-free survival and overall survival after SBRT [51].

In a few studies FDG-PET/CT has been used to define the GTV [50–52]. The actual value of adding FDG-PET to TV delineation however remains unclear due to the lack of pathological validation of the FDG-based TV. Ford et al. suggested that FDG-PET/CT might

be particularly useful in distinguishing the tumor from the duodenum [53]. This might be important considering the frequent duodenal toxicity seen in early SBRT trials. However, this observation is based on only a few cases and so far no studies addressing this issue have been published.

One study evaluated the use of FLT-PET/CT for the detection of pancreatic cancer in 5 patients and compared this to FDG-PET/CT. Using a visual interpretation the primary cancer could be detected from the background activity in only 2 out of 5 patients with FLT-PET, while FDG-PET was able to detect the primary cancer in all five patients [54]. Although only 5 patients were analyzed, there seems to be no place for FLT-PET in AC of the pancreas.

In conclusion, there is currently no evidence defending the use of PET for TV delineation in pancreatic cancer.

Malignancies of the liver

High dose irradiation of unresectable hepatocellular carcinoma (HCC) and liver metastasis is rapidly gaining interest due to recent studies where SBRT or high dose rate (HDR) brachytherapy was used with excellent local control rates and limited toxicity [55–59]. When using such high doses, accurate TV delineation is essential in the prevention of radiation-induced liver disease (RILD).

Hepatocellular carcinoma

The diagnostic accuracy of FDG-PET in HCC for tumor detection is generally poor with a sensitivity ranging between 0% and 50% [60–62]. Two tracers of the lipid metabolism, ^{18}F-fluorocholine (FCH) and ^{11}C-acetate showed promising results in preliminary studies [63–65]. Ho et al. saw a higher sensitivity for ^{11}C-acetate-PET compared to FDG-PET in 32 patients with HCC with ⩽3 lesions (87.3% vs 47.3%, respectively). Comparison with histopathology showed that well-differentiated HCC is detected by ^{11}C-acetate-PET while poorly differentiated types are more often detected by FDG-PET [63]. This complementarity was also found in the study by Park et al. On 90 patients with 110 lesions sensitivity increased with the addition of ^{11}C-acetate to FDG-PET/CT (60.9% vs 75.4% for the single-tracer modalities and 82.7% for dual-tracer PET/CT) [64]. Uptake of ^{11}C-acetate seemed to be associated with large and multiple tumors as a detection of small primary HCC yielded low sensitivities with all tracers. Talbot et al. showed a detection rate of 100% in 12 patients with newly diagnosed or recurrent HCC using FCH-PET/CT compared to only 56% with FDG-PET/CT [65]. These results however are obtained in a retrospective setting in patients with confirmed HCC. Selection of the optimal tracer for each patient and further qualitative improvements of PET/CT are essential for PET to play a role in HCC.

Liver metastases

Hematogenous metastases to the liver are very common and originate from different primary tumors. Liver metastases originating from colon and rectal cancers are considered eligible for curative treatment in case of limited disease [66]. Over the last couple of years, RT is widely gaining ground in the treatment of non-resectable liver metastases [59]. Contrary to what we see in HCC FDG-PET is considered to be highly sensitive for the detecting liver metastases secondary to colorectal cancer [67–69]. So far one study retrospectively reviewed the value of FDG-PET/CT for radiotherapy planning in 19 patients with colorectal liver metastasis treated with HDR brachytherapy for 38 lesions in 25 sessions [70]. Adding the information from FDG-PET to the planning CT resulted in a change in the CTV in 84% of all sessions. An increase was observed in 15 sessions while in 6 sessions the CTV decreased. The median PET/CT-CTV was significantly larger than the CT-CTV with a median increase of 24.5% (p = 0.022). The authors observed a significantly larger rate of early local progression in those patients with incomplete PET/CT CTV coverage. They therefore concluded that PET is particularly informative for pretreated lesions, when CT is inconclusive. This is in contrast to observations by Akhurst et al. who found that preoperative chemotherapy reduces the activity of the glycolytic enzyme hexokinase which resulted in a reduction in sensitivity of standard FDG-PET for colorectal metastasis [71].

In any case, FDG-PET holds promise when considering irradiating liver metastasis up to a high dose, but warrants further research.

Rectal cancer

Classically, in rectal cancer, a three or four beam set-up is used to deliver a short or long course of RT to the posterior pelvis before a total mesorectal excision (TME) is performed. This treatment is generally well tolerated and local control is excellent [1,72]. Accurate GTV delineation has therefore long been considered of minor importance and the main emphasis was put on accurate CTV delineation [73]. The observation that rectal cancer patients with a pathological complete response (pCR) after chemo-RT might not need surgery; the implementation of highly conformal RT techniques and the ability to assess the tumor response early during RT is gradually changing this view [14,74–76]. If dose escalation is considered, accurate knowledge of the exact tumor volume is required to maintain an acceptable small bowel and bladder toxicity. So far three different PET tracers have been tested for radiotherapy planning: FDG, FMISO and FLT. Roels et al. investigated the role of FMISO, FLT and FDG for the definition of the GTV [77]. Patients underwent PET/CT imaging with two different tracers – a combination of FDG and FMISO or a combination of FDG and FLT (Fig. 1). They found that at each time-point, the mean FDG-PET GTV was significantly larger than the FMISO-PET GTV, but not significantly larger than the mean FLT-PET GTV. Mismatch analysis confirmed that FDG, FLT and FMISO-PET reflect different biological characteristics and can be used as a target for dose-escalation RT in rectal cancer. In general FDG and FLT GTVs corresponded better than FDG and FMISO GTVs, probably due to the non-specific FMISO uptake in normoxic bowel wall and diffusion of FMISO through the rectal wall. Moreover, the spatial distribution of FMISO varied considerably during RT, while FDG and FLT uptake was less variable over time. These findings favor the use of FDG and FLT as potential tracers for TV definition in dose-escalation RT and proof that re-imaging is important if these GTVs are used as a target for dose escalation.

A second study by Roels et al. investigated FDG-PET/CT and MRI before the start of treatment, after 10 fractions of radiation and before surgery [24]. The FDG-PET GTV was automatically delineated with two different segmentation algorithms; a modified threshold-based method and a gradient-based method. The mean FDG-derived GTVs showed a tendency to shrink during and after CRT (Fig. 2). They concluded that the FDG-PET GTVs obtained with a gradient-based segmentation technique seemed to fit best with the GTV measured on the pathological specimen. Ciernik et al. found that the automated segmentation of the FDG signal strongly correlated with the CT-derived GTV and the volume as assessed on pathology in 11 patients with rectal cancer [78]. He stated that PET-based delineation can be automated which makes it fast and less prone to inter-observer variation and usable in creating a working PTV (wPTV) based on the PET GTV. There are however some limitations to this study [79]. Firstly, there was no pathological correlation of the PET-based GTV. Secondly; the limited accuracy of FDG-PET in detecting microscopic lymph node invasion makes it unsuitable for the automatic definition of a CTV or PTV [80]. Patel et al. also addressed the question concerning PET and in-
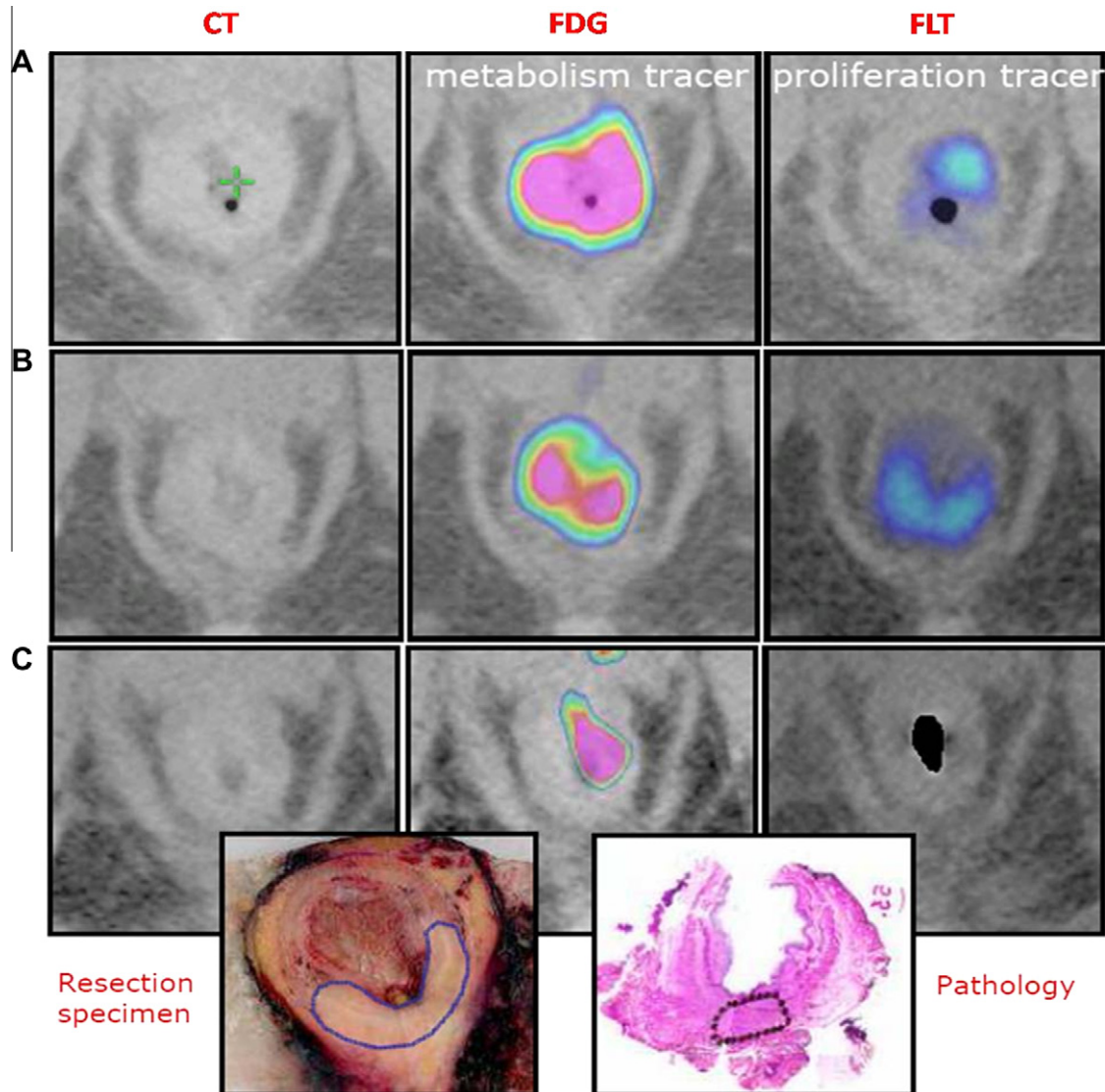
Fig. 1. Comparison of CT-scan, FDG-PET and FLT-PET (columns) before chemoradiotherapy (CRT) (row A), after 10–12 fractions of CRT (row B) and before surgery (row C). The macroscopic and microscopic surgical specimen is shown at the bottom.

ter-observer variability. They compared the nodal and primary tumor GTV contour for a hypothetical boost volume on conventional CT alone and on FDG- and FLT-PET/CT in six rectal cancer patients [81]. Four radiation oncologists delineated primary and nodal GTV on all scans. The boost TVs based on combined PET/CT resulted in lower inter-observer variability compared with CT alone, particularly for nodal disease. Again, this is only based on a limited number of patients and less variability does not necessarily imply more correct delineation. Furthermore, as stated above, visual delineation has the disadvantage that it is less independent and less objective than gradient-based methods.

In conclusion, both FDG- and FLT-PET are promising tracers for the delineation of the GTV in rectal cancer. Before these can be implemented in daily practice improvement of PET-CT is essential. Also accurate definition of the margins around the CTV are essential when delivering high doses onto a highly deformable and mobile organ such as the rectum.

Anal cancer

Concurrent (chemo-)RT has gradually become the mainstay of curative treatment of anal cancer [82,83]. Current treatment guide-lines include FDG-PET as part of the standard pre-treatment work-up in patients diagnosed with anal cancer. Several investigations have shown that with FDG-PET, more involved lymph nodes can be detected than with clinical examination and CT [84,85]. Also, it appears that post-therapy FDG-PET/CT is highly predictive for a tumor response and a long-term clinical outcome [86].

To investigate whether a dose reduction on the inguinal lymph nodes enlarged on CT, but negative on FDG-PET is safe, Mai et al. investigated 39 sequential patients with anal cancer [87]. All patients were treated with combined CRT including elective irradiation of the inguinal lymph nodes up to 36 Gy. On planning CT, a total of 162 inguinal lymph nodes were detected with 16 suspected lymph nodes in nine patients. Three of these lymph nodes in three patients were PET-positive (FDG-PET positivity was defined as normalized SUV > 2.5). Only on these lymph nodes the radiation dose was increased up to 50.4–54 Gy. The authors concluded that reduction of the irradiation dose to CT-enlarged but PET-negative inguinal LN does not result in increased failure. The limited number of patients and affected lymph nodes, the use of a fixed threshold delineation method combined with the retrospective nature of this study does not allow definite conclusions, but they do suggest a future role for FDG-PET in the treatment planning of anal cancer.
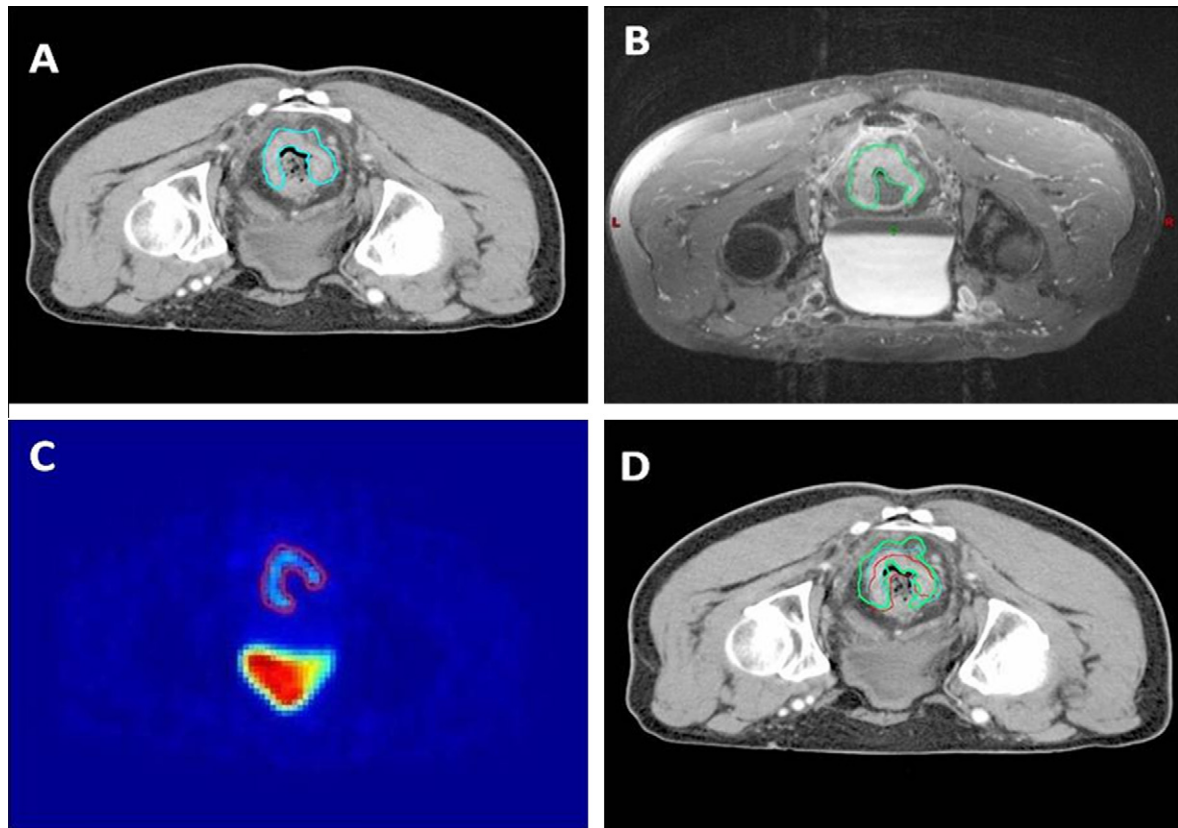
Fig. 2. Manual gross tumor volume (GTV) delineation on CT-scan (A); on T1 weighted MRI image (B) and automated gradient based delineation of the GTV on the FDG-PET(C). Fusion GTV after non rigid registration with a rigid approximation for the tumor to the planning CT (D).

General conclusions and future prospects

- Up to now FDG-PET is mainly used for diagnosis, staging, early response prediction and (re-)staging in different gastro-intestinal tumors.
- Concerning TV definition and delineation FDG-PET shows promising results in esophageal cancer, rectal cancer, colorectal liver metastases and pancreatic cancer. Evidence for the use of FDG-PET in Hepatocellular carcinoma and gastric cancer is lacking and warrants further investigation.
- The limited spatial resolution and low sensitivity in the diagnosis of pathologic lymph nodes makes FDG-PET in general unsuitable for omission of PET-negative lymph node regions. Combination of FDG-PET with CT might increase this sensitivity. The higher specificity allows for inclusion of FDG-PET positive regions in some tumor sites (i.e. esophageal cancer)
- In general the role of FDG-PET in GTV definition and delineation is investigational. Validation of the different segmentation methods, comparison with the pathological specimen and improvements of the PET-CT acquisition are mandatory requirements before its use can be implemented in clinical practice.
- Other tracers are being investigated and some show promising results. So far they have no place in daily practice.

References

[1] Kapiteijn E, Marijnen AM, Nagtegaal ID, et al. Preoperative radiotherapy combined with Total mesorectal excision for resectable rectal cancer. N Engl J Med 2001;345:638–46.
[2] Mariette C, Piessen G, Triboulet JP. Therapeutic strategies in oesophageal carcinoma: role of surgery and other modalities. Lancet Oncol 2007;8:545–53.
[3] Berger B, Claus B. Evidence-based radiation oncology: Oesophagus. Radiother Oncol 2009;92:276–90.
[4] Valentini V, Cellini F, Minsk B, et al. Survival after radiotherapy in gastric cancer: Systematic review and meta-analysis. Radiother Oncol 2009;92:176–83.
[5] Sultana A, Tudur Smith C, Cunningham D, et al. Systematic review, including meta-analyses, on the management of locally advanced pancreatic cancer using radiation/combined modality therapy. Br J Cancer 2007;96:1183–90.
[6] Bjerregaard J, Mortensen M, Jensen M, et al. Long-term results of concurrent radiotherapy and UFT in patients with locally advanced pancreatic cancer. Radiother Oncol 2009;92:226–30.
[7] Abdel-Nabi H, Doerr RJ, Lamonica DM, et al. Staging of primary colorectal carcinomas with fluorine-18 fluorodeoxuglucose whole body PET: Correlation with histopathologic and CT findings. Radiology 1998;206:755–60.
[8] Kantorova I, Lipska L, Belohlavek O, et al. Routine (18)F-FDG PET preoperative staging of colorectal cancer: Comparison with conventional staging and ist impact on treatment decision making. J Nucl Med 2003;44:1784–8.
[9] Bipat S, van Leeuwen MS, Comans EF, et al. Colorectal liver metastases: CT, MR imaging and PET for diagnosis-meta-analysis. Radiology 2005;224:748–56.
[10] Huebner RH, Park KC, Shepherd JE, et al. A Meta-analysis of the literature for whole-body FDG PET detection of recurrent colorectal cancer. J Nucl Med 2000;41:1177–89.
[11] Flanagan FL, Dehdashti F, Siegel BA, et al. Staging of esophageal cancer with 18F-fluorodeoxyglucose positron emission tomography. AJR Am J roentgenol 1997;168:417–24.
[12] Lerut T, Flamen P, Ectors N, et al. Histopathologic validation of lymph node staging with FDG-PET scan in cancer of the esophagus and gastroesophageal junction: A prospective study based on primary surgery with extensive lymphadenectomy. Ann Surg 2000;232:743–52.
[13] Flamen P, Lerut A, Van Cutsem E, et al. The utility of positron emission tomography for the diagnosis and staging of recurrent esophageal cancer. J Thorac Cardiovasc Surg 2000;120:1085–92.
[14] Janssen MH, Ollers MC, Riedl RG, et al. Accurate prediction of pathological rectal tumor response after two weeks of preoperative radiochemotherapy using (18)F-fluorodeoxyglucose-positron emission tomography-computed tomography imaging. Int J Radiat Oncol Biol Phys 2010;77:392–9.
[15] Aerts HJ, Lambin P, De Ruysscher D. FDG for dose painting: a rational choice. Radiother Oncol 2010 [Epub ahead of print].
[16] Been LB, Suurmeijer AJH, Cobben P, Jager P, Hoekstra HJ, Elsinga PH. [18F]FLT-PET in oncology: current status and and opportunities. Eur J Nuc Med Mol Imaging 2004;31:1659–72.

[17] Koh WJ, Rasey JS, Evans ML, et al. Imaging of hypoxia in human tumors with 18F-fluoromisonidazole. Int J Radiat Oncol Biol Phys 1992;41:31–9.

[18] MacManus M, Nestle U, Rosenzweig KE, et al. Use of PET and PET/CT for radiation therapy planning: IAEA expert report 2006–2007. Radiother Oncol 2009;91:85–94.

[19] Siewert JR, Ott K. Are squamous and adenocarcinomas of the esophagus the same disease? Semin Radiat Oncol 2006;17:38–44.

[20] Mamede M, El Fakhri G, Abrue-e Lima P, Gandler W, Nosé V, Gerbaudo VH. Preoperative estimation of esophageal tumor metabolic length in FDG-PET images with surgical pathology confirmation. Ann Nucl Med 2007;21:553–62.

[21] Zhong X, Yu J, Zhang B, et al. Using ^{18}F-fluorodeoxyglucose positron emission tomography to estimate the length of gross tumor in patients with squamous cell carcinoma of the Esophagus. Int J Radiat Oncol Biol Phys 2009;73:136–41.

[22] Yu W, Fu XL, Zhang YJ, et al. GTV spatial conformity between different delineations methods by 18FDG-PET/CT and pathology in esophageal cancer. Radiother Oncol 2009;93:441–6.

[23] Daisne JF, Sibomana M, Bol A, et al. Tri-dimensional automatic segmentation of PET volumes based on measured source-to-background ratios: Influence of reconstruction algorithms. Radiother Oncol 2003;69:247–50.

[24] Roels S, Slagmolen P, Nuyts J, et al. Biological image-guided radiotherapy in rectal cancer: challenges and pitfalls. Int J Radiat Oncol Biol Phys 2009;75:782–90.

[25] Vrieze O, Haustermans K, De Wever W, et al. Is there a role for FGD-PET in radiotherapy planning in esophageal carcinoma? Radiother Oncol 2004;73:269–75.

[26] Shimizu S, Hosokawa M, Itoh K, Fujita M, Takahashi H, Shirato H. Can hybrid FDG-PET/CT detect subclinical lymph node metastasis of esophageal cancer appropriately and contribute to radiation treatment planning? A comparison of image-based an pathological findings. Int J Clin Oncol 2009;14:421–5.

[27] Leong T, Everitt C, Yuen K, et al. A prospective study to evaluate the impact of FDG-PET on CT-based radiotherapy treatment planning for oesophageal cancer. Radiother Oncol 2006;78:254–61.

[28] Moureau-Zabotto L, Touboul E, Lerouge D, et al. Impact of CT and ^{18}F-fluorodeoxyglucose positron emission tomography image fusion for conformal radiotherapy in esophageal carcinoma. Int J Radiat Oncol Biol Phys 2005;63:340–5.

[29] Muijs CT, Schreurs LM, Busz DM, et al. Consequences of additional use of PET information for target volume delineation and radiotherapy dose distribution for esophageal cancer. Radiother Oncol 2009;93:447–53.

[30] Siewert JR, Stein HJ. Classification of adenocarcinoma of the oesophagogastric junction. Br J Surg 1998;85:1457–9.

[31] Power DG, Reynolds JV. Localized adenocarcinoma of the esophagogastric junction - Is there a standard of care? Cancer Treat Rev 2010 [Epub ahead of print].

[32] Matzinger O, Gerber E, Bernstein Z, et al. EORTC-ROG expert opinion: radiotherapy volume and treatment guidelines for neoadjuvant radiation of adenocarcinomas of the gastroesophageal junction and the stomach. Radiother Oncol 2009;92:164–75.

[33] Weber WA, Ott K, Becker K, et al. Prediction of response to preoperative chemotherapy in adenocarcinomas of the esophagogastric junction by metabolic imaging. J Clin Oncol 2001;19:3058–65.

[34] Ott K, Weber WA, Lordick F, et al. Metabolic imaging predicts response, survival and recurrence in adenocarcinomas of the esophagogastri junction. J Clin Oncol 2006;24:4692–8.

[35] Lordick F, Ott K, Krause BJ, et al. PET to assess early metabolic response and to guide treatment of adenocarcinoma of the oesophagogastric junction: the MUNICON phase II trial. Lancet Oncol 2007;8:797–805.

[36] Sobin LH, Gospodarowicz MK, Wittekind C. TNM Classification of Malignant Tumours. 7th ed. New York: Wiley; 2009.

[37] Han D, Yu J, Yu Y, et al. Comparison of (18)F-fluorothymidine and (18)F-fluorodeoxyglucose PET/CT in delineating gross tumor volume by optimal threshold in patients with squamous cell carcinoma of thoracic esophagus. Int J Radiat Oncol Biol Phys 2010;15:1235–41.

[38] Macdonald JS, Smalley SR, Benedetti J. Chemoradiotherapy after surgery compared with surgery alone for adenocarcinoma of the stomach or gastroesophageal junction. N Engl J Med 2001;345:725–30.

[39] Yun M, Lim JS, Noh SH, et al. Lymph node staging of gastric cancer using 18F-FDG PET: A comparison study with CT. J Nucl Med 2005;46:1582–8.

[40] Mukai K, Ishida Y, Okajima K, Isozaki H, Morimoto T, Nishiyama S. Usefulness of preoperative FDG-PET for detection of gastric cancer. Gastric cancer 2006;9:192–6.

[41] Stahl A, Ott K, Weber WA, et al. FDG-PET imaging of locally advanced gastric carcinomas: correlation with endoscopic and histopathological findings. Eur J Nucl Med Mol Imaging 2003;30:288–95.

[42] Yang Q-M, Kawamura T, Itoh H, et al. Is PET-CT suitable for predicting lymph node status for gastric cancer? Hepatogastroenterology 2008;33:782–5.

[43] Ott K, Fink U, Becker K, et al. Prediction of response to preoperative chemotherapy in gastric carcinoma by metabolic imaging: Results of a prospective trial. J Clin Oncol 2003;21:4604–10.

[44] Di Fabio F, Pinto C, Rojas Llimpe FL, et al. The predictive value of 18F-FDG-PET early evualation in patients with metastatic gastric adenocarcinoma treated with chemotherapy plus cetuximab. Gastric Cancer 2007;10:221–7.

[45] Hermann K, Ott K, Buck AK, et al. Imaging gastric cancer with PET and the radiotracers 18F-FLT and 18F-FDG: a comparative analysis. J Nucl Med 2007;48:1945–50.

[46] Moertel C, Frytak S, Hahn R, et al. Therapy of locally unresectable pancreatic carcinoma: a randomized comparison of high dose (6000 rads) radiation alone, moderate dose radiation (4000 rads)5-fluorouracil and high dose radiation 5-fluorouracil: the gastrointestinal tumor study group. Cancer 1981;48:1705–10.

[47] Huguet F, Girard N, Seblain-El Guerche C, et al. Chemoradiotherapy in the management of locally advanced pancreatic carcinoma: a qualitative systematic review. J Clin Oncol 2009;27:2269–77.

[48] Rusthoven KE, Kavanagh BD, Cardenes H, et al. Multi-institutional phase I/II trial of stereotactic body radiation therapy for liver metastases. J Clin Oncol 2009;27:1572–8.

[49] Koong AC, Christofferson E, Le QT, et al. Phase II study to assess the efficacy of conventionally fractionated radiotherapy followed by a stereotactic radiosurgery boost in patients with locally advanced pancreatic cancer. Int J Radiat Oncol Biol Phys 2005;63:230–323.

[50] Chang DT, Schellenberg D, Shen J, et al. Stereotactic radiotherapy for unresectable adenocarcinoma of the pancreas. Cancer 2009;115:665–72.

[51] Schellenberg D, Quon A, Minn AY, et al. (18)Fluorodeoxyglucose PET is prognostic of progression-free and overall survival in locally advanced pancreas cancer treated with stereotactic radiotherapy. Int J Radiat Oncol Bio Phys 2010;77:1420–5.

[52] Schellenberg D, Goodman KA, Lee Florence, et al. Gemcitabine chemotherapy and single-fraction stereotactic body radiotherapy for locally advanced pancreatic cancer. Int J Radiat Oncol Biol Phys 2008;72:678–86.

[53] Ford EC, Hermans J, Yorke E, Wahl RL. ^{18}FDG-PET/CT for image-Guided and intensity-modulated Radiotherapy. J Nucl Med 2009;50:1655–65.

[54] Quon A, Chang ST, Chin F, et al. Initial evaluation of 18F-fluorothymidine (FLT) PET/CT scanning for primary pancreatic cancer. Eur J Nucl Med Mol Imaging 2008;35:527–31.

[55] Dawson LA, McGinn CJ, Tenhaken RK, Walker S, Ensminger W, Lawrence TS. Escalated focal liver radiation and concurrent hepatic artery fluorodeoxyuridine for unresectable intrahepatic malignancies. J Clin Oncol 2000;18:2210–8.

[56] Wulf J, Guckenberger M, Haedinger U, et al. Stereotactic radiotherapy of primary liver cancer and hepatic metastases. Acta Oncol 2006;45:897–906.

[57] Tse RV, Hawkins M, Lockwood G. Phase I study of individualized stereotactic body radiotherapy for hepatocellular carcinoma and intrahepatic cholangiocarcinoma. J Clin Oncol 2008;26:657–64.

[58] Ricke J, Wust P, Stohlmann A, et al. CT-guided interstitial brachytherapy of liver malignancies alone or in combination with thermal ablation: Phase I-II results of a novel technique. Int J Radiat Oncol Biol Phys 2004;58:1496–505.

[59] Lee MT, Kim JJ, Dinniwell R. Phase I study of individualized stereotactic body radiotherapy of liver metastasis. J Clin Oncol 2009;27:1585–91.

[60] Khan MA, Combs CS, Brunt EM, et al. Positron emission tomography scanning in the evaluation of hepatocellular carcinoma. J Hepatology 2000;32:792–7.

[61] Jeng LB, Changlai SP, Shen YY, Lin CC, Tsai CH, Tsai CH. Limited value of 18F–2 deoxyglucose positron emission tomography to detect hepatocellular carcinoma in hepatitis B virus carriers. Hepatogastroenterology 2003;50:2154–6.

[62] Teefey SA, Hildeboldt CC, Dehdashti F, et al. Detection of primary hepatic malignancy in liver transplant candidates: prospective comparison of CT, MR imagin US and PET. Radiology 2003;226:533–42.

[63] Ho C, Yu S, Yeung D. ^{11}C-Acetate PET imaging in hepatocellular carcinoma and other liver masses. J Nucl Med 2003;44:213–21.

[64] Park JW, Kim JH, Kim SK, et al. A prospective Evaluation of ^{18}FDG and ^{11}C-acetate PET/CT for detection of primary and metastatic hepatocellular carcinoma. J Nucl Med 2008;49:1912–21.

[65] Talbot J, Gutman F, Fartoux L, et al. PET/CT in patients with hepatocellular carcinoma using ^{18}[F] fluorocholine: preliminary comparison with ^{18}[F]FDG PET/CT. Eur J Nucl Med Mol Imaging 2006;33:1285–9.

[66] Adson MA, van Heerden JA, Adson MH, et al. Resection of hepatic metastases from colorectal cancer. Arch Surg 1984;119:647–51.

[67] Ogunbiyi OA, Flanagan FL, Dehdashti F, et al. Detection of recurrent and metastatic colorectal cancer: comparison of positron emission tomography and computed tomography. Ann Surg Oncol 1997;4:613–20.

[68] Flamen P, Stroobants S, Van Cutsm E. Additional value of whole-body positron emission tomography with fluorine-18–2-fluoro-deoxy-d-glucose in recurrent colorectal cancer. J Clin Oncol 1997;17:894–901.

[69] Fernandez FG, Drebin JA, Linehan DC, et al. Five-Year Survival After Resection of Hepatic Metastases From Colorectal Cancer in Patients Screened by Positron Emission Tomography With F-18 Fluorodeoxyglucose (FDG-PET). Ann Surg 2004;240:438–50.

[70] Steffen IG, Wust P, Ruehl R, et al. Value of combined PET/CT for radiation planning in CT-Guided percutaneous interstitial high-dose-rate single-fraction brachytherapy for colorectal liver metastases. Int J Radiat Oncol Biol Phys 2010;77:1178–85.

[71] Akhurst T, Kates TJ, Mazumdar M, et al. Recent chemotherapy reduces the sensitivity of 18F Fluorodeoxyglucose positron emission tomography in the detection of colorectal metastases. J Clin Oncol 2005;23:8713–6.

[72] Sauer R, Becker H, Hohenberger W, et alGerman Rectal Cancer Study Group. Preoperative versus postoperative chemoradiotherapy for rectal cancer. N Engl J Med 2004;351:1731–40.

[73] Roels S, Duthoy W, Haustermans K, Penninckx F, Vandecaveye V, Boterberg T, et al. Definition and delineation of the clinical target volume for rectal cancer. Int J Radiat Oncol Biol Phys 2006;65:1129–42.

[74] Habr-Gama A, Perez RO, Nadalin W, et al. Operative versus non operative treatment for stage 0 distal rectal cancer following chemoradiation therapy: long-term results. Ann Surg 2004;240:711–7.

[75] Bujko K, Richter P, Kołodziejczyk M, et al. Preoperative radiotherapy and local excision of rectal cancer with immediate radical re-operation for poor responders. Radiother Oncol 2009;92:195–201.

[76] Engels B, De Ridder M, Tournel K, et al. Preoperative helical tomotherapy and megavoltage computed tomography for rectal cancer: impact on the irradiated volume of small bowel. Int J Radiat Oncol Biol Phys 2009;5:1476–80.

[77] Roels S, Slagmolen P, Nuyts J, et al. Biological image-guided radiotherapy in rectal cancer: is there a role for FMISO or FLT, next to FDG? Acta Oncol 2008;47:1237–48.

[78] Ciernik IF, Huser M, Burger C, Bernard Davis J, Szekely G. Automated functional image-guided radiation treatment planning for rectal cancer. Int J Radiat Oncol Biol Phys 2005;62:893–900.

[79] Roels S, Haustermans K, Gregoir V. In regard to Ciernik et al. Automated functional image-guided radiation treatment planning for rectal cancer. Int J Radiat Oncol Biol Phys 2006;64:1611–5.

[80] International Commission on Radiation Units and Measurements, ICRU Report 50: dose specification for reporting external beam therapy with photons and electrons, ICRU, Bethesda, MD; 1993.

[81] Patel DA, Chang ST, Goodman KA. Impact of Integrated PET/CT on variability of target volume delineation in rectal cancer. Technol Cancer Res Treat 2007;6:31–6.

[82] Nigro ND, Vaitkevicius VK, Consisine Jr B. Combined therapy for cancer of the anal canal: a preliminary report. Dis colon Rectum 1974;17:354–6.

[83] Bartelink H, Roelofsen F, Eschwege F, et al. Concomitant radiotherapy and chemotherapy is superior to radiotherapy alone in the treatment of locally advanced anal cancer: results of a phase III randomized trial of the European Organization for Research and Treatment of Cancer Radiotherapy and Gastrointestinal cooperative Groups. J Clin Oncol 1997;15: 2040–9.

[84] Cotter SE, Grigsby PW, Siegel BA, et al. FDG-PET/CT in the evaluation of anal carcinoma. Int J Radiat Oncol Biol Phys 2006;65:720–5.

[85] Nguyen BT, Joon DL, Khoo V, et al. Assessing the impact of FDG-PET in the management of anal cancer. Radiother Oncol 2008;87:376–82.

[86] Schwarz JK, Siegel BA, Dehdashti F, et al. Tumor response and survival predicted by post-therapy FDG-PET/CT in anal cancer. Int J Radiat Oncol BIol Phys 2008;71:180–6.

[87] Mai SK, Welzel G, Hermann B, Wenz F, Haberkorn U, Dinter DJ. Can the radiation dose to CT-enlarged buy FDG-PET-negative inguinal lymph nodes in anal cancer be reduced? Strahlenther Onkol 2009;185:254–9.

Review

Clinical evidence on PET/CT for radiation therapy planning in prostate cancer

Maria Picchio [a,b,*], Elisabetta Giovannini [a], Cinzia Crivellaro [b], Luigi Gianolli [a], Nadia di Muzio [c], Cristina Messa [b,d,e]

[a] Nuclear Medicine, San Raffaele Scientific Institute, Milan, Italy; [b] Molecular Bioimaging Center, University of Milano-Bicocca, Milan, Italy; [c] Radiation Oncology, San Raffaele Scientific Institute, Milan, Italy; [d] IBFM, National Research Council, Milan, Italy; [e] Nuclear Medicine, San Gerardo Hospital, Monza, Italy

ARTICLE INFO

ABSTRACT

The present chapter is focused on the role of positron emission tomography/computed tomography (PET/CT) and [11C]-labelled Choline ([11C]Choline) for the management of prostate cancer patients for radiation therapy planning.

Although still a matter of debate, PET/CT with [11C]Choline is not routinely recommended for selecting patients for prostate cancer primary radiation treatment. However, due to its high accuracy in detecting and localizing recurrences when a biochemical failure occurs, [11C]Choline PET/CT may play a role in the re-staging phase to distinguish patients with local versus distant relapse, thus influencing patient management (curative versus palliative therapy).

Limited data are currently available on the role of [11C]Choline PET/CT in target volume selection and delineation. According to available literature, [11C]Choline PET/CT is not clinically recommendable to plan target volume both for primary prostate treatment and for local recurrence. Nevertheless, promising data suggested a potential role of [11C]Choline PET/CT as an image guide tool for the irradiation of prostate cancer relapse.

© 2010 European Society for Therapeutic Radiology and Oncology and European Association of Nuclear Medicine. Published by Elsevier Ireland Ltd. All rights reserved. 96 (2010) 347–350

In prostate cancer patients, an accurate visualization of the primary tumor, lymph nodal and distant neoplastic involvement, as well as recurrences after therapy are essential for a proper treatment planning [1–3]. However, the diagnostic accuracy of conventional imaging modalities, such as computed tomography (CT) and magnetic resonance (MR) imaging, is still suboptimal in the management of these patients [4,5]. Positron emission tomography (PET) and particularly integrated PET/CT modalities are showing increasing usefulness, in general, in radiation oncology: (a) to stage the disease, for accurate patient selection to treatment, (b) to select and delineate the target volume, by defining the biological target volumes (BTV), and (c) to re-stage and monitor the disease, by evaluating the biological effect of treatment.

Two-[18F]-fluoro-2-deoxy-D-glucose ([18F]FDG) is the most commonly used PET tracer in oncology [6]. However, in prostate cancer, it presents limitations, mainly due to the low glucose metabolism of prostate cancer cells and due to its physiologic urinary excretion that may interfere with imaging of pelvis [7].

Among the different PET tracers alternatively investigated for imaging prostate, [11C]Choline is currently providing the most promising results in prostate cancer patients. [11C]Choline has a negligible urinary excretion that represents an advantage in visualizing urological malignancies. Choline is an essential component of phospholipids of the cell membrane. The presence of Choline transporters, cell proliferation and up-regulation of Choline kinase are mechanisms suggested for the increased uptake of Choline in neoplastic disease, including prostate cancer [8,9].

[11C]Choline PET/CT

PET/CT with [11C]Choline is a diagnostic tool that is increasingly used in clinical oncology. Its role is mainly recognized in the re-staging of prostate cancer patients when a biochemical relapse occurs. In fact, in patients with a prostate specific antigen (PSA) failure after radical treatment for prostate cancer, PET/CT with [11C]Choline may accurately detect the presence of recurrences. PET/CT with [11C]Choline has been shown to be complementary to conventional imaging modalities, but with the advantage of re-staging prostate cancer in a single step [10–13]. In radiation oncology, the potential roles of PET/CT with [11C]Choline, in both primary and recurrent prostate cancer, are (1) patient selection for treatment and (2) target volume selection and delineation.

* Corresponding author. Address: Nuclear Medicine, San Raffaele Scientific Institute Via Olgettina 60, 20132, Milan, Italy.
E-mail address: picchio.maria@hsr.it (M. Picchio).

Patient selection

The accurate evaluation of the extent of neoplastic disease represents a crucial issue in planning the treatment, both in staging and in re-staging phase. The presence of metastatic disease currently influences the treatment strategies, curative therapy being ineffective and palliative therapy regimens being favored [14,15]. The role of PET/CT with [11C]Choline in distinguishing patients with local or distant disease has been investigated for the planning of both primary and recurrent prostate cancer treatment.

Primary prostate cancer

When a primary prostate cancer is diagnosed, several aspects are to be considered to plan the treatment strategies. As an alternative to radical prostatectomy, definitive radiation therapy may be proposed to patients, offering the same long-term survival results as surgery and providing a quality of life at least as good as that provided by surgery [15].

The choice of treatment, after the appropriate assessment of tumor extension (TNM classification), has to be based on the combination of several prognostic factors, including Gleason score, baseline PSA, age of the patient, patient's co-morbidity, life expectancy and quality of life and d'Amico's prognostic factor classification [15].

The primary extension assessment of prostate cancer is usually performed by conventional imaging modalities including bone scan, CT and MR imaging [15,16]. As previously reported, these modalities may present limitations in detecting prostate cancer metastases, particularly when PSA values are lower than 20 ng/ml [15]. However, the recent development of high-resolution MR imaging with lymphotrophic ultra-small super-paramagnetic iron oxide particles (USPIO) represents a promising approach in the detection of small and otherwise occult lymph node metastases in patients with prostate cancer [15,17,18].

[11C]Choline PET/CT is not suitable for primary prostate cancer detection, mainly due to limited reported values of sensitivity and specificity in localizing tumor within the prostate gland (71.6% and 42.6%, respectively) [19]. PET modality presents a spatial resolution of approximately 5 mm, thus limiting its capability in detecting small lesions. This limitation is particularly relevant at lymph nodal level where small neoplastic deposits may often occur. In fact, although specificity data are quite high (99.8%), the reported sensitivity of [11C]Choline PET/CT in detecting lymph nodal involvement in prostate cancer patients is very low (41.4%) [20]. At present, there is no clinical evidence that a negative [11C]Choline PET/CT finding at lymph nodal level can surely exclude the pres-

ence of the disease at that site [20]. [11C]Choline PET/CT has been proposed to detect bone metastases in prostate cancer patients showing, in a small group of 11 patients, comparable results as detected by MR diffusion-weighted imaging [21]. The high cost of PET/CT modality and the limited availability of systematic comparative studies with conventional bone scintigraphy do not allow a clear clinical recommendation of [11C]Choline PET/CT for the primary staging of bone metastases.

Large prospective studies, also including cost-effectiveness analyses, are needed to assess the role of [11]Choline PET/CT in the clinical practice of patients with a new diagnosis of prostate cancer. Currently, [11C]Choline PET/CT cannot be recommended in selecting patients for primary treatment, mainly due to its low sensitivity in the detection of lymph-node metastasis.

Recurrent prostate cancer

Although there are recent improvements in diagnostic and therapeutical strategies, a significant percentage of prostate cancer recurrences may occur after therapy. Up to 27–53% of all patients undergoing either radiation therapy or radical prostatectomy will develop local or distant recurrences within 10 years after the initial therapy [22]. Typically, the recurrent cancer is indicated when repeated progressive values of serum PSA are higher than 0.2 ng/ml after a prostatectomy and when a PSA value of 2 ng/ml is above the nadir after the radiation therapy [15]. The information on the site of recurrence is crucial for the therapeutic strategy. Patients with local failure may be candidates for salvage radiotherapy after radical prostatectomy while hormonal therapy is preferred when distant metastases occur [23,24]. Thus, it is important to distinguish between local failure only and distant metastatic recurrent involvement. Several parameters may help in differentiating between local and distant relapse including PSA kinetics, patho-histological stage and Gleason score of the prostatectomy specimen. However, only imaging modalities may allow the anatomical localization of recurrences. Following the primary treatment, bone scintigraphy and CT scans are of no additional diagnostic value for PSA serum levels lower than 20 ng/mL. Endorectal MR imaging may help in detecting local recurrences at lower PSA levels, but it is not a routine clinical practice for the early detection of local relapses [15,25].

[11C]Choline PET/CT has been shown to be useful for re-staging patients with prostate cancer with biochemical failure, in particular, for its capability to detect the presence of lymph nodal and bone metastases, and, although with less accuracy, of local recurrences [10,12,26]. In this scenario, the reported sensitivity of [11C]Choline PET is ranging between 38% and 95% [10–12,26–30]
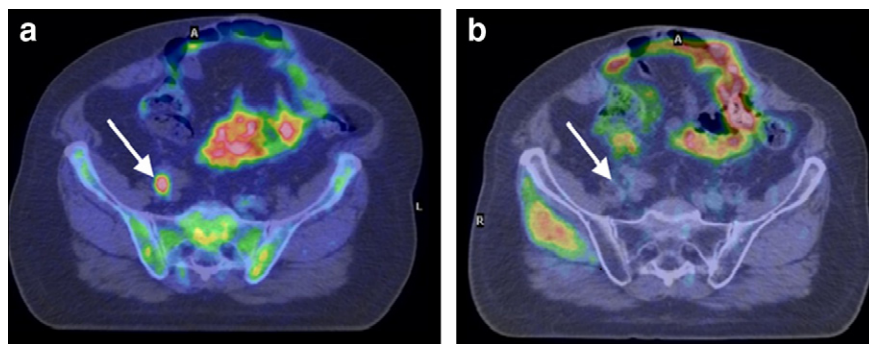

Fig. 1. 75 Year old patient who presented an increase of PSA serum level (2.58 ng/ml) after radical treatment for prostate cancer (Gleason Score = 4 + 3, pT3b pN0). [11C]Choline PET/CT, performed to re-stage prostate cancer, documented a lymph-node metastasis in the right pelvic region (white arrow), as recognized on [11C]Choline PET/CT transaxial fused slices (a). Patient was thus treated by HTT (67.2 Gy/28 fractions) on pelvic lymph nodal chains with a boost on the positive [11C]Choline PET/CT lymph node. Three months after the end of radiation treatment the patient was referred to a second [11C]Choline PET/CT to evaluate treatment response. [11C]Choline PET/CT transaxial fused slices (b) documented a [11C]Choline complete metabolic response at right pelvic lymph node (white arrow). PSA serum value at the time of the second PET/CT examination was significantly decreased (<0.01 ng/mL), thus demonstrating the efficacy of treatment.

Table 1

Tumor site/tracer	Patients selection	Target volume selection	Target volume delineation	Adaptive treatment	Patient outcome
Prostate/11C-Choline	Useful in re-staging phase to (1) exclude from local RT patients with distant mts and (2) refer pts to appropriate therapeutic strategies	No routine use yet in primary treatment Promising data in recurrence treatments, particularly for LN volume selection	No routine use yet	No routine use yet	No data available yet

and particularly, 38–85% in patients previously treated with radical prostatectomy [10–12,26,27,29] and 78–81% in patients previously treated with definitive radiation therapy [27,30].

Several authors showed that the positive detection rate of [11C]Choline PET/CT increases with the increasing PSA values [12,13,29]. In particular, the reported percentages of positive [11C]Choline PET/CT findings are of 19% in patients with a PSA level between 0.2 ng/ml and 1 ng/ml, 46% in those with a PSA level between 1 ng/ml and 3 ng/ml, and 82% in those with a PSA level higher than 3 ng/ml [12].

In general, when a recurrence is suspected after the primary treatment (either radical prostatectomy or radiotherapy), [11C]Choline PET/CT could be suggested as the first procedure in re-staging prostate cancer to guide further treatment decisions [10,11]. Patients with a negative [11C]Choline PET/CT scan, presenting increasing PSA values, should be further examined by conventional imaging modalities to avoid false negative findings at local level. As salvage radiotherapy is indicated in case of local failure, [11C]Choline PET/CT may be of help in documenting the absence of lymph nodal and/or bone metastases.

Conversely, in case of [11C]Choline PET/CT positive findings, the knowledge of the anatomical site of recurrence may be useful to refer patients to the specific tailored therapy, in addition to the conventional anti-hormonal therapy [11]. Choline PET/CT has been previously proposed as an image method to select patients for surgical treatment in case of pelvic and retro-peritoneal lymph node metastases, after the primary treatment [11,31]. The same treatment strategy has been recently translated to radiotherapy treatment [32]. In fact, the high accuracy of [11C]Choline PET/CT in the detection of prostate recurrent disease, in addition to the recent introduction in clinical practice of high conformal intensity modulated treatments, such as helical tomotherapy (HTT), allows new treatment strategies to be proposed [31,33,34] (Fig. 1).

In conclusion, [11C]Choline PET/CT has been established as a diagnostic tool in re-staging patients with biochemical failure after radical treatment for prostate cancer. Its accurate detection and localization of the recurrent disease is the reason why [11C]Choline PET could be proposed as a valid guide for selecting specific patients for specific tailored treatment [22].

Target volume selection and delineation

In prostate cancer, the role of [11C]Choline PET/CT has been investigated for target volume selection and delineation in both primary prostate cancer and its recurrences.

Primary prostate cancer

Although still a matter of debate, [11C]Choline PET/CT is not suitable for the initial diagnosis of prostate cancer, thus not being recommendable for an accurate selection and delineation of target volumes at local level. In fact, prostate cancer is often characterized by multiple foci that may be smaller than PET spatial resolution (approximately 5 mm). Prostate cancer may present values of [11C]Choline uptake, as measured by standardized uptake value (SUV), very variable, thus reflecting a high heterogeneity of pros-

tate cancer metabolic state [35]. In addition, a significant overlap of [11C]Choline uptake between prostate cancer, benign prostate hyperplasia, and healthy tissue has been reported [19,36,37]. The previously reported low [11C]Choline PET/CT accuracy in lymph nodal staging of prostate cancer is the reason why this modality may not be recommended to plan target volumes at lymph nodal level.

Recurrent prostate cancer

In patients with biochemical relapse after prostatectomy, salvage radiotherapy is indicated in case of local failure, at PSA level between 0.2 ng/ml and 1.0 ng/ml. However, [11C]Choline PET/CT is not routinely clinically recommended when PSA serum values are lower than 1.0 ng/ml [15], due to the high incidence of false negative findings [12].

Conversely, [11C]Choline PET/CT presents high values of sensitivity and specificity in detecting distant recurrent sites of the disease [38], especially at lymph nodal level. In radiation treatment planning, [11C]Choline PET/CT may be thus considered to select and delineate target volumes at lymph nodal recurrent sites. The use of [11C]Choline PET/CT to guide HTT treatment on lymph nodal recurrences was initially investigated [34]. Although still experimental, the preliminary results are promising, showing that the treatment is well tolerated with a good rate of local control (significant PSA decrease after HTT in 88% of patients) (Fig. 1). However, further studies with larger population of patients and longer follow-ups are still needed to establish its efficacy (Table 1).

Alternative PET tracers

Two alternative PET tracers that may be considered in planning radiation treatment of prostate cancer patients are [18F]Choline and [11C]Acetate.

[18F]Choline presents a very similar behavior to [11C]Choline in prostate cancer patients. The most striking difference between the two tracers is the urinary elimination that is high for [18F]Choline, being an important disadvantage for imaging prostate region. Conversely, [18F]Choline imaging has the advantage of a longer half-life (approximately 110 min versus 20 min of [11C]Choline) allowing transportation from one single cyclotron Center to several PET Centers [39]. In studies of radiotherapy dose escalation, [18F]Choline has been used to delineate gross tumor volume and to generate the planning target volume in patients with intra-prostatic lesion, attempting to reduce irradiation dose to the bladder and the rectum [40]. However, published data are still too limited to provide valuable conclusions.

Analogously, [11C]Acetate also is a valuable PET tracer for imaging prostate cancer, being used both for primary prostate cancer and metastatic sites [41–43]. The role of [11C]Acetate as an image guide for radiotherapy planning has been evaluated in patients with intra-capsular prostate carcinoma with promising results [44]. However, data are still limited to establish its clinical role in radiotherapy planning.

Conclusion

[11C]Choline PET/CT is an established diagnostic tool in re-staging patients with biochemical failure after primary treatment. This technique is complementary to conventional imaging modalities but with the advantage of re-staging prostate cancer in a single step.

In planning radiation treatment, PET/CT with [11C]Choline has been investigated both for patient selection for treatment and for target volume selection and delineation showing that [11C]Choline PET/CT is not suitable for the selection of patients to be referred to primary radiation treatment for its low sensitivity both at prostate and at lymph nodal levels. Conversely, in the re-staging phase, this modality may be useful to avoid unnecessary local treatment in patients with distant metastases and to select and refer patients to specific treatment strategies.

Further studies are still needed to establish the final clinical role of [18F]Choline and [11C]Acetate for radiation therapy planning in prostate cancer patients.

References

[1] Pinkawa M, Attieh C, Piroth MD, et al. Dose-escalation using intensity-modulated radiotherapy for prostate cancer – evaluation of the dose distribution with and without 18F-choline PET–CT detected simultaneous integrated boost. Radiother Oncol 2009;93:213–9.

[2] Muijs CT, Schreurs LM, Busz DM, et al. Consequences of additional use of PET information for target volume delineation and radiotherapy dose distribution for esophageal cancer. Radiother Oncol 2009;93:447–53.

[3] MacManus M, Nestle U, Rosenzweig KE, et al. Use of PET and PET/CT for radiation therapy planning: IAEA expert report 2006–2007. Radiother Oncol 2009;91:85–94.

[4] Pucar D, Sella T, Schoder H. The role of imaging in the detection of prostate cancer local recurrence after radiation therapy and surgery. Curr Opin Urol 2008;18:87–97.

[5] Grosu AL, Piert M, Weber WA, et al. Positron emission tomography for radiation treatment planning. Strahlenther Onkol 2005;181:483–99.

[6] Senft A, de Bree R, Hoekstra OS, et al. Screening for distant metastases in head and neck cancer patients by chest CT or whole body FDG-PET: a prospective multicenter trial. Radiother Oncol 2008;87:221–9.

[7] Shreve PD, Grossman HB, Gross MD, Wahl RL. Metastatic prostate cancer: initial findings of PET with 2-deoxy-2-[F-18]fluoro-D-glucose. Radiology 1996;199:751–6.

[8] Richter JA, Rodriguez M, Rioja J, et al. Dual tracer (11)C-Choline and FDG-PET in the diagnosis of biochemical prostate cancer relapse after radical treatment. Mol Imaging Biol 2010;12:210–7.

[9] Muller SA, Holzapfel K, Seidl C, et al. Characterization of choline uptake in prostate cancer cells following bicalutamide and docetaxel treatment. Eur J Nucl Med Mol Imaging 2009;36:1434–42.

[10] Picchio M, Messa C, Landoni C, et al. Value of [11C]choline-positron emission tomography for re-staging prostate cancer: a comparison with [18F]fluorodeoxyglucose-positron emission tomography. J Urol 2003;169:1337–40.

[11] Scattoni V, Picchio M, Suardi N, et al. Detection of lymph-node metastases with integrated [11C]choline PET/CT in patients with PSA failure after radical retropubic prostatectomy: results confirmed by open pelvic-retroperitoneal lymphadenectomy. Eur Urol 2007;52:423–9.

[12] Giovacchini G, Picchio M, Coradeschi E, et al. Predictive factors of [(11)C]choline PET/CT in patients with biochemical failure after radical prostatectomy. Eur J Nucl Med Mol Imaging 2010;37:301–9.

[13] Krause BJ, Souvatzoglou M, Tuncel M, et al. The detection rate of [11C]choline-PET/CT depends on the serum PSA-value in patients with biochemical recurrence of prostate cancer. Eur J Nucl Med Mol Imaging 2008;35:18–23.

[14] Heidenreich A, Aus G, Bolla M, et al. EAU guidelines on prostate cancer. Eur Urol 2008;53:68–80.

[15] Heidenreich A, Bolla M, Joniau S, et al. Guidelines on Prostate Cancer. European Association of Urology; 2010. http://www.uroweb.org/guidelines/online-guidelines/.

[16] Groenendaal G, Moman MR, Korporaal JG, et al. Validation of functional imaging with pathology for tumor delineation in the prostate. Radiother Oncol 2010;94:145–50.

[17] Harisinghani MG, Barentsz J, Hahn PF, et al. Noninvasive detection of clinically occult lymph-node metastases in prostate cancer. N Engl J Med 2003;348:2491–9.

[18] Heesakkers RA, Futterer JJ, Hovels AM, et al. Prostate cancer evaluated with ferumoxtran-10-enhanced T2 -weighted MR Imaging at 1.5 and 3.0 T: early experience. Radiology 2006;239:481–7.

[19] Giovacchini G, Picchio M, Coradeschi E, et al. [(11)C]choline uptake with PET/CT for the initial diagnosis of prostate cancer: relation to PSA levels, tumor stage and anti-androgenic therapy. Eur J Nucl Med Mol Imaging 2008;35:1065–73.

[20] Schiavina R, Scattoni V, Castellucci P, et al. 11C-Choline positron emission tomography/computerized tomography for preoperative lymph-node staging in intermediate-risk and high-risk prostate cancer: comparison with clinical staging nomograms. Eur Urol 2008;54:392–401.

[21] Luboldt W, Kufer R, Blumstein N, et al. Prostate carcinoma: diffusion-weighted imaging as potential alternative to conventional MR and 11C-choline PET/CT for detection of bone metastases. Radiology 2008;249:1017–25.

[22] Picchio M, Crivellaro C, Giovacchini G, Gianolli L, Messa C. PET–CT for treatment planning in prostate cancer. Q J Nucl Med Mol Imaging 2009;53:245–68.

[23] Martorana G, Schiavina R, Franceschelli A. Should we perform imaging-guided lymph- node dissection in patients with lymphatic recurrence of prostate cancer after radical prostatectomy? Eur Urol 2009;55:1302–4.

[24] Peterson JL, Buskirk SJ, Heckman MG, et al. Late toxicity after postprostatectomy salvage radiation therapy. Radiother Oncol 2009;93:203–6.

[25] Kershaw LE, Logue JP, Hutchinson CE, Clarke NW, Buckley DL. Late tissue effects following radiotherapy and neoadjuvant hormone therapy of the prostate measured with quantitative magnetic resonance imaging. Radiother Oncol 2008;88:127–34.

[26] Reske SN, Blumstein NM, Glatting G. [11C]Choline PET/CT imaging in occult local relapse of prostate cancer after radical prostatectomy. Eur J Nucl Med Mol Imaging 2008;35:9–17.

[27] de Jong IJ, Pruim J, Elsinga PH, Vaalburg W, Mensink HJ. 11C-Choline positron emission tomography for the evaluation after treatment of localized prostate cancer. Eur Urol 2003;44:32–8 [discussion 8–9].

[28] Rinnab L, Mottaghy FM, Blumstein NM, et al. Evaluation of [11C]-choline positron-emission/computed tomography in patients with increasing prostate-specific antigen levels after primary treatment for prostate cancer. BJU Int 2007;100:786–93.

[29] Castellucci P, Fuccio C, Nanni C, et al. Influence of trigger PSA and PSA kinetics on 11C-Choline PET/CT detection rate in patients with biochemical relapse after radical prostatectomy. J Nucl Med 2009;50:1394–400.

[30] Breeuwsma AJ, Pruim J, van den Bergh AC, et al. Detection of local, regional, and distant recurrence in patients with psa relapse after external-beam radiotherapy using (11)C-choline positron emission tomography. Int J Radiat Oncol Biol Phys 2010;77:160–4.

[31] Jereczek-Fossa BA, Kowalczyk A, D'Onofrio A, et al. Three-dimensional conformal or stereotactic reirradiation of recurrent, metastatic or new primary tumors. Analysis of 108 patients. Strahlenther Onkol 2008;184:36–40.

[32] Van Poppel H. Is radiotherapy useful in node-positive prostate cancer patients after radical prostatectomy? Eur Urol 2009;55:1012–3.

[33] Picchio M, Alongi F, Giovacchini G, et al. 11C-Choline PET/CT image-guided radiotherapic treatment of lymph nodal recurrence in prostate cancer patients. Eur J Nucl Med Mol Imaging 2008;35:388.

[34] Picchio M, Alongi F, Giovacchini G, et al. 11C-Choline PET/CT image-guided tomotherapy treatment of lymph nodal relapse in prostate cancer patients. J Nucl Med 2010;51:1274.

[35] Farsad M, Schiavina R, Castellucci P, et al. Detection and localization of prostate cancer: correlation of (11)C-choline PET/CT with histopathologic step-section analysis. J Nucl Med 2005;46:1642–9.

[36] Reske SN, Blumstein NM, Neumaier B, et al. Imaging prostate cancer with 11C-choline PET/CT. J Nucl Med 2006;47:1249–54.

[37] Yoshida S, Nakagomi K, Goto S, Futatsubashi M, Torizuka T. 11C-Choline positron emission tomography in prostate cancer: primary staging and recurrent site staging. Urol Int 2005;74:214–20.

[38] Rinnab L, Simon J, Hautmann RE, et al. [(11)C]Choline PET/CT in prostate cancer patients with biochemical recurrence after radical prostatectomy. World J Urol 2009;27:619–25.

[39] Husarik DB, Miralbell R, Dubs M, et al. Evaluation of [(18)F]-choline PET/CT for staging and restaging of prostate cancer. Eur J Nucl Med Mol Imaging 2008;35:253–63.

[40] Weber DC, Wang H, Cozzi L, et al. RapidArc, intensity modulated photon and proton techniques for recurrent prostate cancer in previously irradiated patients: a treatment planning comparison study. Radiat Oncol 2009;4:34.

[41] Albrecht S, Buchegger F, Soloviev D, et al. (11)C-Acetate PET in the early evaluation of prostate cancer recurrence. Eur J Nucl Med Mol Imaging 2007;34:185–96.

[42] Vees H, Buchegger F, Albrecht S, et al. 18F-Choline and/or 11C-acetate positron emission tomography: detection of residual or progressive subclinical disease at very low prostate-specific antigen values (<1 ng/mL) after radical prostatectomy. BJU Int 2007;99:1415–20.

[43] Kotzerke J, Volkmer BG, Glatting G, et al. Intraindividual comparison of [11C]acetate and [11C]choline PET for detection of metastases of prostate cancer. Nuklearmedizin 2003;42:25–30.

[44] Seppala J, Seppanen M, Arponen E, Lindholm P, Minn H. Carbon-11 acetate PET/CT based dose escalated IMRT in prostate cancer. Radiother Oncol 2009;93:234–40.

Review

Clinical evidence on PET–CT for radiation therapy planning in cervix and endometrial cancers

Christine Haie-Meder *, Renaud Mazeron, Nicolas Magné

Brachytherapy Service, Institut Gustave Roussy, Villejuif, France

A R T I C L E   I N F O

A B S T R A C T

PET–CT plays an increasing role in the diagnosis and treatment of gynaecological cancers. In cervix cancer, whilst MRI remains the best imaging technique for initial primary tumor staging, PET–CT has been showed to be a highly sensitive method to determine lymph node status, except in patients with early-stage cervical cancer where PET–CT cannot replace surgical exploration of pelvic lymph nodes. In patients with advanced cervical cancer, PET–CT has the potential of showing lymph node metastasis not only within the pelvis, but also outside the pelvis, more particularly in the para-aortic area. PET–CT has also been described as a useful tool in 3-D-based adaptative brachytherapy. In endometrial cancer, the issues are different, as the recent decade has seen a therapeutic decrease in early-stage disease, especially in postoperative radiation therapy, whilst more advanced disease have been approached with more aggressive treatments, integrating chemotherapy and external beam radiotherapy. Lymph node status is also an important issue and PET-Scan may replace lymph node surgical procedure particularly in obese patients.

Recent publications have emphasized the increasing role of PET–CT in the diagnostic and treatment of gynaecological cancers [1–3]. In cervix cancer, the FIGO classification, even if recently reviewed, is still based on clinical examination [4]. The lymph node status, representing one of the main prognostic factors, is not included into the FIGO classification. Surgical staging remains probably the best method to determine lymph node involvement. PET-Scan has been recently showed to be a highly sensitive method to determine lymph node status. To integrate PET–CT into the radiotherapy treatment planning represents a challenging issue [5]. For some authors, FDG-PET even represents a rational choice for dose painting [6]. PET-Scan has also been described as a useful tool in 3-D-based adaptative brachytherapy, even if the recent developments in gynaecological BT have been reported with MRI or ultrasound [7]. In endometrial cancer, the issues are different, as the recent decade has seen a therapeutic decrease in early-stage disease, especially in postoperative radiation therapy, whilst more advanced disease have been approached with more aggressive treatments, integrating chemotherapy and external beam radiotherapy. Lymph node status is also an important issue and PET-Scan may replace lymph node surgical procedure particularly in obese patients.

Cervical cancer

Fluorodeoxyglucose (FDG)-PET

Primary tumor staging

MRI has been showed to be the best exam to assess tumor in cervix cancer, especially to detect tumor extension in the parametria. The accuracy of MRI in the staging of cervical cancer ranges from 80% to 90% compared to 60% to 69% for CT. FDG-PET–CT has been initially used to identify cervical cancer. Wong et al. reported a series of patients with cervix cancer who had a PET–CT in the initial work-up [8]. Their conclusion was that the PET–CT was able to detect 100% of the primary disease and was also able to separate the population with limited disease from patients with metastases. The clinical value of PET–CT was prospectively investigated in a series of 120 consecutive patients with cervix cancer by Loft et al. [9]. Among them, 27 underwent radical hysterectomy and the PET–CT results were compared to histopathological findings. Of the 27 patients, four had PET–CT evidencing pathological foci in the pelvis: one was false-positive and three were true-positive. Integrating the results on lymph

* Corresponding author.
   E-mail addresses: haie@igr.fr, Christine.HAIEMEDER@igr.fr (C. Haie-Meder).

nodes, the authors concluded that FDG-PET–CT had a predictive positive value of 75%, a negative predictive value of 96%, sensitivity of 75%, and specificity of 96%. In Stage IA and limited IB, false-negative PET–CTs are more often reported, when the tumor size is inferior to the PET–CT sensitivity. Moreover, neither PET–CT nor CT is an effective method for detecting parametrial extension. For primary tumor evaluation, MRI remains the best imaging technique for initial primary tumor staging in cervical cancer.

Nodal staging

Nodal status is one of the strongest prognostic factors in patients with cervical cancers. In early-stage disease, the 5-year survival is 90–95% in node negative patients, 50% in positive pelvic node patients, and 20–30% in positive para-aortic node patients. The knowledge of nodal status is therefore fundamental, as it has an impact on treatment modalities. The extension of radiation fields to the para-aortic area depends on the involvement of the para-aortic nodes and a pelvic involvement potentially leads to a boost within involved pelvic nodes. The capacity of lymph node metastasis detection using CT or MRI is mainly dependent on the lymph node size. It is generally admitted that lymph node size greater than 1 cm is considered as abnormal. The sensitivity of MRI was reported to be within the range of 38–89%, and the specificity 78–99% [10].These results were improved with the use of ultrasmall superparamagnetic iron oxide particles (USPIO) [11]. Nodal staging using PET-Scan is still a matter of controversy.

Lymph node staging in early-stage disease. It is generally admitted that PET–CT is of limited value in patients with early-stage cervical cancer and cannot replace surgical exploration of pelvic lymph nodes. Table 1 summarizes the main literature data in this clinical situation.

Lymph node staging in advanced disease. Patients are considered with advanced disease when FIGO Stage is ⩾IB2. In this clinical situation, PET–CT has the potential interest of showing lymph node metastasis not only within the pelvis, but also outside the pelvis, more particularly in the para-aortic area. PET–CT can show distant metastasis, ignored by the standard traditional exams, i.e., CT and MRI. In the literature dealing with PET in the assessment of lymph node involvement in advanced cervical cancers, three different types of analyses have been performed: results of PET compared to CT and/or MRI, results of PET as prognostic factors, especially on the survival, and comparison between PET results and histopathological findings.

Comparison between PET and CT and/or MRI. PET sensitivity has been reported to be significantly higher than MRI. Sugawara et al. reported a 86% FDG-PET sensitivity for pelvic and para-aortic lymph node metastasis, compared with a CT sensitivity of 57%, in a series of 21 patients with advanced cervical cancer [17]. In a series of 32 patients with advanced-stage cervical cancer, Rose et al. reported PET sensitivity and specificity of 75% and 92%, respectively [18]. Sensitivity was higher for pelvic (100%) than para-aortic (75%) lymph node metastases.

Comparison between PET results and histopathological findings. The studies on the correlation of PET–CT results and histopathological findings are of particular interest to determine the need for extension of the radiation fields to the para-aortic area. The main publications are summarized in Table 2. Some authors recommend a para-aortic lymph node dissection prior to the beginning of concomitant chemoradiation, in order to properly define the radiation fields, as PET–CT would overlook 8% of positive para-aortic lymph node patients.

Treatment optimization

External irradiation. As previously stated, pathological uptake of PET may modify treatment strategy, either by extending radiation fields to the para-aortic area, or by modifying the total doses to the involved nodes within the pelvis and/or the para-aortic area. Narayan et al. assessed whether PET–CT or MRI could avoid surgical staging in 27 patients with locally advanced cervical carcinoma planned for radiotherapy [22]. The authors concluded that PET had superior sensitivity to MRI but still missed small-volume disease and they recommended para-aortic lymph node dissection in all patients with positive pelvic lymph nodes on PET. Conversely, the 98% positive predictive value of PET–CT was high enough to avoid pathological confirmation and led to extended field radiotherapy. Belhocine et al. reported that PET staging significantly influenced the treatment decision-making in 18% of the patients [23]. In a prospective cohort of 560 patients evaluating FDG-PET lymph node staging, Kidd et al. evidenced a statistically significant correlation between PET findings with the risk of disease progression and with survival [24].

The dose to lymph nodes has been extensively described by Grigsby et al. [25]. In a series of 208 patients with cervix cancer, lymph nodes were scored as either positive or negative for abnormal FDG uptake PET and lymph node status by CT was classified as <1 cm (negative) or >1 cm (positive). All enlarged lymph nodes detected by CT were PET positive. No patient underwent lymph node dissection. The mean pelvic lymph nodes were dependent on PET and CT findings: PET negative nodes, <1 cm, 66.8 Gy, and 0/76 failures; PET positive nodes, <1 cm, 66.8 Gy, and 3/89 failures; 1.1 to <2 cm, 66.9 Gy, and 0/21 failures; 2.1 to <3 cm, 69.4 Gy, and 2/15 failures; and 3.1 to <4 cm, 74.1 Gy, and 0/5 failures. The mean para-aortic lymph node was 43.3 Gy and no para-aortic failure was observed among 24 patients with PET positive <1 cm, 0/5 failure for 1.1 to <2 cm, and 0/4 failure for 2.1 to <3 cm. The risk of isolated nodal failure was <2%. The reason why patients did not fail in the para-aortic area when they were presented with initial PET positive in the para-aortic area is mainly because these patients were at a high risk of having distant metastases, which represented the

Table 1
FDG-PET for lymph node staging in early-stage disease.

Author	n	Study	FIGO stages	Imaging modality	LN	Se (%)	Sp (%)	PPV (%)	NPV (%)	Nodal status confirmation
Roh et al. [12]	54	P	2 groups IB-IIA < 4 cm:29 IIB-IIIB:25	PET–CT	Overall	38	97	56	94	LND
Reinhardt et al. [13]	35	R	IB-II	PET vs MRI	PELN	91	100	90		LND
					PELN	73	83	64		
Chou et al. [14]	60	P	IA2-IIa ⩽ 4 cm and no LN on MRI	PET	PELN	10	94	25	84	SLN
Sironi et al. [15]	47	P	IA-IB	PET	overall	72	99.7	81	99	LND
Wright et al. [16]	59	R	IA2-IIA	PET–CT > 2002	PELN	53	90	71	80	LND
					PALN	25	98	50	93	LND

Se: sensitivity, Sp: specificity, R: retrospective, P: prospective, SLN: sentinel lymph node, PELN: pelvic lymph node, PALN: para-aortic lymph node.

Table 2
Comparison between FDG-PET results and histopathological findings of para-aortic lymph node dissection in advanced cervix cancer.

Author	n	FIGO stage	CT findings	Se (%)	Sp (%)	PPV (%)	NPV (%)	Accuracy
Lin et al. [19]	50	IB2-IVA	All negative	86	94			92
Yildirim et al. [20]	16	IIB-IVA	All negative	50	83	50	83	75
Boughanim et al. [21]	38	IB2-IIA-B	All negative				92	
Narayan et al. [22]	27	IB-IVB	MRI:3+			100	87	

Se: sensitivity, Sp: specificity, PPV: positive predictive value, NPV: negative predictive value.

main cause of failure. Conversely, dose intensification in the pelvic lymph nodes, as performed in this study, could be of value.

Conversely, Esthappan et al. proposed dose escalation to 59.4 Gy to the positive para-aortic lymph node and 50.4 Gy to the para-aortic region using CT/PET-guided IMRT [26]. The authors proposed guidelines to select treatment parameters needed for the use of CT/PET-guided IMRT for cervical carcinoma with positive para-aortic lymph nodes. If the published data are all in accordance to recommend increasing the dose to pelvic nodes by using the results of PET–CT, further studies are necessary to better define the total dose to the para-aortic nodes as they might not be necessary if the main carcinological events are distant metastases. Recurrent cervical carcinoma can also be salvaged with radiotherapy and PET–CT helps in limiting the irradiated volumes, specially to decrease the risk of complications after surgery [27].

Chemoradiation selection. A meta-analysis of 4580 patients included in randomized studies clearly indicated that the use of concurrent chemoradiation would lead to a significant increase in disease-free and overall survival, with a significant reduction in the development of distant metastasis [28]. The development of PET–CT could represent a useful tool to better select candidates for concomitant chemoradiation. Grigsby et al. compared concomitant chemoradiation with radiotherapy alone in a prospective data registry of 65 patients with FIGO IB2 to IIIB cervix carcinoma with no evidence of lymph node metastasis [29]. Radiation therapy alone was administered to 15 and concomitant chemoradiation using cisplatin to 50 patients. No significant difference in 5-year overall survival for patients with PET-FDG–negative lymph nodes was observed. Loft et al. prospectively assessed the diagnostic value of PET–CT in 120 patients with cervical cancer stage $\geqslant$1B [9]. Sensitivity and specificity of PET/CT for pelvic node diagnosis were 75% and 96%, respectively. Regarding para-aortal nodal disease, sensitivity and specificity were 100% and 94%, respectively. This confirms that the use of whole-body FDG/PET/CT scanning for newly diagnosed cervical cancer with FIGO stage $\geqslant$1B2 has a high sensitivity and specificity and allows a more adapted therapeutic strategy.

Brachytherapy procedure. The use of MRI for brachytherapy planning has been recently investigated. MRI at the time of brachytherapy allows an accurate tumor delineation and dose optimization [30,31]. Recommendations have been published to have reproducible and reliable definitions of targets with limited inter-observer variability [32] A few studies have assessed the use of PET for three-dimensional (3D) brachytherapy. Malyapa et al. compared two-dimensional (2D) treatment planning orthogonal radiography-based brachytherapy with a 3D treatment planning based on 18F-fluoro-deoxyglucose-positron emission tomography in 11 patients with cervical cancer [33]. The patients underwent two PETs: a first one to visualize the tumor and a second one with the FDG placed inside the tandem and ovoid applicators to visualize the treatment source positions for 3-D treatment planning. The authors concluded that this technique was feasible and accurate relative to 2D treatment planning. Lin et al. conducted a dosimetric study comparing intracavitary brachytherapy using a standard plan with a PET-defined tumor volume in 11 patients undergoing a total of 31 intracavitary treatments [34]. The coverage of the target isodose surface for the first implant with and without optimization 73% and 68% ($p = 0.21$). For the mid and final implant, the coverage was 83% and 70% ($p = 0.02$). The dose to point A was significantly higher with the optimized plans for both the first implant ($p = 0.02$) and the mid and last implants ($p = 0.008$). The dose to the 2 cm^3 and 5 cm^3 of bladder or rectum were not significantly different. The authors concluded that FDG-PET-based treatment planning improved dose tumor coverage without significant increase to the bladder and rectum doses. Optimized treatment allowed for improved tumor coverage to the PET defined tumor volume without significantly increasing the dose to bladder or rectum. Physiological tumor volume determination by PET allows a more targeted irradiation with brachytherapy. Lin et al. had demonstrated a mean 50% tumor volume reduction occurring within 20 days from the beginning of irradiation [35].

Other PET tracers

The majority of publications dealing with PET in cervix cancers have studied Fluoro-deoxy-glucose as tracer. Because of limited urinary uptake, (11)C-choline appears as a promising radiopharmaceutical [MacManus]. Torizuka et al. conducted a study comparing (18)F-FDG and (11)C-choline in the imaging of gynaecological tumors in 21 patients with 18 untreated tumors and three suspected recurrence of ovarian cancer [36]. Among them, five had cervical cancer, 4 FIGO Stage IIB, and one Stage IB1. ^{11}C-Choline PET showed uterine cervix cancer in all 5 patients, because of low urinary radioactivity. ^{18}F-FDG PET failed to detect small cervical cancer in one patient, with an intense bladder activity. For nodal staging, three patients had no pathological uptake and the node negativity was later confirmed by surgery. The two other patients presented enlarged parailiac lymph nodes on MRI, ^{18}F-FDG PET clearly detected intense uptake at the level of lymphadenopathy whilst ^{11}C-Choline PET could show an abnormal activity, but this was obscured by physiologic bowel uptake. The authors concluded that ^{11}C-Choline PET may be inferior to ^{18}F-FDG PET for the tumor staging within the abdomen, because of the bowel ^{11}C-Choline uptake.

Tumor hypoxia has been demonstrated by PET with (60)Cu-labeled diacetyl-bis(N(4)-methylthiosemicarbazone) ((60)Cu-ATSM) which is a biomarker of poor prognosis in patients with cervical cancer. In a series of 38 patients with cervical cancer, Dehdashti et al. found an inverse relationship between tumor ((60)Cu-ATSM) uptake and progression-free and survival [37]. Of interest was the absence of correlation between ((60)Cu-ATSM) uptake and (18)F-FDG uptake.

An imaging comparison of 64Cu-ATSM and 60Cu-ATSM in a series of 10 patients with cancer of the uterine cervix was conducted by Lewis et al. [38]. The authors found a better image quality with 64Cu-ATSM, because of lower noise and concluded that 64Cu-ATSM appeared to be a safe radiopharmaceutical with high-quality images of tumor hypoxia.

Endometrial cancer

Fluorodeoxyglucose (FDG)-PET

The validity of FDG-PET has been mainly studied in the preoperative evaluation and the available data have not reached the maturity observed in cervix cancers. One of the main issues in this patient population is to select patients who require lymphadenectomy.

Primary tumor staging

Suzuki et al. examined 30 patients with endometrial cancer and compared PET, CT, MRI, and postoperative findings [39]. FDG-PET was able to detect primary tumors, with a higher sensitivity: 96.7% versus 83.3% for CT/MRI. By contrast, Park et al. detected no difference in sensitivity (91.5% for MRI versus 89.4% for PET), specificity (33.3% for MRI versus 50.5% for PET), accuracy (84.9% for MRI versus 84.9% for PET), positive predictive value (91.5% for MRI versus 93.3% for PET), or negative predictive value (33.3% versus 37.5% for PET) for primary lesions [40].

Nodal staging

Kitajima et al. evaluated the accuracy of pelvic and para-aortic lymph node metastasis detection in 40 patients with stage IA to IIIC [41]. PET/CT was interpreted by two experienced radiologists and was compared with histopathological findings. The overall node-based sensitivity, specificity, and accuracy of PET–CT were 53.3%, 99.6%, and 97.8%, respectively. The authors concluded that due to moderate sensitivity, even if PET–CT is superior to conventional imaging techniques, it should not replace lymphadenectomy. More recently, Kitajima et al. reassessed the accuracy of PET–CT with the integration of contrast-enhanced CT in the detection of pelvic and para-aortic node metastasis [42]. Their conclusion on a series of 45 patients were the same: the sensitivity for detecting metastatic lesions 4 mm or less was 12.5%, for metastasis between 5 and 9 mm 66.7%, and for metastatic lesions of 10 mm or larger 100%. In the series reported by Suzuki, the conclusions were similar: a negative PET in the detection of lymph node metastasis would not justify omitting lymph node dissection if a precise knowledge of the nodal status is necessary [39]. In the series of Park et al. PET/CT showed higher sensitivity but the difference did not reach statistical significance ($p = 0.250$) [40].

Chung et al. evaluated PET/CT in 31 patients with suspected recurrent endometrial cancer [43]. The results showed high sensitivity, specificity, and accuracy being 100%, 94.7%, and 92.3%, respectively. In 22.6% of the patients, PET helped in modifying the diagnosis or the treatment strategy.

So far, no study has been reported on clinical outcome comparing PET–CT and MRI in endometrial cancer, as the treatment of these tumors is mainly surgery. For the same reasons, no data have been published on adaptive treatment.

Other PET tracers

In the study by Torizuka et al., already mentioned in the cervical cancer section, comparing ^{11}C-Choline PET and ^{18}F-FDG PET, in gynaecological cancers, 11 patients presented uterine corpus cancer [36]. All patients underwent surgery after PET examinations. Surgical FIGO staging was Stage 0 for 1 patient (with endometrial hyperplasia), Stage IA (tumor limited to the endometrium) in two patients, Stage IB (invasion of less than 50% of the myometrium thickness) in five patients, Stage IC (invasion of more than 50% of the myometrium thickness) in one patient, and Stage IIIA (serosa invasion) in two patients. Both ^{11}C-choline PET and ^{18}F-FDG PET were true-positive in nine patients for the detection of uterine corpus cancer. Both tracers were negative in the patient with atypical hyperplasia. In one patient with diabetes, ^{11}C-choline PET could detect the tumor, whilst ^{18}F-FDG PET was false-negative. For nodal staging, both ^{11}C-Choline PET and ^{18}F-FDG PET were negative in all 11 patients and the negativity was surgically confirmed. ^{11}C-Choline PET could therefore be an alternative to ^{18}F-FDG PET, especially in patients presenting with diabetes.

Conclusion

FDG PET appears to be an effective imaging technique in lymph node staging of locally advanced cervix carcinoma patients with negative CT findings. The results of PET–CT contribute to select the optimal treatment plan and to customize the radiotherapy planning by modifying radiation fields, and guide the brachytherapy planning. In endometrial cancer patients, this imaging modality may better select treatment strategies, especially in terms of lymphadenectomy. Preliminary published data on cervical cancer have indicated the prognostic value of post-therapeutic PET–CT assessment. Further evaluations in prospective clinical trials are required to assess the clinical benefit of this strategy.

References

[1] Lucignani G. FDG-PET in gynaecological cancers: recent observations. Eur J Nucl Med Mol Imaging 2008;35:2133–9.

[2] Maffione AM, Piva M, Tsamita CS, et al. Positron-emission tomography in gynaecological malignancies. Arch Gynecol Obstet 2009;280:521–8.

[3] Magné N, Chargari C, Vicenzi L, et al. New trends in the evaluation and treatment of cervix cancer: the role of FDG-PET. Cancer Treat Rev 2008;34:671–81.

[4] FIGO Committee on Gynecologic Oncology. Revised FIGO staging for carcinoma of the vulva, cervix, and endometrium. Int J Gynecol Obstet 2009;105:103–4.

[5] Öllers M, Osmans G, van Baardwijk A, et al. The integration of PET–CT scans from different hospitals into radiotherapy treatment planning. Radiother Oncol 2009;91:85–94.

[6] Aerts HJWL, Lambin P, De Ruysscher D. FDG for dose painting: A rational choice. Radiother Oncol 2010;doi:10.1016/j.radonc.2010.05.001.

[7] Poetter R. Image-guided brachytherapy sets benchmarks in advanced radiotherapy. Radiother Oncol 2009;91:141–6.

[8] Wong TZ, Jones EL, Coleman RE. Positron emission tomography with 2-deoxy-2-[(18)F]fluoro-D-glucose for evaluating local and distant disease in patients with cervical cancer. Mol Imaging Biol 2004;6:55–62.

[9] Loft A, Berthelsen AK, Roed H, et al. The diagnostic value of PET/CT scanning in patients with cervical cancer: a prospective study. Gynecol Oncol 2007;106:29–34.

[10] Scheidler J, Hricak H, Yu KK, Subak L, Segal MR. Radiological evaluation of lymph node metastases in patients with cervical cancer. a meta-analysis. JAMA 1997;278:1096–101.

[11] Bellin MF, Roy C, Kinkel K, et al. Lymph node metastases: safety and effectiveness of MR imaging with ultrasmall superparamagnetic iron oxide particles – initial clinical experience. Radiology 1998;207:799–808.

[12] Roh JW, Seo SS, Lee S, et al. Role of positron emission tomography in pre-treatment lymph node staging of uterine cervical cancer: a prospective surgicopathologic correlation study. Eur J Cancer 2005;41:2086–92.

[13] Reinhardt MJ, Ehritt-Braun C, Vogelgesang D, et al. Metastatic lymph nodes in patients with cervical cancer: detection with MR imaging and FDG PET. Radiology 2001;218:776–82.

[14] Chou HH, Chang TC, Yen TC, et al. Low value of [18F]-fluoro-2-deoxy-D-glucose positron emission tomography in primary staging of early-stage cervical cancer before radical hysterectomy. J Clin Oncol 2006;24:123–8.

[15] Sironi S, Buda A, Picchio M, et al. Lymph node metastasis in patients with clinical early-stage cervical cancer: detection with integrated FDG PET/CT. Radiology 2006;238:272–9.

[16] Wright JD, Dehdashti F, Herzog TJ, et al. Preoperative lymph node staging of early-stage cervical carcinoma by [18F]-fluoro-2-deoxy-D-glucose-positron emission tomography. Cancer 2005;104:2484–91.

[17] Sugawara Y, Eisbruch A, Kosuda S, et al. Evaluation of FDG PET in patients with cervical cancer. J Nucl Med 1999;40:1125–31.

[18] Rose PG, Adler LP, Rodriguez M, et al. Positron emission tomography for evaluating para-aortic nodal metastasis in locally advanced cervical cancer before surgical staging: a surgicopathologic study. J Clin Oncol 1999;17:41–5.

[19] Lin WC, Hung YC, Yeh LS, Kao CH, Yen RF, Shen YY. Usefulness of (18)F-fluorodeoxyglucose positron emission tomography to detect para-aortic lymph nodal metastasis in advanced cervical cancer with negative computed tomography findings. Gynecol Oncol 2003;89:73–6.

[20] Yildirim Y, Sehirali S, Avci ME, et al. Integrated PET/CT for the evaluation of para-aortic nodal metastasis in locally advanced cervical cancer patients with negative conventional CT findings. Gynecol Oncol 2008;108:154–9.

[21] Boughanim M, Leboulleux S, Rey A, et al. Histologic results of para-aortic lymphadenectomy in patients treated for stage Ib2/II cervical cancer with negative [18F] fluorodeoxyglucose positron emission tomography scans in the para-aortic area. J Clin Oncol 2008;26:2558–61.

[22] Narayan K, Hicks RJ, Jobling T, et al. A comparison of MRI and PET scanning in surgically staged loco-regionally advanced cervical cancer: potential impact on treatment. Int J Gynecol Cancer 2001;11:263–71.

[23] Belhocine T, Thille A, Fridman V, et al. Contribution of whole-body 18FDG PET imaging in the management of cervical cancer. Gynecol Oncol 2002;87:90–7.

[24] Kidd EA, Siegel BA, Dehdashti F, Rader JS, Mutch DG, Powell MA, Grigsby PW. Lymph node staging by positron emission tomography in cervical cancer: relationship to prognosis. J Clin Oncol 2010;28:2108–13.

[25] Grigsby PW, Singh AK, Siegel BA, Dehdashti F, Rader J, Zoberi I. Lymph node control in cervical cancer. Int J Radiat Oncol Biol Phys 2004;59:706–12.

[26] Esthappan J, Mutic S, Malyapa RS, et al. Treatment planning guidelines regarding the use of CT/PET-guided IMRT for cervical carcinoma with positive paraaortic lymph nodes. Int J Radiat Oncol Biol Phys 2004;58:1289–97.

[27] Haasbek CJA, Uitterhoeve ALJ, Van der Velden J, et al. Long-term results of salvage radiotherapy for the treatment of recurrent cervical carcinoma after prior surgery. Radiother Oncol 2008;89:197–204.

[28] Green J, Kirwan J, Tierney J, et al. Concomitant chemotherapy and radiation therapy for cancer of the uterine cervix. Cochrane Database Syst Rev 2005;3:CD002225.

[29] Grigsby PW, Mutch DG, Rader J, et al. Lack of benefit of concurrent chemotherapy in patients with cervical cancer and negative lymph nodes by FDG-PET. Int J Radiat Oncol Biol Phys 2005;61:444–9.

[30] Chargari C, Magné N, Dumas I, et al. Physics contribution and clinical outcome with 3D MRI-based pulsed dose-rate intracavitary brachytherapy in cervical cancer patients. Int J Radiat Oncol Biol Phys 2009;74:133–9.

[31] Pötter R, Dimopoulos J, Georg P, et al. Clinical impact of MRI assisted dose volume adaptation and dose escalation in brachytherapy of locally advanced cervix cancer. Radiother Oncol 2007;83:148–55.

[32] Dimopoulos JCA, De Vos V, Berger D, et al. Inter-observer comparison of target delineation for MRI-assisted cervical cancer brachytherapy: application of the GYN GEC-ESTRO recommendations. Radiother Oncol 2009;91:166–72.

[33] Malyapa RS, Mutic S, Low DA, et al. Physiologic FDG-PET three-dimensional brachytherapy treatment planning for cervical cancer. Int J Radiat Oncol Biol Phys 2002;54:1140–6.

[34] Lin LL, Mutic S, Low DA, et al. Adaptive brachytherapy treatment planning for cervical cancer using FDG-PET. Int J Radiat Oncol Biol Phys 2007;67:91–6.

[35] Lin LL, Yang Z, Mutic S, Miller TR, Grigsby PW. FDG-PET imaging for the assessment of physiologic volume response during radiotherapy in cervix cancer. Int J Radiat Oncol Biol Phys 2006;65:177–81.

[36] Torizuka T, Kanno T, Futatsubashi M, et al. Imaging of gynaecologic tumors: comparison of (11)C-choline PET with (18)F-FDG PET. J Nucl Med 2003;44:1051–6.

[37] Dehdashti F, Grigsby PW, Lewis JS, Laforest R, Siegel BA, Welch MJ. Assessing tumor hypoxia in cervical cancer by PET with Cu-labeled diacetyl-bis(N4-methylthioemicarbazone). J Nucl Med 2008;49:201–5.

[38] Lewis JS, Laforest R, Dehdashti F, Grigsby PW, Welch MJ, Siegel BA. An imaging comparison of 64Cu-ATSM and 60Cu-ATSM in cancer of the uterine cervix. J Nucl Med 2008;49:1177–82.

[39] Suzuki R, Miyagi E, Takahashi B, et al. Validity of positron emission tomography using fluoro-2-deoxyglucose for the preoperative evaluation of endometrial cancer. Int J Gynecol Cancer 2007;17:890–6.

[40] Park JY, Kim EN, Kim DY, et al. Comparison of the validity of magnetic resonance imaging and positron emission tomography/computed tomography in the preoperative evaluation of patients with uterine corpus cancer. Gynecol Oncol 2008;108:486–92.

[41] Kitajima K, Murakami K, Yamasaki E, et al. Accuracy of 18F-FDG PET/CT in detecting pelvic and paraaortic lymph node metastasis in patients with endometrial cancer. Am J Roentgenol 2008;190:1652–8.

[42] Kitajima K, Murakami K, Yamasaki E, Kaji Y, Sugimura K. Accuracy of integrated FDG-PET/contrast-enhanced CT in detecting pelvic and paraaortic lymph node metastasis in patients with uterine cancer. Eur Radiol 2009;19:1529–36.

[43] Chung HH, Kang WJ, Kim JW, et al. The clinical impact of [(18)F] FDG PET/CT for the management of recurrent endometrial cancer: correlation with clinical and histological findings. Eur J Nucl Med Mol Imaging 2008;35:1081–8.